REGULATION OF HUMAN VASCULAR REDOX STATE IN OBESITY AND INSULIN RESISTANCE

By

Ioannis Akoumianakis

Thesis presented for the degree

Doctor of Philosophy in Cardiovascular Medicine

University of Oxford

St Cross College

Division of Cardiovascular Medicine

Radcliffe Department of Medicine

University of Oxford

Level 6, John Radcliffe Hospital

Oxford, OX3 9DU

Supervisors: Professor Charalambos Antoniades, Professor Keith M Channon

Trinity Term 2019

Acknowledgements

Who would have thought that this would be the trickiest part of the thesis to write! And yet, there are so many people who have made this thesis possible, and I doubt that could emphasize their invaluable contribution enough in the few following lines!

I am grateful to all the current and past members of my research team, the Oxford Translational Cardiovascular Research Group. I am glad to have been a part of such a friendly and diverse group of people working together through all the good and the bad, the moments of frustration and success. I would like to thank, in no particular order: Dr Evangelos K Oikonomou, Dr Marios Margaritis, Miss Laura Herdman, Dr Alexios S Antonopoulos, Dr Ileana Badi, Dr Costas Psarros, Dr Fabio Sanna, Dr Patricia Ciccone, Dr Christos Kotanidis, Dr Maria Cristina Carena, Miss Sheena Thomas, Dr Hidekazu Kondo, Dr Akansha Tarun and Dr Nadia Akawi for their friendship, support and feedback throughout my course ad a DPhil candidate.

I deeply appreciate the valuable contribution of all the research collaborators, both at Oxford University and abroad, who have contributed to the results presented in this thesis. These include (but not limited to) Dr Paulus Wohflart and Dr Norbert Tennagels at Sanofi Aventis Deutschland gmbH and Dr Surawee Chuaipichai, Dr Eileen McNeill, Dr Gillian Douglas, Dr Ashely Hale from Prof Keith Channon's research group for their scientific input and feedback.

I am grateful to all the funding bodies that made this work possible, namely the British Heart Foundation, UK, Sanofi Aventis Deutschland GmbH and the Alexandros S Onassis Public Benefit Foundation, Greece.

I am immensely honoured to have been supervised by Prof Charalambos Antoniades and Prof Keith M Channon. Their interest on my work and their insightful input, mentorship and guidance have been continuous throughout my studies. They comprise life mentors for me and I hope I will maintain their acquaintance, both scientifically and personally, in the future.

Last but not least, I cannot emphasize strongly enough how grateful I am to my family, including my parents and grandparents, my uncles and aunt as well as my brother and cousin, for their companionship and support through it all. I owe everything to them.

Dedication

To my parents and grandparents for making me the person I am today.

To my brother and cousin for their companionship.

Abstract

Insulin resistance (IR) and dysfunctional adipose tissue (AT) secretome are believed to mediate the mechanistic links between metabolic and vascular disease. However, the mechanistic details of the interactions between vascular IR, AT-derived products and vascular disease phenotypes in humans are poorly understood. In the first part of my thesis, I attempted to characterise downstream vascular insulin signalling in patients with atherosclerosis and how this could be modified to regulate vascular insulin sensitivity. In the second part of this work, I explored the role of AT-derived Wnt5a (a novel, AT-secreted glycoprotein with inadequately characterised vascular roles) as a link between metabolic and vascular disease via direct regulation of vascular redox state and endothelial function. For these purposes, I used the Oxford cohort for Fat, Vessels and Fat (OxHVF), a uniquely phenotyped cohort of >1,000 patients undergoing cardiac surgery) to perform observational association studies and functional *ex vivo* bioassays on intact vascular tissues, which were also complemented by appropriate *in vitro* mechanistic experiments. I firstly demonstrated that vascular IR is a universal feature of human atherosclerosis irrespectively of the presence of systemic IR, characterised by disproportionally increased Erk1&2 activation as opposed to Akt activation in response to insulin. This can be reversed by pre-treatment with a dipeptidyl peptidase 4 (DD4) inhibitor, thus identifying vascular insulin-sensitising roles for this class of drugs. In the second part of my thesis, I revealed that systemic Wnt5a bioavailability is increased in obesity, diabetes and vascular disease, while Wnt5a (partially originating from AT) can induce vascular NADPH-oxidase activation via a novel USP17 interaction through paracrine and endocrine ways, also accompanied by endothelial dysfunction, eNOS uncoupling and redox-sensitive VSMC phenotype changes. My findings provide novel links between obesity, insulin resistance and vascular disease mechanisms and pose significant therapeutic implications.

List of publications and presentations during DPhil

Manuscripts contributing to DPhil thesis

Akoumianakis I *et al* (1). "Vascular insulin resistance in patients with cardiovascular disease reversed by DPP4 inhibition: Implications for insulin treatment in diabetes". In Revision, *Sci Transl Med.* 2019

Akoumianakis I *et al* (2). "Adipose tissue-derived Wnt5a as a trigger of vascular disease in obesity: The role of USP17/Rac1-mediated vascular redox signalling". Accepted. *Sci Transl Med.* 2019.

Akoumianakis I, Antoniades C. "Impaired Vascular Redox Signalling in the Vascular Complications of Obesity and Diabetes Mellitus". *Antioxid Redox Signal*. 2018. Doi: 10.1089/ars.2017.7421 [Epub ahead of print]

Akoumianakis I *et al*. "Exploring the Crosstalk between Adipose Tissue and the Cardiovascular System". *Korean Circ J*. 2017;47(5):670-685.

Akoumianakis I, Antoniades C. "Dipeptidyl peptidase IV inhibitors as novel regulators of vascular disease". *Vascul Pharmacol*. 2017;96-98:1-4.

Akoumianakis I, Antoniades C. "The interplay between adipose tissue and the cardiovascular system: is fat always bad?" *Cardiovasc Res*. 2017;113(9):999-1008.

Akoumianakis I *et al.* "Perivascular adipose tissue as a regulator of vascular disease pathogenesis: identifying novel therapeutic targets". *Br J Pharmacol*. 2017 Oct;174(20):3411-3424.

Other published manuscripts during DPhil

Rayner JJ, Abdesselam I, Peterzan MA, Akoumianakis I *et al.* "Very low calorie diets are associated with transient ventricular impairment before reversal of diastolic dysfunction in obesity". *Int J Obes (Lond)* 2018. doi: 10.1038/s41366-018-0263-2. [Epub ahead of print]

Antonopoulos AS, Sanna F, Sabharwal N, Thomas S, Oikonomou EK, Herdman L, Margaritis M, Shirodaria C, Kampoli AM, Akoumianakis I *et al.* "Detecting human coronary inflammation by imaging perivascular fat". *Sci Transl Med*. 2017;9(398).

Margaritis M, Sanna F, Lazaros G, Akoumianakis I *et al*. "Predictive value of telomere length on outcome following acute myocardial infarction: evidence for contrasting effects of vascular vs. blood oxidative stress". *Eur Heart J*. 2017;38(41):3094-3104.

Turnbull CD, Akoumianakis I *et al*. "Overnight urinary isoprostanes as a marker of oxidative stress in obstructive sleep apnoea". *Eur Respir J.* 2017;49(2).

Woodward L, Akoumianakis I (equal author contribution) *et al.* "Unravelling the adiponectin paradox: novel roles of adiponectin in the regulation of cardiovascular disease". *Br J Pharmacol*. 2017;174(22):4007-4020.

Akoumianakis I, Antoniades C. "Is stress response a new link between adipose tissue and atherogenesis? The role of HSPs/HSF1". *Cardiovasc Res.* 2016 Jul 1;111(1):10-2.

Antonopoulos AS, Margaritis M, Verheule S, Recalde A, Sanna F, Herdman L, Psarros C, Nasrallah H, Coutinho P, Akoumianakis I *et al.* "Mutual Regulation of Epicardial Adipose Tissue and Myocardial Redox State by PPAR-γ/Adiponectin Signalling". *Circ Res*. 2016;118(5):842-55.

Akoumianakis I, Antoniades C. "Studying Systemic Oxidative Stress in Heart Failure: Does It Have Any Role in Clinical Practice?" *Hellenic J Cardiol.* 2015;56(5):402-5.

Awards & distinctions during DPhil

August 2018: Akoumianakis I *et al*. *"Insulin triggers oxidative stress in the vascular wall of patients with atherosclerosis, independently of systemic insulin resistance: The beneficial role of DPP-IV inhibition"*. European Society Cardiology Congress 2018 (*young investigator award winner, coronary pathophysiology & microcirculation session).*

August 2018: Akoumianakis I *et al*. *"Perivascular adipose tissue-derived Wnt5a as a regulator of human vascular disease pathogenesis"*. European Society Cardiology Congress 2018 (*best basic science poster award*).

June 2018: Akoumianakis I *et al*. *"Insulin induces oxidative stress in the vascular wall of patients with atherosclerosis independently of systemic insulin resistance: the regulatory role of DPP4 inhibition".* British Cardiovascular Society Conference 2018 (*best poster runner-up*).

September 2017: Akoumianakis I *et al*. *"Insulin triggers oxidative stress in the vascular wall of patients with atherosclerosis independently of diabetes or systemic insulin resistance: the protective effect of DPP-IV inhibition"*. British Atherosclerosis Society Conference 2017 *(early career award).*

Conference abstracts and presentations during DPhil

August 2018: Akoumianakis I *et al*. *"Insulin triggers oxidative stress in the vascular wall of patients with atherosclerosis, independently of systemic insulin resistance: The beneficial role of DPP-IV inhibition"*. European Society Cardiology Congress 2018 (*young investigator award winner, coronary pathophysiology & microcirculation session).*

August 2018: Akoumianakis I *et al*. *"Perivascular adipose tissue-derived Wnt5a as a regulator of human vascular disease pathogenesis"*. European Society Cardiology Congress 2018 (*best basic science poster award*).

June 2018: Akoumianakis I *et al*. *"Insulin induces oxidative stress in the vascular wall of patients with atherosclerosis independently of systemic insulin resistance: the regulatory role of DPP4 inhibition".* British Cardiovascular Society Conference 2018 (*best poster runner-up*).

September 2017: Akoumianakis I *et al*. *"Insulin triggers oxidative stress in the vascular wall of patients with atherosclerosis independently of diabetes or systemic insulin resistance: the protective effect of DPP-IV inhibition"*. British Atherosclerosis Society Conference 2017 *(early career award).*

November 2016: Oikonomou EK, Odutayo A, Akoumianakis I *et al* "*Identifying biological predictors of early saphenous vein graft failure: A meta-analysis of 5,134 patients with*

angiographic follow up in SAFINOUS-CABG collaborative group" (oral presentation), American heart Association Scientific Sessions 2016

September 2016: Turnbull C, Akoumianakis I *et al*. "*Overnight urinary isoprostane levels during CPAP withdrawal as a marker of oxidative stress*" (poster presentation), European Respiratory Society Congress 2016

September 2016: Akoumianakis I *et al* "*Novel insights into the effects of insulin-like growth factor 1 and endothelin signalling on vascular redox state in patients with type 2 diabetes mellitus*" (poster presentation), European Association for the Study of Diabetes Annual Meetings 2016

August 2016: Akoumianakis I *et al*. "*Novel insights into the role of insulin-like growth factor 1 in the regulation of myocardial redox state in humans*" (oral presentation), European Society Cardiology Congress 2016

June 2016: Akoumianakis I *et al*. "*Novel insights into the effects of insulin-like growth factor 1 and endothelin signalling on vascular redox state in patients with type 2 diabetes mellitus*" (oral presentation), American Diabetes Association Scientific Sessions 2016

November 2015: Akoumianakis I *et al*. "*Effects of systemic insulin resistance on redox state and endothelial nitric oxide bioavailability in the human vascular wall*" (poster presentation), American Heart Association Scientific Sessions 2015

November 2015: Akoumianakis I *et al*. "*New roles of the interplay between endothelin and insulin-like growth factor 1 in the regulation of vascular redox state in patients with type 2 diabetes and coronary atherosclerosis*" (poster presentation), American Heart Association Scientific Sessions 2015

September 2015: Antonopoulos A, Margaritis M, Herdman L, Sanna F, Akoumianakis I *et al*. "*Exploring the obesity paradox in secondary prevention: a new biological role of femoral adipose tissue in humans*" (poster presentation), European Society Cardiology Congress 2015

September 2015: Margaritis M, Lazaros G, Patel S, Herdman L, Antonopoulos AS, Akoumianakis I *et al*. "*Telomere length predicts clinical outcomes postrevascularization procedures: its role as a novel biomarker of systemic oxidative stress and cardiovascular ageing*" (oral presentation), European Society Cardiology Congress 2015

Table of contents

LIST OF TABLES **15**

LIST OF FIGURES **16**

LIST OF ABBREVIATIONS **21**

CHAPTER 1 ..... **26**

INTRODUCTION 26

1.1. Atherosclerosis: a major cause of worldwide morbidity and mortality *26*

1.2. Obesity, insulin resistance and diabetes mellitus: global health burdens with vascular implications *28*

1.2.1. Obesity: link with vascular disease 28

1.2.2. Insulin resistance & diabetes mellitus: relationship with vascular disease 30

1.2.2.1. Types of diabetes mellitus and vascular complications 31

1.2.2.2.1. The polyol pathway 33

1.2.2.2.2. The hexosamine pathway 33

1.2.2.2.3. Formation of advanced glycation end-products 34

1.2.2.2.4. Protein kinase C signalling 35

1.2.2.2.5. Epigenetic mechanisms 35

..... *36*

1.3. Redox signalling as a regulator of vascular disease: mechanistic links with obesity, insulin resistance and diabetes mellitus *36*

1.3.1. Types of reactive oxygen species 37

..... 38

1.3.2. Enzymatic sources of vascular reactive oxygen species and their regulation 38

1.3.2.1. NADPH-oxidases 38

..... 39

1.3.2.1.1. NADPH-oxidases regulation in obesity, insulin resistance and diabetes mellitus 40

1.3.2.2. Uncoupled endothelial nitric oxide synthase....41
....44
1.3.2.2.1. Regulation of eNOS in obesity, insulin resistance and diabetes mellitus....44
1.3.2.3. Mitochondrial oxidases....45
1.3.2.3.1. Mitochondrial oxidase regulation in obesity, insulin resistance and diabetes mellitus....45
1.3.2.4. Xanthine oxidase....46
1.3.2.4.1. Regulation of xanthine oxidase in obesity, insulin resistance and diabetes mellitus....46
1.3.3. Endogenous antioxidant systems....47
1.4. Insulin: a universal metabolic regulator with vascular roles 49
1.4.1. Insulin biosynthesis and secretion....49
1.4.2. Insulin signalling....50
1.4.3. Mechanisms of molecular insulin resistance....51
1.4.4. Vascular effects of insulin: implications for insulin-based antidiabetic treatments....52
1.5. Adipose tissue: a dynamic endocrine organ.... 56
1.5.1. Regional variability of adipose tissue biology....59
1.5.1.1. Subcutaneous versus visceral adipose tissue....60
1.5.1.2. Perivascular adipose tissue....61
1.6. Wnt signalling as a novel link between metabolic and vascular disease 63
1.6.1. Wnt ligands: a diverse family of signalling molecules....64
1.6.1.1. Canonical Wnt signalling....66
1.6.1.2. Non-canonical Wnt signalling....67
1.6.2. Wnt signalling and metabolic disease....68
1.6.3. Vascular effects of Wnt signalling....69
1.6.4. Wnt5a: a key non-canonical Wnt ligand with cardiometabolic implications....70
1.7. Hypotheses and aims.... 73
CHAPTER 2 74
OVERVIEW OF THE STUDY DESIGN & METHODS.... 74
2.1. The Oxford cohort for heart, vessels and fat.... 74
2.1.1. Demographic characteristics, risk factor recording, in-hospital and long-term follow-up
....76
2.1.2 Sample collection....78
2.1.2.1. Blood sampling....78
2.1.2.2. Tissue collection & processing....78
2.2. Biomarker measurements.... 80
2.2.1. Enzyme-linked immunosorbent assay....80
....81

2.2.2. Medical laboratory measurements 81
2.3. Measurement of vascular superoxide production 82
2.3.1. Lucigenin-enhanced chemiluminescence 83
2.3.1.1. Quantification of vascular baseline superoxide readout 84
2.3.1.2. Quantification of vascular NADPH-stimulated superoxide readout 85
2.3.1.3. Quantification of vascular Vas2870-inhibitable superoxide readout 86
2.3.1.4. Quantification N(G)-Nitro-L-arginine methyl ester (L-NAME) delta superoxide readout 87
2.3.2. Dihydroethidium staining & confocal microscopy 88
2.4. Organ bath vasomotor studies with human vessels 89
2.5. Gene expression studies 93
2.5.1. RNA isolation & purification 93
2.5.2. Reverse transcription of RNA – cDNA library creation 94
2.5.3. Gene expression studies using quantitative PCR 94
2.6. Measurement of vascular biopterin content 97
..... 98
..... 99
..... 99
..... 99
2.7. Western immunoblotting in vascular tissue 99
2.8. Estimation of Rac1 & p47^{phox} membrane translocation in human vessels 101
2.9. Rac1 activation assay in human vessels 102
2.10. Statistical analysis 103
2.11. Personal contribution 104
CHAPTER 3 106
VASCULAR INSULIN RESISTANCE IN PATIENTS WITH ATHEROSCLEROSIS: IMPLICATIONS FOR INSULIN TREATMENT IN DIABETES 106
3.1. Introduction 107
3.2. Study population & methods 107
3.2.1. Study population 108
3.2.2. Methods 109
3.2.2.1. Ex vivo & in vitro incubations 109
3.2.2.2. Human umbilical vein endothelial cell culture 110
3.2.2.3. Mouse studies 110
3.2.2.4. Immunoprecipitation of IRS1 111
3.2.2.5. Statistical analysis 111
3.3. Results 112

3.3.1. Characterizing the effects of insulin on vascular redox state in humans with atherosclerosis 113
3.3.2. DPP4 inhibition restores "physiological" vascular redox response to insulin in human atherosclerosis 118
3.3.3. Exogenous insulin effects on eNOS in human vessels, which is modulated by DPP4 inhibition 121
3.3.4. Characterizing abnormal vascular insulin signalling in humans with vascular disease 124
3.3.5. Characterizing the insulin-sensitizing properties of DPP4 inhibition 125
..... 129
3.3.6. Clinical implications of the interaction between DPP4 and insulin 129
3.4. Discussion *130*
3.4.1. Beyond glycaemic control: the need to explore the vascular effects of insulin treatment 131
3.4.2. Vascular effects of insulin in humans with atherosclerosis and the concept of vascular insulin resistance 132
3.4.3. DPP4 inhibition as a means of vascular insulin sensitisation 134
3.5. Conclusion *135*

CHAPTER 4 137

ADIPOSE TISSUE-DERIVED WNT5A AS A TRIGGER OF VASCULAR DISEASE 137
4.1. Introduction *137*
4.2. Study population & methods *138*
4.2.1. Study population 138
4.2.1.1. In vivo clinical studies (study 1, 2 and 3) 138
4.2.1.2. Ex vivo studies with human vessels (Study 4) 139
4.2.2. Methods 139
4.2.2.1. Ex vivo & in vitro incubations 139
4.2.2.2. Human primary smooth muscle cell isolation and culture 140
4.2.2.3. Transfection studies with Fzd2 and Fzd5 siRNA 141
4.2.2.4. Transfection studies with UPS17 142
4.2.2.5. shRNA lentiviral particles transduction in immortalised pre-adipocytes 142
4.2.2.6. Wnt5a secretion assay 143
4.2.2.7. Co-culture of human primary VSMC with immortalised pre-adipocytes 143
4.2.2.8. Mouse studies 143
4.2.2.9. Coronary calcium score quantification 145
4.2.2.10. Statistical analysis 145
4.3. Results *146*
4.3.1. Wnt ligand expression profile in adipose tissue depots from patients with atherosclerosis 147

4.3.2. Interactions of Wnt5a with obesity, systemic insulin resistance and diabetes 148
4.3.3. Interactions between Wnt5a and vascular disease 150
4.3.4. Wnt5a as a link between vascular redox state and obesity 153
4.3.5. Effects of Wnt5a on vascular NADPH-oxidases activity 154
4.3.7. Vascular smooth muscle cell-specific effects of Wnt5a 159
4.3.7. Effects of Wnt5a on endothelial function and eNOS coupling 164
4.4. Discussion *166*
4.4.1. Links between Wnt5a signalling and metabolic disease in humans 167
4.4.2. Association of Wnt5a signalling with vascular biology and disease in humans 168
4.4.3. Novel interactions between Wnt5a signalling and arterial redox signalling in humans 169
4.5. Conclusion *172*

CHAPTER 5 174

STUDY LIMITATIONS 174
5.1. Lack of healthy control cohort for clinical associations *174*
5.2. Use of non-atherosclerotic vessels as models of human atherosclerosis *177*
5.3. Lack of control vascular tissue from healthy humans *178*

CHAPTER 6 179

DISCUSSION 179
6.1. The concept of vascular insulin resistance: novel perspectives *179*
6.1.1. Clinical implications 180
6.2. Wnt5a and vascular redox signalling: implications in humans *182*
6.2.1. Clinical implications 184
6.3. Novel aspects of the interplay between metabolic & vascular disease *186*
6.3.1. Vascular disease modifies responses to insulin: implications for treatment of diabetes 186
6.3.2. AT as a sensor of metabolic disease and vascular consequences: the example of Wnt5a 187
6.3.3. Metabolic & vascular disease are involved in a dynamic, bidirectional crosstalk 188
6.4. Future work *189*
6.4.1. Understanding vascular insulin resistance in humans 189
6.4.2. Exploring the spectrum of vascular Wnt5a signalling & consequences 190
6.4.3. The Oxford cohort for heart, vessels and fat: an ongoing target discovery project 191

REFERENCES 193

List of tables

Table 1.1: Summary of representative adipocytokines and their biological roles

Table 1.2: List of Wnt ligands in humans and their predominant signalling pathways

Table 1.3: List of main Wnt receptors

Table 2.1: List of TaqMan probes used in this thesis

Table 2.2: List of antibodies used for Western immunoblotting in this thesis

Table 3.1: Demographic characteristics of patients included in Chapter 3 studies

Table 4.1: Demographic characteristics of patients included in Chapter 4 studies

List of figures

Figure 1.1: Summary of interactions between metabolic & vascular disease

Figure 1.2: Sources and vascular effects of reactive oxygen species (ROS)

Figure 1.3: Overview of NADPH-oxidase isoforms

Figure 1.4: Overview of endothelial nitric oxide synthase (eNOS) structure and regulation

Figure 1.5: Major endogenous antioxidant enzymes

Figure 1.6: Vascular insulin signalling and molecular targets of insulin resistance (IR)

Figure 1.7: Routes of adipose tissue (AT) signalling

Figure 1.8: Canonical Wnt signalling pathway

Figure 1.9: Non-canonical Wnt signalling pathways

Figure 2.1: Overview of the AdipoRedOx study workflow

Figure 2.2: Example internal mammary artery pedicle

Figure 2.3: Example isolated internal mammary artery

Figure 2.4: Processed, opened internal mammary artery rings

Figure 2.5: Example adipose tissue sample

Figure 2.6: Representative standard curves for the ELISA kits used

Figure 2.7: Representative basal superoxide ($O_2^{\cdot-}$) trace

Figure 2.8: Representative NADPH-stimulated superoxide ($O_2^{\cdot-}$) trace

Figure 2.9: Representative Vas2870-inhibitable superoxide ($O_2^{\cdot-}$) trace

Figure 2.10: NADPH-stimulated and Vas2870-inhibitable superoxide ($O_2^{\cdot-}$) correlation

Figure 2.11: Representative L-NAME delta superoxide ($O_2^{\cdot-}$) trace

Figure 2.12: Organ bath Radnotti instrument used for *ex vivo* vasomotor studies

Figure 2.13: Example phenylephrine (PE) dose-response curve

Figure 2.14: Example acetylcholine (Ach) dose-response curve

Figure 2.15: Example sodium nitroprusside (SNP) dose-response curve

Figure 2.16: KingFisher flex magnetic particle processor

Figure 2.17: QuantStudio7 quantitative real-time PCR instrument

Figure 2.18: Tetrahydrobiopterin (BH4) example peak

Figure 2.19: Dihydropterin (BH2) and biopterin (B) example peaks

Figure 3.1: Serum insulin and nitric oxide (NO) bioavailability in humans with coronary atherosclerosis

Figure 3.2: Insulin impairs endothelial function in patients with coronary atherosclerosis

Figure 3.3: Serum insulin is associated with increased vascular oxidative stress and vascular NADPH-oxidases activity in non-diabetic patients with coronary atherosclerosis

Figure 3.4: Exogenous insulin directly increases NADPH-oxidases activity in saphenous vein (SV) segments from patients with coronary atherosclerosis

Figure 3.5: Exogenous insulin increases NADPH-oxidase activity in internal mammary artery (IMA) segments from patients with coronary atherosclerosis, but not in healthy mouse aortae

Figure 3.6: *In situ* visualisation of arterial superoxide ($O_2^{\cdot-}$) in response to insulin treatment

Figure 3.7: Exogenous insulin reduces vascular NADPH-oxidases activity in patients with coronary atherosclerosis on an oral DPP4 inhibitor (DPP4-i)

Figure 3.8: DPP4 inhibition reverses vascular redox responses to insulin in patients with coronary atherosclerosis

Figure 3.9: DPP4 inhibition reverses vascular redox responses to insulin in patients with coronary atherosclerosis

Figure 3.10: The effect of insulin on NADPH-oxidases is mediated by Rac1 activation followed by Rac1/p47phox membrane translocation and regulated by DPP4 inhibition

Figure 3.11: Effects of insulin on endothelial nitric oxide synthase (eNOS) coupling and phosphorylation

Figure 3.12: Insulin reduces tetrahydropterin (BH4) bioavailability, an effect reversed by DDP4 inhibition (DPP4-i)

Figure 3.13: Insulin improves endothelial function *ex vivo* in the presence of DPP4 inhibition (DPP4-i)

Figure 3.14: Downstream insulin signalling in patients with atherosclerosis

Figure 3.15: DPP4 inhibition regulates downstream insulin signalling in human vessels

Figure 3.16: Downstream insulin signalling axes directly regulates vascular redox responses to insulin

Figure 3.17: DPP4 inhibition (DPP4-i) rescues molecular insulin sensitivity via AMP-activated kinase (AMPK)

Figure 3.18: Clinical implications of the interactions between systemic dipeptidyl peptidase 4 (DPP4) activity and insulin levels

Figure 3.19: Summary of vascular insulin signalling regulation

Figure 4.1: Wnt ligand expression profile in human adipose tissue (AT)

Figure 4.2: Plasma Wnt5a bioavailability and metabolic disease

Figure 4.3: Adipose tissue (AT) expression of Wnt5a & Sfrp5 and metabolic disease

Figure 4.4: Perivascular adipose tissue (PVAT) as a local source of Wnt5a in obesity

Figure 4.5: Arterial Wnt receptor expression and metabolic disease

Figure 4.6: Plasma Wnt5a bioavailability is associated with coronary artery disease (CAD)

Figure 4.7: Wnt5a as a link between obesity and arterial redox state

Figure 4.8: Wnt5a directly induces NADPH-oxidases activation in human arteries

Figure 4.9: Phenotyping of Wnt5a-overexpressing TetO mice

Figure 4.10: *In vivo* Wnt5a overexpression stimulates arterial NADPH-oxidase activity in mice

Figure 4.11: Wnt5a induces arterial activation of Rac1 and Nox subunit membrane translocation via non-canonical signalling

Figure 4.12: Rac1 activation mediates the effect of Wnt5a on arterial NADPH-oxidases activity

Figure 4.13: Physiological Wnt5a concentrations selectively activate non-canonical Wnt signalling

Figure 4.14: Wnt5a induces activation of the planar cell polarity (PCP) pathway in human primary vascular smooth muscle cells (VSMCs)

Figure 4.15: Wnt5a increases oxidative stress and NADPH-oxidases activity in human primary vascular smooth muscle cells (VSMCs)

Figure 4.16: Paracrine effect of human primary adipocyte-derived Wnt5a on NADPH-oxidases activity in neighbouring human primary vascular smooth muscle cells (VSMCs)

Figure 4.17: The pro-oxidant effects of Wnt5a in human vascular smooth muscle cells (VSMCs) are mediated by Frizzled 2 (Fzd2) and Frizzled 5 (Fzd5) receptors

Figure 4.18: Wnt5a increases USP17 expression in a redox-sensitive manner in human vascular smooth muscle cells (VSMCs)

Figure 4.19: USP17 transfection in HeLa cells

Figure 4.20: USP17 mediates the long-term effect of Wnt5a on Rac1 activation

Figure 4.21: Wnt5a induces uncoupling of endothelial nitric oxide synthase (eNOS) via tetrahydrobiopterin (BH4) oxidation

Figure 4.22: Wnt5a induces endothelial dysfunction in human vessels *ex vivo*

Figure 4.23: Summary of the effects of Wnt5a on arterial redox state

List of abbreviations

In alphabetical order

Ach: Acetylcholine

ADRF: Adventitium-derived relaxing factor

AGE: Advanced glycation-end-product

AMPK: Adenosine monophosphate-activated kinase

APC: Adenomatous polyposis coli

AT: Adipose tissue

BAT: Brown adipose tissue

BH2: Dihydrobiopterin

BH4: Tetrahydrobiopterin

Bk: Bradykinin

BMI: Body mass index

CamKII: Calmodulin-activated kinase II

CCS: Coronary calcium score

CK1: Casein kinase 1

CVD: Cardiovascular disease

DHE: Dihydroethidium

DM: Diabetes mellitus

DPP4: Dipeptidyl peptidase 4

DPP4-i: Dipeptidyl peptidase 4 inhibitor

eNOS: Endothelial nitric oxide synthase

EpAT: Epicardial adipose tissue

Erk: Extracellular signal-regulate kinase

ET-1: Endothelin 1

FDG: ^{18}F-fluorodeoxyglucose

FFA: Free fatty acid

FMD: Flow mediated dilation

GCK: Glucokinase

GLP1: Glucagon-like peptide 1

GPX: Glutathione peroxidase

GSK3β: Glucogen synthase kinase 3β

Hb1Ac: Haemoglobin 1Ac

4-HNE: 4-hydroxynonenal

HNF: Hepatic nuclear factor

HOMA-IR: Homeostatic model assessment – insulin resistance

HSP90: heat shock protein 90

IL-6: Interleukin 6

IMA: Internal mammary artery

IR: Insulin resistance

JNK: c-Jun N-terminal kinase

KATP: ATP-regulated potassium channel

KHB: Krebs-HEPES buffer

LADA: Latent autoimmune diabetes of adults

LEF: Lymphoid enhancer-binding factor

L-NAME: N(ω)-nitro-L-arginine methyl ester

LRP: Lipoprotein-related protein

MAPK: Mitogen-activated protein kinase

miR: Micro-RNA

MODY: Maturity-onset diabetes of the young

NAD+: Nicotinamide adenine dinucleotide

NADH: Nicotinamide adenine dinucleotide, reduced

NADPH: Nicotinamide adenine dinucleotide phosphate, reduced

NFAT: Nuclear factor of activated T-cells

NF-kB: Nuclear factor kappa beta

NO: Nitric oxide

oxLDL: Oxidised low density lipoprotein

PAME: Palmitic acid methyl ester

PCP: Planar cell polarity (pathway)

PE: Phenylephrine

PET: Positron emission tomography

PI3K: Phosphoinositide-3 kinase

PKA: Protein kinase A

PKC: Protein kinase C

PON: Paraoxonase

PVAT: Perivascular adipose tissue

RAA: Right atrium appendage

RAGE: receptor of advanced glycation end-products

ROS: Reactive oxygen species

ScAT: Subcutaneous adipose tissue

Sfrp: Secreted frizzled-like protein

SNP: Sodium nitroprusside

SOD: Superoxide dismutase

SV: Saphenous vein

T2DM: Type 2 diabetes mellitus

TCF: T-cell factor

TG: Triglycerides

TNFα: Tumour necrosis factor alpha

VAT: Visceral adipose tissue

VSMC: Vascular smooth muscle cell

WAT: White adipose tissue

Wnt5a: Wingless/integrated protein 5a

XO: Xanthine oxidase

Chapter 1

Introduction

This chapter discusses the association of atherosclerosis with dysregulated metabolic states such as obesity, insulin resistance (IR) and diabetes mellitus (DM) as well as how vascular redox signalling may comprise a mechanistic link between these disease entities. It also describes the current knowledge regarding local insulin signalling in the vasculature and the vascular consequences of anti-diabetic medications such as insulin and dipeptidyl peptidase 4 (DPP4) inhibitors (DPP4-i) in diabetic patients. Furthermore, this chapter discusses the divergent roles of different adipose tissue depots in cardiometabolic disease and the properties of Wingless/Integrated protein 5a (Wnt5a), a novel secreted glycoprotein which may be a mechanistic link between obesity, IR and vascular complications.

1.1. Atherosclerosis: a major cause of worldwide morbidity and mortality

Atherosclerosis is characterised by arterial lumen narrowing due to formation of atheromatous plaque build-up, comprising the most common cause of cardiovascular disease (CVD) and resulting in a variety of ischaemic complications following vascular stenosis/thrombosis/occlusion (Hansson, 2005). Despite impressive advances in primary and secondary prevention, atherosclerosis remains a global health burden affecting a massive amount of people and accounting for a significant percentage of overall mortality and morbidity in a worldwide scale (Herrington *et al.*, 2016). Atherosclerosis-related death rates have decreased during recent years in high-income countries, however disease burden and its resulting morbidities remain disappointingly high (Herrington *et al.*, 2016). Furthermore, mortality rates due to atherosclerosis are actually increasing in some low- and mid-income countries (especially in Eastern Europe and Asia) (Herrington *et al.*, 2016). According to the British Heart Foundation 2018 statistics, atherosclerotic disease accounted for 19% of deaths in men and 16% of deaths in women in the United Kingdom in 2016, or ~113,000 deaths in total, and inflicting significant morbidity in more than 650,000 people. These considerations highlight the continuous need for better understanding of the underlying mechanisms of atherosclerosis and discovery of more effective therapeutic interventions to reduce the adverse consequences of this world reaching disease entity.

Atherosclerosis is a multifactorial disease resulting from a complex interplay of genetic susceptibility parameters, demographic risk factors (such as smoking, obesity, hyperlipidaemia and hyperglycaemia) and pathogenic pro-inflammatory and pro-oxidative mechanisms (Weber and Noels, 2011). Recent advances have drastically increased our understanding about the pathogenesis of atherosclerosis and have introduced novel therapeutic options and technologies to more efficiently treat and stratify patients with atherosclerosis (Weber and Noels, 2011; Dadu and Ballantyne, 2014; Antonopoulos *et al.*, 2017). Still, the previously mentioned statistics highlight that clinical residual risk in atherosclerosis remains significantly high in

spite of recent advances, and suggest the presence of unanswered questions regarding the biology of atherosclerosis. Such questions include the mechanistic interactions between vascular and metabolic disease (including obesity, IR and DM) and the spectrum of roles of vascular redox signalling in these interactions.

1.2. Obesity, insulin resistance and diabetes mellitus: global health burdens with vascular implications

Obesity and DM comprise metabolic pandemics with exceedingly high prevalence in adults (Centre for Disease Control, Prevention and others, 2017; Hales *et al.*, 2018). According to the World Health Organisation (WHO), almost 650 million people were obese in 2016, while well over 400 million people suffer from DM. These entities are characterized by overlapping systemic biochemical and biological abnormalities such as hyperlipidaemia, hyperglycaemia, IR, and inflammation (Kaur, 2014). Obesity, in particular, is characterized by increased body fat mass and, perhaps more importantly, by dysregulated body fat distribution (Akoumianakis and Antoniades, 2017b). DM, on the other hand, can be classified into many subtypes with differing pathophysiology, hyperglycaemia always being the ultimate common result (Beckman and Creager, 2016). All of the aforementioned metabolic abnormalities are able to induce profound changes in vascular cell phenotype with regards to various biological processes such inflammatory activation, haemostasis dysregulation, proliferation and migration capacity, and oxidative stress (Rask-Madsen and King, 2013), leading to vascular complications (Figure 1.1).

1.2.1. Obesity: link with vascular disease

Various studies have linked obesity, especially central obesity defined by an increased waist-to-hip ratio, with CVD progression (Antonopoulos *et al.*, 2016). Several underlying

mechanisms are believed to contribute to this association, mainly related with elements of adipose tissue (AT) biology which are dysregulated in obesity (Antonopoulos *et al.*, 2016).

AT inflammation, a hallmark of central obesity, may be a key underlying mechanistic factor behind the association of obesity with CVD (Wellen and Hotamisligil, 2003). Inflamed AT secretes high levels of pro-inflammatory molecules such as resistin, tumour necrosis factor alpha (TNFα), and interleukin 6 (IL-6), which may propagate obesity-related vascular disease via induction of a systemic pro-inflammatory environment (Gu and Xu, 2013).

Consistently, obesity has been associated with increased markers of systemic oxidative stress, namely oxidized low-density lipoprotein (oxLDL) levels and urinary F2- isoprostanes (Savini *et al.*, 2013), as well as with nutrient overload and free fatty acid (FFA) overproduction, all of which can directly influence vascular biology (Matsuda and Shimomura, 2013). Importantly, growing evidence suggests that ‘‘dysfunctional adipocytes’’ exhibit dramatically altered secretome including microRNA-containing micro-vesicles and adipokines (hormones of adipose origin) beyond inflammatory cytokines (Akoumianakis and Antoniades, 2017b), thus leading to profound changes in the endocrine cardiovascular effects of ‘‘dysfunctional’’ AT.

Central obesity is often observed in the context of the metabolic syndrome, a pathophysiological entity characterised by systemic low-grade inflammation, dyslipidaemia, nutrient overload, AT inflammation, IR, hypertension, hyper-coagulant state, and endothelial dysfunction (Kaur, 2014). The metabolic syndrome comprises an important public health problem and it is associated with both microvascular and macrovascular complications (Figure 1.1.) (Kaur, 2014). Several studies have linked the metabolic syndrome and its individual risk factors with CVD, however the specific details of how these concurrent risk factors collude to influence vascular biology are unknown (Tune *et al.*, 2017).

Interestingly, metabolically healthy obese individuals (defined by the absence of metabolic syndrome) may have no increased risk for CVD, although this requires further support by large clinical trials (Eckel *et al.*, 2015). This suggests that obesity is a heterogeneous entity, the direct vascular effects of which are not easy to separate from the concomitant effects of co-existing risk factors in clinical studies. Furthermore, it has now become evident that the regional quality of AT may be much more important than overall AT mass (Akoumianakis and Antoniades, 2017b), as discussed in subsequent sections focusing on the regionally variable crosstalk between AT and the vascular wall. As such, it becomes evident that better understanding is required as to the biological mechanisms that drive the association between obesity and CVD.

1.2.2. Insulin resistance & diabetes mellitus: relationship with vascular disease

DM is an established risk factor for vascular complications via a variety of pathogenic mechanisms (Figure 1.1) (Bhupathiraju and Hu, 2016). Importantly, circulating glucose levels and glycosylated haemoglobin (HbA1c) are regarded as crucial surrogate markers of DM severity, and their regulation has long been the primary goal for the management of the cardiovascular consequences of DM (Lipska and Krumholz, 2017). Conversely, it has recently been revealed that targeting glycaemic control alone is not sufficient to reverse cardiovascular complications in diabetic patients (Green *et al.*, 2015; Marso *et al.*, 2016; Scirica *et al.*, 2013). This suggests that local vascular pathogenic mechanisms must be considered beyond global glycaemic control. In addition, different anti-diabetic medications have widely variable effects on CVD risk (Marso *et al.*, 2016; Scirica *et al.*, 2013; Gerstein *et al.*, 2012; Marso *et al.*, 2017), stressing the need to better understand the ‘‘pleiotropic’’ or ‘‘hypoglycaemia-independent’’ effects of antidiabetic medications used in clinical practice for the management of diabetic patients.

1.2.2.1. Types of diabetes mellitus and vascular complications

The majority of DM cases can be classified as either type 1 or type 2 (Schalkwijk and Stehouwer, 2005). Other, rarer, types of DM have also been described based on specific aetiologies. These include genetic defects in pancreatic β cell function (maturity onset diabetes of the young, or MODY), genetic defects in insulin function (e.g., in the context of lipoatrophy), exocrine pancreatic pathologies, various endocrinopathies, and certain drugs or infections (American Diabetes Association, 2009). Depending on their underlying aetiology, different types of DM have differing risk for vascular complications, suggesting that, although the fundamental cellular mechanisms of diabetic vascular injury may be similar, the varying extent of peripheral IR and hyperglycaemia differentially contribute to cardiovascular risk in different DM types (American Diabetes Association, 2009; Gaya, 2011).

Type 1 DM is an autoimmune disease characterized by primary pancreatic insufficiency and complete loss of insulin secretion (Katsarou *et al.*, 2017). On the contrary, type 2 DM (T2DM) is primarily characterized by peripheral IR, which is often associated with hyperinsulinemia in the early stages of the disease prior to pancreatic failure (American Diabetes Association, 2009). T2DM often appears as part of the metabolic syndrome (Schalkwijk and Stehouwer, 2005). Both types of DM are associated with vascular complications, reflecting the fact that hyperglycaemia, the ultimate result of both DM types, has direct detrimental effects on the vasculature (Brownlee, 2001, 2005). In the case of T2DM, other factors such as obesity, hyperlipidaemia, and abnormal insulin signalling may further contribute to vascular disease (Brownlee, 2001, 2005).

Several forms of non-type 1 DM are also associated with partial or complete insulin deficiency, including permanent neonatal diabetes mellitus (PNDM) and latent autoimmune diabetes in adults (LADA) (Stenstrom *et al.*, 2005; Polak and Cavé, 2007). The underlying mechanisms involve slow β cell degeneration or gene mutations of ATP-regulated potassium

(KATP) channels involved in insulin secretion (Stenstrom *et al.*, 2005; Naylor *et al.*, 2011). The clinical similarities of these entities with type 1 DM are reflected by similar prevalence and pathophysiology of vascular complications as a consequence of hyperglycaemia-induced vascular injury (Polak and Cavé, 2007; Laugesen, Østergaard and Leslie, 2015).

MODY is a genetic, monogenic form of, usually not insulin-dependent, DM appearing in young adults below 25 years old (McDonald and Ellard, 2013). Mutations of the glucokinase (GCK) and the hepatocyte nuclear factors 1 and 4 alpha (HNF1A, HNF4A) gene account for approximately 80% of all MODY cases (McDonald and Ellard, 2013). MODY phenotypes display significant variability with regards to vascular complications, with HNF1A/4A-MODY being particularly associated with severe hyperglycaemia and high rates of macro- and microvascular complications (Gaya, 2011). Such discrepancies may rise from the variable levels of hypoglycaemia as from potential direct vascular effects of different MODY types.

Gestational diabetes is a syndrome often described in women during pregnancy, and it is associated with increased risk of future T2DM development even if it is temporarily reversed during or after pregnancy (Spaight *et al.*, 2016). Gestational diabetes shares similar risk factors with T2DM, however not all women with gestational diabetes will develop T2DM (Kampmann, 2015; Spaight *et al.*, 2016). Importantly, even in the absence of T2DM development, women with history of gestational diabetes may have increased risk for adverse cardiovascular events (Shah, Retnakaran and Booth, 2008; Rydén *et al.*, 2013). The mechanistic basis of this clinical observation is not fully elucidated and could reflect the cumulative adverse effects of metabolic syndrome associated risk factors (even in the absence of clinically evident T2DM).

1.2.2.2. Established mechanisms of diabetic vascular injury

Hyperglycaemia induces a number of cellular disturbances that propagate diabetic complications (Brownlee, 2005), including increased activation of the polyol and hexosamine pathways, increased formation of advanced glycation end-products (AGE), stimulation of protein kinase C (PKC) activity and induction of mitochondrial oxidative stress, which are collectively believed to influence vascular function (Fig. 1.1) (Brownlee, 2001, 2005).

1.2.2.2.1. The polyol pathway

The polyol pathway reduces aldehydes to alcohols under physiological conditions, while aldose reductase, the first enzyme of the polyol pathway, also has low affinity for glucose (Brownlee, 2001). In the context of hyperglycaemia, intracellular glucose levels are increased and partially converted to sorbitol and finally fructose via the polyol pathway with concomitant reduction of NADPH (Brownlee, 2005). These may adversely affect cellular function via sorbitol-mediated osmotic dysregulation, reduced Na+-K+ ATPase activity, disruption of physiological nicotinamide adenine dinucleotide (NADH)/NAD+ balance and reduction of cytosolic NADPH (Brownlee, 2005). Notably, NADH is crucial for maintenance of the intracellular bioavailability of glutathione, an important endogenous antioxidant (18), while changes in NADPH/NAD+ balance may result in oxidative stress and detrimental oxidative modification of DNA, lipids and proteins (Yan *et al.*, 2016). The polyol pathway is an ubiquitous biochemical pathway variably active in a variety of cell types, and its relevance to diabetic complications has been demonstrated in a variety of tissues and cell types ranging from neurons (Brownlee, 2005) to retinal cells (Lorenzi, 2007) and importantly vascular cells, i.e., both vascular smooth muscle (Ramana *et al.*, 2003) and endothelial cells (Oyama *et al.*, 2006).

1.2.2.2.2. The hexosamine pathway

The hexosamine pathway is a minor branch of glycolysis, using a small fraction of total glucose influx to produce hexosamines such as UDP-N-acetylglucosamine (UDP-GlcNAc), UDP-N-acetylgalactosamine (UDP-GalNAc) and CMP-syalic acid, which are important structural subunits of glucosyl modified molecules (e.g., glycoproteins, glycolipids, proteoglycans and gangliosides) (Buse, 2006). UDP-GlcNAc is the major end product of the pathway and a substrate for O-GlcNAc transferase (OGT). This enzyme catalyses the transfer of GlcNAc to serine and threonine protein residues, thus propagating downstream cellular signalling cascades (Buse, 2006). Hyperglycaemia-induced excess production of UDP-GlcNAc and subsequent O-GlcNAc modification of key proteins including insulin response substrate 1 (IRS1) (Buse, 2006; Semba *et al.*, 2014) and Akt (Very *et al.*, 2018) are believed to comprise the basis of hexosamine pathway-related diabetic complications (Buse, 2006; Hart *et al.*, 2011) as displayed in a variety of *in vivo* animal and cell culture models (Buse, 2006; Issad, Masson and Pagesy, 2010). Importantly, O-GlcNAc appears to be switched from a nutrient sensor and physiological compensatory mechanism to a causal contributor of CVD phenotypes such as heart failure and endothelial function in *in vitro* and *in vivo* animal models (Dassanayaka and Jones, 2014), providing a direct underlying link between diabetes and cardiovascular complications.

1.2.2.2.3. Formation of advanced glycation end-products

AGE, the end-products of non-enzymatic lipid and protein glycosylation (Vlassara and Uribarri, 2014), are increased not only in DM but also in obesity and hyperlipidaemia as well as with old age (Goldin *et al.*, 2006). AGE-induced cellular injury results from direct chemical macromolecule modification as well as through receptor-mediated signalling via the receptors for advanced glycation end-products (RAGE) (Brownlee, 2005; Goldin *et al.*, 2006). RAGE signalling regulates processes such as growth, inflammation, and reactive oxygen species (ROS) production in endothelial cells and vascular smooth muscle cells (VSMCs) as well as in

stromal macrophages (Brownlee, 2001; Goldin *et al.*, 2006). Potential clinical relevance of AGE-mediated pathogenic mechanisms has been supported by clinical trials with AGE inhibitors with focus on renal diabetic complications, but more studies regarding diabetic vascular complications are still needed.

1.2.2.2.4. Protein kinase C signalling

PKC is a multi-isoform enzyme activated by diacylglycerol, a molecule that is increased intracellularly in response to hyperglycaemia (Das Evcimen and King, 2007). PKC has been implicated in the regulation of inflammation, proliferation, apoptosis, and ROS generation in a variety of cell types including VSMCs and endothelial cells, ultimately influencing vascular oxidative stress, nitric oxide (NO) bioavailability, vascular permeability and intima thickening (Minami *et al.*, 2003; Jones *et al.*, 2004; Das Evcimen and King, 2007). PKCβ and PKCδ, in particular, have been consistently linked with DM and obesity (Mochly-Rosen, Das and Grimes, 2012), thus contributing to diabetic complications via the aforementioned multitude of effects.

1.2.2.2.5. Epigenetic mechanisms

Hyperglycaemia has been associated with distinct epigenetic changes that persist even after reversal of hyperglycaemia, and this mechanism has been adversely associated with vascular biology (Guzik and Cosentino, 2017). p66Shc, a redox sensor that regulates mitochondrial oxidative stress and promotes redox signalling, is a well-studied example of such epigenetic hyperglycaemia-induced regulation (Paneni *et al.*, 2012), which is believed to contribute to redox signalling and further redox-mediated epigenetic changes via pathways such as that of nuclear factor kappa beta (NF-kB) (Guzik and Cosentino, 2017).

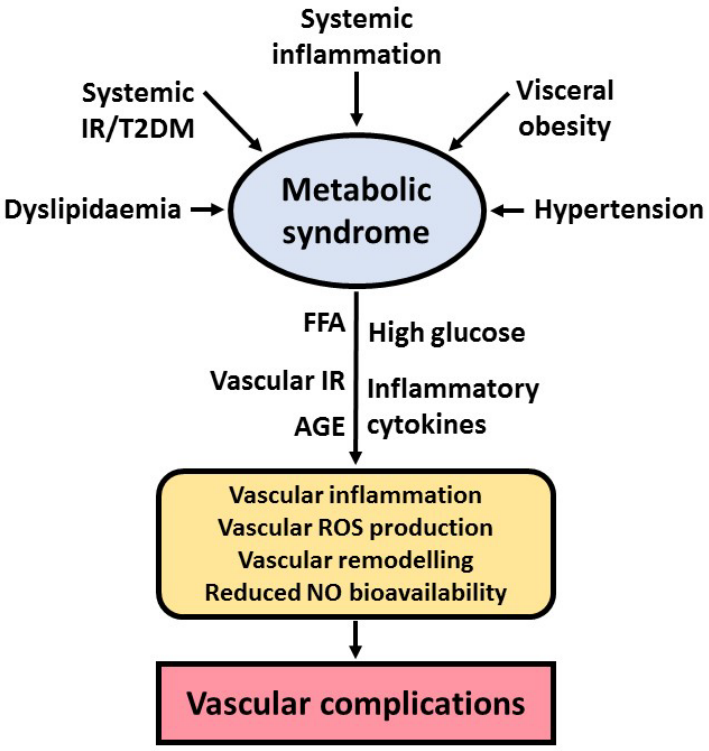

Figure 1.1: Summary of interactions between metabolic & vascular disease. The metabolic syndrome is characterised by systemic inflammation, metabolic disturbances such as dyslipidaemia, visceral obesity, insulin resistance (IR) and type 2 diabetes mellitus (T2DM) as well as cardiovascular abnormalities such as hypertension. These are associated with increased risk of vascular complications via a variety of pathogenic factors such as hyperglycaemia, inflammatory cytokines, increased levels of free fatty acids (FFA) and advanced glycation end-products (AGE), as well as the presence of vascular IR. These mechanisms ultimately regulate vascular phenotypes such as inflammation, reactive oxygen species (ROS) generation, vascular remodelling and nitric oxide (NO) bioavailability. *Adapted by I Akoumianakis et al, Antioxid Redox Sign 2018, doi: 10.1089/ars.2017.7421*

1.3. Redox signalling as a regulator of vascular disease: mechanistic links with obesity, insulin resistance and diabetes mellitus

Low levels of intracellular ROS are required for homeostasis maintenance (Bartosz, 2009). On the other hand, cellular oxidative stress characterised by increased production of ROS, has been associated with a variety of detrimental cellular phenotypes resulting from both direct oxidative damage and more complex redox signalling pathways (Figure 1.2) (Bartosz, 2009; Mittal *et al.*, 2014). ROS production originates from a variety of endogenous enzymatic

systems and it is regulated by endogenous antioxidant mechanisms (Mittal *et al.*, 2014). Dysregulation of this balance has been linked with vascular disease, obesity, IR and DM (Dandona, Aljada and Bandyopadhyay, 2004).

1.3.1. Types of reactive oxygen species

ROS classically refers to any partially reduced molecule or ion containing one or more unpaired electrons, thus having strong oxidising properties (Bartosz, 2009; Mittal *et al.*, 2014), including superoxide anion ($O_2^{\cdot-}$), hydrogen peroxide (H_2O_2), hydroxyl radical ($OH^{\cdot}$) and hypochlorous acid (HOCl) (Thannickal and Fanburg, 2000). ROS are generated as by-products of cellular metabolism via various metabolic pathways, predominantly via mitochondrial oxidases of the electron transport chain but also by cytochrome P450 (Mittal *et al.*, 2014). In addition, significant amounts of ROS can be produced by NADPH-oxidases, enzymes dedicated to ROS production which are under complex pathophysiological regulation (Konior *et al.*, 2014; Mittal *et al.*, 2014). In addition, uncoupled endothelial nitric oxide synthase (eNOS) and xanthine oxidase (XO) can act as sources of ROS under certain circumstances (Li, Horke and Förstermann, 2014; Mittal *et al.*, 2014), as explained in following sections.

$O_2^{\cdot-}$, resulting from one-electron molecular oxygen (O_2) reduction, is the predominant ROS produced by NADPH-oxidases as well as by xanthine oxidase, mitochondrial oxidases and uncoupled eNOS (Li and Förstermann, 2013; Mittal *et al.*, 2014). It is highly reactive with extremely short half-life and the ability to induce rapid macromolecule modifications (Valko *et al.*, 2007; Afanas'ev, 2015). In addition, it can be (spontaneously as well as enzymatically) converted to H_2O_2 (Mittal *et al.*, 2014), a more stable ROS with longer-lasting downstream signalling roles (Veal, Day and Morgan, 2007). H_2O_2 may be neutralised by being converted to water and O_2, or may be used to synthesise $OH^{\cdot}$ in the presence of metal iron ion (Fe^{2+}) (Mittal *et al.*, 2014). In addition, $O_2^{\cdot-}$ can further react with nitric oxide (NO) to form

peroxynitrite ($ONOO^-$), a ROS itself (Pacher, Beckman and Liaudet, 2007). Finally, $O_2^{\cdot-}$ can oxidise a variety of lipids, and the resulting peroxidation products (such as malondialdehyde and 4-hydroxynonenal (4-HNE)) may have novel signalling properties, as shown recently in human models of atherosclerosis (Margaritis *et al.*, 2013; Antonopoulos *et al.*, 2015). These types of ROS thus comprise a dynamic, interconnected and interchangeable network that is extremely difficult to decipher (Fig. 1.2).

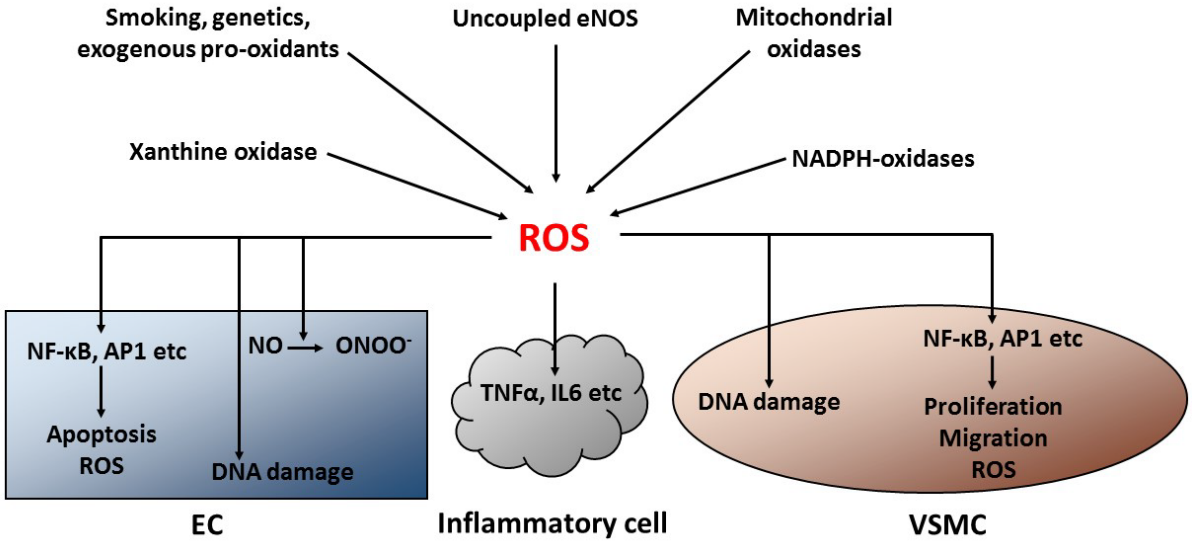

Figure 1.2: Sources and vascular effects of reactive oxygen species (ROS). ROS are synthesised by enzymes such as NADPH-oxidases, mitochondrial oxidases, xanthine oxidase and uncoupled endothelial nitric oxide synthase (eNOS) and further stimulated by genetic and environmental pre-oxidant factors. ROS have detrimental effects on the endothelial cells (ECs), vascular smooth muscle cells (VSMCs) and infiltrating inflammatory cells of the vascular wall. These include direct oxidative DNA damage, oxidation of nitric oxide (NO) to peroxynitrite ($ONOO^-$) and induction of inflammatory signalling by upregulating tumour necrosis α (TNFα), interleukin 6 (IL6), nuclear factor κ beta (NFκB) and activator protein 1 (AP1) signalling. This reinforces local ROS production and induces EC apoptosis while regulating VSMC migration and proliferation. *Adapted by I Akoumianakis et al, Antioxid Redox Sign 2018, doi: 10.1089/ars.2017.7421*

1.3.2. Enzymatic sources of vascular reactive oxygen species and their regulation

1.3.2.1. NADPH-oxidases

NADPH-oxidases, or Nox enzymes, are dedicated to the production of $O_2^{\cdot-}$, and they comprise a major source of ROS in the vascular wall (Konior *et al.*, 2014). Seven NADPH-oxidase isoforms have been described to date (Figure 1.3), namely Nox1–5 and dual oxidase

Duox proteins 1–2 (Duox1-2), which are expressed in vascular cells amongst other cell types (Panday *et al.*, 2015). Nox2 and Nox4 are reportedly major NADPH-oxidase isoforms found in endothelial cells, whereas VSMCs are believed to mainly express Nox4 and Nox1 (Guzik *et al.*, 2004). However, this may be variable depending on the vascular bed and endothelial cell or VSMC subtypes.

NADPH-oxidases are multi-subunit membrane enzymes (Fig. 1.3) (Bedard and Krause, 2007). gp91^{phox} is the catalytic subunit of Nox2, the prototype NADPH-oxidase which was described first in macrophages, while p22phox comprises the catalytic subunit of the other Nox isoforms (Panday *et al.*, 2015). The activity of these catalytic subunits is regulated by several cytosolic proteins that are able to translocate to the membrane upon a variety of stimuli to form the active NADPH-oxidases complex (Konior *et al.*, 2014). Nox2 activity is tightly regulated by the GTPase Rac1 (in its active, GTP-binding form) as well as the p47^{phox}, p67^{phox}, and p40^{phox} proteins, which are in turn subject to regulation via phosphorylation in response to stimulants such as PKC, angiotensin II and TNFα (Li and Shah, 2003; Li, Horke and

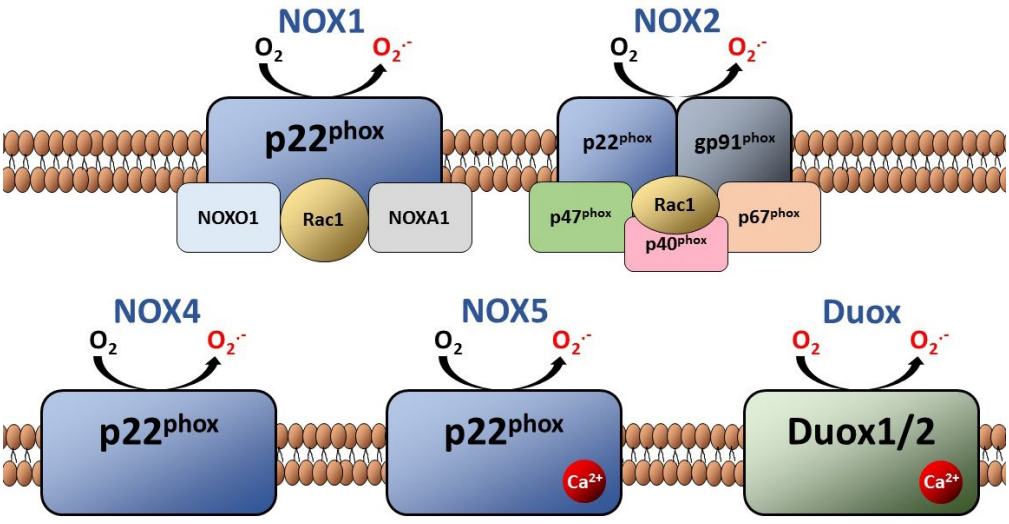

Figure 1.3: Overview of NADPH-oxidase isoforms. NADPH-oxidases exist in seven isoforms, namely Nox1-5 and Duox1&2. All Nox isoforms use p22^{phox} as their catalytic subunit, while gp91^{phox} is a catalytic subunit for Nox2. Nox1/2 activity is regulated by the activation (e.g., via phosphorylation or GTP-binding) and membrane translocation of several regulatory subunits such as Rac1 as well as p47^{phox}, p40^{phox} and p67^{phox} for Nox2 and NOXO1 and NOXA1 for Nox1. Nox5 and Duox1&2 are further believed to be dependent upon intracellular Ca2+ levels. *Adapted by I Akoumianakis et al, Antioxid Redox Sign 2018, doi: 10.1089/ars.2017.7421*

Förstermann, 2013; Panday *et al.*, 2015). NOXO1, NOXA1 are regulators of Nox1 activity,

while active Rac1 can also contribute to Nox1 activity via membrane translocation upon its GTP-activation (Panday *et al.*, 2015). The rest of the Nox isoforms are believed to be Rac1-independent, although their regulation is less studied (Konior *et al.*, 2014).

1.3.2.1.1. NADPH-oxidases regulation in obesity, insulin resistance and diabetes mellitus

Evidence suggests that the gene expression of vascular NADPH-oxidases is upregulated in models of T2DM (Lassègue and Griendling, 2010), and several pathogenic mechanisms are believed to contribute to vascular NADPH-oxidases activity in the context factors can stimulate the activity of these enzymes in the presence of obesity and DM (Gao and Mann, 2009).

As mentioned previously, PKC is an ubiquitous enzyme the activity of which is enhanced in obesity and T2DM (Farese and Sajan, 2012). Amongst its various effects, PKC is able to regulate cellular redox state (Mochly-Rosen, Das and Grimes, 2012). One of the relevant mechanisms may involve Nox2 activation via $p47^{phox}$ phosphorylation (Li, Horke and Förstermann, 2013). PKC also facilitates endothelin-1 (ET1) signalling via multiple pathways (Park *et al.*, 2000; Steinberg, 2015), which can also lead to mitogen-activate protein kinase (MAPK) p38-mediated induction of NADPH-oxidases activity (Rask-Madsen and King, 2013). Evidence also suggests that certain isoforms could regulate Rac1 activation (Gorshkova *et al.*, 2008; Y. Kim *et al.*, 2008) with direct implications for Nox1 and Nox2 activity, although this aspect has not been adequately explored.

AGE are able to regulate ROS production (Ott *et al.*, 2014), which in fact is known to further stimulate glycation reactions, thus establishing a vicious cycle of AGE and ROS burst (Goldin *et al.*, 2006; Ott *et al.*, 2014). In particular, AGE have been shown to upregulate Nox catalytic subunit expression and thus $O_2^{\cdot-}$ generation via RAGE signalling (San Martin *et al.*, 2007; Ott *et al.*, 2014). RAGE signalling has also been shown to upregulate Rac1 expression (Chen *et al.*, 2016), potentially influencing Nox1 and Nox2 activity. NADPH-oxidases

activation, in turn, is believed to propagate many of the detrimental vascular effects of AGE such as endothelial progenitor cell apoptosis, increased vascular permeability and dysregulated endothelial cell gene expression (Warboys, Toh and Fraser, 2009; Ott *et al.*, 2014; Vlassara and Uribarri, 2014).

TNFα is proinflammatory cytokine elevated both systemically and locally in obese humans (Hansson, 2005; Libby, 2012; Esser *et al.*, 2014) and it comprises a causal inducer of systemic and peripheral IR that precedes clinical T2DM (Hotamisligil *et al.*, 1996). In addition, TNFα is able to increase NADPH-oxidases activity in the vasculature (Lassègue and Griendling, 2010), via the atypical ζ isoform of PKC as well as other inflammatory signalling cascades (Frey *et al.*, 2002; Kim *et al.*, 2007). NADPH-oxidase activity, is believed to regulate certain elements of TNFα-induced phenotypes such as vascular cell apoptosis (Basuroy *et al.*, 2009). As such, TNFα is a mechanistic link between obesity, IR, DM and vascular NADPH-oxidases activity.

Vascular NADPH-oxidases are, to a lesser degree, able to use NADH as an alternative substrate (Lassègue, San Martín and Griendling, 2012). Given that excessive activation of the polyol pathway leads to increased cellular NADH/NAD+ as observed in cases of obesity and DM (Rask-Madsen and King, 2013), this pathway may constitute a biochemical parameter regulating vascular NADPH-oxidases activity in the presence of obesity or T2DM.

1.3.2.2. Uncoupled endothelial nitric oxide synthase

eNOS is a homodimeric enzyme that, under physiological conditions, catalyses the production of NO in endothelial cells using L-arginine as a substrate (Fig. 1.4A) (Li and Förstermann, 2013). Tetrahydrobiopterin (BH4) is a co-factor of eNOS that is crucial for its proper catalytic function (Li and Förstermann, 2013). BH4 can be oxidised to dihydrobiopterin (BH2) in the context of increased oxidative stress, and in the absence of this co-factor, eNOS

transfers electrons to molecular oxygen, thus producing $O_2^{\cdot -}$ in endothelial cells rather than NO, a state described as "eNOS uncoupling" (Fig. 1.4B) (Li, Horke and Förstermann, 2014). Levomefolic acide (5-MTHF), the circulating form of folic acid, has the ability to prevent BH4 oxidation, although clinical trials have failed to document a clinically beneficial effect in atherosclerosis (Antoniades *et al*, 2009).

The enzymatic activity of eNOS is delicately regulated by a number of mechanisms (Fig. 1.4) involving protein phosphorylation and allosteric modulation, while the expression of the enzyme can be influenced by a myriad of upstream stimuli such as inflammation, hormonal factors and shear stress (Förstermann and Sessa, 2012). The physiological effects eNOS are the net result of the regulatory mechanisms influencing its activity and its coupling status which determines its chemical product.

eNOS has several phosphorylation sites such as Ser1177, Ser633, Ser114, Ser615, Tyr81, Tyr677 and Thr495 in humans (Mount, Kemp and Power, 2007; Förstermann and Sessa, 2012). Phosphorylation at Ser1177 significantly stimulates eNOS activity (Mount, Kemp and Power, 2007). Various kinases are able to phosphorylate eNOS at Ser1177, namely Akt and AMP-activated kinase (AMPK) in response to insulin, calmodulin-dependent kinase (CamKII) in response to intracellular calcium (Ca^{2+}) increase and protein kinase A (PKA) in response to shear stress (Förstermann and Sessa, 2012). Ser633 phosphorylation also has a less important positive effect on eNOS activity (Mount, Kemp and Power, 2007). On the contrary, Th495 phosphorylation results in reduced eNOS activity, and it is most notably regulated by PKC activity (Förstermann and Sessa, 2012). The other eNOS phosphorylation sites are less extensively studied and comprise a novel field of research which may increase our understanding about eNOS regulation.

Allosteric interactions affect the activity of eNOS beyond protein phosphorylation. Indeed, caveolin-1 is a tonic inhibitor of eNOS, while calmodulin and heat-shock protein 90 (HSP90) are allosteric eNOS activators antagonising caveolin-1 binding (Förstermann and Sessa, 2012). Calmodulin is a Ca^{2+}-binding protein that is involved in allosteric protein-protein interactions in response to increased intracellular Ca^{2+} (Chin and Means, 2000). HSP90 is a chaperone influencing the folding and function of a variety of proteins including eNOS (García-Cardeña *et al.*, 1998). Importantly, calmodulin and HPS90 binding to eNOS act synergistically in antagonising the effects of caveolin-1 (Gratton *et al.*, 2000), while HSP90 binding is believed to

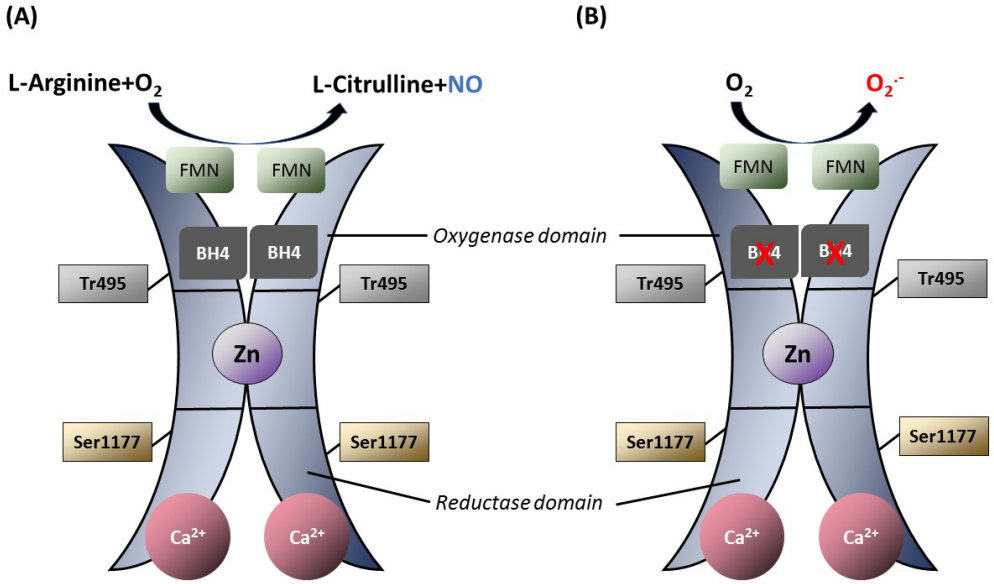

orchestrate the temporal enzymatic regulation of eNOS activity from an early Ca^{2+}-dependent phase to a late, phosphorylation regulated phase (Brouet *et al.*, 2001).

Figure 1.4: Overview of endothelial nitric oxide synthase (eNOS) structure & regulation. eNOS is a homodimer, with each monomer having an oxygenase and reductase domain, several phosphorylation sites such as Ser1177 and Thr495, a flavin mononucleotide (FMN) binding domain and its activity is dependent on the presence of zinc and further regulated by intracellular Ca^{2+} levels. When binding its important co-factor tetrahydrobiopterin (BH4), eNOS produces nitric oxide (NO) (A). In the absence of BH4 (usually resulting from its oxidation), eNOS produces superoxide ($O_2^{\cdot-}$) instead of NO, a condition described as "eNOS uncoupling" (B). *Adapted by I Akoumianakis et al, Antioxid Redox Sign 2018, doi: 10.1089/ars.2017.7421*

1.3.2.2.1. Regulation of eNOS in obesity, insulin resistance and diabetes mellitus

Evidence has linked obesity, IR and T2DM with eNOS uncoupling (Karbach *et al.*, 2014). As mentioned in the previous section, obesity, IR and T2DM are able to increase ROS production via NADPH-oxidases activation, and this could provide a direct mechanistic link with eNOS uncoupling via BH4 oxidation. Indeed, increased vascular and perivascular inflammation as well as eNOS uncoupling due to BH4 oxidation have been reported in several animal models of obesity (Marchesi *et al.*, 2009; Gamez-Mendez *et al.*, 2015; Xia *et al.*, 2016), corroborating the observational studies reporting impaired endothelial function in obese humans (Van Gaal, 2010). Interestingly, inflammation has been shown to increase BH4 bioavailability via induction of GTP cyclohydrolase I (GCHI) expression, which may help preserve endothelial function under inflammatory states (Antoniades *et al*, 2011). In addition, leptin, an adipokine upregulated in obesity, has been shown to induce eNOS uncoupling *in vitro* and in a rodent model of obesity (Korda *et al.*, 2008). Similar mechanisms of eNOS uncoupling have been demonstrated in the context of IR and DM (Rask-Madsen and King, 2007; Huang, 2009).

Cardiometabolic disease has also been associated with alterations in eNOS activity apart from the coupling status of the enzyme. PKC activation is able to reduce eNOS activity (Das Evcimen and King, 2007; Paneni *et al.*, 2013) by phosphorylating the enzyme at Thr495 (Payne *et al.*, 2009). In addition, DM is associated with increased O-GlcNAcylation of Akt, an important stimulator of eNOS activity via Ser1177 phosphorylation, and this results in

inhibition of eNOS activity (Paneni *et al.*, 2013). Furthermore, AGE-RAGE interactions have been shown to result in both decreased eNOS expression and reduced activity in endothelial cells (Ishibashi *et al.*, 2011). These enzymatic activity-regulating effects are less studied than the profound effects of obesity, IR and DM on eNOS uncoupling, and their overall contribution to phenotypes such as endothelial function largely depends on the coupling status of eNOS.

1.3.2.3. Mitochondrial oxidases

Enzymes of the mitochondrial respiratory electron transport chain contribute to cellular ROS generation (Li, Horke and Förstermann, 2014; Mittal *et al.*, 2014). Complexes I (NADH dehydrogenase) and III (ubiquinone-cytochrome b-c1) of the mitochondrial respiratory chain in particular are constant cellular sources of $O_2^{\cdot-}$, influenced by the respiratory rate as well as by the activity of superoxide dismutase 2 (SOD2, an enzyme converting mitochondrial $O_2^{\cdot-}$ to H_2O_2), which is located in the mitochondrial matrix (Förstermann, 2008). Interestingly, mitochondrial dysfunction has been associated with vascular disease (Ramachandran *et al.*, 2002), and experimental studies suggest that mitochondrial oxidative stress may facilitate atherogenesis (Ohashi *et al.*, 2006). However, the *in vivo* significance of mitochondrial ROS in human vascular disease remains to be explored.

1.3.2.3.1. Mitochondrial oxidase regulation in obesity, insulin resistance and diabetes mellitus

Numerous studies have suggested that obesity, IR and DM are linked with mitochondrial dysfunction (Lowell and Shulman, 2005; de Mello *et al.*, 2018), which is in turn linked with excessive ROS generation (Doughan, Harrison and Dikalov, 2008). Diabetes is associated with dysregulated mitochondrial biology and energetics, facilitating mitochondrial ROS overproduction beyond the physiological respiration and overriding endogenous antioxidant defences (Rask-Madsen and King, 2013). In addition, AGE-mediated Nox activation has been linked with increased mitochondrial oxidative stress in pancreatic cells, promoting apoptosis

(Lee *et al.*, 2010). Interestingly, PKC activation has been shown to phosphorylate p66Shc, a protein involved in redox signalling as mentioned previously, facilitating its translocation to the mitochondria and stimulating mitochondrial $O_2^{\cdot-}$ production (Paneni *et al.*, 2013). Consistently, mice lacking p66Shc are resistant to hyperglycaemia-induced oxidative stress and vascular disease progression (Napoli *et al.*, 2003), further supporting an important role for p66Shc in vascular disease regulation in the context of cardiometabolic disease. Nevertheless, these mechanistic links between metabolic disease and mitochondrial oxidative stress remain to be put in broader context with regards to their vascular consequences.

1.3.2.4. Xanthine oxidase

XO is involved in purine catabolism, converting hypoxanthine to xanthine and xanthine to uric acid while producing ROS such as $O_2^{\cdot-}$ and H_2O_2 as a by-product (Pacher, 2006). These ROS react with NO rapidly to form $ONOO^-$, an inhibitor of XO (Montezano *et al.*, 2015). The role of XO in redox state regulation is complex, considering that the enzyme in a potential source of ROS, but is tightly regulated by ROS-NO interactions and further produces uric acid, a significant endogenous antioxidant (Pacher, 2006; Pacher, Beckman and Liaudet, 2007). However, experimental studies have linked XO with vascular inflammation, endothelial dysfunction and ischaemia-reperfusion injury, thus proposing a redox-related pathophysiological role for this enzyme in CVD (Pacher, 2006).

1.3.2.4.1. Regulation of xanthine oxidase in obesity, insulin resistance and diabetes mellitus

The molecular mechanisms via which XO activity may be regulated in the context of obesity, IR and DM are still controversial. Experimental studies have demonstrated that obesity is associated with impaired endothelial function in a high fat diet-fed animal model via upregulation of XO activity (Erdei *et al.*, 2006), while XO inhibition reverses arterial stiffness

and endothelial dysfunction in obese mice fed with Western type diet (Lastra *et al.*, 2017). Furthermore, XO has been associated with production of ROS in type 1 DM (Desco *et al.*, 2002), an observation which has been confirmed in streptozotocin-induced diabetes in mice (Matsumoto *et al.*, 2003). In addition, allopurinol, a XO inhibitor, has been shown to attenuate the development of diabetic cardiomyopathy in mice (Rajesh *et al.*, 2009). These results suggest that metabolic disease is associated with elevated XO activity, which in turn may exert pathophysiological cardiovascular roles at least partially via ROS production. However, the underlying molecular mechanisms of these interactions remain unclear.

1.3.3. Endogenous antioxidant systems

Several endogenous antioxidant systems exist to ensure tight regulation of cellular redox state. These include antioxidant enzymes (Fig. 1.5) as well as smaller, endogenously synthesised non-protein molecules with direct antioxidant properties (Förstermann, 2008). Importantly, dysregulation of these antioxidant systems may contribute to cellular oxidative stress (Förstermann, 2008).

Endogenous antioxidant enzymes include SOD1-3 (which catalyse the conversion of the highly reactive $O_2^{\cdot-}$ to oxygen and H_2O_2) (Fukai and Ushio-Fukai, 2011), catalase (which converts H_2O_2 to water and oxygen) (Li, Horke and Förstermann, 2014), and the paraoxonase (PON, lactonases existing in three isoforms) family of enzymes (Förstermann, Xia and Li, 2017). In addition, glutathione peroxidases (GPX) reduce a wide range of lipid peroxides to

their corresponding alcohols, whereas they are also able to convert H_2O_2 to water and oxygen, and as such they also comprise important antioxidant enzymes (Förstermann, Xia and Li, 2017). Finally, the thioredoxin system is another important antioxidant system utilising NADPH to reduce ROS products such as oxidised proteins via electron flux through thioredoxin reductase and thioredoxin.

Importantly, obesity has been associated with changes in endogenous antioxidant enzyme function. Indeed, SOD activity has been shown to be significantly reduced in several rodent models of obesity (Bełtowski *et al.*, 2000), while the expression of SOD and GPX was significantly reduced in aortae of high fat diet-fed rats compared to healthy controls (Roberts *et al.*, 2006). This transcriptional dysregulation of antioxidant enzymes in obesity has further been confirmed by additional *in vivo* animal studies (Furukawa *et al.*, 2004). In addition, genetic studies have linked dysregulated activities of antioxidant enzymes (including SOD, GPX and catalase) with the pathogenesis of DM (Banerjee and Vats, 2014). Antioxidant enzymes thus comprise an additional mechanistic link between metabolic disease and dysregulated redox signalling which warrants further investigation.

In addition to the aforementioned antioxidant enzymes, a number of small non-protein molecules can behave as endogenous antioxidants, including glutathione, uric acid, bilirubin, and vitamin C, all of which behave as ROS scavengers while also potentially mediating the enzymatic production of ROS (Förstermann, 2008).

1.4. Insulin: a universal metabolic regulator with vascular roles

Insulin is a hormone secreted by the pancreas that regulates whole body glucose metabolism (Kahn and Flier, 2000). These effects are predominantly mediated by receptor-mediated effects on the liver, AT, skeletal muscle and brain (Kahn and Flier, 2000; Dimitriadis *et al.*, 2011; Thorens, 2011). Importantly, due to the widespread expression of insulin receptor, insulin has pleiotropic effects in peripheral tissues that may be glucose-independent (Odegaard and Chawla, 2013). Vascular cells, in particular, are subject to the effects of insulin signalling, which regulates processes such as cell proliferation, vascular tone and redox state (Muniyappa *et al.*, 2007).

Systemic IR is a hallmark of the metabolic syndrome that accompanies obesity and precedes the onset of clinical T2DM, and it refers to the inability of physiological circulating insulin levels to successfully regulate blood glucose (Kahn and Flier, 2000). Therefore, it is associated with hyperinsulinaemia as a compensatory mechanism (Kahn and Flier, 2000). On the other hand, cellular IR reflects the impairment of physiological insulin receptor downstream signalling in response to insulin (Shulman, 2000). Cellular IR in organs that are crucial for systemic glucose handling (such as the liver and skeletal muscle) is believed to be the underlying mechanism of the presence of systemic IR (Kahn and Flier, 2000).Conversely, the specific downstream consequences of peripheral IR in tissues such as the vasculature are less clear. Given the dysregulation of insulin levels and downstream signalling in cardiometabolic disease, a more focused examination of physiological and pathophysiological vascular insulin signalling is crucial to better understand the links of obesity, IR and DM with vascular disease.

1.4.1. Insulin biosynthesis and secretion

In pancreatic β cells, transcription and translation of the *insulin* gene results in the synthesis of protein precursor called preproinsulin (Fu, R. Gilbert and Liu, 2013). This precursor undergoes a number of post-translational modifications to form proinsulin and eventually

insulin by final removal of a sequence of amino acids called peptide C from the proinsulin molecule (Fu, R. Gilbert and Liu, 2013). Mature insulin consists of two individual peptide chains (a 21-amino acid chain A and a 30-amino acid chain B) linked by disulfide bonds (Fu, R. Gilbert and Liu, 2013). *Insulin* gene transcription is regulated by nutrient stimuli, with glucose being by far the most potent physiological stimulus upregulating insulin expression (Fu, R. Gilbert and Liu, 2013).

Once synthesised, insulin is stored intracellularly in secretory granules, along with peptide C and other β cell products (Henquin, 2009; Fu, R. Gilbert and Liu, 2013). Glucose is a potent stimulator of insulin secretion, which occurs in two phases, the rapid phase reflecting the rapid release of already synthesised insulin and the slow phase resulting from secretion of newly synthesised insulin molecules (Fu, R. Gilbert and Liu, 2013; Harcourt, Penfold and Forbes, 2013). The molecular mechanisms of glucose-stimulated insulin secretion involve activation of KATP channels and increase in intracellular calcium in response to increased intracellular glucose concentration (Henquin, 2009). Interestingly, these pathways are amplified in response to excess hyperglycaemia, but this amplification potential is lost in diabetic patients (Henquin, 2000). Insulin secretion is also further regulated by metabolic parameters such as free amino and fatty acids, catecholamines, as well as endogenous hormones such as incretins (Rorsman and Braun, 2013).

1.4.2. Insulin signalling

Insulin exerts its signalling effects upon binding to its respective surface receptors (Lizcano and Alessi, 2002). Insulin receptors are proteins with tyrosine kinase activity in their intracellular ends that exist as monomers in the plasma membrane of target cells, and they undergo dimerization upon binding to insulin (Lizcano and Alessi, 2002). Following this dimerization, insulin receptor monomers undergo cross-phosphorylation at tyrosine residues to

occur in their intracellular ends, which then phosphorylate a variety of post-receptor molecules including the IRSs (such as IRS1) and Shc protein (Lizcano and Alessi, 2002). These post-receptor mediators can direct downstream insulin signalling toward two distinct pathways, namely the phosphoinositide 3-kinase (PI3K)/Akt or the MAPK pathway, both involved in wide reaching critical aspects of cellular biology depending on the target cell type (Lizcano and Alessi, 2002). The insulin pathway is summarised in Fig. 1.6.

1.4.3. Mechanisms of molecular insulin resistance

The definition of IR is two-fold, either describing an impaired response to the effects of insulin with regards to cellular glucose uptake or, strictly speaking, a molecular dysregulation of the insulin pathway (Shulman, 2000). Interestingly, in the former case, the insulin pathway may be intact but its effects could be antagonised by other parallel metabolic pathways (Shulman, 2000). On the other hand, dysregulation of the molecular insulin signalling pathway may have crucial pleiotropic and glucose-independent effects in tissues such as the vasculature which are not as crucial for overall glucose metabolism (Muniyappa *et al.*, 2007; Odegaard and Chawla, 2013).

The predominant theory for IR is related to chronic nutrient overload which results in the accumulation of multiple toxic metabolic by-products in various tissue and cell types (Shulman, 2000; Samuel and Shulman, 2012). These are believed to mainly affect the downstream metabolic responses to insulin, although they may be accompanied by changes of the insulin pathway itself (Samuel and Shulman, 2012). For example, FFA induce IR via a series of metabolic reactions leading to increased intracellular citrate levels which inhibit phosphofructokinase, a rate-controlling enzyme in glycolysis, eventually leading to increased intracellular glucose concentrations and decreased glucose uptake (Shulman, 2000).

Inflammation has been revealed as an important mediator of molecular IR via direct targeting of the insulin pathway (Figure 1.6) (Khodabandehloo *et al.*, 2016). Indeed, proinflammatory mediators that are increased in obesity and DM, including TNFα and downstream proteins such as PKC and c-Jun N-terminal kinase (JNK), have been shown to result in abnormal phosphorylation of IRS1 at serine instead of tyrosine residues (Samuel and Shulman, 2012; Khodabandehloo *et al.*, 2016). Importantly, such molecular IR appears to selectively impair the responsiveness of the PI3K/Akt axis compared with the MAPK pathway, thus creating a crucial imbalance between the signalling axes (Potenza, Addabbo and Montagnani, 2009). Crucially, metabolic nutrient overload in tissues such as the AT promotes inflammation, thus creating an interrelated network of mediators that synergistically promote cellular IR (Samuel and Shulman, 2012).

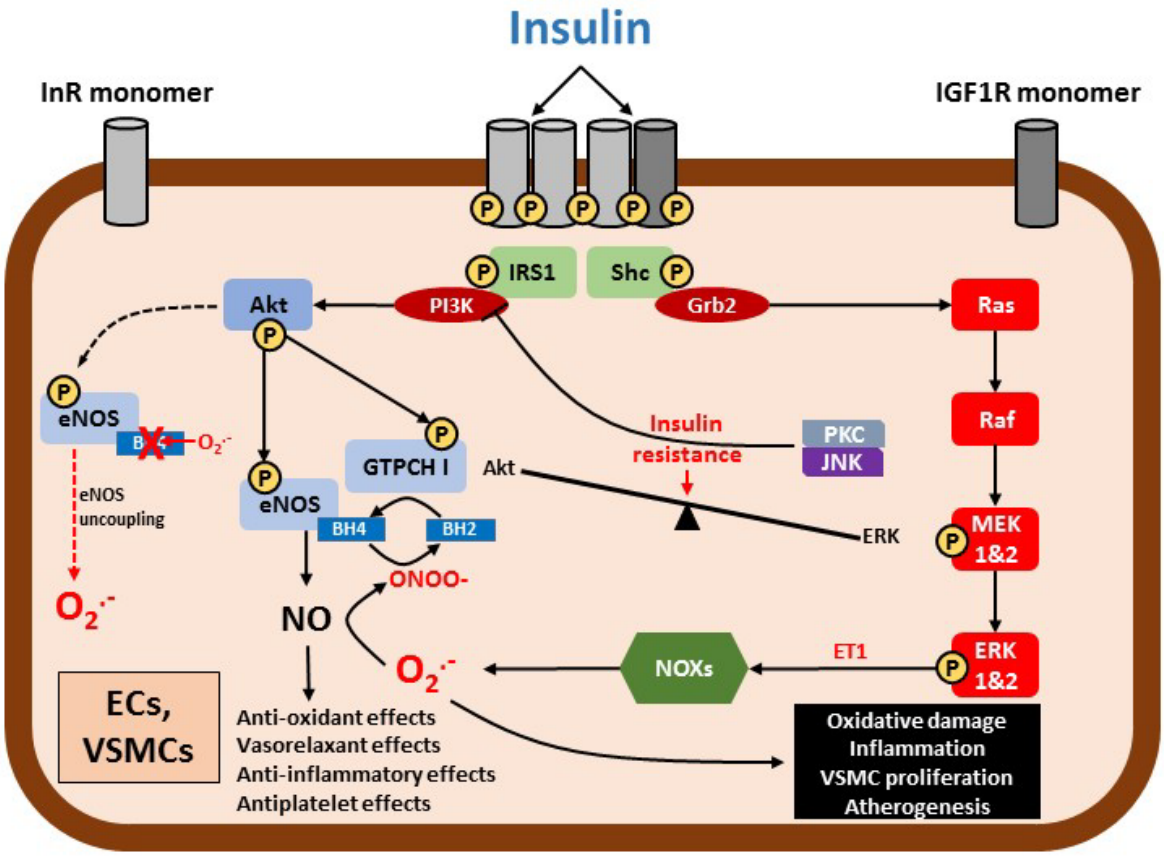

Figure 1.6: Vascular insulin signalling and molecular targets of insulin resistance (IR). Insulin induces dimerization of insulin receptor (InR) or insulin-like growth factor 1 receptor (IGF1R) monomers, which then undergo cross-phosphorylation at Tyr sites and induce Tyr phosphorylation of downstream proteins such as insulin receptor substrate 1 (IRS1) and Shc. IRS1 directs signalling towards the phosphoinositide 3-kinase (PI3K)/Akt pathway, which under normal conditions increases eNOS activity via Ser1177 phosphorylation and eNOS coupling via activation of GTP-cyclohydrolase I (GTPCHI), the enzyme responsible for tetrahydrobiopterin (BH4) formation. This increases nitric oxide (NO) bioavailability inducing vasoprotective effects .Shc regulates the mitogen-activated protein kinase (MAPK) insulin pathway, leading to Erk1&2 phosphorylation, endothelin 1 (ET1) signalling enhancement and NADPH-oxidases activation. This increases superoxide ($O_2^{\cdot-}$) generation, BH4 oxidation, eNOS uncoupling, reduced NO bioavailability and overall detrimental vascular effects. Molecular insulin resistance via protein kinase C (PKC) or c-Jun N-terminal kinase (JNK) mainly influences IRS1 phosphorylation and thus the PI3K/Akt pathway as opposed to the MAPK pathway, potentially resulting in relative overactivation of NADPH-oxidases activation in response to

1.4.4. Vascular effects of insulin: implications for insulin-based antidiabetic treatments

Insulin signalling in the vasculature has multiple effects (Potenza, Addabbo and Montagnani, 2009). Insulin via Akt is able to activate eNOS by Ser1177 phosphorylation enhancing L-arginine transport and also improving BH4 bioavailability, thus resulting in increased NO bioavailability and enhanced vasorelaxation under physiological conditions in humans (Mcneill *et al.*, 1998; Fisslthaler *et al.*, 2003; Konopatskaya *et al.*, 2003; Sobrevia and González, 2009). On the other hand, stimulation of the MAPK pathway by insulin is able to increase vascular ET1 signalling in cell culture and animal models (Potenza, Addabbo and Montagnani, 2009), thus being potentially able to induce activation of NADPH-oxidases as well as proliferation of VSMCs (115, 138). Consistently, MAPK kinases such as extracellular signal-regulated kinases 1&2 (Erk1&2) are able to directly regulate Rac1 (Ray, Vaidya and Johnson, 2007), while NADPH-oxidases have been shown to comprise downstream targets of insulin (San José, Bidegain, Pablo A Robador, *et al.*, 2009). Consequently, the integrated vascular effects of insulin depend on the post-receptor balance between the two signalling axes (Fig. 1.6).

Under physiological conditions, the net vascular effects of insulin are mainly mediated by the Akt pathway, resulting in increased eNOS activity and coupling and improved NO bioavailability, therefore being considered protective for vessel homeostasis (Muniyappa *et al.*, 2007). Accordingly, these vascular effects are lost in individuals with obesity and systemic IR (Williams *et al.*, 1996; Jiang *et al.*, 1999), something that is likely not solely attributed to the

systemic effects of obesity and IR, but rather to direct dysregulation of local, vascular responses to insulin (Katakam *et al.*, 2005; Muniyappa *et al.*, 2007). It is postulated that selective inhibition of the PI3K/Akt axis of insulin signalling in the context of post-receptor IR can result in an excessive activation of the MAPK pathway (Figure 1.6) (Wanstall *et al.*, 2001; Schulman and Zhou, 2009) which could theoretically enhance vascular oxidative stress, although this has not been directly addressed in human vessels. Interestingly, ROS production at low levels, particularly via Nox4, has been proposed to be involved in the preservation of cellular insulin sensitivity by inhibiting protein tyrosine phosphatases, enzymes that de-phosphorylate and deactivate insulin receptor (Mahadev *et al.*, 2004). Therefore, ROS possibly have a Janus-like relationship with insulin signalling, being required for its tight regulation but being potentially detrimental upon excessive production.

The previous considerations propose the interesting notion that insulin treatment in diabetic patients could have unpredictable effects on the human vasculature resulting from vascular insulin signalling independently of effects on hyperglycaemia. Consistently, recent clinical trials have revealed that treatment with insulin analogues such as glargine (outcome reduction with an initial glargine intervention, or ORIGIN trial) and degludec (trial comparing cardiovascular safety of insulin degludec versus insulin glargine in patients with type 2 diabetes at high risk of cardiovascular events, or DEVOTE) did not significantly improve adverse cardiovascular events in diabetic patients despite achieving excellent glycaemic control (Gerstein *et al.*, 2012; Marso *et al.*, 2017). Conversely, the LEADER (liraglutide effect and action in Diabetes: evaluation of cardiovascular outcome results) trial recently demonstrated that liraglutide, an analogue of glucagon-like peptide 1 (GLP1, an incretin stimulating insulin secretion), significantly reduced cardiovascular complications in diabetic patients independently of glycaemic control (S. P. Marso *et al.*, 2016). These clinical trial examples strongly suggest that glycaemic control is not an adequate marker of vascular consequences,

and local vascular responses to different antidiabetic agents should be considered. Interestingly, a number of novel antidiabetic drugs have displayed peripheral insulin-sensitising effects and may be crucial in the reversal of human vascular responses to insulin. GLP1 receptor signalling, target by GLP1 or GLP1 analogues, has shown the ability to improve insulin sensitivity and may be of relevance in the vasculature (Okerson and Chilton, 2012).

Accordingly, DPP4-i are a novel class of drugs, initially thought to solely act via increasing GLP1 bioavailability, which have also demonstrated pleiotropic effects with potential insulin-sensitising and vasoprotective properties (Fadini and Avogaro, 2011). DPP4 is a peptidase existing both in transmembrane and soluble forms, which cleaves X-proline or X-alanine dipeptides from the N-terminal end of a variety of polypeptides including chemokines, growth factors and incretins (Fadini and Avogaro, 2011; Akoumianakis and Antoniades, 2017a). DPP4-mediated cleavage of dipeptides from the N-terminal end of GLP1 results in inactivation of this peptide; therefore DPP4-i is crucial to glucose metabolism and hence diabetes management by increasing GLP1 bioavailability and facilitating its stimulating actions with regards to pancreatic insulin secretion and peripheral insulin sensitising effects (Renner *et al.*, 2016). However, DPP4-i may affect the function of multiple DPP4 substrates such as neuropeptide Y, peptide YY, brain natriuretic peptide (BNP), interleukin 10 and various chemokines (Akoumianakis and Antoniades, 2017a; Duan *et al.*, 2017). As such, it has been hypothesised to potentially have pleiotropic effects on the vascular wall by affecting vascular cell biology as well as immune responses to vascular disease. Indeed, DPP4-i has been associated with attenuated vascular inflammation and oxidative stress, although it may have adverse effects via stimulating sympathetic signalling (Duan *et al.*, 2017). Overall, DPP4-i may be a promising antidiabetic medication option with pleiotropic vascular effects, which warrants further investigation.

1.5. Adipose tissue: a dynamic endocrine organ

AT has recently emerged as an endocrine organ, secreting a variety of cytokines as well as adipokines (hormones of adipocyte origin), which elicit a variety of local and systemic responses, influencing lipid and glucose metabolism and regulating systemic inflammation. As such, AT may be actively involved in the pathophysiology of cardiometabolic disease (Akoumianakis and Antoniades, 2017b). Importantly, anatomically distinct AT depots display different biological characteristics in health and disease (Antonopoulos *et al.*, 2016).

The complexity of the role of AT in CVD is highlighted by the so-called "obesity paradox", namely the clinical observation that, in advanced cardiometabolic disease states, moderately obese patients (defined mainly by body mass index or BMI, in kg/m^2) demonstrate lower cardiovascular morbidity compared with lean individuals (Antonopoulos *et al.*, 2016). Although several alternative theories have been proposed to explain this observation, it is generally accepted that a major component of the obesity paradox may originate from the anatomical and biological heterogeneity of AT and the inability of BMI (the classical marker of obesity) to reflect these crucial elements (Antonopoulos *et al.*, 2016). Consequently, alterations in the biology and regional distribution of AT appear to be equally important as (if not more important than) overall AT mass with regards to cardiometabolic disease pathogenesis and cardiovascular risk. To this end, further research is required regarding the interactions of regional AT biology with vascular disease mechanisms.

Adipocytokines comprise protein products secreted by AT, able to exert local (paracrine) and systemic (endocrine) signalling roles (Tilg and Moschen, 2006). These include cytokines secreted by immune cells (e.g., macrophages, lymphocytes) infiltrating the AT as well as adipokines secreted by adipocytes (Tilg and Moschen, 2006; Akoumianakis and Antoniades,

2017b). AT is able to secrete a wide variety of such molecules, and dynamically alter the composition of its secretome in the context of disease states such as obesity, IR and T2DM (Tilg and Moschen, 2006; Rasouli and Kern, 2008).

Adipocytokines exert their signalling roles via three distinct routes of signalling, namely the endocrine, paracrine-autocrine and the vasocrine route (Fig. 1.7) (Akoumianakis and Antoniades, 2017b). Secreted adipocytokines may enter the circulation via the vessels providing blood supply to the AT, being able to travel via the systemic circulation to remote anatomical regions (endocrine route) (Akoumianakis and Antoniades, 2017b). In addition, adipocytokines secreted by cells of the AT may diffuse locally in the interstitial space, affecting neighbouring cells (paracrine-endocrine route) (Akoumianakis and Antoniades, 2017b). This mode of signalling is an important way of crosstalk between the vascular wall and its surrounding perivascular AT (PVAT) (Margaritis *et al.*, 2013; Akoumianakis, Tarun and Antoniades, 2016). Vasocrine signalling is a more controversial concept that shares characteristics with endocrine and paracrine signalling (Akoumianakis and Antoniades, 2017b). Indeed, according to this mode of signalling, adipocytokines such as TNFα may diffuse into the lumen of small arterioles and exert local biological effects in downstream regions of the microcirculation (Yudkin, Eringa and Stehouwer, 2005). This mode of signalling has wider range effects compared to paracrine signalling; however, in contrast with endocrine signalling,

it is unlikely to result in systemic changes of adipocytokine levels (Yudkin, Eringa and Stehouwer, 2005). and its effects are rather limited to individual vascular beds (Yudkin, Eringa and Stehouwer, 2005; Gu and Xu, 2013).

Table 1.1: Summary of representative adipocytokines and their biological roles

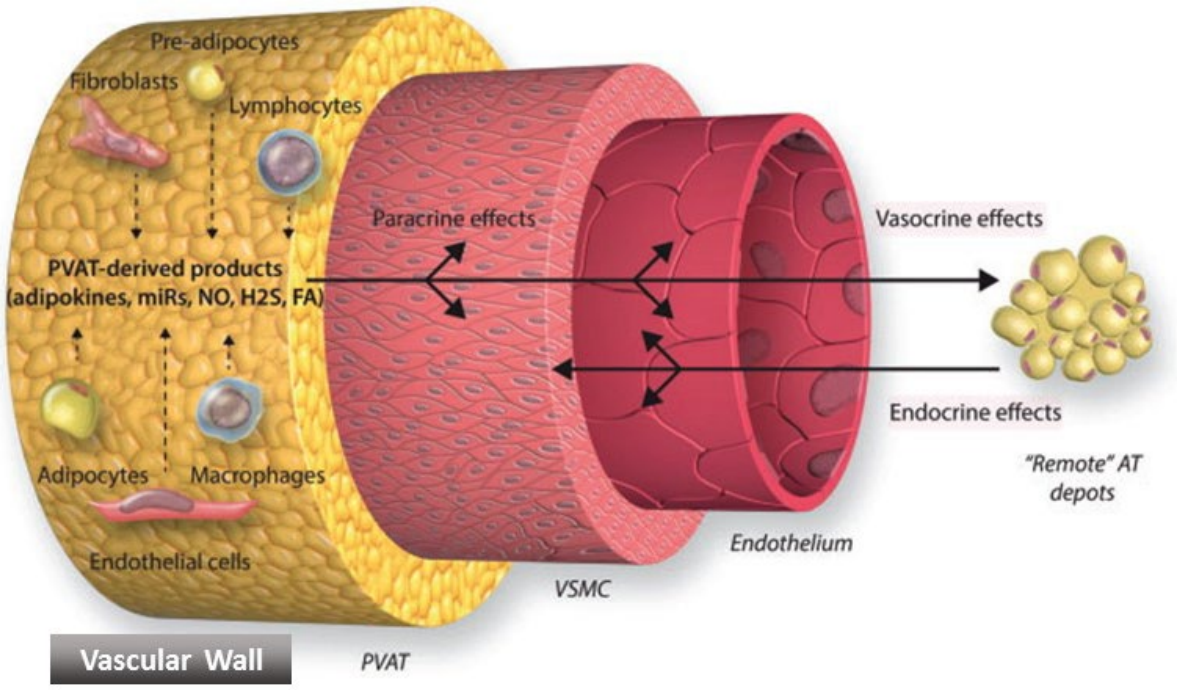

Figure 1.7: Routes of adipose tissue (AT) signalling. Remote AT depots can influence the vascular wall via products secreted in the circulation (endocrine effects). On the other hand, signalling products secreted from perivascular AT (PVAT) cells can reach the vascular smooth muscle cell (VSMC) and endothelial layers by diffusion, exerting local roles (paracrine effects). Such products include adipokines, microRNAs (miRs), gaseous messengers such as nitric oxide (NO) and hydrogen sulfide (H_2S) and fatty acids (FA). Some such products may diffuse deep enough to reach the vascular lumen from outside, thus exerting regional effects in downstream vascular beds via the local circulation (vasocrine effects). *Adapted by I Akoumianakis et al, Cardiovasc Res. 2017;113(9):999-1008.*

Adipose tissue product	Functions
Adiponectin	Insulin-sensitizing, anti-oxidant, and anti-inflammatory properties
Leptin	Hyperleptinaemia and leptin resistance are associated with cardiometabolic disease, but the direct effects of this hormone in different disease settings are controversial

Omentin	Insulin-sensitizing and anti-oxidant effects
Resistin	Promotion of insulin resistance, inflammation, and oxidative stress
TNF	Wide range of pro-inflammatory effects, induction of oxidative stress & insulin resistance
IL-6	Potent pro-inflammatory properties, induction of oxidative stress
Angiotensinogen/AngII/Aldosterone	Pro-oxidant and pro-inflammatory roles on the vascular wall

TNF: Tumour necrosis factor; IL-6: Interleukin 6; AngII: Angiotensin II

AT is also able to secrete a variety of non-protein products beyond adipocytokines. These include microRNA (miR) molecules (Thomou *et al.*, 2017), gaseous messengers such as NO and H_2S (Akoumianakis, Tarun and Antoniades, 2016) and metabolites such as methyl palmitate (Gollasch, 2017). MiRs are small, non-coding RNA molecules that can be secreted via exosome and they have the ability to bind complementary mRNA sequences, thus inhibiting their translation (Ameres and Zamore, 2013). NO and H_2S, on the other hand, are gaseous molecules with short half-life which can be synthesised and secreted by AT, being responsible for a variety of paracrine effects with particular implications regarding cardiovascular biology (Akoumianakis, Tarun and Antoniades, 2016). Finally, AT secretes a variety of metabolites which may have endocrine and paracrine effects (Akoumianakis and Antoniades, 2017b). Palmitic acid methyl ester (PAME), a fatty acid metabolite, comprises such an example with direct cardiovascular implications due to its ability to induce vasorelaxation and attenuate local inflammation (Lee *et al.*, 2011; Gollasch, 2017), regulating vascular tone especially in the context of paracrine PVAT-vascular wall interactions (Lee *et al.*, 2011).

1.5.1. Regional variability of adipose tissue biology

As mentioned previously, obesity has long been defined on the basis of BMI > 30 kg/m^2, a global index of adjusted whole body fat mass (Hubert *et al.*, 1983). On the other hand, this fails to capture the regional variability of AT distribution (Antonopoulos *et al.*, 2016). Consistently, lots of experimental and observational studies have highlighted the biological and functional

differences of superficial (subcutaneous) versus deep (visceral) AT depots (Wajchenberg, 2000) and further identified PVAT as a unique AT depot of particular importance for vascular biology (Akoumianakis, Tarun and Antoniades, 2016). Crucially, the various AT depots can adjust their secretome in response to various stimuli such as inflammation and other secreted signals, e.g., brain natriuretic peptide (BNP) which have been shown to exert opposing effects on the secretion of adipokines such as adiponectin (Antonopoulos *et* al, 2014).

1.5.1.1. Subcutaneous versus visceral adipose tissue

Subcutaneous AT (ScAT) is located under the skin, and it is believed to serve as a protective barrier as well as a physiological buffer for excessive energy intake by accumulating FFA and glycerol as triglycerides (TG) (Ibrahim, 2010). Around 80% of total AT mass is found in the subcutaneous region, and when the energy-storing capacity of ScAT is exceeded, excess fat may be accumulated in deeper anatomical regions, in the abdominal or thoracic visceral area (Ibrahim, 2010). Visceral AT (VAT), in turn, is characterised by increased inflammatory infiltration and smaller, less differentiated adipocytes (Ibrahim, 2010; Antonopoulos *et al.*, 2017), and phenotypic changes in this depot are believed to drive the pathophysiological consequences of obesity by secreting a variety of inflammatory adipocytokines and other products that propagate systemic IR, systemic inflammation and cardiovascular disease (Després, 2006; Ibrahim, 2010; Akoumianakis and Antoniades, 2017b; Piché *et al.*, 2018). Experimental human models in ScAT and thoracic AT (ThAT) have shown that inflammation and BNP can differentially regulate AT secretome; in particular, inflammation reduces adiponectin secretion while BNP increases adiponectin secretion (Antonopoulos *et al*, 2014), supporting the notion that these AT depots comprise dynamic endocrine organs.

Clinical association studies support the notion that visceral obesity contributes to metabolic disease complications as opposed to subcutaneous adiposity. Indeed, excessive VAT (male-type obesity), is associated with increased clinical cardiometabolic complication risk, while

gluteal (subcutaneous) fat deposition (female-type obesity) may be protective against CVD since it presumably reflects increased expanding capacity of ScAT (Piché *et al.*, 2018). This concept of ScAT expandability reflects the ability of the body to handle energy uptake without visceral or intra-organ deposition, and may be influenced by genetic and environmental factors that could, at least partially, explain the variability of the obesity phenotype observed amongst individuals (Piché *et al.*, 2018). Based on these considerations, the WHO has redefined obesity based on the waist and hip circumferences, the ratio of which reflects the relative accumulation of VAT versus ScAT and is believed to be a more relevant biomarker than BMI (WHO, 2011).

1.5.1.2. Perivascular adipose tissue

PVAT surrounds the wall of most human vessels, with no clear anatomical barrier between the two (Siegel-Axel and Häring, 2016), and corresponds to only ~ 3% of total body AT mass (Lee, Després and Koh, 2013). Nevertheless, PVAT has some unique properties owning to its close proximity with the vascular wall (Siegel-Axel and Häring, 2016).

PVAT often simulates characteristics of brown AT (BAT) (Gu and Xu, 2013), such as the presence of abundant vasculature, along with adipocytes containing many small lipid droplets and ample mitochondria (Saely, Geiger and Drexel, 2011). In contrast, most other AT depots in adults fall under the white AT (WAT) type, containing lipid-rich adipocytes with single lipid droplets (Saely, Geiger and Drexel, 2011). BAT utilizes energy for heat production, while WAT mainly has energy-storing functions; furthermore, both types have secretory properties (Saely, Geiger and Drexel, 2011; Wang, Zhao and Lin, 2015). Interestingly, obesity is associated with loss of the BAT-like properties of PVAT, but the biological relevance of this phenomenon is unknown (Gu and Xu, 2013).

PVAT secretes a variety of products that exert paracrine effects on the neighbouring vascular wall (Akoumianakis, Tarun and Antoniades, 2016). The secretome of PVAT is

influenced by stimuli such as inflammation, obesity and IR, which affect the differentiation status of adipocytes as well as the degree and polarization of its infiltrating inflammatory cells (Siegel-Axel and Häring, 2016). Changes in the secretome of PVAT, in turn, may have important consequences on vascular biology in the context of obesity, IR and DM (Gu and Xu, 2013). Evidence suggests that the secretome of PVAT has a net anti-inflammatory, antioxidant and vasodilatory effect in healthy individuals via molecules such as adiponectin, NO and other adventitium-derived relaxing factors (ADRFs) (Akoumianakis, Tarun and Antoniades, 2016). Obesity, IR and DM, however, induce a phenotypic switch in PVAT, enhancing the secretion of proinflammatory adipocytokines such as TNFα and resistin (Akoumianakis, Tarun and Antoniades, 2016).

Observational studies have corroborated the clinical relevance of PVAT function on vascular disease. Local expansion of peri-coronary AT has been independently associated with coronary calcification, atherosclerotic plaque burden and vulnerability as well as with cardiovascular risk factors such as plasma cholesterol and intima-media thickness in animal and human studies (Greif *et al.*, 2009; Liu *et al.*, 2010; Park *et al.*, 2013; Siegel-Axel and Häring, 2016; Sinha *et al.*, 2016). Peri-coronary AT assumes a pro-inflammatory phenotype in the context of coronary atherosclerosis in mice (Iacobellis, 2015). In addition, coronary spasm-induced angina has been linked with increased PVAT inflammation by ^{18}F-fluorodeoxyglucose (FDG) positron emission tomography (PET) in humans (Ohyama *et al.*, 2018). However, harnessing the full potential of PVAT-vascular wall interactions in humans remains challenging.

Recently, a new concept has emerged whereby PVAT may be a recipient of biological signals originating from the underlying vascular wall, adjusting its secretome in response to such signals (Akoumianakis, Tarun and Antoniades, 2016). Indeed, increased vascular

oxidative stress in human internal mammary artery (IMA) segments was found to result in the formation of lipid peroxidation products such as 4-HNE, which could diffuse to the neighbouring PVAT and increase the expression of adiponectin, a vasoprotective molecule, presumably as a local compensatory defence mechanism (Margaritis *et al.*, 2013; Antonopoulos *et al.*, 2015). The crosstalk between PVAT and the vasculature is thus bi-directional, with PVAT both secreting products that influence vascular biology (outside-to-inside signalling) and receiving vascular products that modify its secretome (inside-to-outside signalling). As this protective mechanism has been discovered in atherosclerosis-free vessels (IMA), it may potentially contribute to the well-established resistance of these arteries to atherosclerosis. Recently, it was shown that vascular inflammation could induce reduced perivascular adipocyte differentiation via the vascular secretion of inflammatory cytokines, resulting in reduced PVAT lipid content which could be detected computed tomography (CT) (Antonopoulos *et al.*, 2017). This example highlights that deciphering the mutual interactions between PVAT and the vascular wall could enhance our ability to treat, predict and prevent CVD complications.

1.6. Wnt signalling as a novel link between metabolic and vascular disease

Wnt signalling includes a evolutionarily conserved spectrum of signalling pathways with universal cell targets (Wiese, Nusse and van Amerongen, 2018) and the ability to regulate crucial cell processes such as cell proliferation, migration and apoptosis (Reya and Clevers, 2005; Schulte and Bryja, 2017).

Although Wnt signalling has long been linked with the pathogenesis of carcinogenesis and tumour expansion and metastasis (Reya and Clevers, 2005; Wiese, Nusse and van Amerongen, 2018), recent evidence suggests that it is also involved in regulating inflammation and IR

(Catalán *et al.*, 2014; Fuster *et al.*, 2015; Zuriaga *et al.*, 2017), therefore potentially contributing to cardiometabolic disease. Importantly, AT secretes several Wnt signalling ligands such as Wnt5a (Ouchi *et al.*, 2010; Catalán *et al.*, 2014; Fuster *et al.*, 2015), which is upregulated in obesity (Ouchi *et al.*, 2010; Zuriaga *et al.*, 2017). These ligands may comprise mechanistic mediators of metabolic syndrome-related vascular complications (Ouchi *et al.*, 2010; Marinou *et al.*, 2012).

Wnt Ligand	Predominant Wnt Pathway Involved
Wnt1	Canonical
Wnt2	Canonical
Wnt2b	Canonical
Wnt3	Canonical
Wnt3a	Canonical
Wnt4	Non-canonical
Wnt5a	Non-canonical
Wnt5b	Non-canonical
Wnt6	Non-canonical
Wnt7a	Non-canonical
Wnt7b	Non-canonical
Wnt8a	Canonical
Wnt8b	Canonical
Wnt9a	Non-canonical
Wnt9b	No-canonical
Wnt10a	Canonical
Wnt10b	Canonical
Wnt11	Non-canonical
Wnt16	Non-canonical

Table 1.2: List of Wnt ligands in humans and their predominant signalling pathways

1.6.1. Wnt ligands: a diverse family of signalling molecules

The Wnt signalling pathways are receptor-mediated, being activated upon binding of a Wnt receptor to a secreted Wnt ligand (Reya and Clevers, 2005). The family of Wnt ligands consists of 19 glycoproteins in mammals (Kikuchi, Yamamoto and Sato, 2009). Wnt ligands undergo a variety of post-translational modifications including glycosylation and palmitoleic

acid modifications (Logan and Nusse, 2004; Wiese, Nusse and van Amerongen, 2018). As a result of these modifications, Wnt ligands display moderate water solubility and thus rapidly form local protein-protein interactions, exerting paracrine signalling effects (Wiese, Nusse and van Amerongen, 2018).

Wnt ligands bind to a variety of membrane receptors belonging mainly to the Frizzled (Fzd) family of G protein-coupled 7-transmembrane receptors (Logan and Nusse, 2004). This interaction is often facilitated by co-factors of the lipoprotein-related protein (LRP) family (mainly LRP5 and LRP6), especially in the context of canonical Wnt signalling as described below (Marinou *et al.*, 2012). Tyrosine-protein kinase transmembrane receptors Ror1 and Ror2 and Ryk protein also comprise less well-characterised Wnt receptors outside the Fzd family (Marinou *et al.*, 2012). The exact chain of events leading to downstream Wnt signalling propagation is not known, but it is believed to involve complex intracellular regulatory protein interactions with Wnt receptors (Wiese, Nusse and van Amerongen, 2018). Dsh, in particular, is a protein which is able to directly interact with Fzd receptors and is believed to be crucial for downstream signal transduction (Logan and Nusse, 2004).

Wnt signalling is subject to rapid regulation at the ligand-receptor interaction level (Schulte and Bryja, 2017). Indeed, Wnt ligands can bind to secreted frizzled-like proteins (Sfrp1-5 in humans), which share structural similarities with the Fzd receptors and thus can bind to Wnt ligands, preventing their interactions with Fzd receptors (Marinou *et al.*, 2012). In addition, LRP5/6 are regulated by interactions with a family of Dickkopf (Dkk) proteins which comprise potent canonical Wnt signalling inhibitors.

Wnt receptors/co-receptors
Fzd2
Fzd5
Ror1
Ror2

Ryk LPR5 LPR6

Two main signalling Wnt pathways have been described to date, namely the canonical and the non-canonical Wnt pathway (Marinou *et al.*, 2012). The non-canonical pathway can be further subclassified to the planar cell polarity (PCP) and the Ca^{2+}-dependent pathway (Marinou *et al.*, 2012).

Table 1.3: List of main Wnt receptors

1.6.1.1. Canonical Wnt signalling

Canonical Wnt signalling involves gene transcription regulation via β-catenin signalling (Fig. 1.8) (Clevers and Nusse, 2012). In the absence of Wnt ligand stimulation, β-catenin forms a protein complex with axin and adenomatous polyposis coli (APC), which attract protein kinases such as casein kinase 1 (CK1) and glycogen kinase synthase 3β (Clevers and Nusse, 2012). These kinases phosphorylate β-catenin, which then is

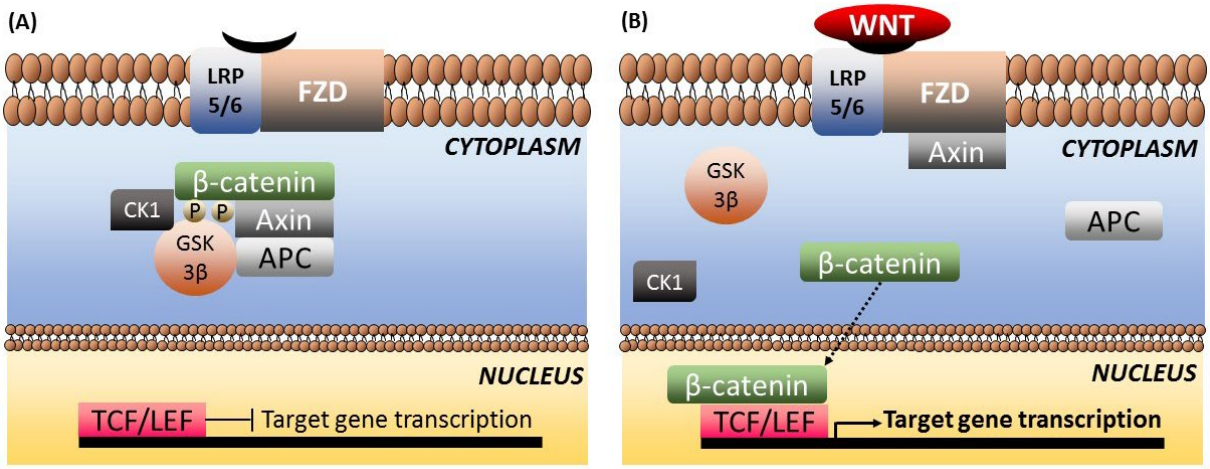

Figure 1.8: Canonical Wnt signalling pathway. In the absence of a Wnt ligand, β-catenin forms a proteolytic complex with axin, adenomatous polyposis coli (APC) and the kinases casein kinase 1 (CK1) and glycogen kinase synthase 3β (GSK3β), which phosphorylate β-catenin and lead to its degradation (A). When a canonical Wnt ligand binds to its Frizzled (Fzd) receptor along with co-receptors such as lipoprotein-related proteins (LRP) 5 & 6, the receptor complex interacts with axin, preventing the formation of the proteolytic complex and allowing β-catenin to translocate to the nucleus, interact with the T cell factor (TCF)/lymphoid-enhancer binding factor (LEF), reversing its ability to constitutively inhibit target genes (B). This results in increased gene expression of Wnt target genes.

degraded via ubiquitination-involving processes (Logan and Nusse, 2004). However, upon Wnt binding, the Fzd-LRP5/6 receptor complex interacts with axin thus disrupting the aforementioned degradation complex (Clevers and Nusse, 2012). This allows β-catenin to translocate to the cell nucleus, where it interacts with the T cell factor (TCF)/lymphoid-enhancer binding factor (LEF), reversing their constitutive inhibitory effect on target gene

transcription (Kikuchi, Yamamoto and Sato, 2009; Clevers and Nusse, 2012). Canonical Wnt signalling upregulates the expression of numerous genes such as c-Myc and cyclin D1, which are involved in cell cycle, affecting cell proliferation versus apoptosis and consequently being involved in disease entities such as tumorigenesis and stem cell-related diseases, e.g., haematological and bone disorders (Clevers and Nusse, 2012).

1.6.1.2. Non-canonical Wnt signalling

Following the description of the prototype, β-catenin-dependent (canonical) Wnt signalling pathway, it became evident that certain Wnt ligands were also able to exert a wide range of biological effects in β-catenin-independent ways (James, Conrad and Moon, 2008). These non-canonical Wnt signalling events can occur either via the PCP or the Ca^{2+}-dependent pathway (Fig. 1.9) (James, Conrad and Moon, 2008).

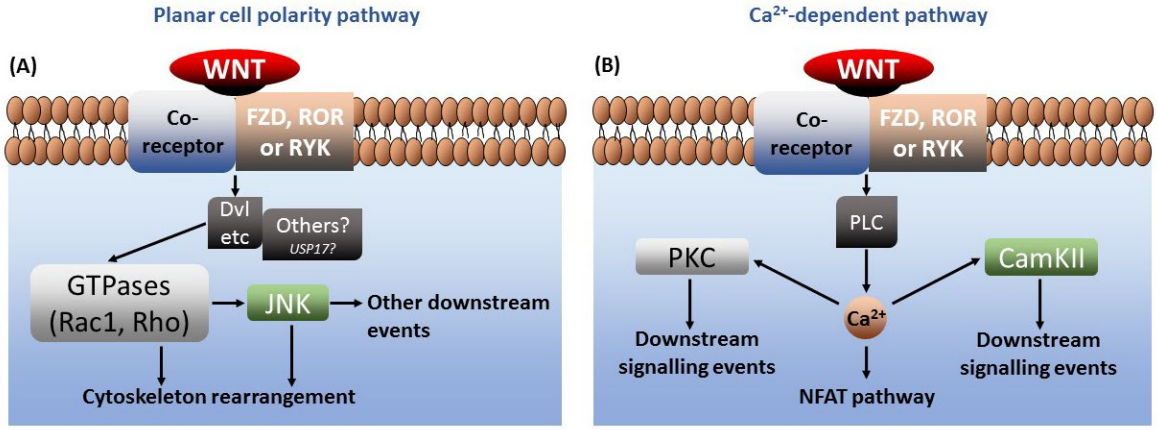

Figure 1.9: Non-canonical Wnt signalling pathways. Non-canonical Wnt ligand binding to receptor such as Frizzled (Fzd), Ror1/2 and Ryk along with poorly characterised co-receptors (different to LRP5/6) can initiate the planar cell polarity (PCP) pathway (A) or the Ca2+-dependent pathway (B). The PCP pathway involves Dishevelled (Dvl)-mediated activation of small GTPases such as Rac1 and Rho, which can directly regulate cytoskeleton rearrangement as well as activate c-Jun N-terminal kinase (JNK). JNK, in turn, can regulate cytoskeleton rearrangement and other downstream processes. The Ca^{2+}-dependent pathway results in phospholipase (PLC)-mediated increase of intracellular Ca^{2+} concentration, which increases the activity of C^{a+}-sensitive kinases such as protein kinase C (PKC) and calmodulin-activated kinase II (CamKII), while stimulating the Ca^{2+}-sensitive nuclear factor of T cells (NFAT) pathway. These mediators are able to influence a multitude of downstream signalling events.

The PCP pathway is initiated upon binding of a Wnt ligand to Fzd/Ror/Ryk receptors (James, Conrad and Moon, 2008). Although the exact downstream chain of events is not fully understood, this ligand-receptor interaction leads to Dishevelled (Dvl) protein-mediated GTP-activation of small GTPases such as RhoA and Rac1 (James, Conrad and Moon, 2008; Marinou

et al., 2012). This can directly induce cytoskeleton polarisation, affecting cell motility (James, Conrad and Moon, 2008), while it can also stimulate activation of JNK via phosphorylation (Nomachi *et al.*, 2008). JNK, in turn, is an established mediator of inflammation also involved in molecular IR induction (Han *et al.*, 2013), thus potentially linking PCP signalling with metabolic disease.

Regulation of intracellular Ca^{2+} levels comprises another way via which Wnt ligands can exert β-catenin-independent effects (James, Conrad and Moon, 2008). Wnt signalling has been found to work in synergy with phospholipase C to increase intracellular Ca^{2+} levels (Slusarski, Corces and Moon, 1997), eventually resulting in the activation of the Ca^{2+}-sensitive kinases PKC and CamKII (James, Conrad and Moon, 2008). In addition, Ca^{2+}-dependent Wnt signalling is able to activate the Ca^{2+}-sensitive nuclear factor of T cells (NFAT) pathway (James, Conrad and Moon, 2008), which is able to influence the transcription of various genes and is important in immune response regulation (Crabtree and Olson, 2002). Ca^{2+}-dependent Wnt signalling has mainly been explored in the context of embryonic development and its clinical relevance in adults is less clear.

1.6.2. Wnt signalling and metabolic disease

Plenty of evidence has linked Wnt signalling with obesity pathogenesis. Indeed, canonical Wnt signalling is believed to inhibit pre-adipocyte differentiation and stem cell commitment to adipocytes, while it may also facilitate local AT inflammation, further suppressing atherogenesis (Christodoulides *et al.*, 2009). By decreasing the energy-storing capacity and expandability of AT, canonical Wnt signalling may contribute to fat accumulation in organs such as the liver, facilitating the metabolic complications of obesity (Laudes, 2011; Gustafson *et al.*, 2013). Consistently, mutations of the gene encoding for LRP5, a key canonical Wnt

signalling co-receptor, differentially regulate body fat distribution and susceptibility to obesity, confirming a link between canonical Wnt signalling and obesity (Loh *et al.*, 2015).

On the other hand, the role of non-canonical Wnt signalling on AT biology is less well-understood. Non-canonical Wnt ligands such as Wnt5a are generally believed to promote adipogenesis directly and by inhibit β-catenin signalling via PKC- and CamKII-mediated β-catenin degradation (James, Conrad and Moon, 2008; Christodoulides *et al.*, 2009). However, Wnt5a has also been shown to inhibit adipogenesis via interactions with peroxisome proliferator-activated receptor γ signalling *in vitro* (Takada *et al.*, 2007). In addition, non-canonical Wnt5a signalling has been associated with AT inflammation independently of AT expansion (Fuster *et al.*, 2015). It is likely that the non-canonical effects of Wnt signalling may be dependent on ligand concentrations and receptor subtypes (Christodoulides *et al.*, 2009).

Wnt signalling has also been implicated in the pathogenesis of IR, the underlying cause of T2DM. This could indirectly result from the aforementioned effects of Wnt signalling on adipogenesis, which limit AT expandability, promote AT inflammation and facilitate fat deposition in the liver and skeletal muscle, ultimately compromising physiological glucose metabolism and promoting systemic IR (Christodoulides *et al.*, 2009). On the other hand, non-canonical Wnt signalling, especially the PCP pathway, may directly induce molecular IR via JNK activation and subsequent serine phosphorylation of IRS1 (James, Conrad and Moon, 2008; Han *et al.*, 2013; Catalán *et al.*, 2014; Fuster *et al.*, 2015).

1.6.3. Vascular effects of Wnt signalling

Wnt signalling has gradually emerged as a potentially significant mediator or vascular disease. Mutations in the *LRP6* gene have been independently associated with carotid artery stenosis in hypertensive patients (Sarzani *et al.*, 2011), while the non-canonical Wnt ligand Wnt5a has been found to be highly expressed in atherosclerotic lesions and its levels increase

in the circulation of humans with atherosclerosis (Christman *et al.*, 2008; Malgor *et al.*, 2014). Dkk1, an LRP5/6 inhibitor, is another Wnt signalling factor that has been linked with atherosclerosis in observational human studies, being highly expressed in atherosclerotic lesions and increased in the circulation of patients with atherosclerosis (Ueland *et al.*, 2009).

Experimental studies have further linked Wnt signalling with atherosclerosis mechanisms. Wnt5a, in particular, appears to be upregulated in macrophages of atherosclerotic lesions in humans (Bhatt and Malgor, 2014), while it may directly induce vascular IR and endothelial dysfunction as well as upregulated proinflammatory cytokine expression in human endothelial cells via non-canonical Wnt signalling (Kim *et al.*, 2010; Bretón-Romero *et al.*, 2016). On the contrary, canonical Wnt signalling may have protective, anti-inflammatory effects in atherosclerosis (Foulquier *et al.*, 2018). To this end, LRP5 appears to regulate monocyte differentiation to macrophages and macrophage uptake of cholesterol, while LRP5-knocout mice display increased plasma cholesterol, increased aortic lipid infiltration and larger atherosclerotic plaque burden (Foulquier *et al.*, 2018). Furthermore, Dkk1 has been shown to enhance the inflammatory interaction between platelets and endothelial cells via β-catenin inhibition (Ueland *et al.*, 2009). On the other hand, canonical Wnt signalling may contribute to VSMC proliferation and intima media thickness (Foulquier *et al.*, 2018). Non-canonical Wnt signalling could further affect VSMC by Rac1- and Rho- mediated migration, although this has not been explicitly studied in such cells (Marinou *et al.*, 2012). The contribution of VSMC migration versus proliferation to vascular disease is still controversial overall, since it may help stabilise atherosclerotic plaques but could also propagate long-term atherosclerotic disease progression (Bennett, Sinha and Owens, 2016).

1.6.4. Wnt5a: a key non-canonical Wnt ligand with cardiometabolic implications

Wnt5a is involved in complex Wnt signalling that is mainly mediated via non-canonical Wnt signalling and regulated by interactions with Sfrp proteins such as Sfrp5 (Kikuchi *et al.*, 2012). However, its ability to regulate canonical Wnt signalling is still controversial (Bhatt and Malgor, 2014). Although Wnt5a has been shown to directly induce β-catenin signalling in VSMCs, this was achieved with a supraphysiologic concentration of 300ng/ml (Mill *et al.*, 2014). It has been proposed that Wnt5a is predominantly a non-canonical Wnt ligand that, depending on ligand concentration and receptor type bioavailability, may stimulate or inhibit canonical Wnt signalling (Bhatt and Malgor, 2014). As mentioned before, Wnt ligands may be neutralised by proteins of the Sfrp family (Reya and Clevers, 2005; Schulte and Bryja, 2017). Sfrp5, in particular, has been shown, to selectively interact with non-canonical Wnt ligands such as Wnt5a and Wnt11 (Li *et al.*, 2008), and the balance between Wnt5a and Sfrp5 may be relevant as an index of non-canonical Wnt signalling capacity (Ouchi *et al.*, 2010).

Wnt5a has been proposed to regulate inflammatory responses and contribute to diseases such as obesity, IR and DM. Wnt5a is involved in macrophage activation (Pereira *et al.*, 2008) and facilitates the production of inflammatory cytokines and chemokines in a variety of tissue types and disease settings (Kikuchi *et al.*, 2012; Rauner *et al.*, 2012; Zhao *et al.*, 2014). Furthermore, Wnt5a is upregulated in AT from obese humans, where it facilitates AT inflammation (Catalán *et al.*, 2014). This proinflammatory effect of Wnt5a on AT is, in fact, independent of AT expansion (Fuster *et al.*, 2015), and may further be facilitated by the concomitant downregulation of its antagonist Sfrp5 in AT, as described in animal and human models of obesity (Ouchi *et al.*, 2010; Zuriaga *et al.*, 2017). The circulating ratio of Wnt5a to Sfrp5 has also been linked with T2DM (Lu *et al.*, 2013). The mechanistic link of Wnt5a with IR and DM is still unresolved, but it likely results indirectly from the inflammatory consequences of Wnt5a signalling on AT, while Wnt5a may also have direct molecular IR-

inducing effect in various cells types via JNK signalling (Kikuchi *et al.*, 2012; Fuster *et al.*, 2015; Bretón-Romero *et al.*, 2016).

Wnt5a has recently emerged as a regulator of vascular disease (Foulquier *et al.*, 2018). Although the complexity of Wnt signalling challenges the description of the integrated vascular effects of Wnt5a, it is evident that this non-canonical Wnt ligand may contribute to vascular disease pathogenesis via regulation of endothelial cell proliferation and migration (Masckauchán *et al.*, 2006; Cheng *et al.*, 2008), stimulation of endothelial cell inflammation (Kim *et al.*, 2010), propagation of vascular calcification (Woldt *et al.*, 2012) and induction of vascular IR and endothelial dysfunction (Bretón-Romero *et al.*, 2016). Observational and translational studies have corroborated the aforementioned *in vitro* findings, proposing a clinically relevant role for Wnt5a in vascular disease in humans (Foulquier *et al.*, 2018), demonstrating that Wnt5a is elevated in human macrophage-rich atherosclerotic plaque areas and in the circulation of patients with atherosclerosis (Christman *et al.*, 2008; Malgor *et al.*, 2014; Foulquier *et al.*, 2018), while Wnt5a-JNK signalling causes endothelial dysfunction in the context of human T2DM (Bretón-Romero *et al.*, 2016).

In summary, Wnt5a has emerged as a regulator of metabolic and vascular disease mainly via inflammatory pathogenic mechanisms (Kikuchi *et al.*, 2012; Foulquier *et al.*, 2018). However, the clinical translation of these observations in vascular disease remains elusive. In addition, the endocrine versus paracrine contribution of Wnt5a signalling in the human vascular wall is not explored. Furthermore, via its ability to induce Rac1 activation, Wnt5a may have direct links with NADPH-oxidases activity and vascular redox signalling, a major determinant of vascular pathophysiology, something that has not been explored previously.

1.7. Hypotheses and aims

This thesis explores two main hypotheses: a) Dysregulated vascular insulin signalling is a pathophysiological link between metabolic disease and atherosclerosis, resulting from the presence of vascular IR, and harnessing this link may have therapeutic implications in diabetic patients; b) AT-derived Wnt5a is a novel mechanistic link between metabolic disease and atherosclerosis via stimulating non-canonical Wnt signalling which could regulate vascular redox state.

In order to fully address these overall hypotheses, this thesis set specific experimental hypotheses, aiming to:

1. Explore the direct effects of insulin treatment (both human insulin and insulin analogues) on vascular redox state and endothelial function in humans with atherosclerosis
2. Explore the underlying mechanisms of the aforementioned effects and characterise vascular post-receptor insulin signalling in humans with atherosclerosis
3. Explore pharmacological strategies to reverse the presence of vascular insulin IR in humans with atherosclerosis
4. Discover links between dysfunctional PVAT and vascular redox state
5. Investigate the relationship of Wnt5a with clinical parameters of atherosclerosis
6. Characterise the biosynthetic ability of human AT with regards to Wnt5a and other Wnt ligands in obesity and systemic IR/DM
7. Determine the direct effects of Wnt5a on human vascular redox state and endothelial function in humans with atherosclerosis
8. Characterise downstream Wnt5a signalling in human vessels from patients with atherosclerosis

Chapter 2

Overview of the study design & methods

This chapter provides an overview of the study population, the participant recruitment process, the demographic characteristics of the patients enrolled as well as the background and details of the experimental procedures used for this thesis. More extensive details are provided in subsequent chapters regarding the relevant methods and study subsets used for individual experimental parts of this thesis.

2.1. The Oxford cohort for heart, vessels and fat

For the purposes of the experimental procedures described in this thesis, I used human samples from the Oxford cohort for Heart, Vessels and Fat (OxHVF), an ongoing project of the Division of Cardiovascular Medicine, University of Oxford aiming to create a large, extensively phenotyped cohort of patients undergoing cardiac surgery. The OxHVF cohort includes multiple clinical studies exploring cardiovascular disease pathogenesis. For the purposes of this thesis, I mainly used biological material and data from the AdipoRedOx study (REC 11/SC/0140). I also used some biological material and information from the Oxford risk factors and non-invasive imagine (ORFAN) study (REC 15/SC/0545) as explained in Chapter 4 of this thesis. A subset of this population was used as a "healthy control" group without coronary atherosclerosis and also to examine calcified plaque progression. More details for the subset of ORFAN patients used in this thesis are provided in Chapter 4.

The AdipoRedOx study includes male or female patients aged 18 years or above, diagnosed with cardiac disease and scheduled for coronary artery bypass graft (CABG) surgery or valve replacement/repair surgery, who are willing and able to give informed consent for participation

in the study. Exclusion criteria included the presence of active infectious diseases (e.g., hepatitis, HIV), active auto-immune or idiopathic diseases (e.g., rheumatoid arthritis, inflammatory bowel disease, psoriasis), active malignancy, end-stage liver or renal failure (requiring dialysis) and recent unstable coronary syndrome (within the previous 8 weeks). Patients receiving non-steroidal anti-inflammatory drugs, dietary supplements or antioxidant vitamins were also excluded from the study. In this dataset, 250 patients undergone CABG surgery at the Ippokration hospital, University of Athens, Greece were also included.

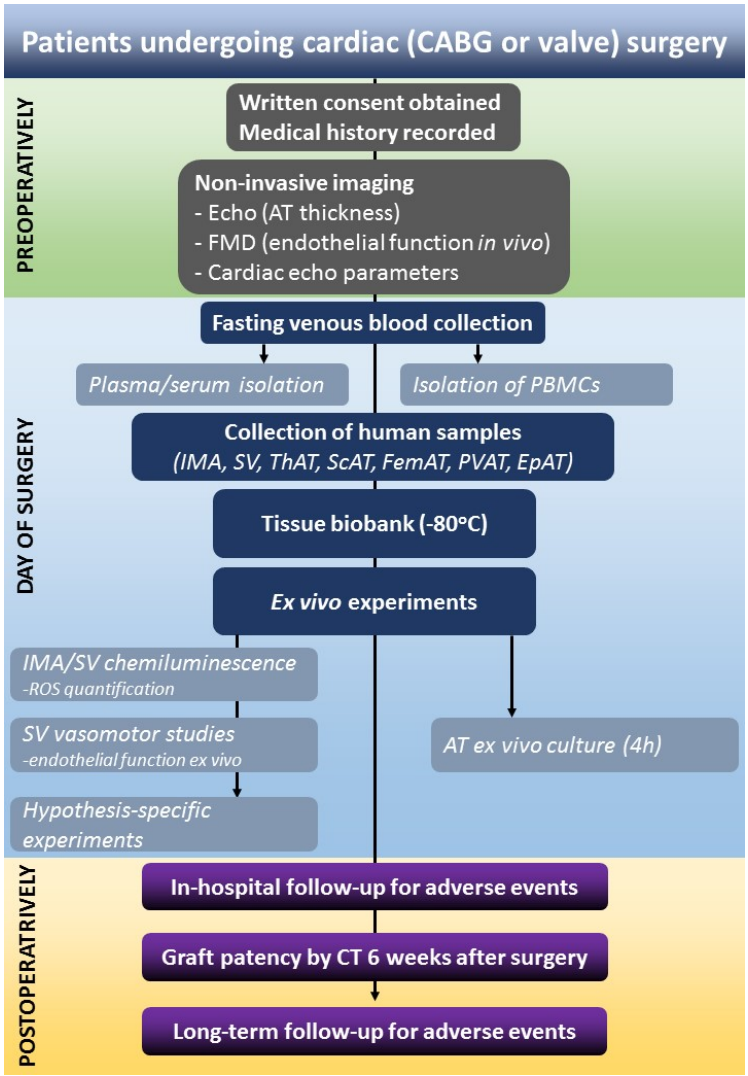

Figure 2.1: Overview of the AdipoRedOx study workflow. Patients undergoing coronary artery bypass grafting (CABG) or valve surgery are recruited and subjected to non-invasive ultrasonographic imaging to assess the thickness of various adipose tissue (AT) depots, flow-mediated dilation (FMD) of the branchial artery and cardiac echo parameters. On the day of surgery, fasting blood is collected and used for plasma, serum and peripheral blood mononuclear cell isolation. Internal mammary artery (IMA), saphenous vein (SV) as well as thoracic (ThAT), subcutaneous (ScAT), femoral (FemAT), epicardial (EpAT) and perivascular (PVAT) AT samples are collected and snap-frozen to generate tissue biobanks or used fresh for a number of *ex vivo* experiments. These include baseline evaluation of the superoxide ($O_2^{\cdot-}$) sources in vascular and myocardial samples, baseline characterisation of endothelial function and AT biosynthetic activity (via 4h culture) as well as individual prospectively designed experiments to test specific hypotheses. Following surgery, patients are followed-up for in-hospital adverse events, while graft patency is evaluated in CABG patients after 6 weeks by cardiac computed tomography (CT). Patients then enter a long-term follow-up phase where adverse events are recorded.

The recruitment process can be summarised as follows. Written informed consent is sought from all participants, which is followed by documentation of a full medical history with

emphasis on cardiovascular diseases. Non-invasive echo-based imaging studies are also performed upon recruitment for all patients. Prior to surgery, fasting blood is collected and used for plasma and serum isolation, which are then aliquoted and snap-frozen at -80ºC for subsequent experiments. During surgery, adipose tissue, vascular and myocardial samples are collected, transferred to the lab as soon as possible and processed for various bio-assays routinely performed with fresh vascular and adipose tissue samples. Additional tissue samples and blood are snap-frozen and stored at -80ºC for future experiments. Surplus fresh tissue is used for specific *ex vivo* experiments as required. An overview of the recruitment process and experimental workflow for AdipoRedOx is presented in Fig. 2.1.

2.1.1. Demographic characteristics, risk factor recording, in-hospital and long-term follow-up

Different subsets of the AdipoRedOx study cohort been used in individual chapters of my thesis. This is due to the fact that not all tissue samples were available for all patients and for all types of experiments. Detailed tables of demographics are provided in subsequent chapters for the study subsets used in each individual chapter.

As part of the routine recruitment process, full cardiovascular history is recorded, including information regarding traditional risk factors for cardiovascular disease (i.e., hyperlipidaemia, diabetes mellitus, smoking status and hypertension), family history of cardiovascular disease, New York Heart Association (NYHA) classification of heart failure, Canadian Cardiovascular Society grading of angina pectoris and cardiovascular medication profile. These are obtained either through the patients' medical records or through direct discussion with the participants. Additional information is sought in medical notes with regards to the angiographic extent of coronary artery disease, left ventricular ejection fraction, previous myocardial infarctions and their territories, previous transient ischaemic attacks (TIA)/stroke, presence of peripheral vascular disease (PVD), previous percutaneous transluminal coronary angioplasty (PTCA) and

any other relevant medical conditions. In addition, measurements of body mass index (BMI), waist and hip circumference are performed by nursing staff or the researcher obtaining consent.

Following surgery, information regarding EuroSCORE II, on- or off-pump CABG, clamp/total bypass time (in case of on-pump), number of vein and arterial grafts used are routinely obtained from the operative notes filed in the medical records. Participants are also followed-up during their hospitalisation for events such as post-operative atrial fibrillation, need for inotropic support and need for blood transfusion or administration of frozen plasma and platelets. Days spent in the cardiothoracic critical care unit as well as total length of stay are also recorded.

In addition to routinely in-hospital outcome monitoring, long-term mortality outcome data following surgery were collected on 15 December 2017 by linking the Office for National Statistics (ONS) data with National Health Service (NHS) Digital (previously the Health and Social Care Information Centre). Patients had previously provided consent and the collected data was first stored in a secured network and subsequently link-anonymized and analysed. All patients were followed-up from the day of surgery until the date of NHS Digital data collection (December 15, 2017) or death. Right-censoring was applied for all patients that were alive at the time of data collection. Follow-up time was defined as the number of days between the time of surgery and December 15, 2017 (for patients that were alive), or date of death. Adjudication of the cause of death was defined based on the International Statistical Classification of Diseases and Related Health Problems 10th Revision (ICD-10) codes, as reported in the ONS data. Cardiac mortality was defined as any death due to proximate cardiac causes (including myocardial infarction and chronic ischemic heart disease), corresponding to the ICD-10 codes of I20-I25 (ischemic heart diseases) and I30-53 (other forms of heart disease).

2.1.2 Sample collection

2.1.2.1. Blood sampling

Venous blood samples were obtained from the central line cannula after 8 hours of fasting, on the morning of surgery. The samples were immediately distributed to standard BD Vacutainer tubes. Orange Serum Separator Tubes were used for serum collection, while various anti-coagulants were sued for plasma collections (i.e., Li+/heparin (green), citrate (blue) and K2EDTA (purple)). The blood samples were immediately transferred to the Cardiovascular Clinical Research Facility (CCRF) laboratory, Division of Cardiovascular Medicine, University of Oxford, located on Level 1, Heart Centre, main John Radcliffe Hospital. Two K2EDTA vials of whole blood were frozen at -80ºC for future DNA extraction. The remainder of the plasma vials were spun at 3,000 g at 4°C for 15 minutes in a Labofuge 400R (Heraeus Instruments) centrifuge. Serum vials were kept at room temperature for 30 min, to allow blood to clot according to serum collection protocol, and were subsequently processed similarly to the plasma tubes after 30min, when the tubes were spun at 3,000 g for 15min and serum was collected. Plasma and serum were split into aliquots in barcode-labelled vials and kept at -80ºC until further processing.

2.1.2.2. Tissue collection & processing

Tissue samples were harvested by the surgeon performing the procedure and transferred in sterile ice-cold Krebs Henseleit buffer (KHLB, NaCl 120mM, KCl 4.7mM, $CaCl_2$ 2.5mM, $MgSO_4$ 1.2mM, KH_2PO_4 1.2mM, $NaHCO_3$ 25mM, glucose 5.5mM, pH=7.4, oxygenated for 5 min (95% O_2/5% CO_2)).

The following types of samples were collected:

- Pedicle left IMA, with its perivascular adipose tissue (peri-IMA PVAT) attached.

- Long saphenous vein (SV), with its perivascular adipose tissue (peri-SV PVAT) attached.
- ScAT, obtained from the site of the sternotomy.
- ThAT, excised from the mediastinal cavity, outside the pericardial sac.
- Femoral adipose tissue (FemAT), which was obtained from the subcutaneous region of the leg incision site.

Figure 2.2: Example internal mammary artery pedicle

All surgical samples were obtained before cannulation of the right atrium and before heparin administration. Each sample was always obtained at the same stage of the operation to limit inter-patient variability. All samples were kept on ice during the process and immediately transferred to the laboratory once sample collection was completed.

Figure 2.3: Example isolated internal mammary artery

SV and IMA samples were placed in a petri dish with a small amount of KHLB and gently flushed with sterile saline using a 25G needle and syringe to remove residual blood and clots. The PVAT surrounding the vessel was carefully dissected using sterile forceps and scalpel. Vessels (IMA and SV) were carefully cut into rings with a single slice using a 15 scalpel blade. Two SV and IMA rings were used for luminometry experiments to estimate superoxide generation and the specific contribution of NADPH-oxidases and uncoupled eNOS as described later. Up to four additional SV rings were used for organ bath vasomotor studies, to estimate

Figure 2.4: Processed, opened internal mammary artery rings

endothelial function *ex vivo* as explained in subsequent sections. Additional vascular rings were used for mechanistic *ex vivo* experiments as required.

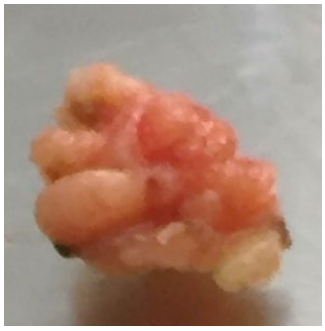

Figure 2.5: Example adipose tissue sample

All AT samples were cut into separate pieces using sterile scissors and/or scalpel. The pieces were washed in sterile phosphate buffered saline (PBS). Adventitia and connective tissue were removed and discarded. Adipose tissue pieces were kept at -80ºC in 1mL phenol (TRI reagent, Sigma) in order to be processed at a later stage for RNA isolation as explained later. For ScAT, ThAT and FemAT, large enough specimens were obtained to allow for additional pieces to be snap-frozen at -80ºC until further processing or used fresh for *ex vivo* adipose tissue explant culture as described later.

2.2. Biomarker measurements

2.2.1. Enzyme-linked immunosorbent assay

Enzyme-linked immunosorbent assay (ELISA) comprises a robust, commercially available method to quantify the levels of a target protein in a variety of biological samples such as plasma, serum and tissue/cell culture supernatants. Although procedural details vary slightly between different ELISA kits, the general process of this widely used technique is as follows: samples of interest along with quality controls and standards are incubated in 96-microplate wells pre-coated with anti-target primary antibody. This initial incubation step ensures that the target protein of each sample is captured by the antibody in the bottom of each well, and the remainder of samples is removed by multiple washes. Subsequently, a second, enzyme-conjugated anti-target primary antibody (having affinity for a different epitope of the target protein) is added to each well, resulting in a sandwich-type binding of the target protein.

Enzyme substrate is next added to each well, and absorbance of the enzymatic product at a specified wavelength (usually 450nm) is measured after stopping the well reaction with an appropriate stop solution at a kit-specific time point. A standard curve is then created using the absorbance values of the standards and the known standard concentrations, and the concentration of the target protein in each unknown sample is interpolated from the standard curve based on individual absorbance readings.

For the purposes of my project, ELISA was used to quantify the levels of Wnt5a (Cloud Clone Corp, SEP549Hu) and Sfrp5 (MyBiosource, MBS702373) in the plasma of the AdipoRedOx study participants. Plasma samples were diluted 1:2 prior to Wnt5a measurements or 1:400 prior to Sfrp5 measurements. Transgenic mouse plasma samples were also used undiluted to quantify systemic levels of Wnt5a by using a commercially available ELISA kit (Cloud Clone Corp, SEP549Mu). Representative standard curves for each kit are presented in Fig. 2.5.

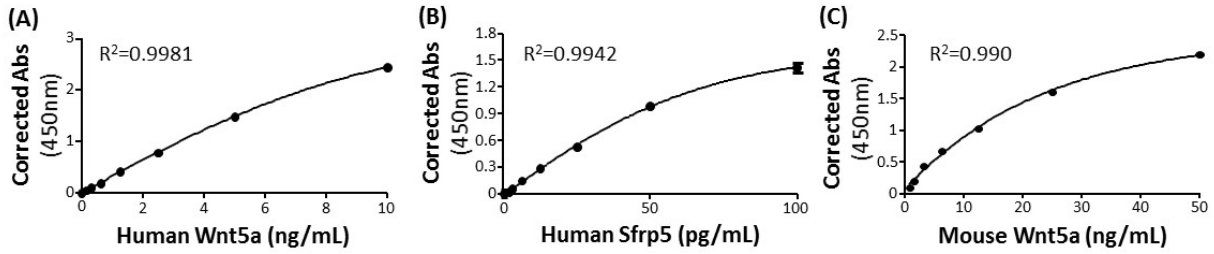

Figure 2.6: Representative standard curves for the ELISA kits used. Representative standard curves are presented for human Wnt5a (panel A, SEP549Hu), human Sfrp5 (panel B, MBS702373) and mouse Wnt5a (panel C, SEP549Mu). Curves were interpolated by non-linear curve fit by matching standard concentrations with corrected absorbance (Abs) at 450nm, and representative R-sq. coefficients are presented for each kit.

2.2.2. Medical laboratory measurements

Serum glucose and insulin were measured in clinical labs. Serum glucose was measured by the hexokinase method using commercially available kits (Abbott, Wiesbaden Germany). Serum insulin was measured by a chemiluminescent microparticle immunoassay using commercially available kits (Abbott, Wiesbaden Germany).

Homeostatic model assessment of systemic IR (HOMA-IR) was calculated by using the formula (glucose x insulin)/405, with glucose measured in mg/dL and insulin in mU/L. HOMA-IR is an established and frequently used surrogate marker of IR, reflecting the serum insulin concentration needed to maintain a given concentration of glucose, hence high HOMA-IR values indicate impaired glucose tolerance. Although proposed cut-off values vary amongst studies, it is generally believed that HOMA-IR should ideally be below 1.5 to indicate normal insulin sensitivity. HOMA-IR has certain limitations which influence its ability to reflect the whole IR milieu. Indeed, HOMA-IR is based on the post-absorptive feedback between insulin and glucose and is thus more reflective of hepatic IR (Thompson *et al.*, 2014), but may not accurately reflect tissue-specific variations in peripheral IR (Hoffman, Vicini and Cobelli, 2004). In addition, HOMA-IR appears to be a more sensitive marker of IR in the context of obesity, whilst this is compromised in individuals with normal or near normal weight, presumably because of the interference of adiposity & obesity with the insulin-glucose feedback (Kim, Abbasi and Reaven, 2004). However, HOMA-IR correlates well with clinical markers of IR such as adiposity as well as clinical outcomes such as cardiovascular risk, and is still useful in concisely reflecting the overall variations in whole body IR phenotype at any given point (Buchanan, Watanabe and Xiang, 2010; Thompson *et al.*, 2014), as used for the purposes of this work.

Serum DPP4 activity was also measured by a colorimetric kinetic commercially available kit according to the manufacturer's instructions (Enzo, BML-AK499-0001) in fasting serum samples.

2.3. Measurement of vascular superoxide production

Two methods were used in this thesis to detect and quantify vascular $O_2^{\cdot-}$:

- Lucigenin chemiluminescence was routinely used to quantify $O_2^{\cdot -}$
- Dihydroethidium (DHE) staining was employed to confirm the chemiluminescence results and allow for *in situ* visualisation of $O_2^{\cdot -}$ within the vascular wall.

2.3.1. Lucigenin-enhanced chemiluminescence

Vascular $O_2^{\cdot -}$ was routinely measured in intact, longitudinally opened vascular rings by lucigenin (5μM) enhanced chemiluminescence based on previously published methods (Margaritis *et al.*, 2013). Lucigenin is able to produce chemiluminescence upon reacting with $O_2^{\cdot -}$ anions, and measurement of this chemiluminescence can be used as a surrogate of $O_2^{\cdot -}$ levels in the system measured (Münzel *et al.*, 2002). The underlying mechanism is believed to include one-electron reduction of lucigenin (LC^{2+}) to lucigenin cation radical ($LC^{\cdot +}$), which then reacts with $O_2^{\cdot -}$ to generate light (Vásquez-Vivar *et al.*, 1997):

$LC^{2+} + e^- \rightarrow LC^{\cdot +}$

$LC^{\cdot +} + O_2^{\cdot -} \rightarrow$ products + chemiluminescence

Multiple studies have concluded that lucigenin chemiluminescence is one of the most sensitive methods of $O_2^{\cdot -}$ quantification (Münzel *et al.*, 2002; Guzik and Channon, 2005). On the other hand, the specificity of this method has been questioned because of the potential ability of lucigenin itself to generate $O_2^{\cdot -}$ via a mechanism described as redox cycling, where lucigenin (in concentrations greater than 20μM) reacts with oxygen to produce $O_2^{\cdot -}$ (Münzel *et al.*, 2002). However, its usefulness as a means of $O_2^{\cdot -}$ quantification when used at low concentrations (such as 5μM) has since been confirmed (Guzik and Channon, 2005). Therefore, lucigenin enhanced chemiluminescence with 5μM lucigenin remains a sensitive and specific method of $O_2^{\cdot -}$ quantification where the redox cycling phenomenon is not relevant.

The use of intact vascular segments instead of homogenates was selected on the basis of validation experiments previously run in my group reporting a strong correlation of the readouts recorded in intact tissue versus homogenates from same patients (Antonopoulos *et al.*, 2015), with the additional benefit of preserving the structural heterogeneity and cell type separation observed within the vascular wall, yielding more physiological responses.

2.3.1.1. Quantification of vascular baseline superoxide readout

In this thesis, lucigenin (5µM) enhanced chemiluminescence was the main vascular $O_2^{\cdot-}$ quantification method used routinely for both the baseline phenotyping of vascular redox state in oxHVF patients and the individual *ex vivo* experiments described in subsequent sections. This was achieved on a single-tube FB12 luminometer set to 37ºC to mimic the *in vivo* situation. Vascular segments were equilibrated in Krebs HEPES buffer (KHB, NaCl 99mM, KCl 4.7mM, $MgSO_4$ 1.2mM, KH_2PO4 1mM, $CaCl_2$ 1.9mM, NaHCO3 25mM, Glucose

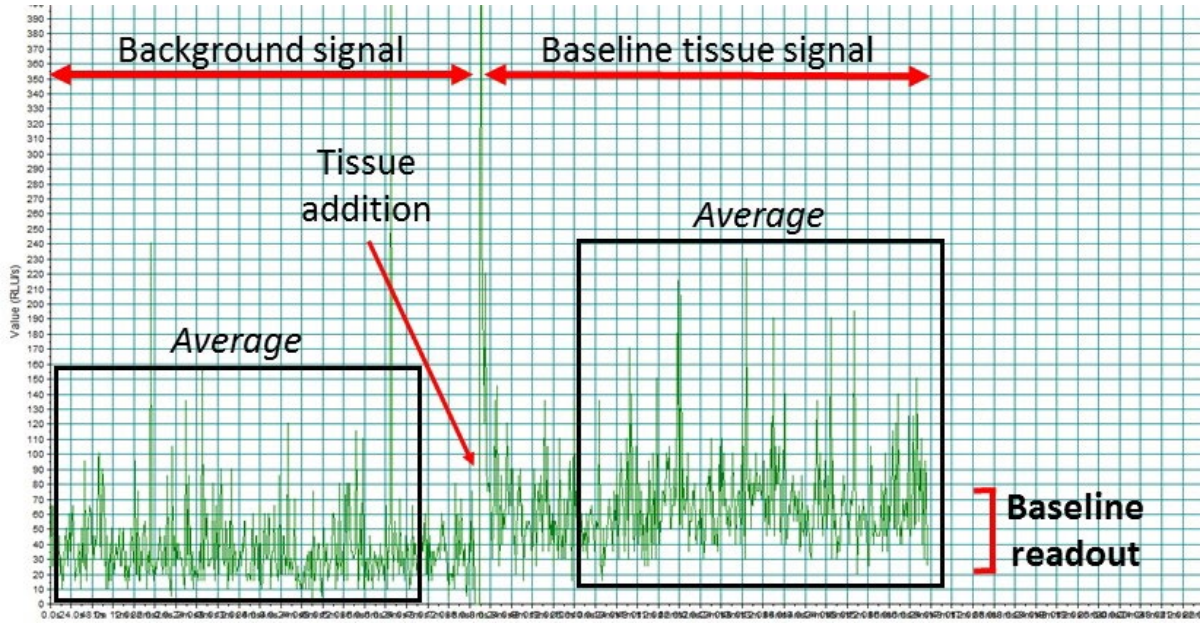

Figure 2.7: Representative basal superoxide ($O_2^{\cdot-}$) trace. The background signal is first recorded, which contains krebs hepes buffer plus lucigenin 5µM in the luminescence vial. Vascular tissue addition results in a signal increase, which corresponds to the baseline (unstimulated) tissue signal. Subtraction of the background from the tissue signal yields the baseline readout, which upon tissue mass correction reflects the baseline production of $O_2^{\cdot-}$ produced per mg of human vascular tissue.

11.1mM, NaHEPES 20mM) at 37ºC with 95% O_2/5% CO_2 for a pre-determined duration (20min for baseline cohort measurements; different incubations times for individual *ex vivo*

mechanistic experiments are described in relevant chapter methods sections). KHB with lucigenin was added in the luminometry vial and the stable background instrument signal was recorded. Vascular rings were then added in the luminometry vial and the new stable signal was recorded after plateau achievement. The final readout was calculated after subtracting the background signal from the baseline signal and expressed per mg of tissue. This signal reflects the baseline vascular $O_2^{\cdot-}$ production (Fig. 2.6).

2.3.1.2. Quantification of vascular NADPH-stimulated superoxide readout

To further increase the specificity of the assay and separate the isolated contributions of individual enzymatic $O_2^{\cdot-}$ sources to the overall baseline vascular $O_2^{\cdot-}$ production, additional stimulation and/or inhibition techniques were employed as described previously (Margaritis *et al.*, 2013, 2017; Antonopoulos *et al.*, 2015). To evaluate the contribution of NADPH-oxidases,

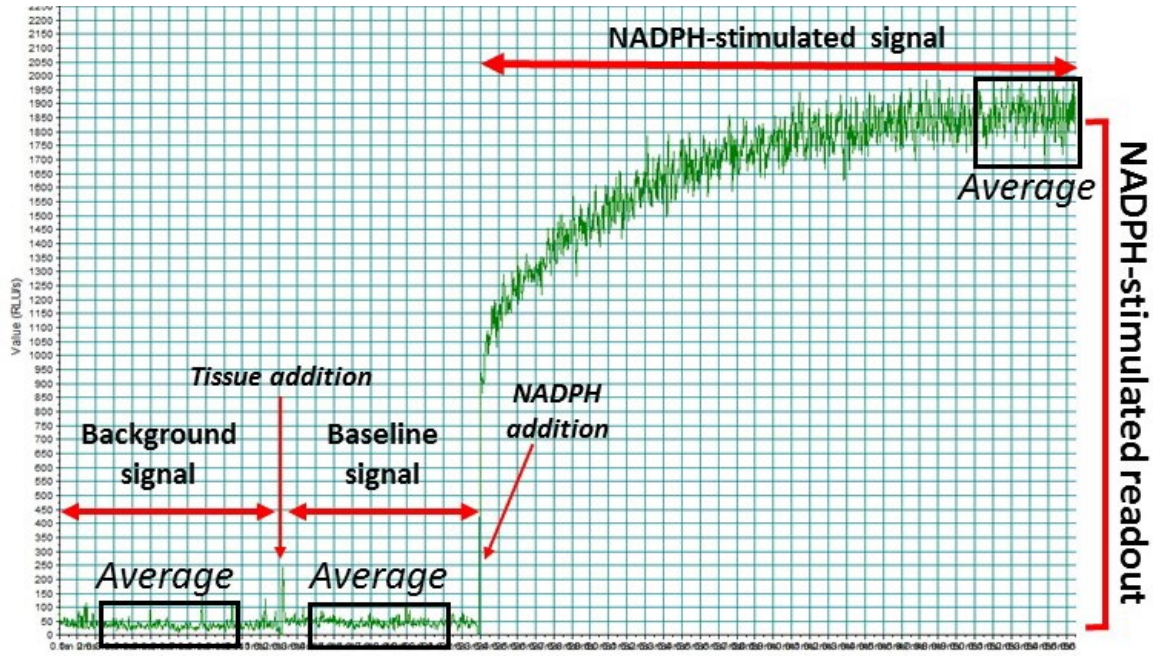

Figure 2.8: Representative NADPH-stimulated superoxide ($O_2^{\cdot-}$) trace. Following the recording of the background and the baseline tissue signal, NADPH 100μM is added in the reaction vial. This supra-physiological concentration saturates all NADPH-utilising catalytic enzyme sites, resulting in a massive increase of $O_2^{\cdot-}$. This corresponds to the NADPH-stimulated signal. The corrected NADPH-stimulated readout is then calculated by subtracting the background from the NADPH-stimulated signal, and is finally expressed per mg of vascular tissue. Considering that NADPH-oxidases are the main enzymes utilising NADPH, this readout is believed to reflect the activity of NADPH-oxidases in the human tissue sample tested.

I stimulated the vascular segments with NADPH at a supra-physiological concentration of 100μM after recording the baseline signal, resulting to saturation of the NADPH-oxidases

molecules. The recorded luminescence signal was drastically amplified with this intervention, acting as a chemical surrogate marker of NADPH-oxidases activity (Fig. 2.7). The final NADPH-stimulated readout was calculated after subtracting the background signal and expressed per mg of tissue.

2.3.1.3. Quantification of vascular Vas2870-inhibitable superoxide readout

NADPH is a substrate mainly, but not only, for NADPH-oxidases. Therefore, I also routinely used Vas2870 400µM 30min, an established irreversible inhibitor of NADPH-oxidases, to inhibit the NADPH-stimulated signal (Fig. 2.8). This intervention typically

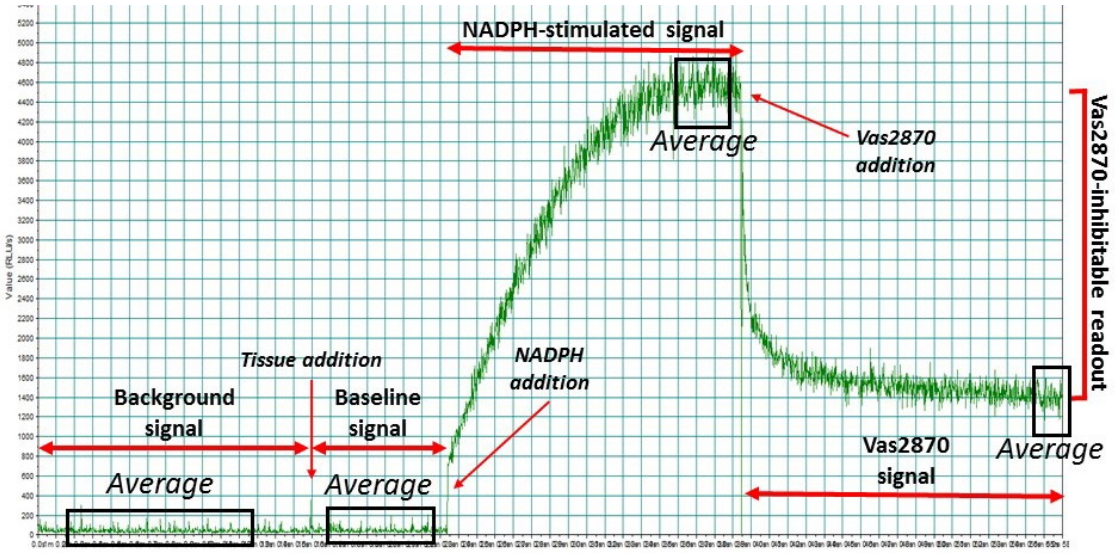

Figure 2.9: Representative Vas2870-inhibitable superoxide ($O_2^{\cdot-}$) trace. Following the recording of the background, baseline and NADPH-stimulated signal, Vas2870 400µM is added in the reaction vial to specifically inhibit NADPH-oxidases. This results in a reduction of the real-time from its NADPH plateau, corresponding to the Vas2870 signal. Subtraction of the Vas2870 30min signal from the NADPH-plateau corresponds to the Vas2870-inhibitable readout, namely the fraction of the NADPH-stimulated signal that is inhibited by Vas2870 and thus comes directly from NADPH-oxidases. This is expressed per mg of tissue and reflects the vascular NADPH-oxidases activity.

resulted in a ~65% inhibition of the NADPH-stimulated signal. The Vas2870-readout was

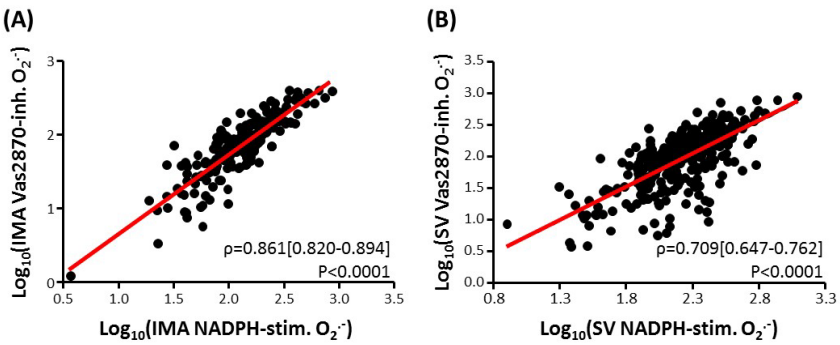

Figure 2.10: NADPH-stimulated and Vas2870-inhibitable superoxide ($O_2^{\cdot-}$) correlation. The NADPH-stim. readout was significantly and strongly correlated with the Vas2870-inh. readout in internal mammary artery (IMA, panel A) but also in saphenous vein (SV, panel B).

calculated by subtracting the Vas2870 30min signal from the NADPH-stimulated plateau and expressed per mg of tissue.

The vascular NADPH-stimulated and Vas2870-inhibitable signals are highly correlated in AdipoRedOx cohort (Fig. 2.10), confirming that NADPH-oxidases are not the only, but the single most important enzymes using NADPH as a substrate in human vascular tissue.

2.3.1.4. Quantification N(G)-Nitro-L-arginine methyl ester (L-NAME) delta superoxide readout

The coupling status of eNOS and the contribution of uncoupled eNOS to overall $O_2^{\cdot-}$ generation was evaluated by using the competitive eNOS inhibitor N(gamma)-nitro-L-arginine methyl ester (L-NAME, 1mM) as described previously (Margaritis *et al.*, 2013).

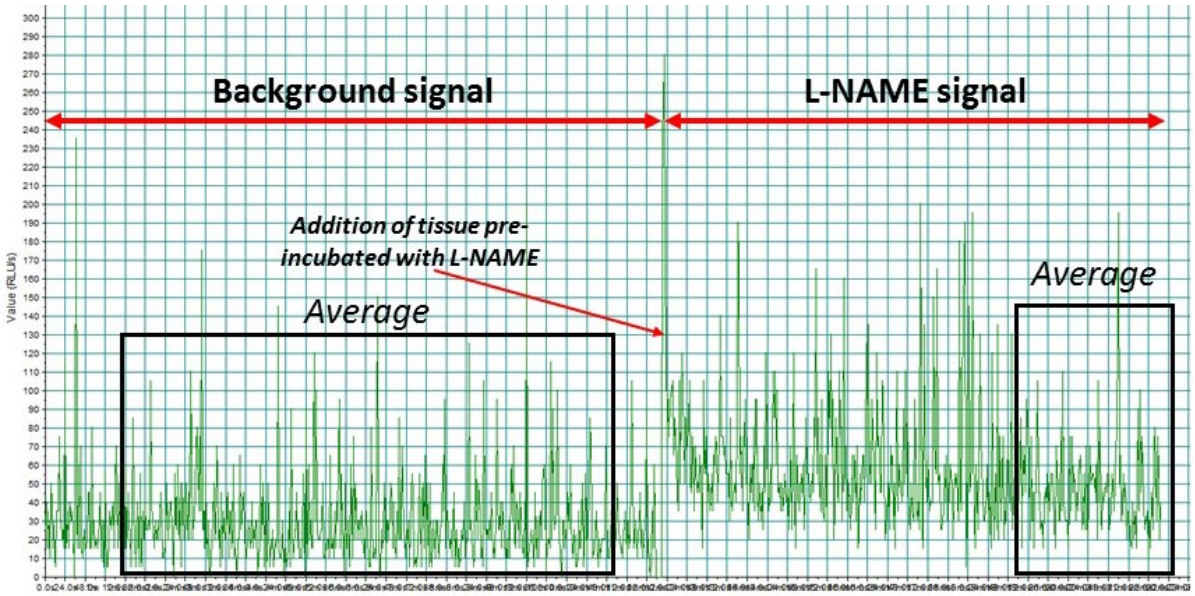

Figure 2.11: Representative L-NAME delta superoxide ($O_2^{\cdot-}$) trace. Background signal was recorded and then the L-NAME reading was obtained by adding vascular tissue incubated with L-NAME. Background was subtracted by this L-NAME reading, which was then adjusted for sample weight in mg. The baseline $O_2^{\cdot-}$ readout was quantified on a second ring from same patients, and it was subtracted from the weight-adjusted L-NAME reading. This final readout reflects the coupling status of endothelial nitric oxide synthase.

KHB with L-NAME 1mM and lucigenin 5µM was used to record the background signal, and vascular tissue pre-incubated with L-NAME 1mM for 20min at 37ºC with 95% O_2/5% CO_2 was then added. The tissue plateau was corrected by subtracting the background and dividing by the vascular ring weight (Fig. 2.10). From this value, the normalised baseline readout

(recorded using a second ring from same patients) was subtracted. This second ring was equilibrated for 20min at 37°C with 95% O_2/5% CO_2 and used for recording of the baseline, NADPH-stimulated and Vas2870-inhibitable readouts explained previously. The final L-NAME readout reflects the coupling status of eNOS. Positive values indicate that eNOS was mainly coupled in the measured tissue, while negative values reflect the presence of significant eNOS uncoupling.

2.3.2. Dihydroethidium staining & confocal microscopy

The results of certain *ex vivo* mechanistic results were further validated by *in situ* visualisation of vascular $O_2^{\cdot -}$ generation in intact tissue sections detected by confocal microscopy following DHE staining. DHE is a cell-permeable molecule able to react with intracellular ROS, leading to formation of ethidium which then binds to nuclear DNA exhibiting red fluorescence, allowing for a semi-quantitative evaluation of intracellular ROS levels (Benov *et al.*, 1998). Reaction of DHE with $O_2^{\cdot -}$, in particular, results in the formation of a specific product, 2-hydroxyethidium, which can be accurately and quantitatively detected by high pressure liquid chromatography (HPLC) (Zhao *et al.*, 2005). Although measurement of 2-hydroxyethidium by HPLC is considered to be the gold standard for $O_2^{\cdot -}$ quantification in terms of specificity, it is not sensitive enough and requires large effect sizes to yield reliable results. On the other hand, DHE staining is not equally specific for $O_2^{\cdot -}$ and can react with other ROS such as hydrogen peroxide or peroxynitrite (Griendling *et al.*, 2016). This is a limitation of DHE staining, and its use should be combined with other methods of $O_2^{\cdot -}$ quantification.

For the purposes of this thesis, *in situ* $O_2^{\cdot -}$ production was visualised in cryosections of IMA segments placed in optical cutting temperature (OCT) compound (VWR, USA) after being subject to certain *ex vivo* incubations in select patients (as described in following chapters) and snap frozen in -80°C until processed. On the day of the assay, cryosections (30μm) were

obtained on a microcryotome (-30ºC) at the Wellcome Trust Centre for Human Genetics, Old Road Campus, University of Oxford. Sections were mounted onto glass slides, marked with a PAP pen and incubated with KHB or KHB+Vas2870 (400 µM to inhibit NADPH-oxidases) for 30 minutes at 37ºC. Buffer was then removed and sections were incubated in the dark with DHE (2µM) for 5 minutes at 37ºC. Buffer was then quickly aspirated after 5min and reactions stopped with fresh ice-cold KHB. The sections were secured with a cover slip on ice and kept in the dark until fluorescence microscope visualisation.

Fluorescence images of the vascular wall were obtained from each vessel quadrant on a Zeiss LSM 510 META laser scanning confocal microscope at the Wellcome Trust Centre for Human Genetics, Old Road Campus, University of Oxford. Images were obtained by using an excitation wavelength of 488nm and an emission wavelength of 585nm. In all cases, cryosections from individual patients were processed and visualised on the same day and vascular rings ±Vas2870 were analysed in parallel with identical imaging parameters in a blinded fashion.

2.4. Organ bath vasomotor studies with human vessels

Endothelial function *ex vivo* was evaluated in an organ bath setting using SV rings from patients of the AdipoRedOx study undergoing CABG surgery. The underlying principle is based on the ability of acetylcholine (Ach) to induce endothelium-dependent vasorelaxation *ex vivo* by stimulating NO production via muscarinic receptor signalling (Wanstall *et al.*, 2001).

Vasomotor studies were performed in a Radnotti double-walled 15ml glass chamber organ bath set-up consisting of four functional experimental chambers. Each experimental chamber is fitted with a metal hook fixed on an immobile support, while a second hook hangs from a non-absorbable suture attached to a force transducer (AD Instruments). The force transducers

are connected to an amplifier (Octal Bridge Amp – AD Instruments) and reader (PowerLab 8/35 – AD Instruments), in turn connected to a desktop computer using LabChart software (AD Instruments). Vascular rings are stabilised between the two hooks, and tension exerted on the force transducer via the upper hook and its associated suture generates an electric signal from the transducer, which travels through the amplifier and reader and is finally converted into grams of tension by the software.

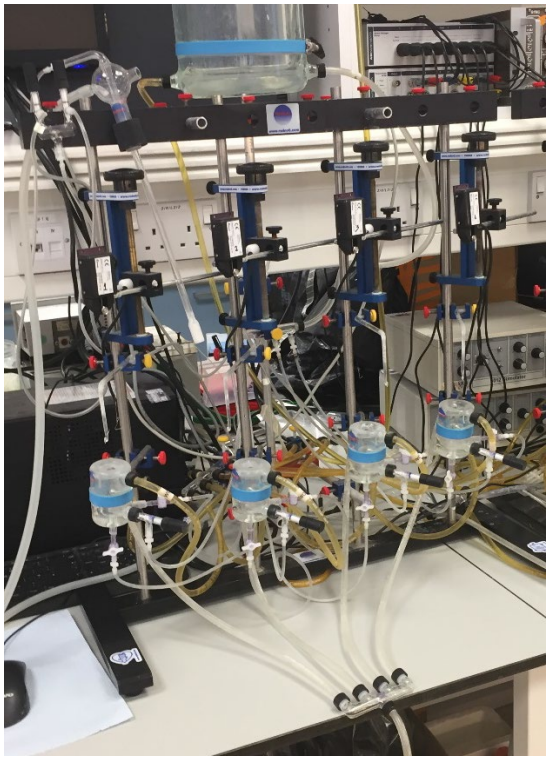

Figure 2.12: Organ bath Radnotti instrument used for *ex vivo* vasomotor studies. This instrument was used for evaluation of endothelial function *ex vivo* in saphenous vein segments.

SV rings were positioned so that the two metal hooks were inserted through the ring lumen with minimal force just to keep the rings in place. The chambers were then filled with oxygenated KHLB and raised, immersing the vascular rings with KHLB, which was stored in a 2L double-walled glass tank. The system was equilibrated at 37ºC via water flowing in the inter-wall space of both the chambers and tank from a pump-fitted water bath (Grant Instruments) set to 37ºC. KHLB in the chambers and the storage tank was continuously oxygenated with 95% O_2/5% CO_2 via a built-in air delivery system. Flow of KHLB in and out of the chambers and gas supply was controlled by individual valve setups in each chamber.

At first, SV rings were equilibrated at minimal tension in the organ bath for 30 minutes and then gradually subjected to passive 1g force increments every 3min until achieving a resting tension of 3g. Once this resting tension was achieved, vessel viability was determined by assessing the contractile responses to potassium chloride (KCl 60 mmol/L). Vessel rings failing

to constrict in response to KCl were deemed non-viable and the experiment was aborted. Viable rings were washed 3 times with KHLB and allowed to return to a resting tension of 3g.

The next phase of the routine experimental procedure comprised the evaluation of contractile responses to phenylephrine (PE, α-adrenergic agonist). A PE-induced constriction dose-response curve was created by adding increasing concentrations of PE in the experimental chamber (PE, 10^{-9} M to 10^{-5} M). At the end of the PE curve, rings were washed 3 times with new KHLB and allowed to return to a resting tension of 3g.

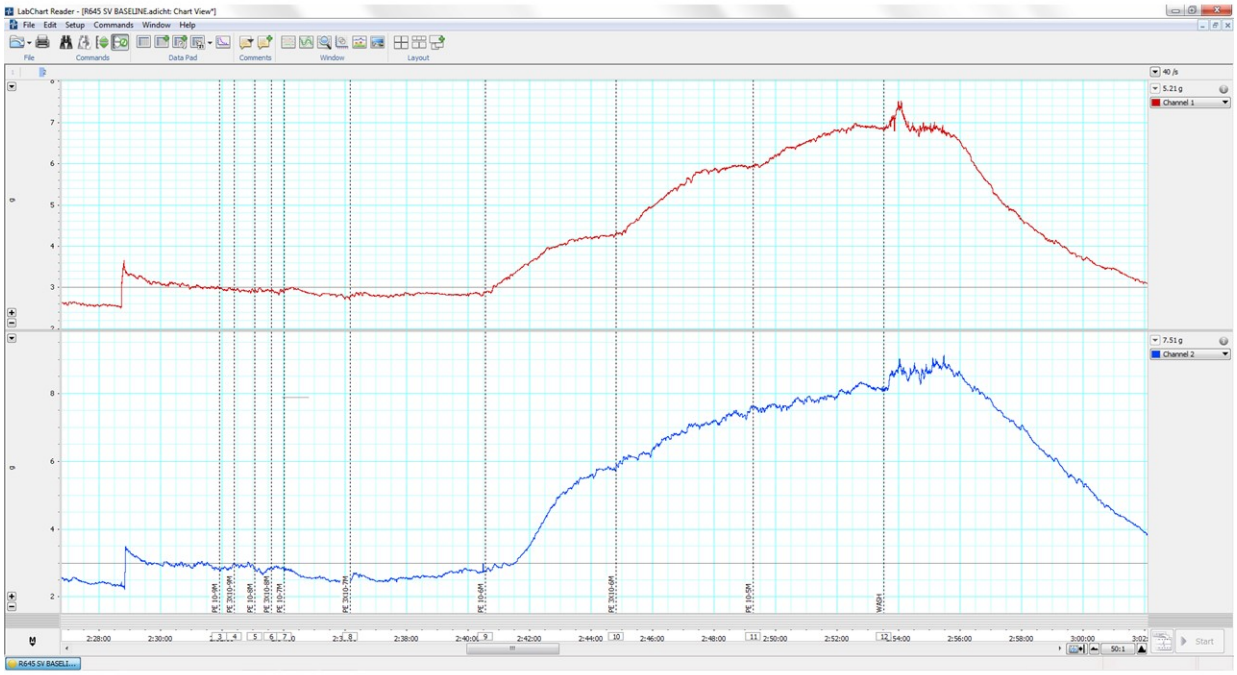

Figure 2.13: Example phenylephrine (PE) dose-response curve. Saphenous vein responses to PE were examined over a range of PE concentrations (10^{-9}M – 10^{-5}M).

Endothelial function *ex vivo* was evaluated at this stage by performing an Ach-induced relaxation dose-response curve (ACh, 10^{-9} M to 10^{-5} M) following pre-constriction with PE $3x10^{-6}$ M. Rings were finally washed and allowed to equilibrate back to 3g resting tension.

For mechanistic *ex vivo* experiments testing the effect of certain interventions on endothelial function *ex vivo*, rings were then incubated with the intervention(s) of interest or

vehicle for a pre-defined period of time. At the end of this incubation step, the PE pre-constriction/Ach dose response step was repeated. Post-incubation Ach curves were corrected for the pre-incubation curves per each individual ring, and the effect of the intervention(s) of interest was then evaluated comparing control versus treatment-incubated rings. More information about specific *ex vivo* setups is provided in subsequent chapters.

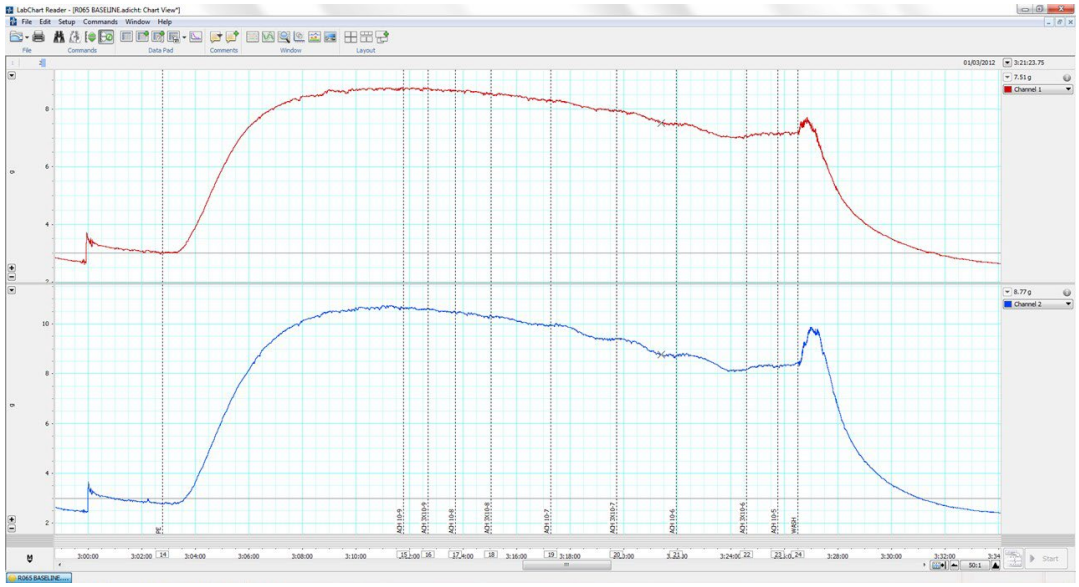

Figure 2.14: Example acetylcholine (Ach) dose-response curve. Saphenous vein responses to Ach were examined over a range of Ach concentrations (10^{-9}M – 10^{-5}M) following pre-constriction with PE 3µM.

At the end of each experiment, rings were pre-contracted again with PE $3x10^{-6}$ M and exposed to L-NAME 100µM in-chamber for 20min, and relaxations in response to the

Fi were
ex and
en

endothelium-independent NO donor sodium nitroprusside (SNP, 10^{-10} M to 10^{-6} M) were evaluated. In the context of eNOS inhibition, these relaxations reflect the muscular component of vascular relaxation, i.e., the ability of the vascular smooth muscle cells to respond to NO.

All readings were recorded using LabChart software. Vasodilatory responses were measured off-line from the LabChart file and expressed as a percentage of the pre-constricted tension.

2.5. Gene expression studies

2.5.1. RNA isolation & purification

Samples were kept in 1mL phenol (TRI reagent, Sigma) at -80ºC until processed. RNA was separated by phenol:chloroform extraction and purified by an automated magnetic beads based method, using the MagMAX MirVana total RNA isolation kit (Thermo Fisher Scientific) on a KingFisher flex magnetic particle processor.

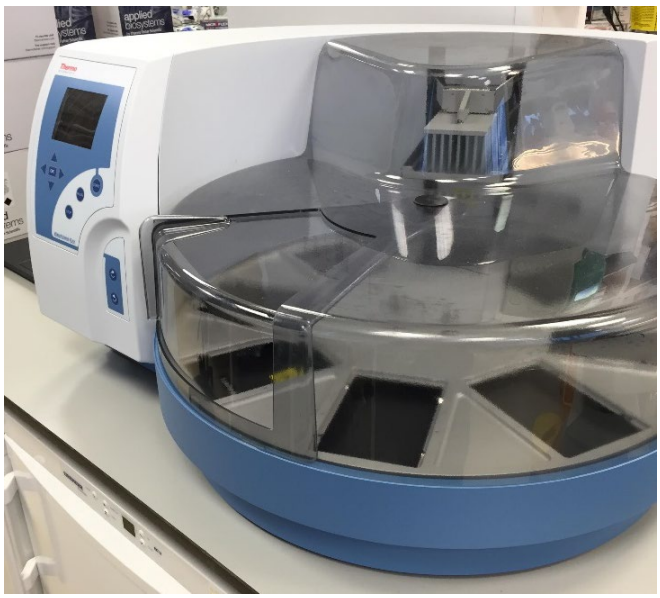

Figure 2.16: KingFisher flex magnetic particle processor. This instrument was routinely used for semi-automated purification of RNA for the purposes of this thesis.

Samples were thawed on ice and homogenised for 1min using a pre-cooled Polytron homogeniser (Kinematica AG). Chloroform was added to the homogenates (200µL for a 1:5 chloroform:phenol ratio). Samples were vigorously shaken by hand for 1min, then left to rest at room temperature for 3min, and finally spun at 13,300 rpm for 15 min, at 4ºC. 500µL of the clear, aqueous phase containing the RNA were then

transferred in deep 96-well plates and mixed with 300μL of isopropanol and 20μL of beads binding mix. Additional 96-well plates were prepared for washing, DNase treatment, release of RNA from the magnetic beads and elution. All plates were mounted on the KingFisher flex magnetic particle processor and RNA purification was performed in an automated way. At the end of the process, purified RNA quality and quantity were determined using a Nanodrop® ND-1000 Spectrophotometer. The 260/280 ratio was greater than 2.0 for ~97% of the samples (greater than 1.9 for virtually all samples), while the 260/230 ratio was greater than 1.5 for all samples.

2.5.2. Reverse transcription of RNA – cDNA library creation

RNA was reverse-transcribed to cDNA using the SuperScript VILO master mix (Thermo Fisher Scientific) according to the manufacturer's instructions. Up to 1μg of RNA was reverse-transcribed in every reaction. Reaction conditions were as follows: 25°C for 10 minutes (primer extension step), 42ºC for 2 hours (cDNA synthesis step) and finally 5 min at 85ºC (reverse transcriptase inactivation step).

Part of the cDNA was used to create 100μL of diluted working cDNA plates that were subsequently used for gene expression assays. TE buffer (10mM Tris HCl, 1mM EDTA, pH=8.0) was used as diluent and the working plate cDNA concentration was 1.85ng/μL. Another part of the cDNA of all samples across the library was pulled together to generate a standard sample which was then used for the analysis of the gene expression assays as described below. The remainder of the cDNA was snap-frozen at -80ºC and stored as stock.

2.5.3. Gene expression studies using quantitative PCR

Gene expression assays were performed by inventoried TaqMan probes (Applied Biosystems). Quantitative PCR reactions were run in triplicates in 384 well plates using 5ng of cDNA per reaction (2.7μL of cDNA, 3.0μL of TaqMan gene expression master mix and 0.3μL of TaqMan

probe per reaction). A standard curve with serial dilutions (1:10, 1:25, 1:50, 1:100 and 1:200) of the cDNA standard mentioned previously was run in individual plates to calculate the plate amplification efficiency. Runs were performed on a QuantStudio 7 Flex real-time PCR system (Thermo Fisher Scientific).

The analysis of the results was performed using the Pfaffl method (Pfaffl, 2001), where the target gene expression was corrected for an endogenous normalising gene and finally expressed relative to the highest standard which was run on every plate, minimising the between-plates variability. Calculations were based on the following equation:

$$Rel.Expression = \frac{E_{TG}{}^{-(Ct_{TG,S}-Ct_{TG,R})}}{E_{HK}{}^{-(Ct_{HK,S}-Ct_{HK,R})}}$$

Where:

E_{TG}: Efficiency of the PCR reaction for the target gene

$Ct_{TG,S}$: Ct value of each experimental sample for the target gene

$Ct_{TG,R}$: Ct value of the reference sample (highest standard) for the target gene

E_{HK}: Efficiency of the PCR reaction for the housekeeping gene

$Ct_{HK,S}$: Ct value of each experimental sample for the housekeeping gene

$Ct_{HK,R}$: Ct value of the reference sample (highest standard) for the housekeeping gene

This formula is equivalent to the $2^{-\Delta\Delta Ct}$ when both efficiencies are equal to 2. All probes displayed an efficiency ranging from 1.85-2.05 and all standard curves had R^2>0.97 upon linear curve fitting.

Figure 2.17: QuantStudio7 quantitative real-time PCR instrument. This instrument was used for all PCR results presented in this thesis.

Table 2.1: List of TaqMan probes used in this thesis

Target Gene	TaqMan Probe ID
Human PPIA	Hs99999904_m1
Human GAPDH	Hs02786624_g1
Human SFPR5	Hs00169366_m1
Human WNT5A	Hs00998537_m1
Human WNT5B	Hs01086864_m1
Human WNT1	Hs00180529_m1
Human WNT3A	Hs00263977_m1
Human WNT3	Hs00902257_m1
Human WNT9A	Hs01573829_m1
Human WNT9B	Hs00287409_m1
Human WNT10A	Hs00228741_m1
Human WNT10B	Hs00928823_m1
Human WNT11	Hs01045906_m1
Human WNT6	Hs00362452_m1
Human WNT4	Hs01573505_m1
Human WNT2	Hs00608224_m1
Human WNT16	Hs00365138_m1
Human WNT2B	Hs00921614_m1
Human WNT7A	Hs01114990_m1
Human WNT7B	Hs00536497_m1
Human WNT8A	Hs00230534_m1
Human WNT8B	Hs00610126_m1
Human FZD2	Hs00361432_s1
Human FZD5	Hs00258278_s1
Human ROR1	Hs00938677_m1

Mouse WNT5A	Mm00437347_m1
Mouse 18S RNA	Mm04277571_s1

2.6. Measurement of vascular biopterin content

Vascular BH4, BH2 and biopterin (B) contents were quantified by HPLC followed by electrochemical (for BH4) and fluorescent (for BH2 and B) detection.

Vascular rings of SV or IMA having undergone certain *ex vivo* incubations were snap-frozen and stored at -80°C until assayed. On the day of the assay, vessel rings were subjected to 3 freeze/thaw cycles in re-suspension buffer (50 mM phosphate buffered saline, 1 mM Dithioerythritol (DTE), 1mM EDTA, pH=7.4) to induce endothelial cell lysis, and samples were centrifuged for 15 min at 13,000 rpm, 4ºC to remove the tissue leftovers. Supernatants were transferred to new, pre-cooled micro tubes and ice-cold precipitation buffer (H_3PO_4 1M, trichloroacetic acid (TCA) 2M and DTE 1mM) was added. Samples were vigorously mixed and then centrifuged for 10min at 13,000 rpm, 4°C.

Samples were injected onto an isocratic HPLC system and quantified using sequential electrochemical (Coulochem III, ESA Inc., UK) and fluorescence (Jasco, UK) detection. HPLC separation was performed using 250mm, ACE C-18 columns (Hichrom, UK) and ultrapure electrochemical grade mobile phase consisting of 50mM sodium acetate, 5mM citric acid, 48µM EDTA and 160 µM DTE (pH=5.2) at a flow rate of 1.3 ml/min. BH4 was measured directly by the electrochemical detector (background currents of +500 nA and -50 nA were used for the detection of BH4 on electrochemical cells E1 and E2, respectively). BH2 and B were measured as separate chromatographic picks in the same sample using a Jasco FP2020 fluorescence detector serially connected to the electrochemical detector. Quantification of BH4, BH2 and B was by comparison with external standards (1nM – 0.1µM) prepared from

10 µM BH4, BH2 and B (Schircks, Zurich) stocks with serial dilutions in ice-cold re-suspension buffer. Individual standard curves were constructed with fresh standards for individual batch runs. Representative peaks are presented in Figures 2.17 and 2.18.

All samples were loaded on the HPLC auto-sampler in random coded batches (of up to 24 samples), blinded to the group identity of each sample, while analysis was also blinded. Results were eventually expressed as pmol/g of vascular tissue.

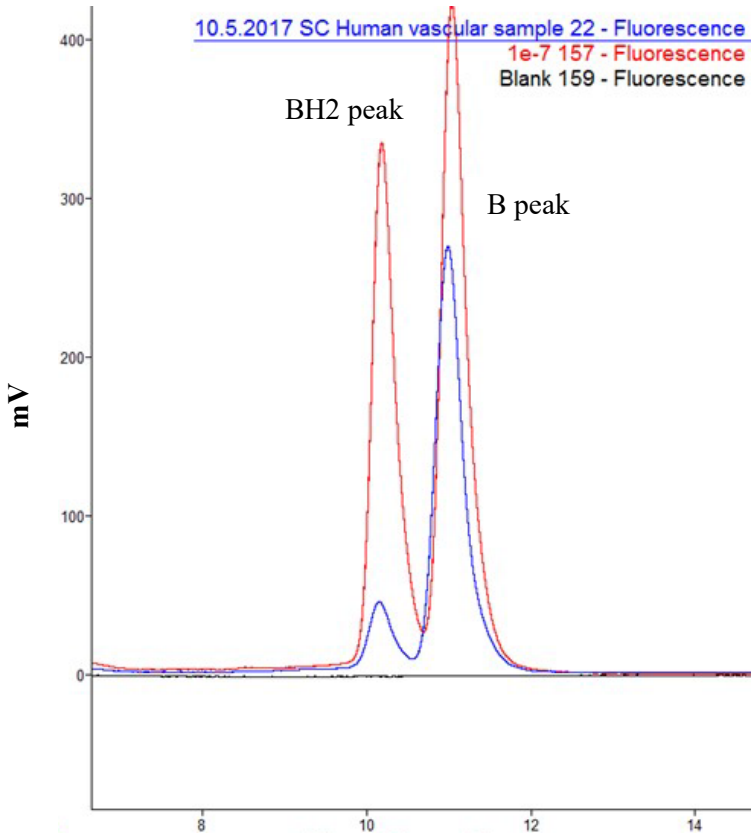

Figure 2.18: Dihydropterin (BH2) and biopterin (BH4) example peak. BH2 and B were both measured by sequential electrochemical detection and quantified by interpolation of standard curve constructed from serial BH4 standard dilutions. The blue peaks indicate an example experimental sample while the red and black lines indicate the highest BH4 standard (0.1µM) and blank respectively in a single run.

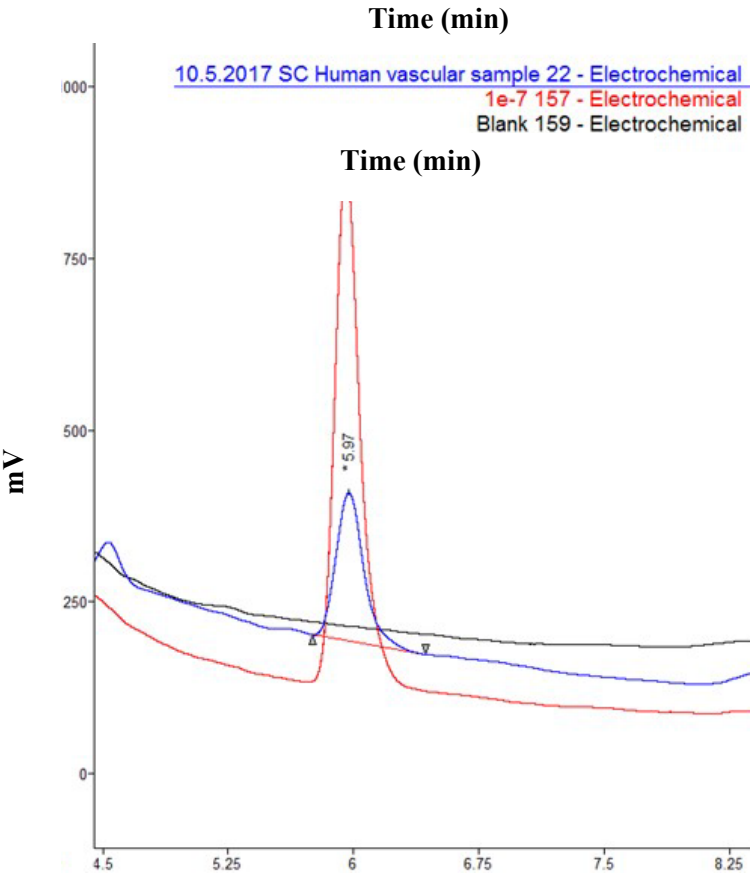

Figure 2.19: Tetrahydrobiopterin (BH4) example peak. BH4 of experimental samples was detected by fluorescence measurement and quantified by interpolation of standard curve constructed from serial BH4 standard dilutions. The blue peak indicates an example experimental sample while the red and black lines indicate the highest BH4 standard (0.1µM) and blank respectively in a single run.

2.7. Western immunoblotting in vascular tissue

Phosphorylated and total protein levels were semi-quantified using Western immunoblotting analysis. This method includes protein separation by a polyacrylamide gel, transfer of separated proteins on nitrocellulose membranes and incubation of the membranes with primary antibodies with specific affinity for the proteins of interest (either phosphorylated or total).

Vascular tissue samples were homogenized in radioimmunoprecipitation assay (RIPA) buffer (10µL per mg tissue) supplemented with protease and phosphatase inhibitor cocktails (Cell Signalling Technologies) in an LT tissue lyser (Qiagen) for 2min by pre-cooled steel beads. Homogenates were centrifuged at 13,000 rpm for 15 minutes at 4 ºC to get rid of debris, and supernatant protein concentrations were quantified by a commercially available bicinchoninic acid assay kit (BCA^{TM} Protein Assay kit, Pierce, UK).

Protein lysates (10-20µg) were then mixed with denaturing agent (dithiothreitol) and LDS NuPAGE loading buffer (Thermo Scientific, UK), so that all components reached 1x concentration and sample volumes were equal (ranging from 20-27µl). Samples were then denatured by incubation at 95°C for 5 minutes, and separated by protein electrophoresis using precast 10-well 4-20% gradient Bis-Tris/SDS gels (Thermo Scientific, UK) in an XCell SureLock mini-gel NuPAGE system. All gel wells were filled with an equal amount of volume and protein, with precision plus protein kaleidoscope pre-stained protein standard used as protein molecular weight marker (Biorad). MOPS (3-(N-morpholino)propanesulfonic acid) buffer was used as running buffer and electrophoresis was carried out at 120 Volts for 1.5 hours by a BioRad PowerPac Basic.

After electrophoresis completion, proteins were transferred to nitrocellulose membranes (Amersham Protran 0.2 µm, GE Healthcare, UK) by using a BioRad wet transfer system (100V for 1.5 hours at 4°C) using 1X NuPAGE transfer buffer with 10% methanol per gel. Successful transfer of proteins to the membrane was visually confirmed with Ponceau S staining. Ponceau S was then washed with water, and membranes were subjected to blocking with 5% skimmed milk (Blotting grade blocking agent, BioRad) or 5% bovine serum albumin (BSA, Sigma Aldrich) in tris-buffered saline/tween 20 buffer (TBST) at room temperature. Membranes were next washed with TBST thrice (10min per wash) at room temperature and incubated overnight at 4°C with a primary antibody according to the manufacturer's instructions.

The following day, membranes were washed thrice with TBST (10min per wash) at room temperature and incubated for 1 hour at room temperature with anti-IgG-horseradish-peroxidase (HRP) conjugated secondary antibody with affinity to IgG of the species source for the primary antibody. Membranes were then washed with TBST thrice. ECL select reagent (Amersham, GE life sciences) was used to initiate the HRP reaction, and protein bands were finally visualised with a BioRad Chemidoc MP Imaging System.

When protein phosphorylation was examined, western blotting for phosphorylated protein bands was followed by membrane stripping using Restore™ Western Blotting Stripping Buffer (ThermoScientific) for 15min at room temperature, and Western blotting was repeated as described above using a primary anti-total protein antibody. All membranes were finally blotted for the house-keeping protein, GAPDH, which served as an endogenous loading control. Bands were quantified by densitometric analysis with the ImageLab software and phosphorylated protein levels were adjusted for the total protein levels on the same membrane. For all other proteins, adjustments were made with GAPDH on the same membrane.

Table 2.2: List of antibodies used for Western immunoblotting in this thesis.

Target Protein	Supplier and Catalogue No	Dilution Details
Akt	Cell Signalling technology, 4691	1:2,000 in milk with 5% TBST
p-Akt (ser473)	Cell Signalling Technology, 4060	1:2,000 in BSA with 5% TBST
eNOS	BD Transduction Labs, 610296	1:1,000 in BSA with 3% TBST
p-eNOS (ser1177)	Cell Signalling Technology, 9570	1:1,000 in BSA with 3% TBST
Erk1&2	Cell Signalling Technology, 4695	1:1,000 in milk with 5% TBST
p-Erk1&2 (Thr202/Tyr204)	Cell Signalling Technology, 4370	1:1,000 in BSA with 5% TBST
AMPKα	Cell Signalling Technology, 5832	1:1,000 in milk with 5% TBST
p-AMPKα (Thr172)	Cell Signalling Technology, 2535	1:1,000 in BSA with 5% TBST
IRS1	Cell Signalling Technology, 2390	1:1,000 in BSA with 3% TBST
p-IRS1 (ser307)	Cell Signalling Technology, 2491	1:1,000 in milk with 3% TBST
Rac1	Cell Signalling Technology, 8631	1:1,000 in BSA with 5% TBST
$p47^{phox}$	Cell Signalling Technology, 4301	1:1,000 in milk with 5% TBST
p-JNK (Thr183/Tyr185)	Cell Signalling Technology, 4671	1:1,000 in BSA with 5% TBST
JNK	Cell Signalling Technology, 9258	1:1,000 in milk with 5% TBST
anti-active β catenin	Millipore, 05-665	1:1,000 in milk with 5% TBST
GAPDH HRP-conjugated	Sigma, G9295	1:20,000 in milk with 5% TBST

TBST: Tris-buffered saline with 0.1% tween

2.8. Estimation of Rac1 & $p47^{phox}$ membrane translocation in human vessels

Human vascular tissue was used to evaluate the degree of Rac1 and $p47^{phox}$ translocation to the membrane for active NADPH-oxidases subunit formation. To achieve this, I first lysed the samples using an LT tissue lyser (as described previously) in ice-cold HEPES buffer (20 mmol/L HEPES, 150 mmol/L NaCl, and 1 mmol/L EDTA, pH=7.4) supplemented with protease inhibitor cocktail (Roche, UK, 1 tablet per 10ml of buffer). Homogenates were centrifuged at 13,000g for 15min at 4ºC to remove cell nuclei and unbroken cells.

Parts of the supernatants (corresponding to 250-450µg of total protein) were further centrifuged at 100,000g for 60min at 4°C using an OptimaMAX XP ultracentrifuge (Beckman Coulter) to separate the membrane from the cytosolic proteins. Pellets containing the membrane protein fraction, were re-suspended in HEPES buffer containing 1% Triton for 20 min on ice and used for the measurement of membrane-translocated Rac-1 and $p47^{phox}$ protein by Western immunoblotting, as described in paragraph 2.10.

The remaining part of the supernatants (10-15µg) was used for Western immunoblotting for total Rac1 or $p47^{phox}$ as described in paragraph 2.7, which served as the normalising proteins for quantification of membrane-translocated Rac1 and $p47^{phox}$.

2.9. Rac1 activation assay in human vessels

Rac1 activation in vascular samples was performed by a commercially available affinity precipitation assay kit according to the manufacturer's instructions (Cell Signalling Technologies). Samples were firstly homogenised in 500µl of lysis buffer plus 1mM phenylmethylsulfonyl fluoride (PMSF, a protease inhibitor recommended by the manufacturer) and centrifuged at 13,000g for 15min at 4ºC to remove debris. A volume of supernatant corresponding to a given amount of protein for each individual patient (ranging from 350-500µg) was then mixed with glutathione resin and PAK1-PBD beads in appropriate spin cup

columns and incubated at 4ºC for 1 hour to allow for binding of GTP-bound GTPases to glutathione via glutathione S transferase (GST) interactions. Samples were then spun at 6,000g for 30sec so that the unbound proteins were removed. Samples were next washed thrice with wash buffer (supplied with the kit), and the glutathione resin-bound GTPases of each sample were eluted in 2x SDS buffer (supplied with the kit) containing 200mM dithiothreitol, which resulted in the dissociation of the active GTPases from the resin. Spin cups containing the resin were discarded and the eluted samples were heated at 95ºC for 5min and used for western immunoblotting for Rac1 using a mouse monoclonal anti-Rac1 antibody provided with the kit. Total Rac1 was also quantified by Western immunoblotting using the leftover of the whole lysates as described in paragraph 2.7. Rac1 activation was estimated as the ratio of GTP-bound Rac1 to total Rac1 in each sample.

2.10. Statistical analysis

In the results of all experiments presented in the following chapters, continuous variables were tested for normal distribution using the Kolmogorov-Smirnov test. Non-normally distributed variables were log-transformed for analysis and are presented as median [25^{th}-75^{th} percentile] or on log-transformed scale. Normally distributed variables are presented as mean ± SEM.

In the clinical association studies, continuous variables between 3 groups were compared by using one-way ANOVA (or Kruskal-Wallis tests for non-normally distributed variables) followed by Bonferoni post-hoc test for individual comparisons, while comparisons between 2 groups were performed by unpaired t-tests (or Mann Whitney U tests for non-normally distributed variables). Correlations between continuous variables were assessed by using bivariate analyses, and Pearson's coefficients were estimated. Whenever a non-normally

distributed variable failed to follow normal approximation after log-transformation, non-parametric analysis was used and Spearman's coefficient was estimated.

For all *ex vivo* experiments where a paired design was followed, Wilcoxon's signed rank tests, paired Student's t-tests or multiple comparisons tests were applied followed by post-hoc correction for multiple comparisons as appropriate.

Multivariate analyses were also applied to evaluate the interactions between variables of interest. Linear regression analysis was performed when the dependent variable was continuous while logistic regression was employed to examine a binary categorical variable. Finally Cox regression was used to evaluate the effect of variables of interest on categorical endpoints (i.e., cardiac mortality events).

Power calculations and specific tests used are presented in a separate statistical analysis section in each chapter. All statistical tests were performed by using SPSS v23.0 (IBM Analytics). $P<0.05$ was considered statistically significant.

2.11. Personal contribution

Throughout my project, I performed laboratory-based experiments and performed statistical analysis at the cardiovascular medicine lab, Level 5 West Wing, John Radcliffe hospital. I was also involved in patient recruitment at the cardiothoracic ward, level 2, main John Radcliffe Hospital.

Patient recruitment, surgical sample collection and baseline *ex vivo* experiments (vascular $O_2^{\cdot-}$ quantification and vasomotor studies) for oxHVF patients recruited before August 2014 were not performed by me. For the purposes of my project, I used biological material from those patients (i.e., snap-frozen tissues and plasma) to isolate RNA and gene expression studies as well as circulating biomarker measurements. I also used demographic characteristics and

archived quantitative data (i.e., *ex vivo* vascular $O_2^{\cdot-}$ quantification and vasorelaxation readouts) from these patients to perform new statistical analyses.

Sample collection and baseline *ex vivo* experiments for all AdipoRedOx patients recruited after August 2014 were performed by me. I also performed all RNA extractions and qPCRs presented in this thesis, as well as all the prospective mechanistic experiments (including $O_2^{\cdot-}$ quantification, vasomotor studies and signalling experiments following specific *ex vivo* incubations) with both human and mouse tissue. Furthermore, I significantly contributed to the creation of the sample bioresource associated with OxHVF, by generating cohort-wide cDNA libraries for AT and IMA, and by performing hundreds of baseline *ex vivo* experiments (L-NAME and NADPH-Vas2870 chemiluminescence experiments, vasomotor studies).

AdipoRedOx patient recruitment was performed by Miss Laura Herdman or myself. Pre-operative flow mediated dilation (FMD) was performed by Miss Laura Herdman and Dr Alexios S Antonopoulos. Insulin and glucose measurements were performed by Dr Costas Psarros. Wnt5a and Sfpr5 measurements were performed by Dr Alexios S Antonopoulos and myself. Mouse breeding, colony maintenance, *in vivo* mouse treatments, mouse tissue harvesting and mouse genotyping were performed by Dr Patricia Ciccone and Dr Fabio Sanna, while the gene expression studies and *ex vivo* $O_2^{\cdot-}$ measurements on mouse tissues were performed by myself. Cell culture studies were predominantly carried out by Dr Fabio Sanna and Dr Amy Chiu, while I contributed to the downstream processing of cell lysates in certain experiments as described in individual Chapters. Recruitment, plasma collection and data processing for ORFAN study participants was done by Miss Sheena Thomas and Dr Evangelos K Oikonomou, while I ran plasma Wnt5a & Sfrp5 ELISAs and performed statistical analysis with data from these patients.

Chapter 3

Vascular insulin resistance in patients with atherosclerosis: Implications for insulin treatment in diabetes

This Chapter explores the concept of vascular IR and the insulin-sensitising properties of DPP4-i. Observational associations are first provided between serum insulin and parameters of vascular redox state and endothelial function, followed by discussion of the mechanistic experiments performed to explore the underlying mechanisms. This work is currently in Revision (Akoumianakis I *et al*, 2019a).

3.1. Introduction

Insulin is believed to have overall vasoprotective roles via activation of the PI3K/Akt signalling pathway, resulting in increased eNOS activity and coupling, increased NO bioavailability and improved endothelial function (Muniyappa *et al.*, 2007). On the other hand, such effects are abolished in obesity (Katakam *et al.*, 2005), while aggressive glycaemic control with insulin treatment has failed to improve cardiovascular risk in diabetic patients in clinical trials (Gerstein *et al.*, 2012; Marso *et al.*, 2017). These observations suggest that metabolic disease may be characterised by vascular IR, while insulin treatment may have unexpected vascular effects independently of its systemic glucose-lowering effects. Importantly, disproportionate activation of the MAPK pathway in response to insulin, as often observed in the context of cellular IR, could actually have detrimental effects on the vasculature (Muniyappa *et al.*, 2007), although this has never been explored before.

Several hypoglycaemic agents display pleiotropic peripheral insulin-sensitising effects. DPP4-i, in particular, has recently emerged as a treatment strategy with a number of pleiotropic effects which has been associated with improved endothelial function and reduced oxidative stress in the vasculature in *in vitro* and animal studies (Fadini and Avogaro, 2011). These could be mediated by its ability to regulate vascular insulin signalling (Akoumianakis and Antoniades, 2017a), however this has not been addressed before.

I hypothesised that insulin treatment may have detrimental effects in the vasculature of patients with atherosclerosis which would be determined by the presence of vascular IR and could be regulated by novel strategies of local insulin sensitization.

3.2. Study population & methods

3.2.1. Study population

The experimental work outlined in Chapter 3 includes 580 patients of AdipoRedOx study for the clinical cohort associations (study 1). In addition, vascular samples from 81 of the aforementioned AdipoRedOx patients (study 2) were used fresh for an number of *ex vivo* experiments including vascular $O_2^{\cdot -}$ quantification, evaluation of endothelial function *ex vivo* as well as downstream insulin signalling by Western immunoblotting (as explained in the relevant sections of Chapter 2).

Study participants provided written informed consent. Exclusion criteria included any active infectious, auto-immune, idiopathic, kidney and liver disease, malignancy and recent unstable coronary syndrome (within the previous 8 weeks). Patients receiving non-steroidal anti-inflammatory drugs, dietary supplements or antioxidant vitamins were also excluded from the study. The demographic characteristics of the participants are provided in Table 3.1.

Table 3.1: Demographic characteristics of Chapter 3 study participants

	Study 1	**Study 2**
Participants (n)	580	81
Age (years)	66.8±0.4	68.7±1.0
Males (%)	81.1	87.7
Hypertension (%)	72.8	80.0
Hyperlipidaemia (%)	77.8	93.8
T2DM (%)	21.6	33.1
Smoking		
Active (%)	10.0	7.4
Past (%)	54.0	51.9
BMI (kg/m^2)	28.5±0.2	28.5±0.4
HOMA-IR in non-diabetics	1.16[0.73-1.83]	1.26[0.53-1.82]
Serum insulin (mU/L)	5.5[3.4-8.3]	7.2[3.0-15.1]
Serum glucose (mg/dL)	96[83-113]	114[80-135]

Medication		
Antiplatelet (%)	81.6	84.0
ACEi/ARBs (%)	61.8	69.1
Statins (%)	82.0	86.4
βblockers (%)	66.0	75.3
CCB (%)	25.6	29.7
Insulin (%)	7.4	8.6
Oral hypoglycaemic (%)	15.6	24.7

T2DM: Type 2 diabetes mellitus; BMI: Body mass index; HOMA-IR: Homeostatic model assessment – insulin resistance; ACEi: Angiotensin converting enzyme inhibitor; ARB: Angiotensin receptor blocker; CCB: Calcium channel blocker. Age and BMI are presented as mean±SEM; HOMA-IR, serum insulin and serum glucose are presented as median[25^{th}-75^{th} percentile]

3.2.2. Methods

3.2.2.1. Ex vivo & in vitro incubations

Human IMA and SV segments were exposed to exogenous insulin treatment *ex vivo* for 20min at 37ºC and 95% O_2/5% CO_2 conditions in KHB. For this purpose, two insulin analogues (insulin glargine 10nM, insulin degludec 100nM) and human soluble insulin 10nM were used.

To evaluate the effect of DPP4-i on insulin responses, I also used human IMA and SV segments and incubated them with KR62436 70μM (Sigma, a chemical DPP4-i) starting 15min prior to the insulin incubations at 37ºC and 95% O_2/5% CO_2 conditions in KHB.

In a sub-group of patients, vascular segments were pre-incubated with compound C (an inhibitor of AMPK) 10μM for 20min before the aforementioned experimental conditions, in order to evaluate the role of AMPK in the crosstalk between DPP4-i and insulin signalling.

Healthy mouse aortic tissue and/or human umbilical vein endothelial cells were exposed to similar insulin/DPP4-i protocols as biological, atherosclerosis-free, controls, as explained in following sections.

3.2.2.2. Human umbilical vein endothelial cell culture

HUVECs were cultured at 37 °C in DMEM medium supplemented with 10 % fetal bovine serum and 100 U/mL penicillin, 100 U/mL streptomycin in humidified 5 % CO_2 incubator. Insulin incubations were performed with 10nM insulin glargine for 20min in the absence or presence of a DPP4 inhibitor (KR62436, Sigma, at 70μM), and cells were then lysed with RIPA buffer supplemented with protease and phosphatase inhibitors for Western blotting. Baseline cell culture and *in vitro* incubations were performed by Dr Fabio Sanna. I performed Western blotting experiments with the cell lysates and analysed the results.

3.2.2.3. Mouse studies

Wild-type C57BL/6 mice were used as biological, atherosclerosis-free controls to evaluate the effects of insulin treatment on vascular redox state. Animals were culled, aortic tissues were collected in ice-cold KHB and incubated *ex vivo* with exogenous insulin (glargine 10nM, degludec 100nM and human soluble insulin 10nM). Insulin-incubated and control segments were finally used fresh for baseline, NADPH-stimulated and Vas2870-inhibitable $O_2^{\cdot-}$ quantification by lucigenin chemiluminescence as explained in relevant sections of Chapter 2. All experimental steps up until aortic tissue harvesting were performed by Dr Fabio Sanna. I performed the *ex vivo* incubations and ran and analysed the lucigenin chemiluminescence experiments.

All animal studies were conducted with ethical approval from the Local Ethical Review Committee in accordance with the UK Home Office regulations (Guidance on the Operation of Animals, Scientific Procedures Act, 1986) and were approved by the Local Ethical Review Committee. Mice were housed in a specific pathogen-free environment, in Tecniplast Sealsafe IVC cages (floor area 542 cm^2) with a maximum of six other mice. Mice were kept in a 12 h

light/dark cycle and in controlled temperatures (20–22°C) and fed normal chow and water ad libitum.

3.2.2.4. Immunoprecipitation of IRS1

Vascular segments were homogenised in a weight-adjusted volume of RIPA buffer (Cell Signalling Technology, #9806) containing a protease and phosphatase inhibitor cocktail (Cell Signalling Technology, #5871 and #5870 respectively), debris removed by centrifugation at 13,000 rpm for 15 minutes, at 4 ºC. Following pre-treatment of the protein lysates with A/G agarose beads (ThermoFischer Scientific, #20423), protein concentrations of samples were quantified by the Pierce BCA protein assay kit. 300-500mg of total protein from all samples were then adjusted to an equal volume of 200µL and incubated with primary anti-IRS1 antibody (Cell Signalling Technology, #3407) overnight at 4ºC. Protein A agarose beads (Cell Signalling Technology, #9863) where then added to the samples and incubated for 2h at 4ºC to allow interaction with the antibody-bound target proteins. Samples where then washed and centrifuged to pellet the immunoprecipitated proteins, which were finally re-suspended in reducing loading buffer. Samples were heated at 95ºC for 5 min and then stored in -80ºC until used for Western immunoblotting.

3.2.2.5. Statistical analysis

Continuous variables were tested for normal distribution using the Kolmogorov-Smirnov test. Non-normally distributed variables were log-transformed for analysis.

In the clinical studies, continuous variables between 3 groups were compared by using one-way ANOVA followed by Bonferoni post-hoc test for individual comparisons. For the organ bath experiments, the effect of “serum insulin tertile” on vasorelaxations in response to ACh & BK was evaluated by using two-way ANOVA for repeated measures (examining the

effect of “Ach, BK or SNP concentration” x “serum insulin tertile” interaction on “vasorelaxations”) in a full factorial model.

Sample size calculations were based on previous data from our laboratory. For the *ex vivo* experiments, sample size calculations were performed based on our previous experience on this model, and I estimated that with a minimum of 5 pairs of samples (serial rings from the same vessel) we would be able to identify a change of $\log(O_2^{\cdot-})$ by 0.48 with α=0.05, power 0.9 and SD for a difference in the response of the pairs of 0.25. Analysis of paired *ex vivo* mechanistic experiments was done by multiple comparisons tests with post-hoc correction as appropriate.

For the *ex vivo* organ bath experiments, where serial rings from the same vessel were incubated with multiple interventions, I performed Friedman tests (paired non-parametric equivalent of ANOVA) and paired Wilcoxon signed rank tests or t-tests for individual comparisons followed by Bonferoni post-hoc correction for multiple testing as appropriate.

To test the cumulative association of serum DPP4 activity and serum insulin with cardiac mortality rates, I created a dichotomous categorical variable by splitting the population of Study 1 into two groups, one with patients in the high tertile for both serum DPP4 activity and serum insulin and one in the intermediate tertiles for those two biomarkers. The combined effect of serum insulin and DPP4 activity on cardiac mortality was then examined by multivariate Cox regression survival analysis after adjusting for traditional cardiovascular risk factors [age per decade of years, sex, hyperlipidaemia, hypertension, diabetes, active smoking and NYHA class as a dichotomous variable (class 0-1 vs class 3-4)].

3.3. Results

3.3.1. Characterizing the effects of insulin on vascular redox state in humans with atherosclerosis

I first investigated the association between circulating insulin levels and endothelial function in a cohort of non-diabetic patients from study 1 (n=110). Interestingly, high serum insulin levels were associated with significantly reduced vasorelaxations of human vessels in response to ACh (Fig. 3.1A) and Bk (Fig. 3.1B), but not to SNP (Fig. 3.11C), suggesting an inverse association between serum insulin levels and NO bioavailability in the human endothelium (Ach and Bk are both considered vasodilators the effects of which are mediated via NO, hence they reflect the ability of the endothelium to respond by regulating NO production).

To explore whether the inverse association between insulin levels and endothelial function is causal, I then exposed human vessels from both diabetic patients and non-diabetic patients without evidence of systemic IR (HOMA-IR<2.9) to exogenous insulin *ex vivo*, using both long-acting insulin analogues (glargine M1 metabolite or degludec), and human insulin.

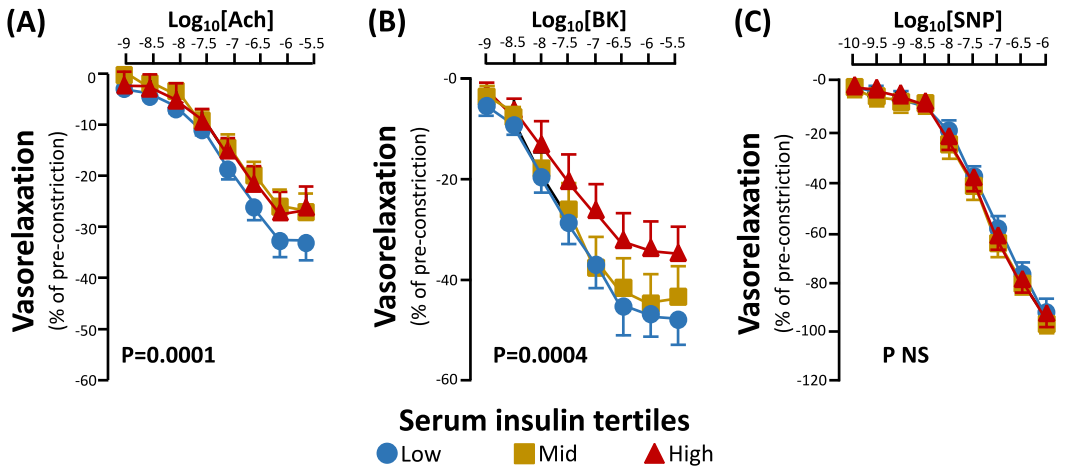

Figure 3.1: Serum insulin and nitric oxide (NO) bioavailability in humans with coronary atherosclerosis. Low insulin levels were associated with impaired endothelium-dependent *ex vivo* vasorelaxations in response to acetylcholine (Ach, panel A, n=110) or bradykinin (Bk, panel B, n=38), without affecting the endothelium-independent *ex vivo* vasorelaxations in response to sodium nitroprusside (SNP, panel C, n=92). P-values are calculated by two-way ANOVA for repeated measures with treatment x group interaction. I Akoumianakis *et al* (1), *Sci Transl Med* (in Revision).

All insulin types significantly reduced vasorelaxations in response to ACh but not to SNP in all patients (Fig. 3.2A-D), suggesting a class effect of insulin on the vascular wall in patients with vascular disease, even in the absence of diabetes or systemic IR. Although this was not designed to compare non-T2DM versus T2DM endothelial responses, panels 3.2A and 3.2B demonstrate very minor differences in Ach vasorelaxations in the two groups, which may reflect a favorable effect of overall antidiabetic treatment but should be interpreted with caution due to the relatively small numbers (for such a comparison).

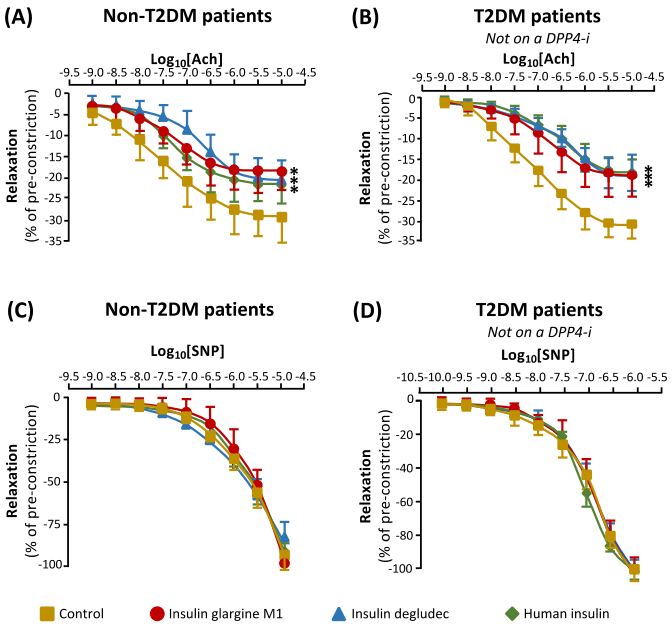

Figure 3.2: Insulin impairs endothelial function in patients with coronary atherosclerosis. All insulin types used impaired the endothelium-dependent Ach-mediated vasorelaxations in non-diabetic (panel A) and diabetic patients (not on an oral DPP4-i, panel B), without affecting the endothelium-independent SNP vasorelaxations (panels C-D). n=6 pairs for all panels. *P<0.05 vs control by two-way ANOVA for repeated measures with treatment x group interaction. I Akoumianakis *et al* (1), *Sci Transl Med* (in Revision).

To understand how insulin could cause endothelial dysfunction in vessels from patients with vascular disease, I then explored the interactions between insulin levels and vascular redox state in non-diabetic patients from Study 1. Serum insulin was marginally non-significantly correlated with basal $O_2^{\cdot-}$ in IMA (Rho=0.21, P=0.09) or SV (Rho=0.15, P=0.10), but when I focused on NADPH-stimulated and Vas2870-inhibitable readouts (which are more sensitive markers of NADPH-oxidases activity), I observed that increased serum insulin levels were associated with increased NADPH-oxidases activity in human vessels (IMA and SV, Fig. 3.3A-D, Vas2870 is a pan-NOX inhibitor of NADPH-oxidases).

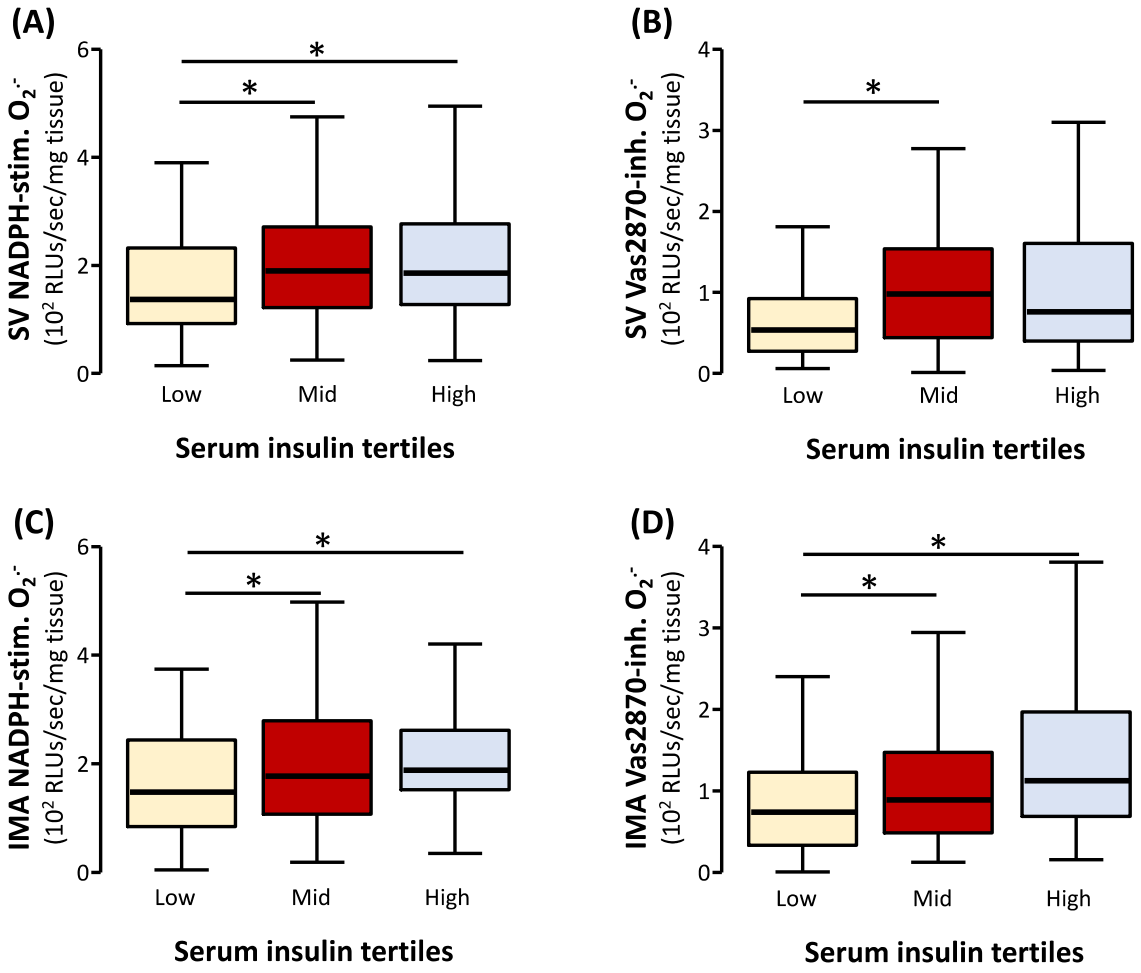

Figure 3.3: Serum insulin is associated with increased vascular oxidative stress and vascular NADPH-oxidases activity in non-diabetic patients with coronary atherosclerosis. Serum insulin levels were positively associated with vascular NADPH-oxidases activity as quantified by the NADPH-stimulated superoxide ($O_2^{\cdot-}$) and Vas2870-inhibitable $O_2^{\cdot-}$ in both saphenous vein (SV, panels A-B) and internal mammary artery (IMA, panels C-D) segments from non-diabetic patients with coronary atherosclerosis without insulin resistance (HOMA-IR<2.9, n=173). *P<0.05 vs low tertile after Kruskal Wallis (non-parametric equivalent of ANOVA) followed by post-hoc multiple comparisons analysis. I Akoumianakis *et al* (1), *Sci Transl Med* (in Revision).

To examine whether exogenous insulin administration could causally increase oxidative stress in the human vascular wall, I exposed SV obtained from study 2 patients to human insulin and insulin glargine M1 (used as a representative insulin analogue and named as "insulin" in the subsequent results sections) *ex vivo* and demonstrated that insulin increased SV NADPH $O_2^{\cdot-}$ generation in diabetic patients as well as and in patients without diabetes or systemic IR (Fig. 3.4A, 3.4D). This was due to activation of vascular NADPH oxidases as documented by the increase of NADPH-stimulated (Fig. 3.4B, 3.4E) as well as the Vas2870-inhibitable $O_2^{\cdot-}$ (Fig. 3.4C, 3.4F) production.

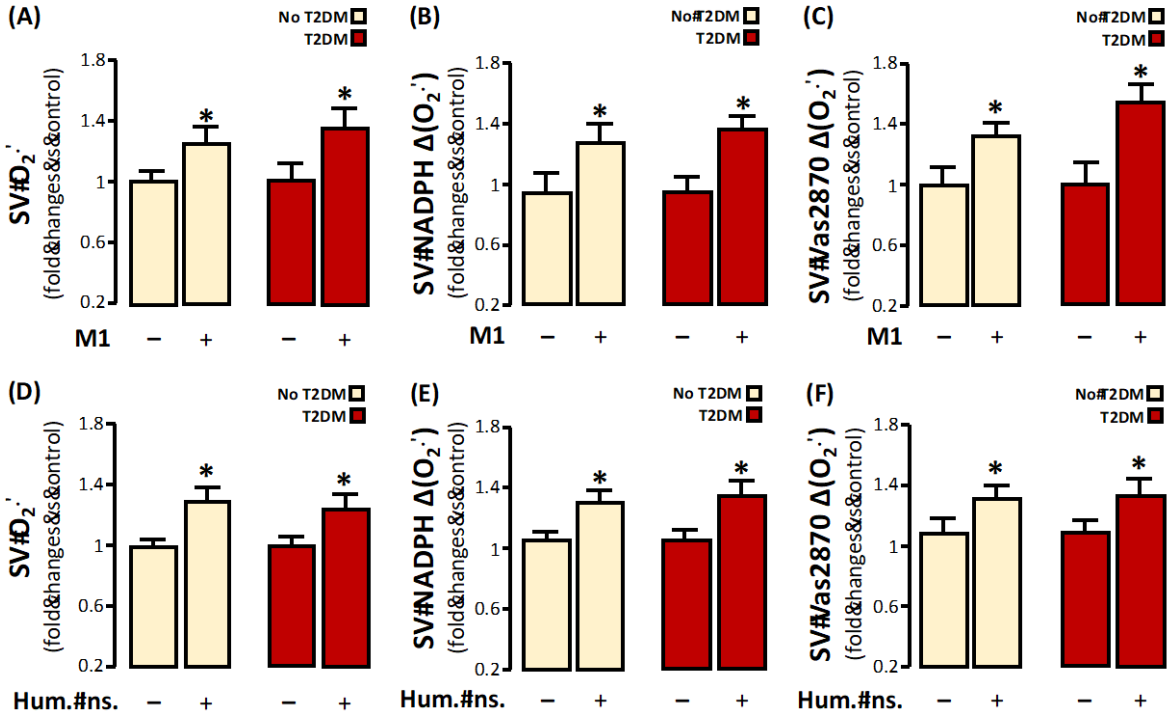

Figure 3.4: Exogenous insulin directly increases NADPH-oxidases activity in saphenous vein (SV) segments from patients with coronary atherosclerosis. Insulin glargine M1 10nM increased basal (panel A), NADPH-stimulated (panel B) and Vas2870-inhibitable (C) superoxide ($O_2^{\cdot-}$) in both non-diabetic and diabetic patients (n=5-7 pairs per panel). The same pattern was observed with human insulin 10nM (panels D-F, n=7-12 pairs per panel). *P<0.05 vs respective controls (for non-T2DM and T2DM) after post hoc multiple comparison analysis. I Akoumianakis *et al* (1)*, Sci Transl Med* (in Revision).

To confirm that the effect of insulin on NADPH-oxidases activity is relevant in human arteries, I exposed IMA segments from diabetic patients and patients without systemic IR or T2DM to insulin.

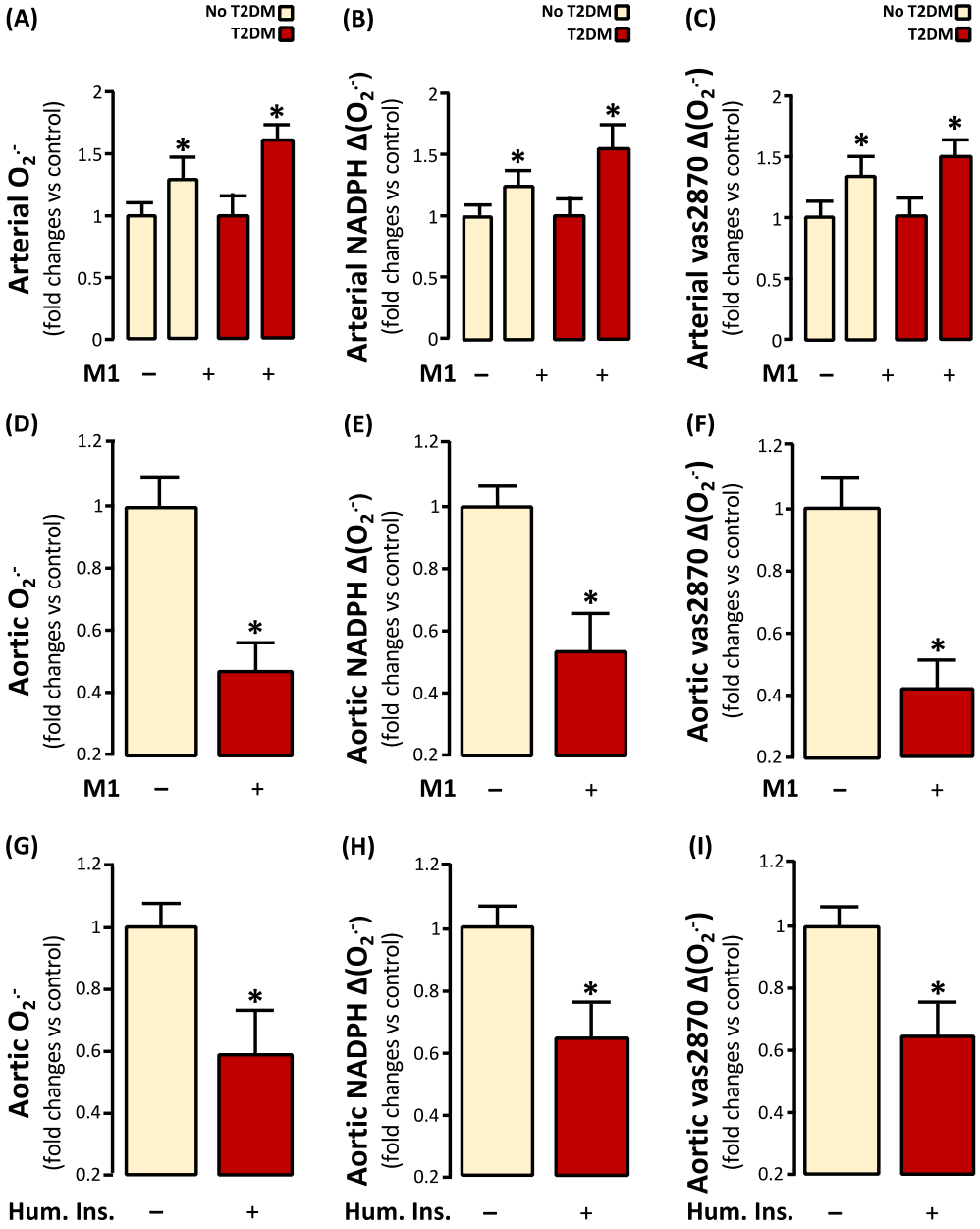

Figure 3.5: Exogenous insulin increases NADPH-oxidase activity in internal mammary artery (IMA) segments from patients with coronary atherosclerosis, but not in healthy mouse aortae. Insulin glargine M1 10nM increased basal (panel A), NADPH-stimulated (panel B) and Vas2870-inhibitable (C) superoxide ($O_2^{\cdot-}$) in IMA from both non-diabetic and diabetic patients (n=5-7 pairs per panel). However, both insulin glargine M1 10nM and human insulin 10nM significantly reduced basal (panels D & G), NADPH-stimulated (panels E & H) and Vas2870-inhibitable (panels F & I) $O_2^{\cdot-}$ in aortic tissue from healthy, atherosclerosis-free wild-type mice (n=5 pairs per panel). *P<0.05 vs control by Wilcoxon signed rank tests after post hoc multiple comparisons analysis in panels A-C. I Akoumianakis *et al* (1)*, Sci Transl Med* (in Revision).

I found that insulin treatment stimulated NADPH-oxidases-derived $O_2^{\cdot-}$ production in arteries from patients with coronary atherosclerosis (Fig. 3.5A-C). To test whether this was associated with the presence of vascular disease, I also exposed mouse aortae from healthy wild-type animals to similar insulin treatment protocols, and I observed that insulin markedly reduced

NADPH-oxidases activity in mouse aortae, providing a positive control for my interventions (Fig. 3.5D-I).

Finally, I further confirmed the ability of insulin to induce NADPH-oxidases activity by *in situ* visualization of $O_2^{\cdot-}$ production in insulin-treated IMA segments from patients with coronary atherosclerosis (Fig. 3.6). Vas2870 was used to reverse the effect on NADPH-oxidases, confirming the specificity of the signal.

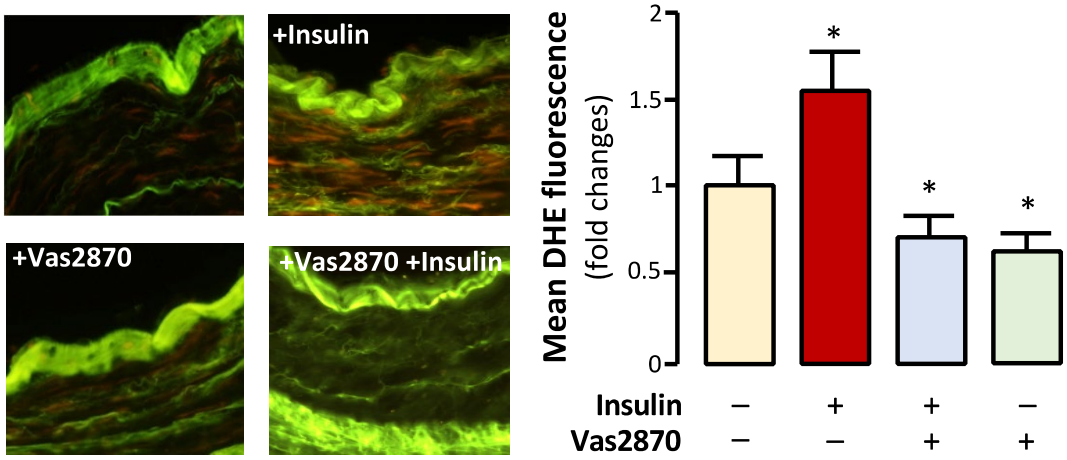

Figure 3.6: *In situ* visualisation of arterial superoxide ($O_2^{\cdot-}$) in response to insulin treatment. Human internal mammary artery (IMA) segments were incubated with insulin (glargine M1, 10nM) then sectioned and $O_2^{\cdot-}$ was visualised by dihydroethidium (DHE). Red signal indicates DHE oxidation, while the green signal reflects the endogenous tissue fluorescence background. Insulin increased $O_2^{\cdot-}$ generation in the arterial wall, and this was reversed by Vas2870 inhibtion, confirmed that the observed effect was mediated by an increase in NADPH-oxidases activity. Quantification of the fluorescence signal confirmed the increase in response to insulin which was reversed by NADPH oxidase inhibition by Vas2870. *P<0.05 vs control after post hoc analysis or multiple corrections. I Akoumianakis *et al* (1)*, Sci Transl Med* (in Revision).

3.3.2. DPP4 inhibition restores "physiological" vascular redox response to insulin in human atherosclerosis

My results so far clearly indicate that insulin has a class stimulatory effect on vascular NADPH-oxidases activity in human atherosclerosis, independently of the presence of diabetes or systemic IR. Although this was an extremely reproducible finding across patients (either with diabetes or not) and vessel types (IMA or SV), I observed that *ex vivo* insulin incubations resulted in significant reduction in NADPH-stimulated and Vas2870-inhibitable vascular $O_2^{\cdot-}$

in certain vascular segments, and I noted that this response was only observed in those diabetic patients receiving an oral DPP4-i prior to vessel harvesting (Fig. 3.6A-C).

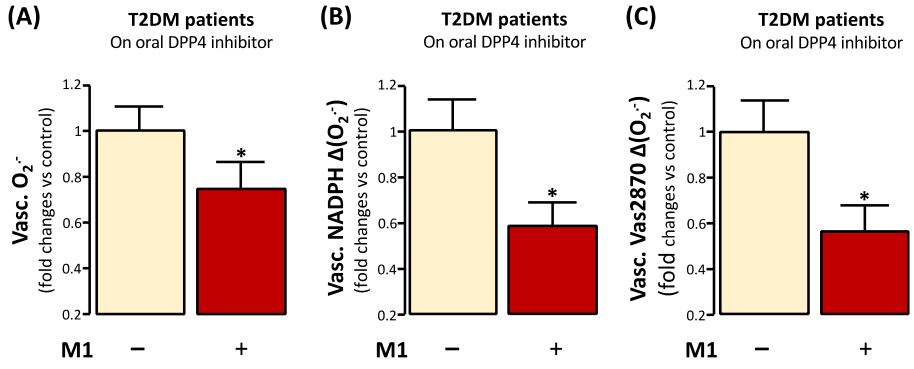

Figure 3.7: Exogenous insulin reduces vascular NADPH-oxidases activity in patients with coronary atherosclerosis on an oral DPP4 inhibitor (DPP4-i). Insulin glargine M1 10nM significantly decreased basal (panel A), NADPH-stimulated (panel B) and Vas2870-inhibitable (C) superoxide ($O_2^{\cdot-}$) in vascular segments from diabetic patients on an oral DPP4-i as part of their antidiabetic treatment (n=5 pairs per panel). *P<0.05 vs control by Wilcoxon signed rank tests. I Akoumianakis *et al* (1), *Sci Transl Med* (in Revision).

To explore the hypothesis that DPP4-i may modify vascular insulin responses, I exposed human vessels (equally represented by diabetic and non-diabetic patients) to insulin in the presence or absence of KR62436, a chemical DPP4-i. Pre-incubation of SVs and IMAs with DPP4-i reversed their response to insulin, leading to reduced NADPH-oxidases activity (Fig. 3.8), which was also replicated with human insulin (Fig. 3.9).

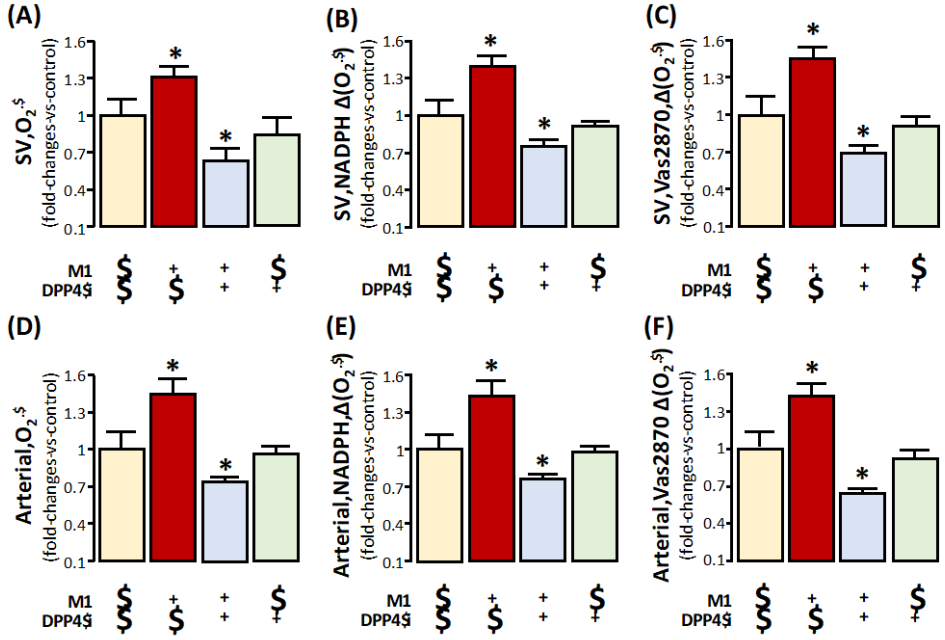

Figure 3.8: DPP4 inhibition reverses vascular redox responses to insulin in patients with coronary atherosclerosis. Insulin glargine M1 10nM significantly decreased basal (panels A & D), NADPH-stimulated (panels B & E) and Vas2870-inhibitable (panels C & F) superoxide ($O_2^{\cdot-}$) in human saphenous veins (SVs) and internal mammary arteries (IMAs) in the presence of DPP4 inhibition (n=5 pairs per panel). *P<0.05 vs control by Wilcoxon signed rank tests. I Akoumianakis *et al* (1), *Sci Transl Med* (in Revision).

To understand the underlying mechanisms via which insulin and DPP4 regulate NADPH-oxidases activity in human vessels, I explored their direct effects on the activation of NADPH-oxidases subunit Rac1. Insulin activated Rac1 (Fig. 3.10A), triggering membrane translocation of both Rac1 and $p47^{phox}$ subunits of NADPH-oxidases (Fig. 3.10B-C). These effects were reversed after pre-treatment of these vessels with DPP4-i, in which case insulin led to significant de-activation of Rac1 (Fig. 3.10A) and prevented the membrane translocation of Rac1 and $p47^{phox}$ (Fig. 3.10B-C). Importantly, DPP4-i had no direct effects on Rac1 activation or Rac1/$p47^{phox}$ membrane translocation (Fig. 3.10). These findings imply that targeting DPP4

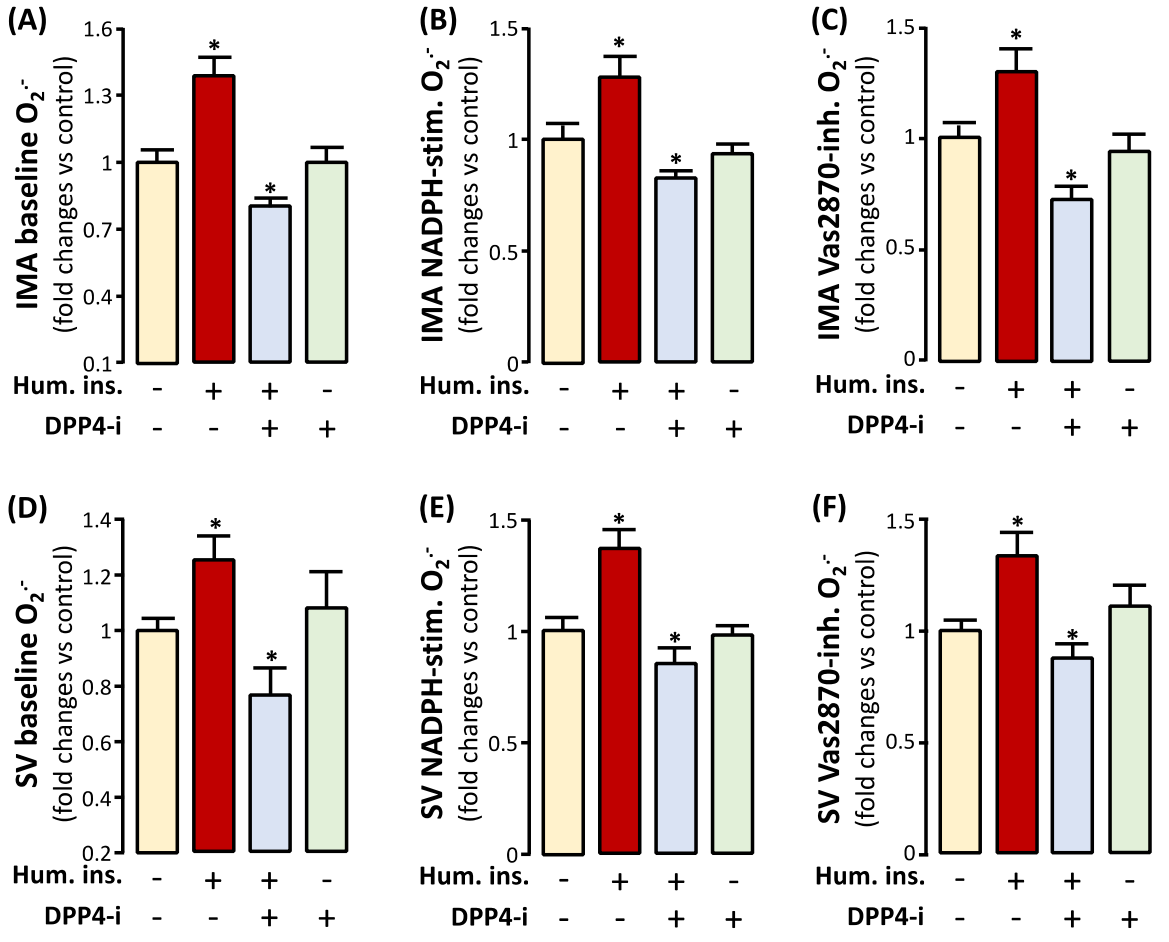

Figure 3.9: DPP4 inhibition reverses vascular redox responses to insulin in patients with coronary atherosclerosis. Human insulin 10nM significantly decreased basal (panels A & D), NADPH-stimulated (panels B & E) and Vas2870-inhibitable (panels C & F) superoxide ($O_2^{\cdot-}$) in human saphenous veins (SVs) and internal mammary arteries (IMAs) in the presence of DPP4 inhibition (n=5 pairs per panel). *P<0.05 vs control after post hoc analysis for multiple comparison. I Akoumianakis *et al* (1), *Sci Transl Med* (in Revision).

is may be required to ensure physiological insulin signaling in human vessels, at least in diabetic patients with vascular disease requiring insulin treatment.

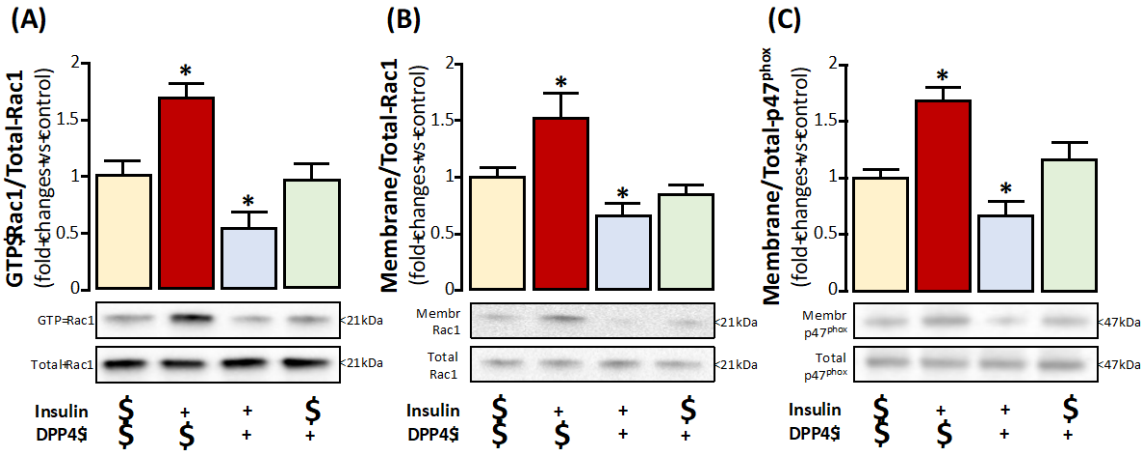

Figure 3.10: The effect of insulin on NADPH-oxidases is mediated by Rac1 activation followed by Rac1/p47^{phox} membrane translocation and regulated by DPP4 inhibition. Insulin glargine M1 10nM significantly increased Rac1 GTP-activation (panel A), resulting in increased membrane translocation of Rac1 (panel B) and p47^{phox} (panel C). These effects of insulin were completely reversed by DPP4 inhibition, while DPP4-I had minimal effects itself (panels A-C). *P<0.05 vs control after post hoc analysis for multiple comparisons. I Akoumianakis *et al* (1), *Sci Transl Med* (in Revision).

3.3.3. Exogenous insulin effects on eNOS in human vessels, which is modulated by DPP4 inhibition

To better understand how exogenous insulin controls vascular NO bioavailability and redox state in human vessels, I next investigated the direct effects of insulin on eNOS activity and coupling in the human vessels from patients with vascular disease. Insulin directly induced vascular eNOS uncoupling, documented by a striking increase in LNAME-inhibitable $O_2^{\cdot-}$ (Fig. 3.11A). This suggests that insulin causes a switch of eNOS function from NO production to $O_2^{\cdot-}$ production, further dysregulating vascular redox signaling. Treatment of these vessels with DPP4-i reversed the effects of insulin on eNOS coupling (Fig. 3.11A), confirming that insulin treatment together with DPP4-i, improves vascular redox signaling through restoration of eNOS coupling in human atherosclerosis.

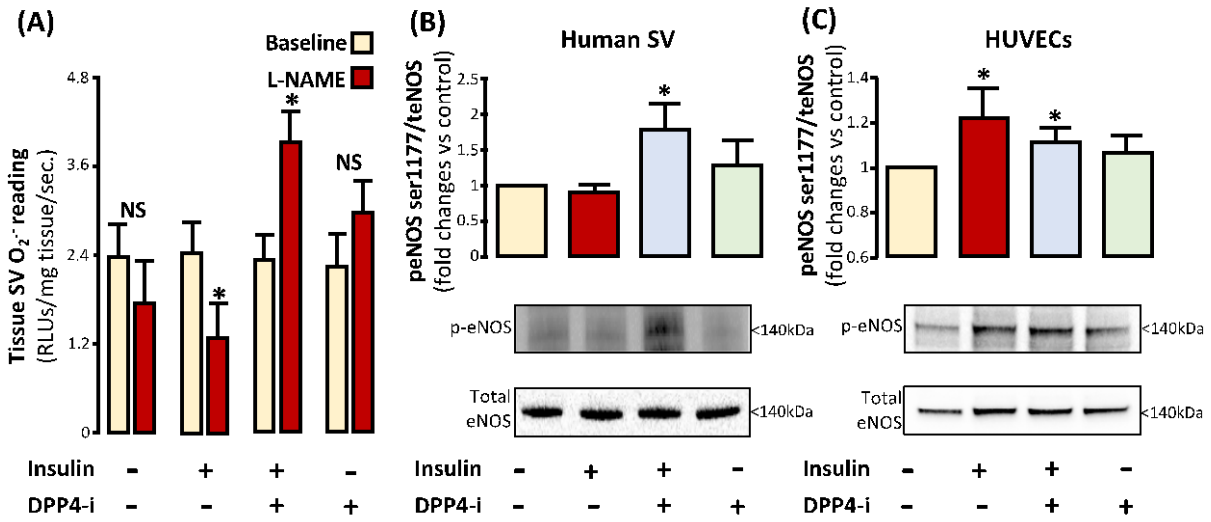

Figure 3.11: Effects of insulin on endothelial nitric oxide synthase (eNOS) coupling and phosphorylation. Insulin glargine M1 10nM significantly induced eNOS uncoupling (evidenced by reduced L-NAME reading from baseline suggesting that eNOS contributes to superoxide $O_2^{\cdot-}$ production), and this effect of insulin was completely reversed in the presence of DPP4 co-inhibition (DPP4-i, panel A). Insulin alone did not induce eNOS phosphorylation at ser1177, but significantly did so in the presence of DPP4 inhibition (panel B). In contrast, insulin was able to induce eNOS ser1177 phosphorylation in a healthy *in vitro* model of endothelial cells, where DPP4 inhibition conveyed no additional benefit (panel C). *P<0.05 after post hoc analysis for multiple comparisons vs respective baseline readings (A) or vs control (B-C). I Akoumianakis *et al* (1)*, Sci Transl Med* (in Revision).

Given that in *in vitro* models insulin has been shown to affect eNOS activity via Akt-mediated ser1177 phosphorylation (Scherrer *et al.*, 1994), I next explored the effects of insulin on eNOS phosphorylation status in humans with vascular disease. I found that insulin alone did not induce vascular eNOS phosphorylation at the activation site Ser1177, whereas significant Ser1177 activation was observed in the presence of DPP4-i (Fig. 3.11B). In contrast, insulin elicited a stimulatory effect on eNOS ser1177 phosphorylation in human umbilical vein endothelial cells used as a biological positive control, and DPP4-i conveyed no additional benefit in that context (Fig. 3.11C), highlighting the discrepancy in vascular insulin responses between humans with vascular disease and disease-free *in vitro* and *in vivo* models.

I next hypothesized that increased oxidative stress resulting from insulin-stimulated NADPH-oxidases activity could induce oxidation of tetrahydrobiopterin (BH4), an essential

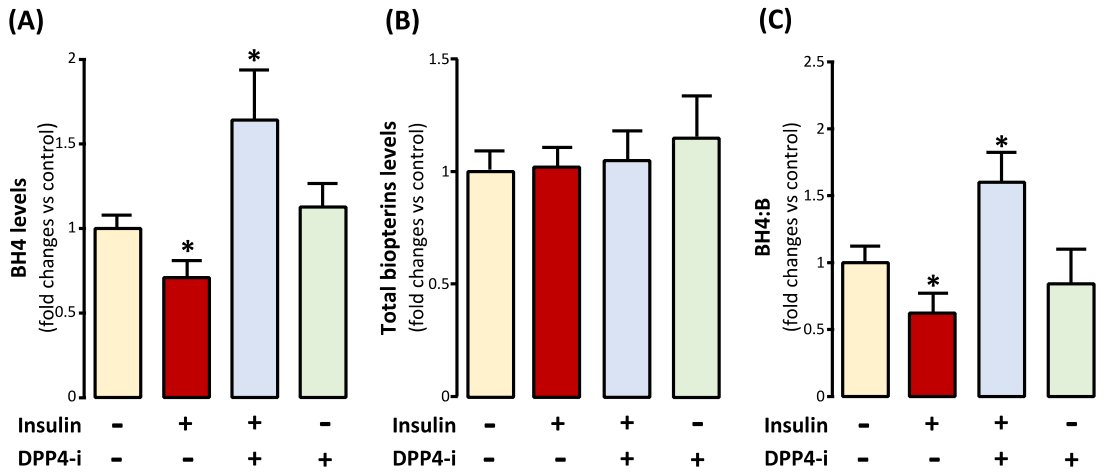

Figure 3.12: Insulin reduces tetrahydropterin (BH4) bioavailability, an effect reversed by DDP4 inhibition (DPP4-i). In human internal mammary artery (IMA) segments, nsulin glargine M1 10nM significantly induced BH4 oxidation (panel A) without affecting total biopterins content (panel B), disrupting the reduced-to-oxidised biopterin ratio (panel C). In the presence of DPP4 inhibition, insulin had the opposite effects, increasing BH4 bioavailability, while DPP4-i had little effect itself (panels A-C). *P<0.05 vs control after post hoc analysis for multiple comparisons. I Akoumianakis *et al* (1)*, Sci Transl Med* (in Revision).

cofactor required for maintaining eNOS enzymatic coupling. Indeed, I found that insulin reduces vascular BH4 bioavailability without affecting total biopterin content [which includes dihydrobiopterin (BH2) and biopterin (B)], resulting in a reduction of the BH4/B (i.e., reduced biopterin to oxidized biopterin) ratio and leading to eNOS uncoupling (Fig. 3.12). Conversely, in the presence of DPP4-i, insulin significantly increased vascular BH4 content and the ratio of BH4/total biopterins, reflecting reduced $O_2^{\cdot-}$ production and improved eNOS coupling (Fig. 3.12).

Given that insulin can improve eNOS coupling, increase BH4 bioavailability and concomitantly stimulate phosphorylation and activation of eNOS in the presence of DPP4-i, I hypothesized that DPP4-i would regulate vasomotor responses to insulin, leading to insulin-induced improvements of endothelial NO bioavailability. Accordingly, I found that insulin significantly impaired the vasorelaxation of human vessels to ACh, but in the presence of DPP4-i, insulin had the opposite effect, improving ACh-induced vasorelaxations (Fig. 3.13A). These effects were endothelium-specific and did not affect the endothelium-independent vasorelaxations to SNP (Fig. 3.13B).

3.3.4. Characterizing abnormal vascular insulin signalling in humans with vascular disease

Given that insulin induces oxidative stress and endothelial dysfunction in vessels from patients with vascular disease (in contrast with the expected beneficial vascular effects of insulin in healthy vessels), I hypothesized that these dysregulated vascular redox responses to insulin could reflect abnormal downstream insulin signaling in the context of vascular IR. As such, I investigated the balance between phosphorylation (activation) of vascular Akt vs. Erk1&2, as

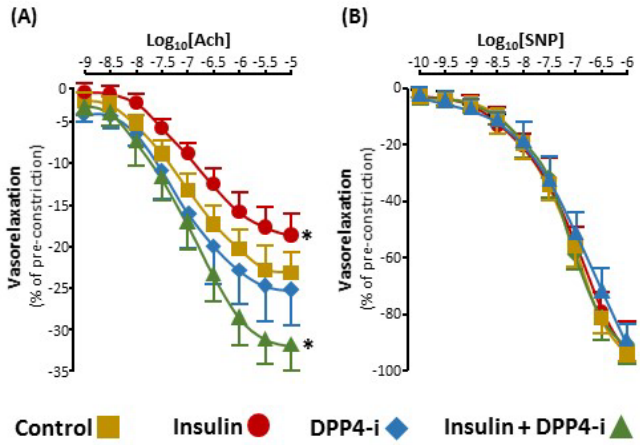

Figure 3.13: Insulin improves endothelial function *ex vivo* in the presence of DPP4 inhibition (DPP4-i). Insulin glargine M1 10nM significantly improved endothelium-dependent acetylcholine (Ach)-mediated relaxations in the presence of DPP4-i, contrary to the effects of insulin alone (panel A). Insulin or DPP4-i did not affect endothelium-independent relaxations in response to sodium nitroprusside (SNP, panel B). *P<0.05 vs control by two-way ANOVA for repeated measures with group x treatment interaction, n=5 pairs per panel. I Akoumianakis *et al* (1), *Sci Transl Med* (in Revision).

representative downstream mediators of the two insulin signaling axes dysregulated in IR. I observed that in vessels from patients with vascular disease, insulin did not stimulate Akt phosphorylation while it significantly induced phosphorylation of Erk1&2, resulting in a dysregulated balance between the two signaling axes in vessels from both non-diabetic (Fig. 3.14A-B) and diabetic (Fig. 3.14C-D) patients. Aortic rings from healthy wild-type mice were used as positive controls, confirming that insulin significantly induces Akt phosphorylation much more so than Erk1&2 in the normal vessel wall (Fig. 3.14E-F). In line with my previous findings, vascular segments from diabetic patients treated with oral DPP4-i responded to insulin stimulation in a way that was opposite to all other vessels obtained from the patients with vascular disease (Fig. 3.14G-H), and resembled the vascular responses of healthy mice

(Fig. 3.14E-F). These results confirm that there is a selective dysregulation of downstream insulin signaling in vessels from patients with vascular disease, in favor of Erk1&2 activation (over Akt), indicating the presence of vascular IR.

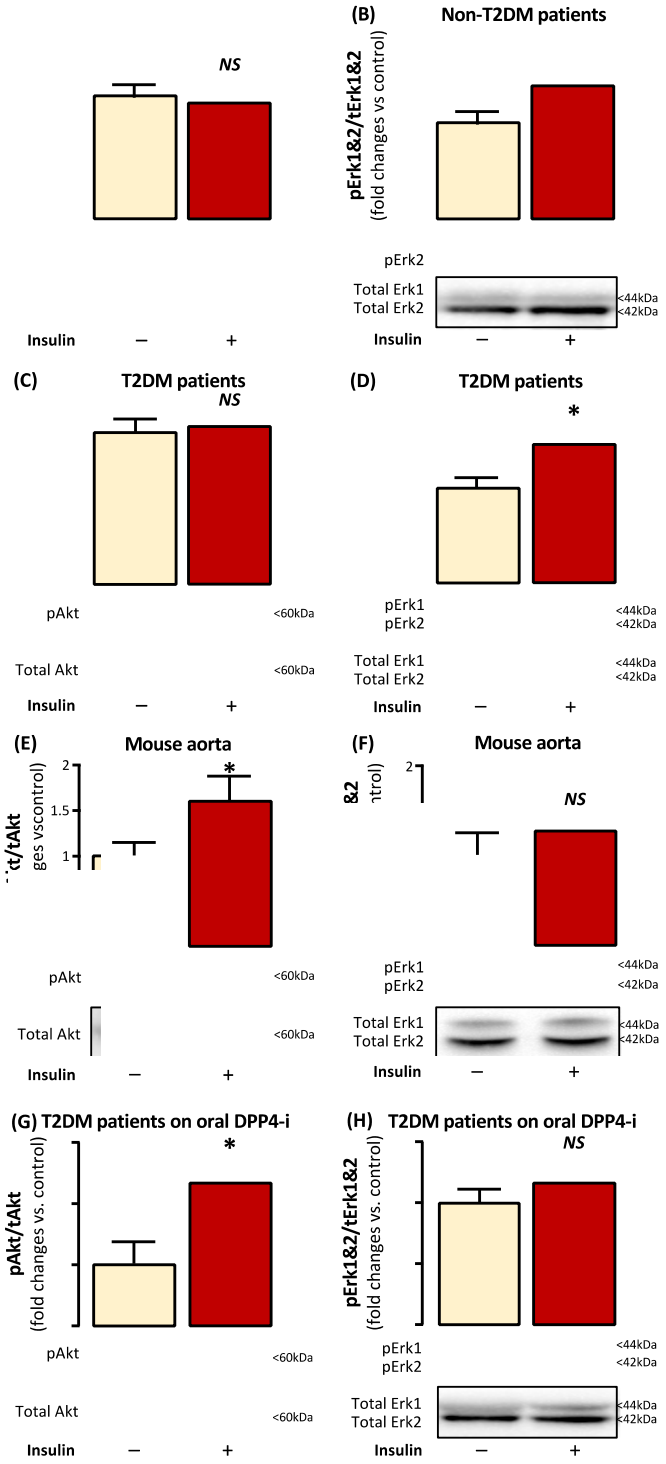

Figure 3.14: Downstream insulin signalling in patients with atherosclerosis. Insulin glargine M1 10nM activated Erk1&2 much more so than Akt in human vessels of non-diabetic and diabetic patients (panels A-F), indicating the presence of molecular insulin resistance. On the contrary, insulin induced marked Akt phosphorylation over Erk1&2 phosphorylation in aortae from atherosclerosis-free wild-type mice as well as in human vessels of diabetic patients on an oral DPP4 inhibitor (panels G-L). *P<0.05 vs control by Wilcoxon sign-rank tests, n=5 pairs per panel. I Akoumianakis *et al* (1), *Sci Transl Med* (in Revision).

3.3.5. Characterizing the insulin-sensitizing properties of DPP4 inhibition

To understand the mechanisms by which DPP4-i regulates downstream insulin and redox signaling in the vascular wall of patients with atherosclerosis, I first examined whether DPP4-i can restore physiological vascular insulin signaling (that favors Akt activation, over Erk1&2) in human vessels. In the presence of DPP4-i, insulin increased the activation of Akt over Erk1&2 in both human arteries (Fig. 3.15A-C) and veins (Fig. 3.15D-F). These were also replicated with human insulin (Fig. 3.15G-I), confirming that this is a class effect.

To prove that these differing insulin signaling pathway axes drive the previously observed redox responses to insulin, I first examined whether insulin activates Rac1 in the presence of an Erk1&2 inhibitor. I found that Erk1&2 inhibition by using 3-(2-Aminoethyl)-5-((4-ethoxyphenyl)methylene)-2,4-thiazolidinedione (Erk-i) abolished the ability of insulin to stimulate Rac1 GTP-activation, suggesting that Erk1&2 signaling is responsible for the insulin-mediated activation of NADPH-oxidases in human vascular disease (Fig. 3.16A). On the contrary, the combination of insulin with DPP4-i did not induce vascular eNOS phosphorylation in the presence of the Akt inhibitor wortmannin (Fig. 3.16B), suggesting that the DPP4-i-induced effect of insulin on eNOS phosphorylation is dependent upon activation of Akt.

To examine whether the DPP4-i/insulin interaction is mediated by changes in the activation of downstream insulin signaling substrate IRS1, I explored the direct effect of insulin and DPP4-i on IRS1 phosphorylation status. I observed that DPP4-i significantly reduced the phosphorylation of IRS1 at Ser307, a phosphorylation site linked with molecular IR (Fig. 3.17A).

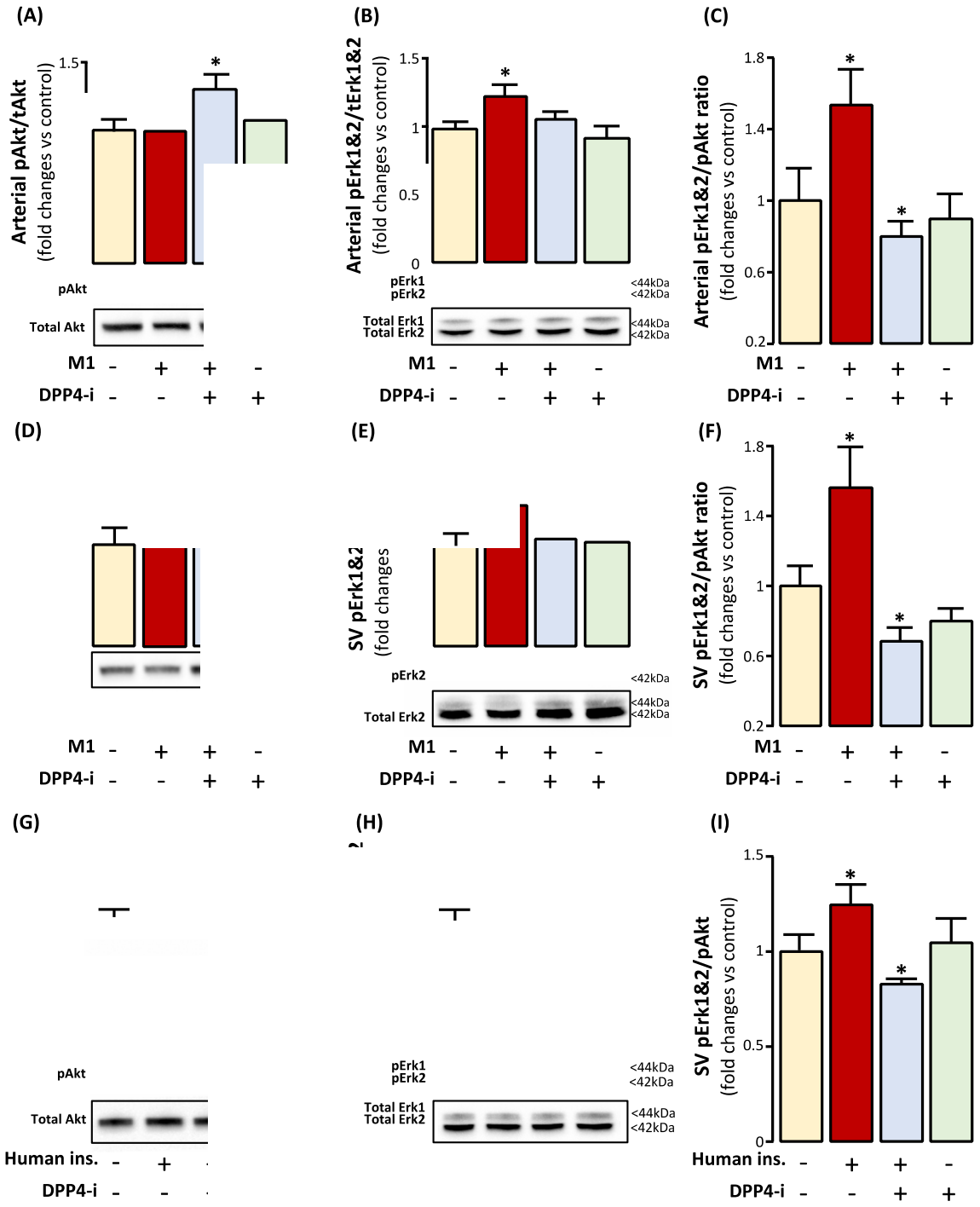

Figure 3.15: DPP4 inhibition regulates downstream insulin signalling in human vessels. Insulin glargine M1 10nM activated Erk1&2 much more so than Akt in human arteries (panels A-C) and veins (panels D-F). Combination of insulin and DPP4 inhibitor (DPP4-i) treatment, however, favoured Akt phosphorylation over Erk1&2 phosphorylation (panels A-F). These were replicated with human insulin, confirming a class effect (panels G-I). *P<0.05 vs control after post hoc analysis for multiple comparisons. I Akoumianakis *et al* (1), *Sci Transl Med* (in Revision).

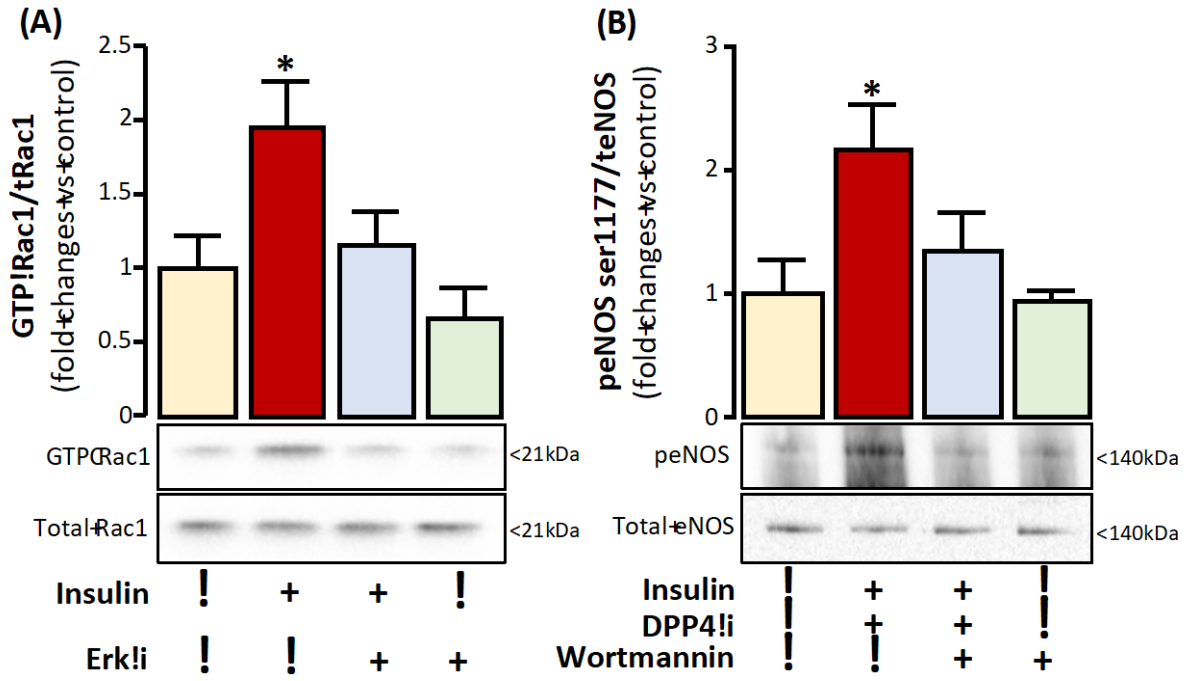

Figure 3.16: Downstream insulin signalling axes directly regulates vascular redox responses to insulin. Erk1&2 inhibition (Erk-i) abolished the ability of insulin glargine M1 10nM to activate Rac1 in human vessels, suggesting that the effect of insulin on NADPH-oxidases is via Erk1&2 (panel A). On the other hand, Akt inhibition by wortmannin abolished the ability of insulin to phosphorylate human vascular eNOS at ser1177 in the presence of DPP4 inhibition (panel B) suggesting that the effect of insulin on eNOS is mediated via Akt in the context of DPP4 inhibition. *P<0.05 vs control after post hoc analysis for multiple comparisons. I Akoumianakis *et al* (1)*, Sci Transl Med* (in Revision).

To further identify potential links of DPP4 inhibition with IRS1, I then explored the ability of DPP4-i to regulate the activation of AMP-activate kinase (AMPKα2), a molecule with known insulin-sensitizing properties, which has recently been linked with DPP4 signaling in *in vitro* models (Zeng *et al.*, 2014; Kornelius *et al.*, 2015). I found that DPP4-i was able to induce phosphorylation AMPKα2 at its activation site Thr172 (Fig. 3.17B). Pre-incubation of human vessels with compound C, an AMPK inhibitor, abolished the ability of DPP4-i to reverse the insulin-stimulated vascular NADPH-oxidase activation (Fig. 3.17C). AMPK inhibition abolished the ability of DPP4-i to rescue insulin sensitivity by reducing the phosphorylation of IRS1 at Ser307 (Fig. 3.17D). These findings suggest that DPP4-i restores vascular insulin sensitivity and elicits antioxidant responses to insulin via an AMPK-mediated mechanism.

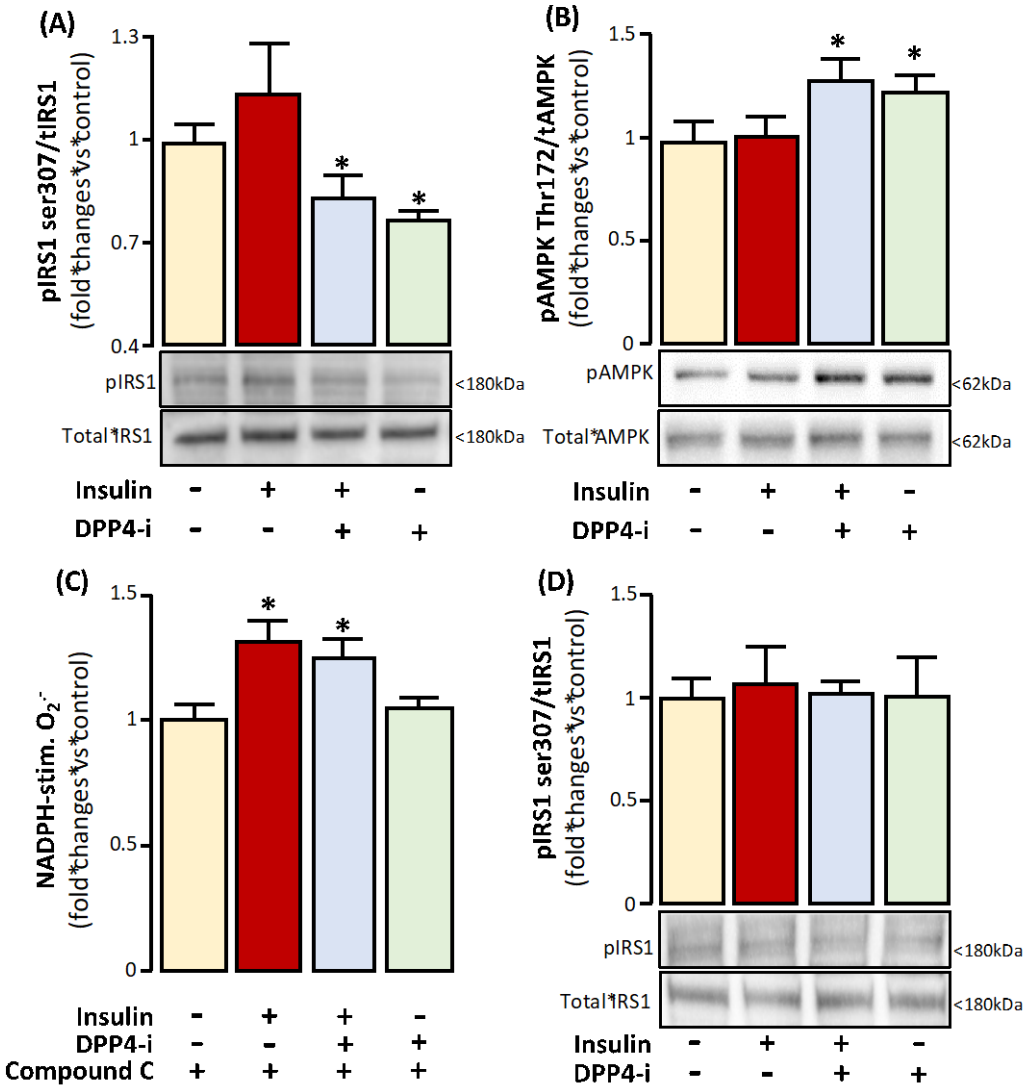

Figure 3.17: DPP4 inhibition (DPP4-i) rescues molecular insulin sensitivity via AMP-activated kinase (AMPK). DPP4-i directly reversed phosphorylation of insulin receptor substrate 1 (IRS1) at Ser307, a site linked with molecular insulin resistance (panel A). DPP4-i also induced phosphorylation of AMPK at its activation site Thr172 (panel B). AMPK inhibition by compound C abolished the ability of DPP4-i to reverse the effect of insulin treatment on NADPH-oxidases activity (panel C) as well as its ability to reduce IRS1 Ser307 phosphorylation (panel D). *P<0.05 vs control by Wilcoxon sign-rank tests, n=5 pairs per panel. I Akoumianakis *et al* (1), *Sci Transl Med* (in Revision).

3.3.6. Clinical implications of the interaction between DPP4 and insulin

To explore the value of systemic DPP4 activity and insulin levels as biomarkers of vascular redox state in patients with coronary artery disease, I then stratified the patients of Study 1 in subgroups depending on plasma DPP4 activity and insulin levels. I observed that patients in the lowest tertile of both DPP4 activity and insulin levels were characterized by markedly lower NADPH-oxidases activity and $O_2^{\cdot-}$ production in IMA compared to patients in the highest

tertile of DPP4 activity and insulin levels, as evaluated by measuring arterial NADPH-stimulated (Fig. 3.18A) and Vas2870-inhibitable (Fig. 3.18B) $O_2^{\cdot-}$ production. This confirmed a cumulative effect of high serum insulin and high DPP4 activity on vascular oxidative stress, introducing their potential role as combined biomarkers in patients with atherosclerosis.

I next explored the predictive value of DPP4 activity and insulin levels on cardiovascular and all-cause mortality, in patients in Study 1. 49 deaths were recorded in total, 21 of which were classified as cardiac. Patients within the high tertile for both serum DPP4 activity and serum insulin displayed significantly higher risk for cardiac death compared to the rest of the study 1 population (HR[95%CI]=3.60[1.12-11.63], P^{+}=0.032, after adjusting for traditional cardiovascular risk factors, namely age, sex, diabetes, hyperlipidemia, hypertension, active smoking and NYHA class (Fig. 3.18C)

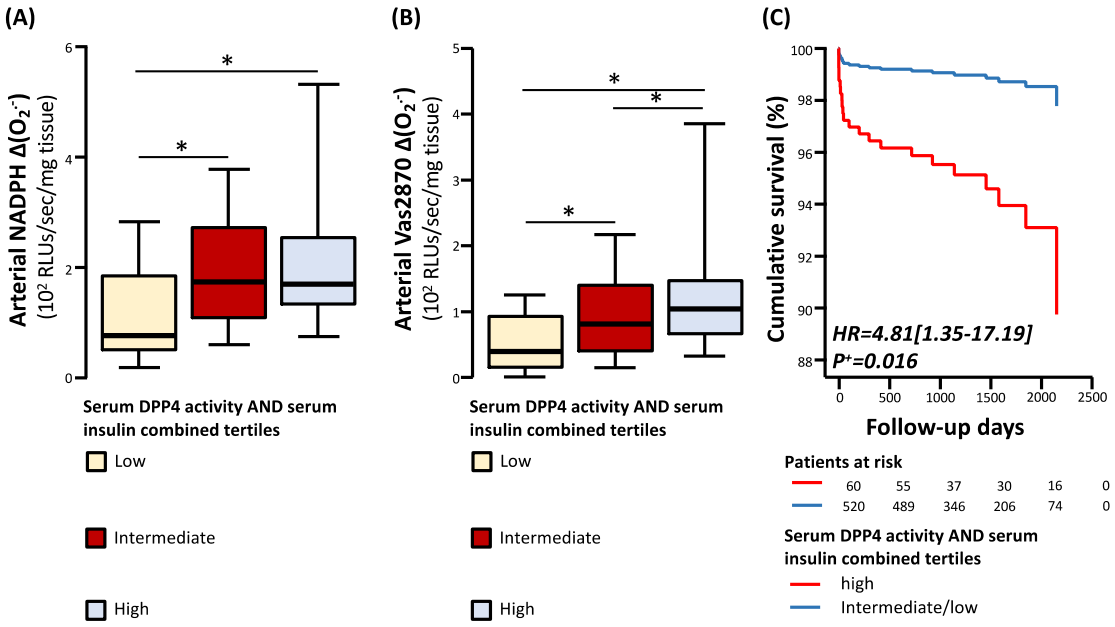

Figure 3.18: Clinical implications of the interactions between systemic dipeptidyl peptidase 4 (DPP4) activity and insulin levels. In study 1, internal mammary artery (IMA) segments from patients in the low tertile for both serum insulin levels and serum DPP4 activity displayed strikingly reduced production of NADPH-stimulated (panel A) and Vas2870-inhibitable (panel B) superoxide ($O_2^{\cdot-}$) production compared to those from patients in the high tertile for both serum insulin levels and serum DPP4 activity, reflecting differences in vascular NADPH-oxidases activity. Patients in the high tertile for both serum insulin levels and serum DPP4 activity (group 1) displayed significantly increased relative risk for cardiac death compared to the rest of the patients of Study 1 (group 2, panel C). P-values in panels A-B are calculated by Kruskal Wallis tests followed by post-hoc multiple comparison analysis vs low tertile. P* in panel C derive from Cox regression model for group 1 vs group 2 after adjusting for other risk factors (age, sex, diabetes, hyperlipidaemia, hypertension, NYHA class). I Akoumianakis *et al* (1), *Sci Transl Med* (in Revision).

This study demonstrates for the first time that the vessels from patients with vascular disease display consistent functional and molecular features of local vascular wall IR, even in the absence of diabetes or systemic IR. This results in dysregulated downstream insulin signalling, leading to increased vascular oxidative stress (via Rac1-mediated activation of NADPH oxidases) and endothelial dysfunction (by inducing eNOS uncoupling). Importantly, pharmacological inhibition of DPP4 restores physiological insulin signalling in vessels from patients with vascular disease, allowing insulin treatment to exert antioxidant and vasoprotective actions. Furthermore, high circulating insulin levels and high serum DPP4 activity in humans are adversely associated with cardiovascular outcomes. These exciting findings may comprise one of the mechanistic explanations as to why aggressive glycaemic control fails to improve clinical outcomes in secondary prevention and identify a new rationale for clinical trials to test the impact of combined DPP4-i and insulin treatment on clinical outcomes in patients with diabetes and vascular disease.

3.4.1. Beyond glycaemic control: the need to explore the vascular effects of insulin treatment

Hyperglycaemia has long been considered as the main therapeutic target for the prevention of vascular complications in diabetes (Schalkwijk and Stehouwer, 2005). However, aggressive lowering of blood glucose has resulted in inconsistent effects on cardiovascular outcomes (Knatterud *et al.*, 1978; Turner, 1998; Cosmi *et al.*, 2018), which may reflect the differing vascular effects of the pharmacological means used to achieve glycaemic control, or the pathophysiologic importance of other dysregulated pathways in T2DM that are not directly related to hyperglycaemia. Indeed, insulin treatment as a means to reduce hyperglycaemia is associated with increased risk for acute ischaemic events and cardiovascular (Margolis, Hoffstad and Strom, 2008; Roumie *et al.*, 2014) or all-cause mortality (McEwen *et al.*, 2012).

The ORIGIN and DEVOTE trials found that basal insulin glargine or insulin degludec respectively had no beneficial long-term effect on cardiovascular complications (Gerstein *et al.*, 2012; Marso *et al.*, 2017). In contrast, non-insulin antidiabetic medications such as liraglutide have been associated with improved long-term cardiovascular outcomes in diabetic patients (S. P. Marso *et al.*, 2016). This controversy highlights the unmet need to understand the direct effects of insulin on the vasculature in people with diabetes, who are at major risk for cardiovascular disease.

3.4.2. Vascular effects of insulin in humans with atherosclerosis and the concept of vascular insulin resistance

In vitro and *animal* studies have demonstrated that insulin exerts direct vasodilatory effects via Akt-mediated increase in nitric oxide bioavailability (Muniyappa *et al.*, 2007; Potenza, Addabbo and Montagnani, 2009). On the other hand, endothelium-specific IR has been associated with increased endothelial dysfunction in mouse studies (Duncan *et al.*, 2008; Kearney, 2013). Importantly, in this study I demonstrated an inverse association between circulating insulin levels and endothelial function, in patients with atherosclerosis, even in the absence of systemic IR. I also demonstrated that exogenous insulin (glargine, degludec or human soluble insulin) treatment induces endothelial dysfunction in human vessels, independently of the presence of diabetes or systemic IR. This is the first study demonstrating that insulin treatment impairs endothelial function in humans with atherosclerosis, even in the absence of diabetes or systemic IR, and provides direct evidence, in humans, of IR at the level of the vasculature that is distinct from systemic IR and/or hyperglycaemia.

Oxidative stress is a key feature of atherogenesis (Akoumianakis and Antoniades, 2017b) and vascular free radicals drive vascular complications in diabetes (Matsuda and Shimomura, 2013; Guzik and Cosentino, 2017). Insulin typically exerts antioxidant effects on the vascular

cells, by activating Akt signalling, resulting into activation of endothelial nitric oxide synthase(eNOS) and suppression of NADPH-oxidases (Muniyappa *et al.*, 2007). However, in conditions of IR, insulin may have the opposite effect, triggering oxidative stress by activating MAPK, at least *in vitro* (San José, Bidegain, Pablo A. Robador, *et al.*, 2009; Abhijit *et al.*, 2013), and this could potentially lead to oxidative degradation of NO and subsequent endothelial dysfunction. Here, I demonstrated for the first time that insulin directly stimulates NADPH-oxidases activity in human arteries and veins via GTP-activation of Rac1 and membrane translocation of active Rac1 and $p47^{phox}$, an effect associated with increased oxidation of eNOS co-factor BH4 and eNOS uncoupling. Interestingly, this was a very consistent result across all patients with advanced atherosclerosis, diabetic or not, and it was independent of IR. My results are the first to propose that insulin administration (synthetic or human) also induces eNOS uncoupling in vessels from patients with atherosclerosis. On the contrary, I confirmed that insulin supresses oxidative stress and restores eNOS uncoupling in aortic tissue form wild type mice by reducing the activity of NADPH-oxidases. This highlights the significant discrepancy between human vessels from patients with atherosclerosis and other disease-free models, implying dysregulation of insulin signalling in vessels from patients with atherosclerosis.

Insulin signalling is regulated by changes in the phosphorylation status of insulin receptor substrates such as IRS1 at Tyr sites (Pessin and Saltiel, 2000), and physiological signalling triggers phosphorylation of Akt (Pessin and Saltiel, 2000). In the presence of diabetes and IR, IRS1 is phosphorylated at Ser residues instead, and downstream dysregulated insulin signalling leads to activation of MAPK (Erk1&2) rather than Akt (Pessin and Saltiel, 2000; Shulman, 2000; Khodabandehloo *et al.*, 2016). While Akt has been linked with eNOS phosphorylation and NO production (Zeng *et al.*, 2000), Erk1&2 activation has been associated with induction of cellular redox signalling (Luo *et al.*, 2012; Bretón-Romero *et al.*, 2016). Although

dysregulated insulin signalling was found in adipocytes of patients with IR (Tan *et al.*, 2015), its presence has not been investigated in human vessels, while its potential role in the development of vascular complications of diabetes in humans is unknown.

In this work I demonstrated that insulin failed to induce Akt phosphorylation in the vascular wall of patients with coronary atherosclerosis while significantly activating Erk1&2, a reflection of vascular IR even in the absence of diabetes. These findings were in contrast with the effects observed when I incubated healthy murine aortic tissue with the same insulin types and concentrations. This local, vascular resistance to insulin in the context of vascular disease may be due to an increased sensitivity of the vasculature to the systemic inflammatory environment of atherosclerosis (F. Kim *et al.*, 2008; Alexopoulos, Katritsis and Raggi, 2014; Domingueti *et al.*, 2016), a consequence of nutrient overload (Nolan *et al.*, 2015) or it may comprise a surrogate marker of senescence and aging (Tsuneki *et al.*, 2008; Keske *et al.*, 2016) considering that most patients with advanced atherosclerosis are relatively elderly.

3.4.3. DPP4 inhibition as a means of vascular insulin sensitisation

Following my observation that human arteries and veins from patients with vascular disease have a consistent IR phenotype independently of diabetes or signs of systemic IR, I hypothesised that physiological insulin signalling could be restored if a pharmacological strategy for vascular insulin sensitization is applied before insulin treatment initiation. DPP4 is a transmembrane glycoprotein, with a soluble isoform, that cleaves N-terminal dipeptides from proteins such as GLP1, reducing their bioavailability (Kim, Yu and Lee, 2014). DPP4 promotes IR in obesity and diabetes (Lamers *et al.*, 2011), so that its pharmacological inhibition may be a therapeutic target in diabetes and IR. Although direct evidence of an interaction between DPP4 and insulin signalling is limited, it has been suggested that DPP4 induces IR in adipocytes (Lamers *et al.*, 2011), while DPP4-i improves insulin sensitivity (Kornelius *et al.*,

2015). However, the vascular implications of DPP4-i in humans and its interactions with vascular insulin signalling are unknown.

In this study I demonstrated that pre-treatment of patients with an oral DPP4-i completely reversed vascular insulin signalling in patients with atherosclerosis, shifting it from Erk1&2 toward Akt activation, and led to an insulin-induced reduction of NADPH-oxidases activity. To examine whether this was due to systemic effects of DPP4-i or due to the direct inhibition of DPP4 in the human vascular wall, I used *ex vivo* models of human vessels, where I demonstrated that pre-incubation of these vessels with a DPP4-i reversed dysregulated insulin signalling leading to improved vascular redox state . This occurred via AMPK-mediated reduction of IRS1 Ser307 phosphorylation, a change that is known to regulate IR in *in vitro* and mouse models (Zeng *et al.*, 2014; Kornelius *et al.*, 2015).

Indeed, in the presence of DPP4-i, insulin reduced Rac1 activation, supressed NADPH-oxidases activity, restored BH4 bioavailability and improved eNOS coupling and NO bioavailability. Interestingly, beyond reversal of insulin signalling, DPP4 inhibition on its own had no effects on vascular redox state or NO bioavailability, a finding compatible with the clinical trials showing no benefit from DPP4-i on cardiovascular complications of diabetes. Finally, in a prospective study arm, I showed that high DPP4 plasma activity and high circulating insulin levels were predictive of higher cardiac mortality in the study population.

3.5. Conclusion

In conclusion, I showed for the first time that IR is present at the molecular level in the vasculature of humans with coronary atherosclerosis even in the absence of diabetes or markers of systemic IR. This results in dysregulated downstream insulin signalling characterised by

Erk1&2 activation, increased NADPH-oxidases activity and endothelial dysfunction. In this context, DPP4-i conveys direct insulin-sensitizing effect, and therefore pharmacological combination of insulin treatment with DPP4-i may prove to be of clinical benefit. These findings call for randomised clinical trials to explore the effect of insulin on clinical outcomes of patients taking DPP4-i.

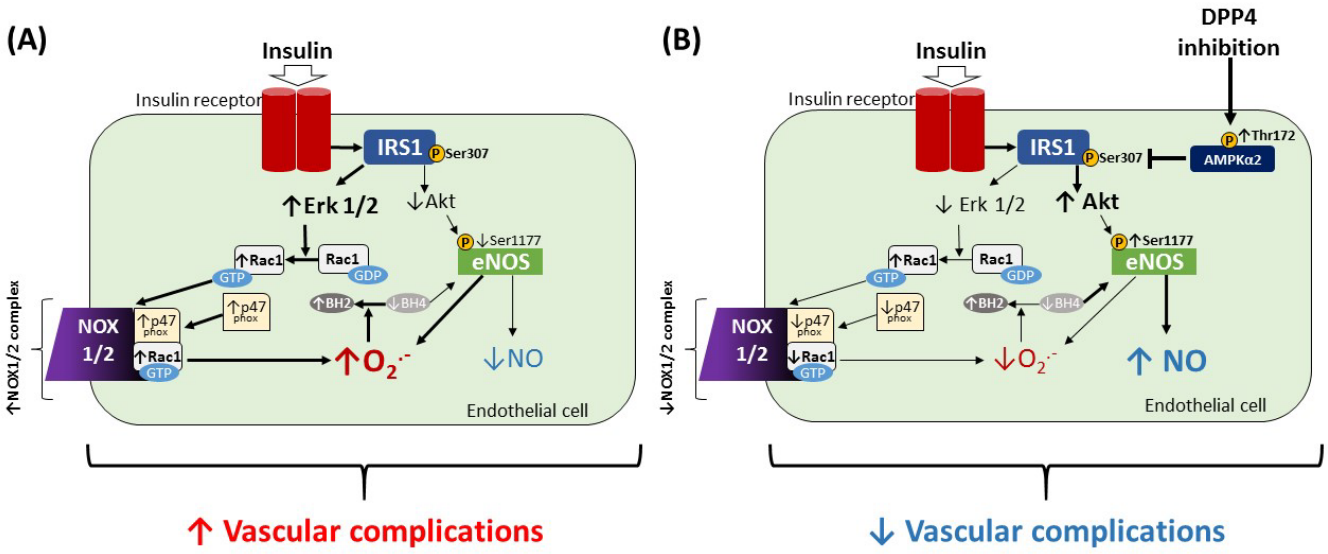

Figure 3.19: Summary of vascular insulin signalling regulation. Insulin disproportionately stimulates the activation of Erk1&2 compared to the Akt signalling axis in the vascular wall of humans with coronary atherosclerosis, presumably. This results in GTP-activation and membrane translocation of Rac1, which along with p47phox forms the active NADPH-oxidases complex, leading to increased oxidative stress, oxidation of tetrahydrobiopterin (BH4), uncoupling of endothelial nitric oxide synthase (eNOS), impairment of endothelial dysfunction and propagation of vascular complications. DPP4 inhibition increases vascular activation of AMP-activated kinase (AMPK), which restores insulin sensitivity by reducing the phosphorylation of insulin response substrate 1 (IRS1) at ser307 and reverses the vascular responses to insulin. The net effect includes marked insulin-mediated activation of Akt, activation (via phosphorylation) of eNOS combined with reduced oxidative stress and improved BH4 availability. Vascular insulin sensitisation with a DPP4 inhibitor may be able to improve the in vivo cardiovascular effects of insulin treatment in diabetic patients, thus reducing the risk for long-term adverse cardiovascular events. I Akoumianakis *et al* (1), *Sci Transl Med* (in Revision).

Chapter 4

Adipose tissue-derived Wnt5a as a trigger of vascular disease

This Chapter explores the role of Wnt5a released by AT as a causal mediator of vascular disease via regulation of vascular redox state. Observational results are first provided exploring the interactions of circulating and AT-derived Wnt5a with obesity, vascular oxidative stress and the presence and progression of vascular disease. These are followed by mechanistic experiments investigating the cellular effects of Wnt5a signalling on vascular redox state. This work is due for publication by *Science Translational Medicine* (Akoumianakis I *et al*, 2019b).

4.1. Introduction

As mentioned in Chapter 1, AT is a dynamic organ with regional biological variability, secreting a wide range of adipocytokines with vascular effects (Akoumianakis and Antoniades, 2017b). PVAT exerts paracrine effects on the vascular wall, while "remote" AT depots such as ScAT and ThAT exert endocrine effects by enriching the circulating adipocytokine pool. Evidence suggests that obesity is associated with a shift of the AT secretome from a vasoprotective/anti-atherogenic to a pro-atherogenic phenotype (Akoumianakis, Tarun and Antoniades, 2016; Akoumianakis and Antoniades, 2017b), highlighting the need for better understanding of the links between AT biology and vascular (patho)physiology.

Recent work suggests that AT secretes Wnt5a and Sfrp5 (Ouchi *et al.*, 2010), both molecules with potential vascular effects (Marinou *et al.*, 2012; Bretón-Romero *et al.*, 2016) which are involved in non-canonical Wnt signalling. Imbalance in the AT production of Wnt5a and Sfrp5 in obesity may result in a 'vicious cycle' of increased AT inflammation and IR (Ouchi *et al.*, 2010; Fuster *et al.*, 2015), indirectly triggering vascular complications of obesity.

Via its link with Rac1 signalling, Wnt5a may have vascular effects regarding NADPH-oxidases activity and oxidative stress (key features of atherogenesis), although this has never been explored in human vascular disease.

I hypothesised that Wnt5a secreted from the AT may be associated with obesity and systemic IR/T2DM, having potentially detrimental vascular effects via redox state regulation through non-canonical Wnt signalling.

4.2. Study population & methods

4.2.1. Study population

Study protocols were in agreement with the Declaration of Helsinki and all patients provided written informed consent prior to enrolment. The demographic characteristics of the participants of all study arms are presented in table 4.1.

4.2.1.1. In vivo clinical studies (study 1, 2 and 3)

Study 1 comprised 1,004 prospectively enrolled patients undergoing cardiac surgery at the John Radcliffe hospital, Oxford University NHS Foundation Trust, UK and Ippokration Hospital, Athens, Greece. Exclusion criteria included inflammatory, neoplastic, renal or hepatic diseases. Fasting blood samples were obtained on the morning of the surgery and used for plasma isolation for circulating biomarker measurements. During surgery, segments of IMA with its surrounding PVAT, ThAT and ScAT from the chest were collected, transferred to the lab on ice, and processed for baseline *ex vivo* experiments, vasomotor studies and measurement of vascular $O_2^{\cdot -}$.

Study 2 included 70 individuals with CAD (from AdipoRedOx study) and 70 controls without CAD (from ORFAN study, confirmed with coronary CT angiography) matched with the CAD group for age, gender and BMI, used for cross-sectional studies comparing circulating Wnt5a and Sfrp5 levels.

Study 3 consisted of 68 individuals that underwent two non-contrast CT scans 3-5 years apart (subset of ORFAN study, mean interval of 4.1 years), to study progression of atherosclerotic disease in the coronary arteries. The development of new calcification and the progression of existing calcified atherosclerotic plaques were compared between the two scans.

4.2.1.2. Ex vivo studies with human vessels (Study 4)

The human *ex vivo* study (study 4) included 77 AdipoRedOx study patients recruited for prospective mechanistic experiments. Human IMA and saphenous vein (SV) segments were collected during surgery and transferred to the lab on ice. IMA samples were processed in the lab as explained in relevant sections, subjected to *ex vivo* incubations and ultimately used for vascular $O_2^{\cdot-}$ quantification and downstream signalling evaluation as described later.

4.2.2. Methods

4.2.2.1. Ex vivo & in vitro incubations

Fresh, intact human IMA samples were cut into sequential rings and opened longitudinally to expose the endothelial surface. Each segment was then equilibrated for 45 minutes in oxygenated (95% O_2/5% CO_2) KHB (pH 7.4) at 37°C, where carrier (sterile PBS), Wnt5a 100ng/mL (R&D Systems, 645-WN/CF) and/or Sfrp5 300ng/mL (R&D Systems, 6266-SF) was added. The vascular segments were then used fresh for superoxide ($O_2^{\cdot-}$) quantification or snap-frozen in -80^{o}C until processed later.

Table 4.1: Demographic characteristics of the Chapter 4 study participants

	Study 1	Study 2		Study 3	Study 4
		Non-CAD	***CAD***		
Participants (n)	1,004	70	70	68	77
Age (years)	64.8±0.5	61.1±0.8	61.3±1.5	60.4±1.04	67±1
Males (%)	81.3	42.9	47.1	39.7	81.8
Hypertension (%)	70.6	22.9	78.6***	27.9	74.0
Hyperlipidaemia (%)	87.1	27.1	68.6***	44.1	90.9
T2DM (%)	23.5	2.9	24.3***	36.8	23.4
Smoking					
Active (%)	14.9	4.3	15.7*	6.6	7.8
Past (%)	49.8	44.3	44.3	32.8	51.9
BMI (kg/m^2)	28.0±0.15	28.3±0.7	28.4±0.5	28.1±0.7	28.4±0.5
Medication					
Antiplatelet (%)	73.1	15.7	90.0***	18.0	89.6
ACEi/ARBs (%)	62.3	21.4	77.1***	36.1	62.3
Statins (%)	78.2	22.9	68.6***	41.0	92.2
βblocker (%)	65.2	24.3	70.0***	23.0	75.3
CCB (%)	23.9	14.3	27.1	13.1	23.4
Insulin (%)	13.3	0.0	10.0**	0.0	5.2
Oral hypoglycaemic (%)	17.5	2.9	10.0	11.5	20.8

T2DM: Type 2 diabetes mellitus; BMI: Body mass index; ACEi: Angiotensin converting enzyme inhibitor; ARB: Angiotensin receptor blocker; CCB: Calcium channel blocker Continuous variables are presented as mean±SEM; ***P<0.01* vs CAD, ****P<0.001* vs non-CAD by Chi-square tests.

For the *ex vivo* experiments involving Rac1 inhibition, human IMA and mouse aorta segments were pre-incubated with a Rac1 inhibitor, NSC23766 100μM (R&D systems, catalogue number 2161) for 15min prior to any experiment.

For the visualisation of vascular $O_2^{\cdot-}$ production, IMA were incubated in the presence or absence of Wnt5a as described earlier, and snap-frozen in optical coherence tomography (OCT) medium until used for oxidative fluorescent microtopography as explained later.

4.2.2.2. Human primary smooth muscle cell isolation and culture

VSMC culture work was done by Dr Fabio Sanna. Human SV explants were washed and digested with 0.25% trypsin for 10min following adventitia removal. The digested tissue was

diced into 1mm^2 sections and seeded in Dulbecco's modified eagle media (DMEM)+20% FBS. VSMCs were grown in Media 231 supplemented with smooth muscle growing supplement (SMGS) (Life Technologies Ltd) in a cell culture incubator at 37^{o}C and 5% CO_2 following the first passage.

For characterisation purposes, VSMCs were plated on a 6-well plate for 24h, culture media was removed and cells were fixed with 4% paraformaldehyde. To permeabilise the cells, 0.2% Triton in PBS was added for 10min at room temperature and cells were then washed thrice with PBS and blocked with 10% bovine serum albumin (BSA). Cells were incubated overnight at 4°C with mouse monoclonal anti-CD31 (Sigma, P8590) or mouse monoclonal anti-α-smooth muscle actin (Sigma, A5228) primary antibody and secondary antibody goat-anti mouse Alexa Fluor 488 conjugated (ab150113, Abcam) for 1 hour at room temperature. Following 3 washes with PBS, the cells were dried and mounted with Slow Fade Gold Anti Fade with DAPI (S36939, ThermoFisher) before visualization with fluorescence inverted microscope (Olympus IX71).

4.2.2.3. Transfection studies with Fzd2 and Fzd5 siRNA

Fzd2, Fzd5 siRNA (ON-TARGET plus SMART pool) and negative control siRNA (ON-TARGET plus non-targeting pool) were purchased from Dharmacon and used to knock-down Fzd2 and Fzd5 receptors in human VSMCs, respectively. Briefly, 1x10^6 cells were seeded in a 6 well plate for 24 h, and medium was replaced by Optimem on the day of transfection. Lipofectamine RNAiMax (Thermo Fisher Scientific) was used to transfect VSMCs with 100 pmoles of siRNA according to the instructions provided by the manufacturer. 24 h post-transfection, Optimem was replaced by Medium 231 plus SMGS. To test the transfection ability as well as the toxicity of lipofectamine RNAiMax on primary VSMCs, BlockiT Alexa Fluor Red Fluorescent control (14750100, ThermoFisher) was used as transfection control.

4.2.2.4. Transfection studies with UPS17

HeLa cells from passage 10-17 were cultured in growth medium DMEM with 10% fetal calf serum (FCS), 1% penicillin/streptomycin, and 200 mM L-glutamine at 37 °C in a 5% CO_2 humidified incubator. Cells were starved overnight, and transfected with pRS-USP17 shRNA (TG321147, Origene Technologies) using FuGENE6 (E2691, Promega).

Total RNA was isolated using Trizol, followed by chloroform and isopropanol extraction, washing by ethanol and dissolving in DEPC-H_2O. USP17 mRNA expression was detected as described previously (*18*). Briefly, 1 μg total RNA was applied using the OneStep RT–PCR kit (210210, Qiagen). The primer sets for USP17 are:

5′-CAGTGAATTCGTGGGAATGGAGGACGACTCACTCTAC-3′ (forward)

5-AGTCATCGATCTGGCACACAAGCATAGCCCTC-3′ (reverse)

We used β-actin as a housekeeping gene by the following primers:

5′-GGACTTCGAGCAAGAGATGG-3′ (forward)

5′-AGCACTGTGTTGGCGTACAG-3′ (reverse)

Clones with undetectable USP17 expression were used for 8h incubations with Wnt5a 100ng/mL and Rac1 activation was assessed compared to transfection controls.

4.2.2.5. shRNA lentiviral particles transduction in immortalised pre-adipocytes

An immortalised human pre-adipocyte cell line from subcutaneous abdominal AT was kindly donated by Constantinos Christodoulides and Fredrik Karpe, generated as described by Todorčević et al (Todorčević *et al.*, 2017).

Immortalized human pre-adipocytes were cultured in a 6 well-plate until 50% confluence. On the day of the infection, media was replaced with culture media containing 5 µg/mL of hexadimethrine bromide. Immortalized pre-adipocytes were transduced with the appropriate amount of shRNA lentiviral transduction particles to downregulate Wnt5a at a multiplicity of infection of 100. 24 h post post-incubation, transduced cells were selected with 0.5 µg/mL puromycin. Wnt5a downregulation was then confirmed by qRT-PCR and Western blotting as described in relevant sections.

4.2.2.6. Wnt5a secretion assay

Human immortalised pre-adipocytes were grown to ~90% confluence in T75 flasks, washed three times with PBS and cultured with 0.1% BSA. After 24 h, medium was collected and centrifuged at 10,000 g for 10 min. Supernatant was concentrated using Amicon Ultra-15 centrifugal filter system 10KMWCO (Millipore) and centrifuged at 5,000 g at room temperature for 1 h. 20 µg of concentrated supernatant total protein were finally analysed by Western blotting.

4.2.2.7. Co-culture of human primary VSMC with immortalised pre-adipocytes

VSMCs were co-cultured with human pre-adipocytes using trans-well plate (0.4 µm polycarbonate filter, Corning) for 24 h. Human pre-adipocytes were cultured in the bottom chamber and VSMCs in the top one.

4.2.2.8. Mouse studies

A doxycycline-inducible Wnt5a-overexpressing transgenic mouse model was used to evaluate the *in vivo* vascular effects of Wnt5a. FVB/N Tg(tetO-Wnt5a)17Rva/J mice were obtained from Jackson Laboratories (stock #022938), and crossed to mixed background C57BL/6, 129/SV, FVB CAGG-rtTA (generated by Dr Lukas Dow in the lab of Dr Scott Lowe at Memorial Sloan Kettering Cancer Centre, USA) (38). Mice were backcrossed to C57BL/6

background seven times prior to the study. TetO-Wnt5a+ and rtTA+ mice were then crossed obtaining double transgenic mice, rtTA+ single transgenic mice were kept as control animals. 2mg/mL doxycycline hyclate (J60579, Alfa Aesar) was administered, to both double transgenic tetO-Wnt5a+/ rtTA+ and control tetO-Wnt5a-/rtTA+ animals via the drinking water, containing 5% sucrose overnight to induce Wnt5a expression. DNA extracted from experimental animal ear notches was used for genotyping with the following PCR primers:

C57BL/6, FVB CAG-rtTA

CCM 5'- CGAAACTCTGGTTGACATG - 3'

CTG 5'- ATGCCCTGGCTCACAAATAC - 3'

CWT 5'- TGCCTATCATGTTGTCAAA – 3'

C57BL/6, FVB/N Tg(tetO-Wnt5a)17Rva/J

17815 5'- ACAAAGACGATGACGACAAGC – 3'

17816 5'- CGCACCTTCTCCAATGTACTG – 3'

oIMR7338 5'- CTAGGCCACAGAATTGAAAGATCT – 3'

oIMR7339 5' – GTAGGTGGAAATTCTAGCATCATCC – 3'

Following overnight induction of Wnt5a overexpression, experimental animals were sacrificed and plasma & tissues snap-frozen in -80^{o}C until used for circulating Wnt5a measurements as well as RNA isolation and reverse transcription to confirm the transgene overexpression as explained below. Aortic tissue was also collected and used fresh to quantify $O_2^{\cdot-}$ production by lucigenin chemiluminescence as explained below.

Animal studies were ethically approved from the Local Ethical Review Committee in accordance with the UK Home Office regulations (Guidance on the Operation of Animals, Scientific Procedures Act, 1986) and were approved by the Local Ethical Review Committee.

Mice were housed in a specific pathogen-free environment, in Tecniplast Sealsafe IVC cages (floor area 542 cm^2) with a maximum of six other mice. Mice were kept in a 12h light/dark cycle in controlled temperatures (20–22°C) and fed normal chow and water ad libitum.

Mouse colony maintenance, transgene overexpression and tissue harvesting was performed by Dr Patricia Ciccone and Dr Fabio Sanna. I performed all the experiments on mouse tissue presented in this thesis.

4.2.2.9. Coronary calcium score quantification

For study 3, a non-contrast prospectively ECG-triggered axial acquisition CT scan was obtained (2.5-3.0 mm axial slice thickness, tube energy of 120 kV) at both time points (baseline and follow-up) with the carina and the diaphragm used as cranial and caudal landmarks respectively. In all patients, the baseline scan was acquired using a 64-slice LightSpeed Ultra CT scanner (General Electric Healthcare), whereas all follow-up scans were performed in a 320-slice Aquilion One scanner (Toshiba Medical Systems). Coronary calcium score (CCS) was measured on a dedicated workstation (Aquarius Workstation® V.4.4.13, TeraRecon Inc., Foster City, CA, USA) according to the Agatston method (Agatston *et al.*, 1990). Coronary calcification progression was defined as any change in CCS ≥ 1, while new onset calcification was evaluated in those patients having CCS=0 at the time of the baseline scan. CCS quantification was performed by Dr Evangelos Oikonomou. I performed the plasma Wnt5a and Sfrp5 measurements for study 3 as well as the relevant statistical analysis.

4.2.2.10. Statistical analysis

Continuous variables were tested for normal distribution by the Kolmogorov-Smirnov test. Non-normally distributed variables are presented as median[25^{th}-75th percentile] and whiskers (Tukey). Normally distributed variables are presented as mean ± SEM. Comparisons of continuous variables between two groups were performed using unpaired t test or Man-

Whitney U-test, while comparisons between 3 or more groups were performed using one-way ANOVA or Kruskal-Wallis followed by Bonferroni or Dunn's post hoc correction for multiple comparisons. Paired comparisons were performed using paired t tests or Wilcoxon signed-rank tests followed by multiple comparisons analysis as appropriate. For between-groups serial changes I used two-way ANOVA for repeated measures.

To examine whether the association between obesity and vascular NADPH-oxidase activity is independent of Wnt5a/Sfrp5 expression in PVAT, I performed multivariate linear regression where NADPH-stimulated $O_2^{\cdot-}$ was used as dependent variable and obesity classification, age, sex, diabetes, hypertension and smoking (with/without *WNT5A*/*SFRP5* expression tertiles in PVAT) were used as independent variables. Standardised beta coefficients are presented.

To address whether plasma Wnt5a, Sfrp5 and their ratio were independently associated with CAD in the nested case-control study 2, I performed multivariate linear egression in which the presence of CAD was used as dependent variable and hypertension, hyperlipidaemia, smoking and plasma wnt5a or sfrp5 or wnt5a/sfrp5 ratio were used as independent variables. The standardised beta is presented for each variable.

To examine whether coronary calcified plaque progression or new onset calcification were associated with plasma Wnt5a, I performed multivariate linear regression where calcified plaque progression and new onset calcification were used as dependent variables and plasma wnt5a, age and sex were used as independent variables.

All statistical tests were two-tailed and were performed using SPSS version 20.0. $P<0.05$ was considered statistically significant.

4.3. Results

4.3.1. Wnt ligand expression profile in adipose tissue depots from patients with atherosclerosis

I first explored the gene expression profile of all 19 Wnt ligands in human PVAT, ThAT and ScAT. *WNT5A* was the most highly expressed Wnt ligand in PVAT (Fig. 4.1A), while *WNT11* was the most highly expressed Wnt ligand in ThAT and ScAT, with *WNT5A* still being among the four most highly expressed Wnt ligands in these depots (Fig. 14.1B-C). As both Wnt5a and Wnt11 are known to be non-canonical Wnt signalling pathway activators, and considering that Wnt5a may be a more important paracrine regulator secreted from PVAT, I next focused on the potential role of Wnt5a as a mediator of the vascular complications of obesity via non-canonical Wnt signalling.

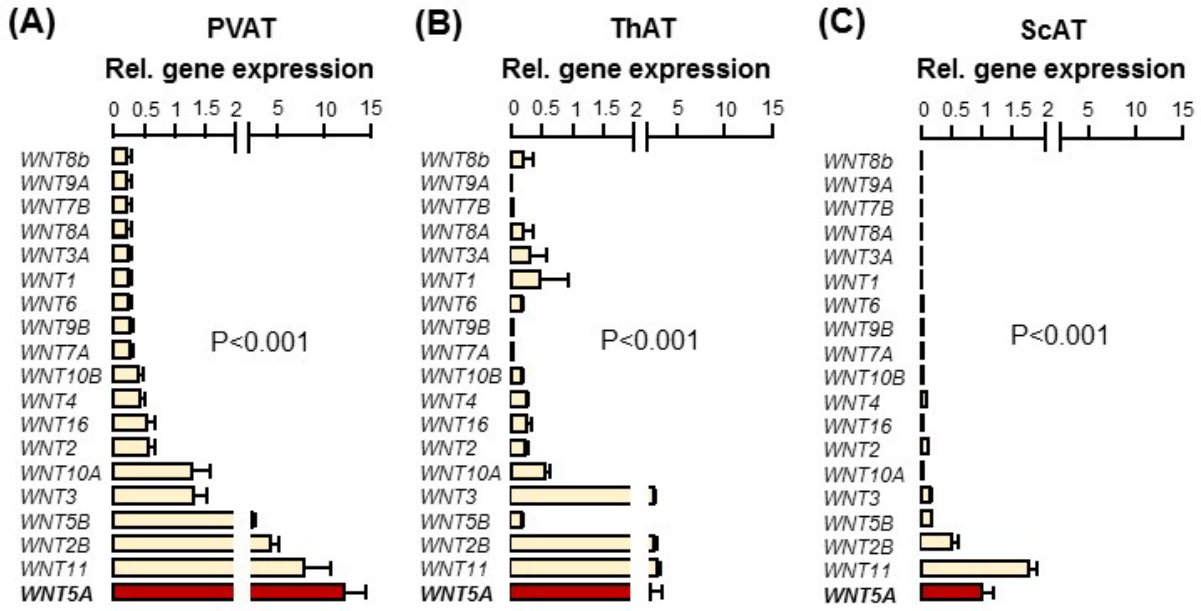

Figure 4.1: Wnt ligand expression profile in human adipose tissue (AT). In an initial pilot study, I evaluated the gene expression of the 19 Wnt ligands in human perivascular (PVAT) (panel A), thoracic (ThAT) (panel B) and subcutaneous (ScAT) AT (panel C) in n=54 patients of study 1. The non-canonical Wnt5a and Wnt11 ligands were the most highly expressed Wnt ligands in all AT depots, with Wnt5a being the most highly expressed Wnt in PVAT. P-values calculated by Kruskal-Wallis tests in all panels. Adapted from I Akoumianakis *et al* (2), *Sci Transl Med* (Accepted).

4.3.2. Interactions of Wnt5a with obesity, systemic insulin resistance and diabetes

Considering that Wnt5a is neutralised by Sfrp5 via protein-protein interactions, I used the circulating Wnt5a/Sfrp5 ratio as an index of overall Wnt5a bioavailability in consistency with previously published observational studies. I first observed that, in obesity, circulating Wnt5a was elevated (Fig. 4.2A), circulating Sfrp5 was decreased (Fig. 4.2B) and their ratio was increased (Fig. 4.2C). Systemic IR and diabetes were non-significantly associated with plasma Wnt5a (Fig. 4.2D) or Sfrp5 (Fig. 4.2E) individually, however they were positively associated with the circulating Wnt5a/Sfrp5 ratio (Fig. 4.2F).

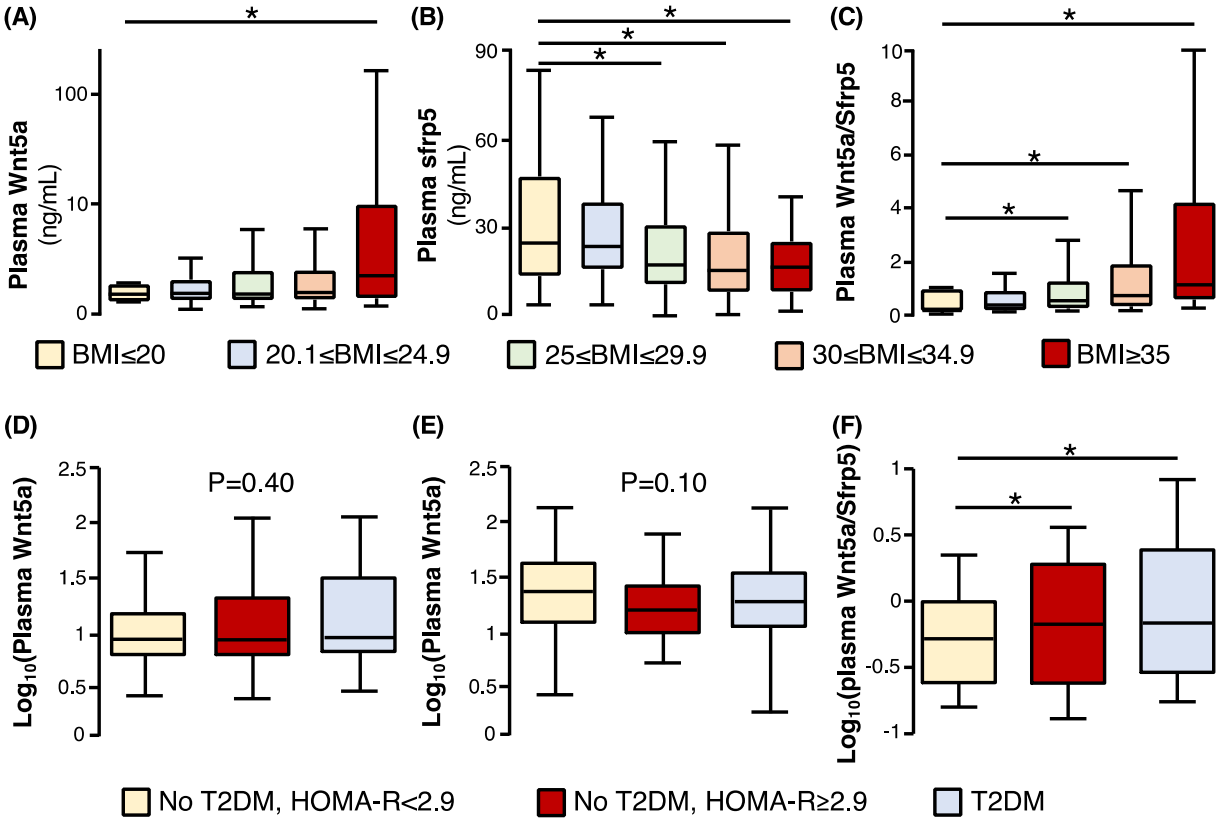

Figure 4.2: Plasma Wnt5a bioavailability and metabolic disease. In obesity, circulating Wnt5a was elevated (A), circulating Sfrp5 was decreased (B) and plasma Wnt5a/Sfrp5 was increased (C). Systemic insulin resistance (HOMA-IR≥2.9) and type 2 diabetes mellitus (T2DM) were non-significantly associated with plasma Wnt5a (D) or Sfrp5 (E), however they were associated with increased plasma Wnt5a/Sfrp5 (F). *P<0.05 vs low BMI group or no T2DM/HOMA-IR<2.9 for all relevant panels after post hoc analysis for multiple comparisons; P-values are calculated by one-way ANOVA in panel B. Adapted from I Akoumianakis *et al* (2), *Sci Transl Med* (Accepted).

I next focused on AT as a source of Wnt5a and Sfrp5, exploring whether the adipose secretion of these molecules was influenced by the presence of obesity and/or systemic IR and T2DM. I observed a positive association between BMI and the gene expression of Wnt5a/Sfrp5 in human ThAT (Fig. 4.3A) but not in human ScAT (Fig. 4.3B).

This suggests that increased Wnt5a/Sfrp5 gene expression in visceral adiposity (i.e. ThAT) could be linked with obesity-related vascular disease in humans. On the other hand, adipose expression of Wnt5a/Sfrp5 was not associated with the presence of systemic IR or T2DM (Fig. 4.3C-D), suggesting that, while these metabolic abnormalities are characterised by systemic increase in Wnt5a/Sfrp5, this is not reflected in AT. On the contrary, obesity, which can be regarded as an AT-specific disease, is associated with dysregulation of Wnt5a/Sfrp5 both in AT and in the circulation.

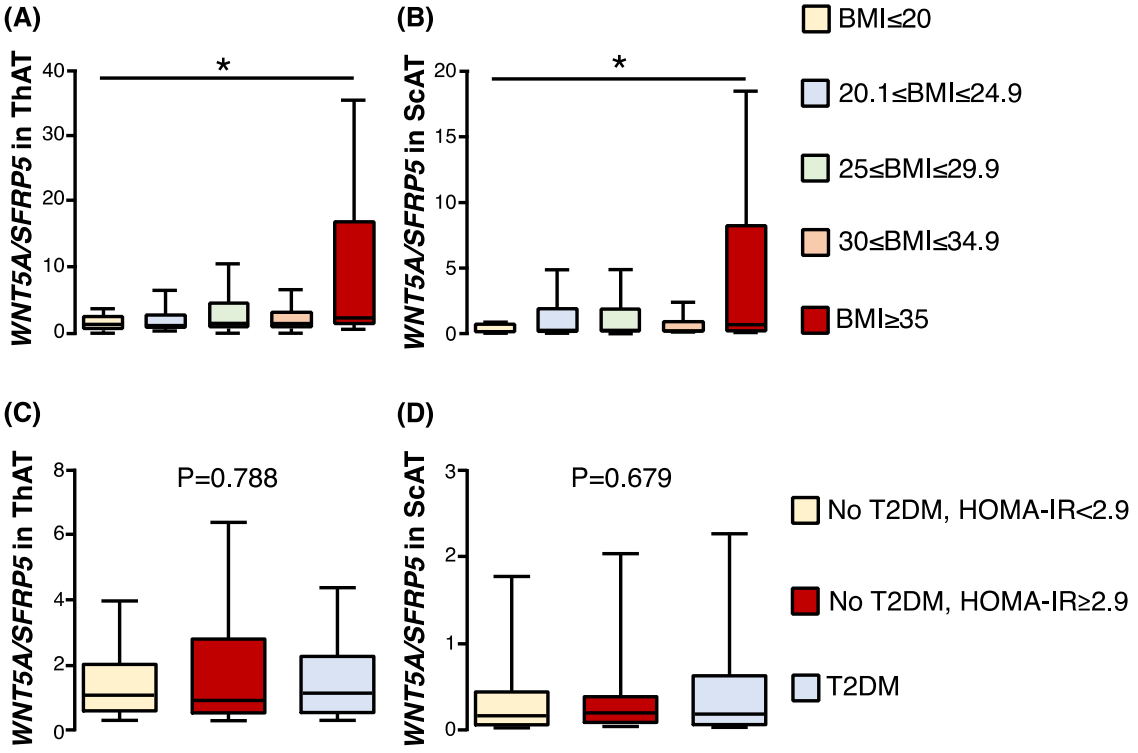

Figure 4.3: Adipose tissue (AT) expression of Wnt5a & Sfrp5 and metabolic disease. Obesity was associated with increased expression of Wnt5a/Sfrp5 in human thoracic (ThAT, panel A), but not subcutaneous (ScAT, panel B) AT. In addition, the presence of systemic insulin resistance (HOMA-IR≥2.9) or type 2 diabetes mellitus (T2DM) was not associated with changes in Wnt5a/Sfr5 expression in either ThAT (panel C) or ScAT (panel D). *P<0.05 vs low BMI group after post hoc analysis for multiple comparisons. P-values are calculated by Kruskal-Wallis tests in panels C-D. Adapted from I Akoumianakis *et al* (2), *Sci Transl Med* (Accepted).

Having established that metabolic disease is associated with changes in systemic and AT-derived Wnt5a bioavailability, I next focused on PVAT as a potential local source of Wnt5a in the context of obesity. I found that obesity was associated with increased local expression of Wnt5a relative to its antagonist Sfrp5 in PVAT surrounding the human IMA (Fig. 4.4A). On the other hand, the expression of Wnt5a in IMA was negligible compared to that of it surrounding PVAT (Fig. 4.4B), suggesting that local Wnt5a signalling is mainly paracrine and not autocrine, being driven by PVAT and not IMA. No changes in PVAT Wnt5a expression were observed in patients with systemic IR or T2DM.

Figure 4.4: Perivascular adipose tissue (PVAT) as a local source of Wnt5a in obesity. Obesity was associated with increased expression of Wnt5a/Sfrp5 in PVAT (panel A). Arterial expression of Wnt5a was negligible compared to its surrounding PVAT, suggesting that local Wnt5a signalling is driven by PVAT (panel B). *P<0.05 vs low BMI group after post hoc analysis for multiple comparisons in panel A; **P<0.001 by Mann Whitney U test in panel B. Adapted from I Akoumianakis *et al* (2), *Sci Transl Med* (Accepted).

4.3.3. Interactions between Wnt5a and vascular disease

I next hypothesised that Wnt5a signalling may have implications for vascular disease. To address this hypothesis, I first screened the gene expression of the Wnt5a receptors in human IMA. I observed that obesity and systemic IR were associated with increased expression of Wnt receptors in human IMA (Fig. 4.5). This suggests that not only is metabolic disease associated with increased bioavailability of Wnt5a (in the circulation and/or AT), but it is also accompanied by increased sensitivity of the human vasculature to the downstream effects of Wnt5a signalling.

In order to evaluate the association between the Wnt5a/Sfrp5 ratio and CAD in humans, I designed a case control study (study 2), whereby 70 patients with CAD were matched for age, gender and BMI with 70 controls without CAD [confirmed by computed tomography (CT) angiography as having no coronary plaque causing>50% luminal stenosis]. Patients with CAD had significantly higher levels of plasma Wnt5a/Sfrp5 ratio (Fig. 4.6A) compared to controls. The presence of CAD was associated with circulating Wnt5a (Bstand=0.23, P=0.00), Sfrp5 (Bstand β=-0.21, P=0.00) and their ratio (Bstand=0.21, P=0.00) independently of traditional risk factors that differed significantly between the Study 2 cohorts (Fig. 4.6B).

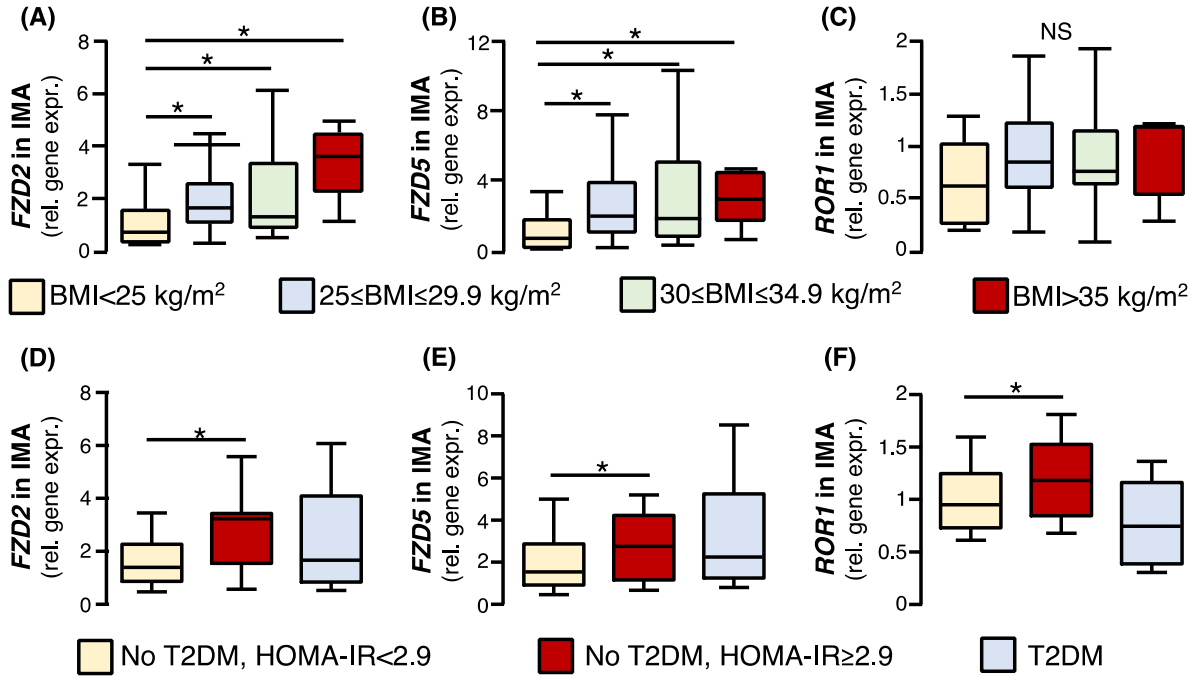

Figure 4.5: Arterial Wnt receptor expression and metabolic disease. Obesity was associated with increased expression of Fzd2 (panel A) and Fzd5 (panel B) in internal mammary artery (IMA) segments. A non-significant trend was observed for Ror1 expression. In addition, systemic insulin resistance (HOMA-IR≥2.9) was associated with increased expression all Wnt receptors (panels D-F) in human IMA. *P<0.05 vs low BMI group after post hoc analysis for multiple comparisons in panels A-B; P-value assessed by Kruskal Wallis test in panel C; *P<0.05 vs no T2DM/HOMA-IR<2.9 in panels D-F. Adapted from I Akoumianakis *et al* (2), *Sci Transl Med* (Accepted).

To explore the potential value of Wnt5a as a surrogate biomarker of vascular disease progression in humans, I designed a validation study (study 3) that involved individuals

scanned at two different time points 3-5 years apart for evaluation of coronary calcified plaque burden by non-contrast CT.

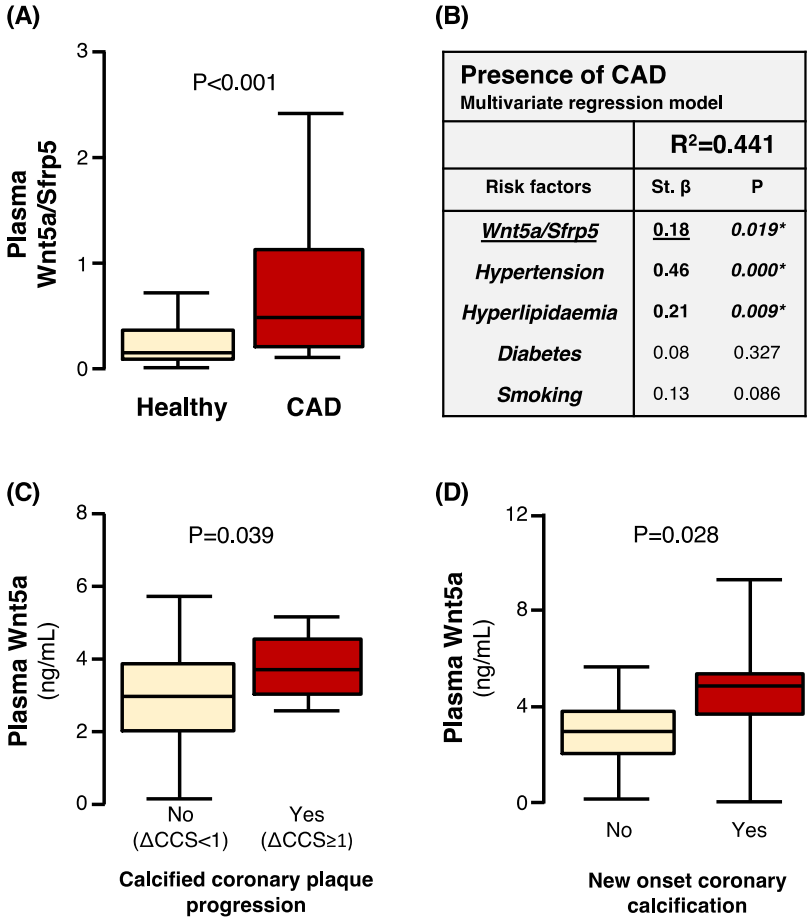

Figure 4.6: Plasma Wnt5a bioavailability is positively associated with coronary artery disease (CAD). Patients with CAD of study 2 had significantly increased circulating Wnt5a bioavailability compared to age-and sex-matched healthy controls (panel A). This association with the presence of CAD was independent of other traditional vascular risk factors (panel B). In study 3, plasma Wnt5a was retrospectively associated with coronary calcified plaque progression and new onset coronary calcification (panels C-D). The baseline CCS in the non-progression group ranged from 0 to 199.5 while the progression group CCS ranged from 0 to 847 P-values in panels A and C-D are calculated by Mann Whitney U tests. Adapted from I Akoumianakis *et al* (2), *Sci Transl Med* (Accepted).

Plasma Wnt5a levels were significantly elevated in patients demonstrating calcified plaque progression [which was defined a difference in coronary calcium score (CCS) ≥1, Fig. 4.6C] or new onset calcification (Fig. 4.6D). The baseline CCS in the non-progression group ranged from 0 to 199.5 while the progression group CCS ranged from 0 to 847. Upon multivariate regression analysis, plasma Wnt5a was associated with progression of calcification (Bstand=0.242, P=0.047) and new onset calcification (Bstand=0.367, P=0.03) independently of age and sex.

4.3.4. Wnt5a as a link between vascular redox state and obesity

I next hypothesised that Wnt5a bioavailability could be a mechanistic link with metabolic disease via altering human arterial redox state. Indeed, I observed that arterial oxidative stress and NADPH-oxidases activity in particular were increased in obesity (Fig. 4.7A-B).

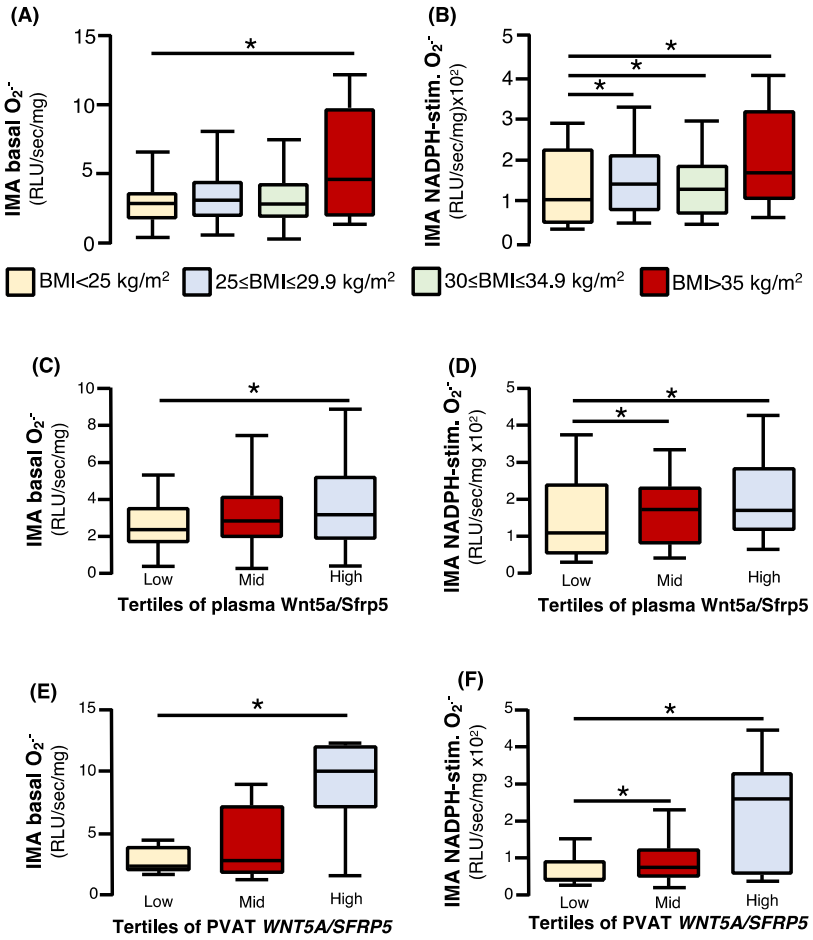

Figure 4.7: Wnt5a as a link between obesity and arterial redox state. Obesity was associated with increased basal (panel A) and NADPH-oxidases-derived (panel B) superoxide ($O_2^{\cdot-}$) in human internal mammary arteries (IMA). On the other hand, basal and NADPH-oxidases-derived $O_2^{\cdot-}$ in human IMA were also positively associated with Wnt5a bioavailability in the systemic circulation (panels C-D) and in perivascular adipose tissue (PVAT, panels E-F). *P<0.05 vs low BMI group (panels A-B) or vs low tertile (panels C-F) after post hoc analysis for multiple comparisons. Adapted from I *Akoumianakis et al* (2), *Sci Transl Med* (Accepted).

Considering that systemic and PVAT-derived Wnt5a are increased in obesity, I next explored whether local or systemic Wnt5a bioavailability were associated with arterial redox state in humans. Indeed, I found that basal and NADPH-oxidases-derived $O_2^{\cdot-}$ generation in human IMA from study 1 patients were positively associated with Wnt5a bioavailability both in plasma (Fig. 4.7C-D) and in PVAT (Fig. 4.7E-F).

To gain causal insights and understand whether the association between obesity and NADPH-oxidases activity in the human arteries is dependent on the Wnt5a/Sfrp5 ratio in PVAT, we performed multivariate analysis where arterial NADPH-stimulated $O_2^{\cdot-}$ was used as

dependent variable, and obesity classification (Bstand.=0.366, P=0.04), diabetes (Bstand.=0.015, P=0.931), smoking (Bstand.=0.08, P=0.693), sex (Bstand.=-0.196, P=0.315), age (Bstand.=0.098, P=0.563) were used as independent variables. When the Wnt5a/Sfrp5 gene expression in PVAT was included in the model (Bstand.=0.362, P=0.039), obesity lost its significant predictive value for arterial NADPH-stimulated $O_2^{\cdot-}$ (Bstand.=0.316, P=0.07), suggesting that the effects of obesity on human arterial redox state are Wnt5a-dependent.

4.3.5. Effects of Wnt5a on vascular NADPH-oxidases activity

To address whether the associations between Wnt5a/Sfrp5 and human vascular redox state are causal, I next used *ex vivo* models of human IMAs (study 4).

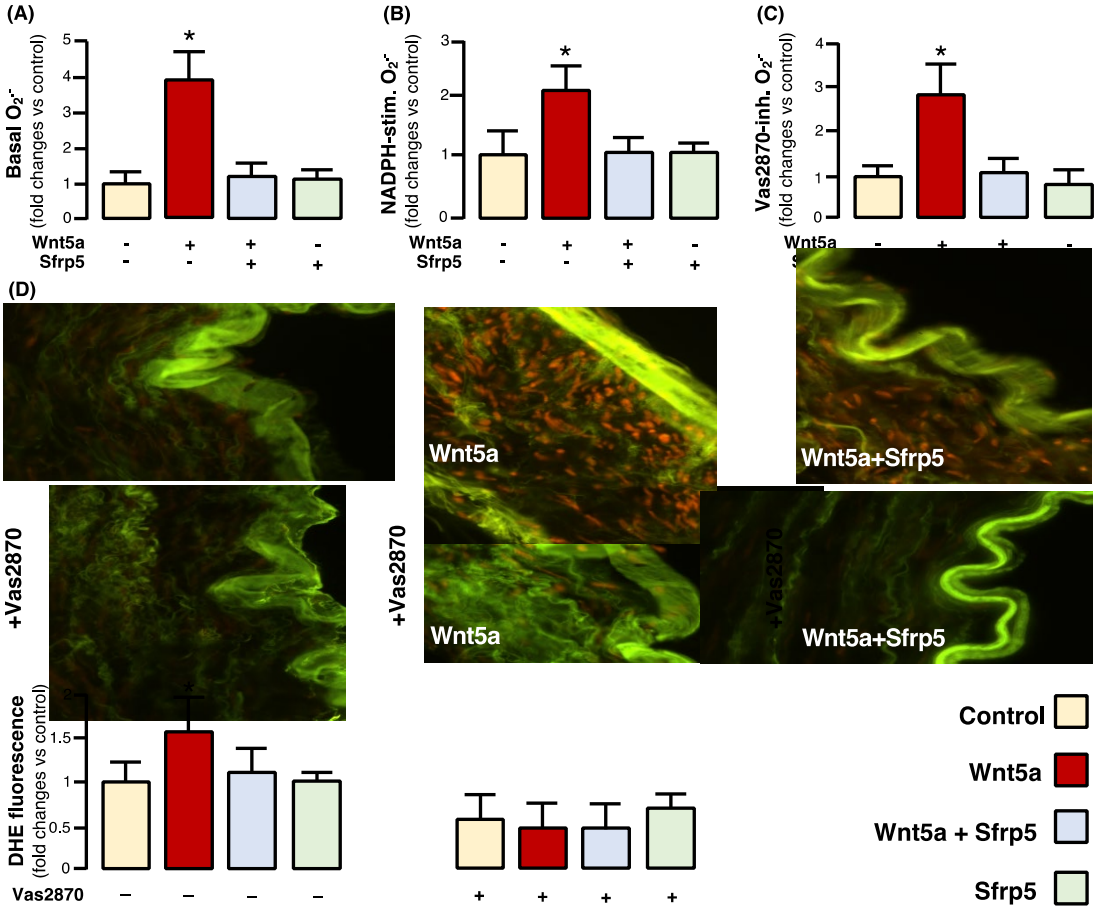

Figure 4.8: Wnt5a directly induces NADPH-oxidases activation in human arteries. In study 4, incubation of internal mammary artery (IMA) segments with Wnt5a 100ng/ml increased basal (panel A, n=12 pairs), NADPH-stimulated (panel B, n=12 pairs) and Vas2870-inhibitable (panel C, n=12 pairs) superoxide ($O_2^{\cdot-}$) generation, which was reversed by Sfpr5. Dihydorethidium (DHE) staining in combination with use of the specific NADPH-oxidases inhibitor Vas2870 confirmed the specificity of these observations and allowed for localisation of the vascular source of $O_2^{\cdot-}$, suggesting that it mainly originates from NADPH-oxidases in the vascular smooth muscle cells layer of the human IMA (panel D). *P<0.05 vs control after post hoc analysis for multiple comparisons. Adapted from I Akoumianakis *et al* (2), *Sci Transl Med* (Accepted).

In these experiments, serial IMA rings were incubated with Wnt5a (100 ng/ml), Sfrp5 (300 ng/ml) or the combination of the two for 45 minutes, and $O_2^{\cdot -}$ generation was evaluated using lucigenin chemiluminescence and confirmed with DHE staining. The concentration of Wnt5a was selected on the basis of being towards the top of the physiological levels of plasma Wnt5a detected in patients of study 1 (range: 1-112 ng/ml). I observed that Wnt5a induced a 4-fold increase in arterial basal $O_2^{\cdot -}$, an effect prevented by co-incubation with Sfrp5 (Fig. 4.8A). Similarly, NADPH-stimulated $O_2^{\cdot -}$ was increased (>2-fold) by Wnt5a incubation, an effect prevented by Sfrp5 (Fig. 4.8B), and the same was observed when measuring the signal inhibited by the specific Nox inhibitor Vas2870 (Fig. 4.8C). The specificity of the signal and the structural $O_2^{\cdot -}$ localization within the human arterial wall were also examined using DHE staining of human IMAs. Incubation of human IMAs with Wnt5a for 45 minutes increased $O_2^{\cdot -}$ generation, mainly from the VSMCs layer, an effect partially attenuated by Sfrp5 and completely reversed by Vas2870 (Fig. 4.8D), confirming that the effect was dependent upon NADPH-oxidases.

To further determine the causality of these findings *in vivo*, I used tissues from a doxycycline-inducible TetO mouse model ($Wnt5a^+/rtTA^+$ mice) where global overexpression of Wnt5a was induced. Mouse work was conducted by Dr Patricia Ciccone and Dr Fabio Sanna. Using harvested tissues from sacrificed experimental animals, I first confirmed the successful gene overexpression of mouse Wnt5a in a variety of tissues (Fig. 4.9). Importantly, Wnt5a was successfully overexpressed in mouse peri-renal (4.10A) and subcutaneous AT (4.10B) as well as in the systemic circulation (4.10C) compared to doxycycline-treated $wnt5a^-/rtTA^+$ littermate controls. When examining fresh aortic tissue from these mice, I observed that $Wnt5a^+/rtTA^+$ mice demonstrated significantly higher basal, NADPH-stimulated and Vas2870-inhibitable aortic $O_2^{\cdot -}$ generation (Fig. 4.10D-F) compared to $Wnt5a^-/rtTA^+$ controls, confirming that *in vivo* overexpression of Wnt5a leads to activation of arterial NADPH-oxidases.

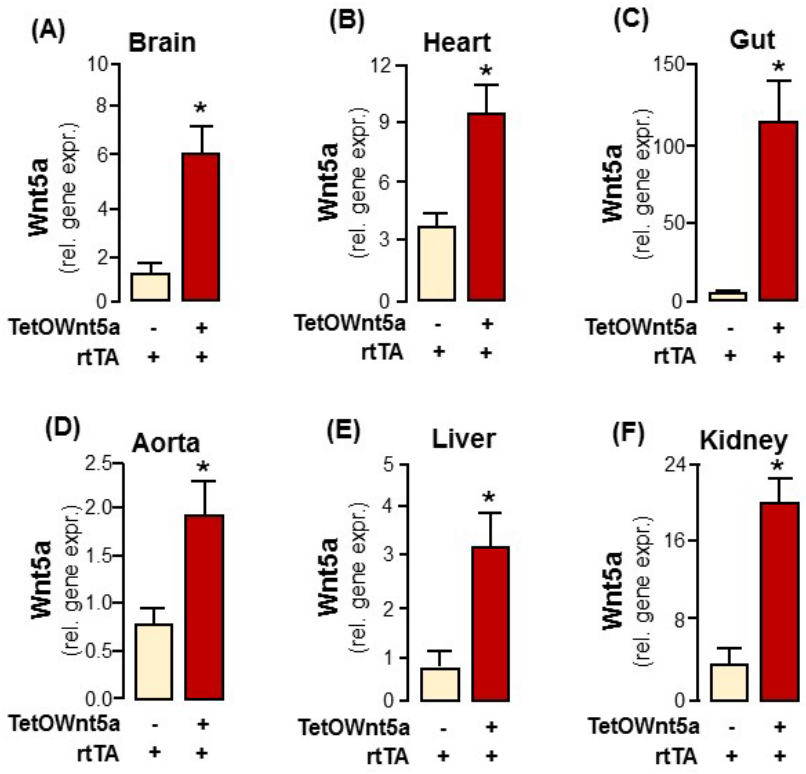

Figure 4.9: Phenotyping of Wnt5a-overexpressing TetO mice. Overnight doxycycline treatment resulted in significantly increased mouse Wnt5a gene expression in a variety of mouse tissues including brain (panel A), heart (panel B), gut (panel C), aorta (panel D), liver (panel E) and kidney (panel F) in rtTA+/Wnt5a+ mice compared to rtTA+/Wnt5a- controls. *P<0.05 by Mann Whitney U tests, n=5 per group for all panels. From I Akoumianakis *et al* (2), *Sci Transl Med* (Accepted).

Investigating the mechanism by which Wnt5a affects human arterial NADPH-oxidases activity, I found that Wnt5a activated the non-canonical PCP Wnt signalling pathway, documented by c-Jun N-terminal kinase (JNK) phosphorylation (an established surrogate marker of PCP activation) in human IMAs as well as in the aortas of $wnt5a^{+}/rtTA^{+}$ mice (Fig.

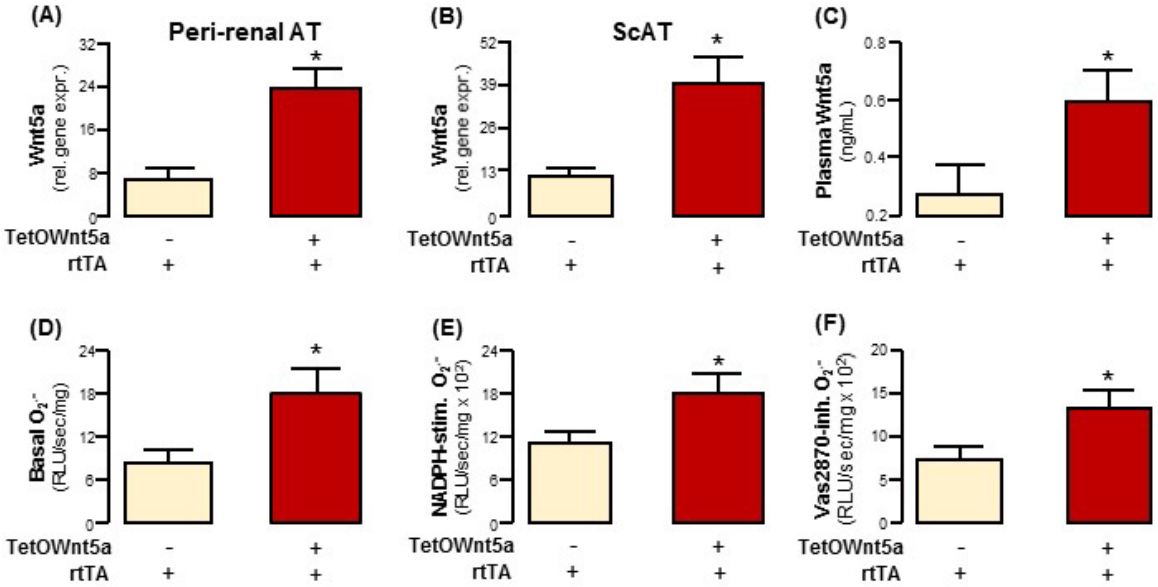

Figure 4.10: *In vivo* Wnt5a overexpression stimulates arterial NADPH-oxidases activity in mice. rtTA+/Wnt5a+ mice displayed increased adipose tissue (AT) production of Wnt5a (panels A-B) and elevated circulating Wnt5a levels (panel C) as well as increased aortic basal (panel D), NADPH-stimulated (panel E) and Vas2870-inhibitable (panel F) superoxide (O_2^-) production. *P<0.05 by Mann Whitney U tests, n=5 per group for all panels. From I Akoumianakis *et al* (2), *Sci Transl* Med (Accepted).

4.11A-B). Importantly, Wnt5a induced activation of Rac1 (Fig. 4.11C) in human arteries, leading to membrane translocation of Rac1 and p47^{phox} subunits of NADPH-oxidases (Fig. 4.11D-E), which are crucial for the activation of the Nox1 and Nox2 isoforms of NADPH-oxidases.

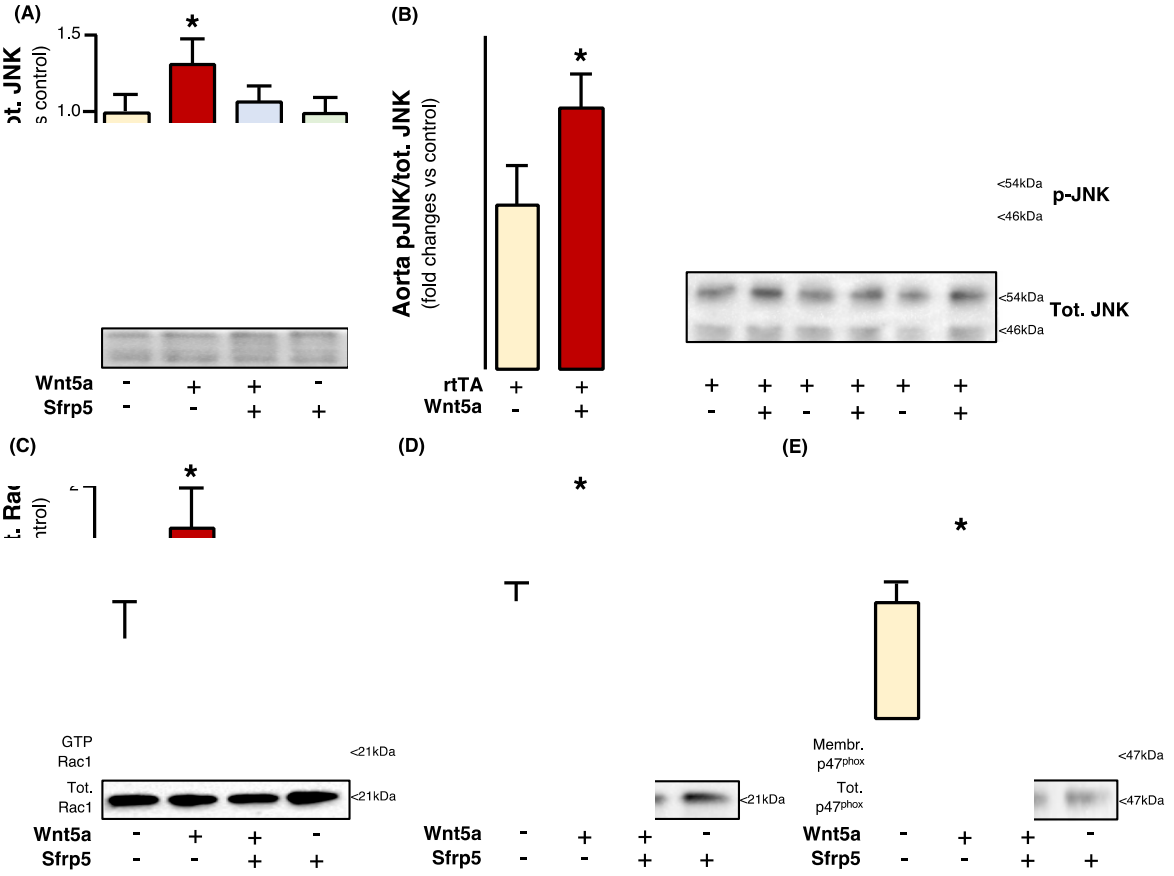

Figure 4.11: Wnt5a induces arterial activation of Rac1 and Nox subunit membrane translocation via non-canonical signalling. Wnt5a induced phosphorylation of c-Jun N-terminal kinase (JNK), a marker of non-canonical Wnt signalling, in both human internal mammary arteries (IMA, panel A) and mouse aortae (panel B). Wnt5a also increased the GTP-activation of Rac1 (panel C), followed by membrane translocation of Rac1 (panel D) and p47^{phox} (panel E), presumably to form active membrane Nox1/Nox2 complexes. *P<0.05 vs control after post hoc analysis for multiple comparisons in panels A, C-E; *P<0.05 vs control mice by Mann Whitney U in panel B. Adapted from I Akoumianakis *et al* (2)*, Sci Transl Med* (Accepted).

The key role of Rac1 in the Wnt5a-mediated NADPH-oxidases activation was further shown by demonstrating that the specific Rac1 inhibitor NSC23766 prevented the Wnt5a-induced increase of basal, NADPH-stimulated and Vas2870-inhibitable $O_2^{\cdot-}$ in both human IMAs (Figures 4.12A-C) and the aortas of Wnt5a$^+$/rtTA$^+$ mice (Figure 4.12D-F).

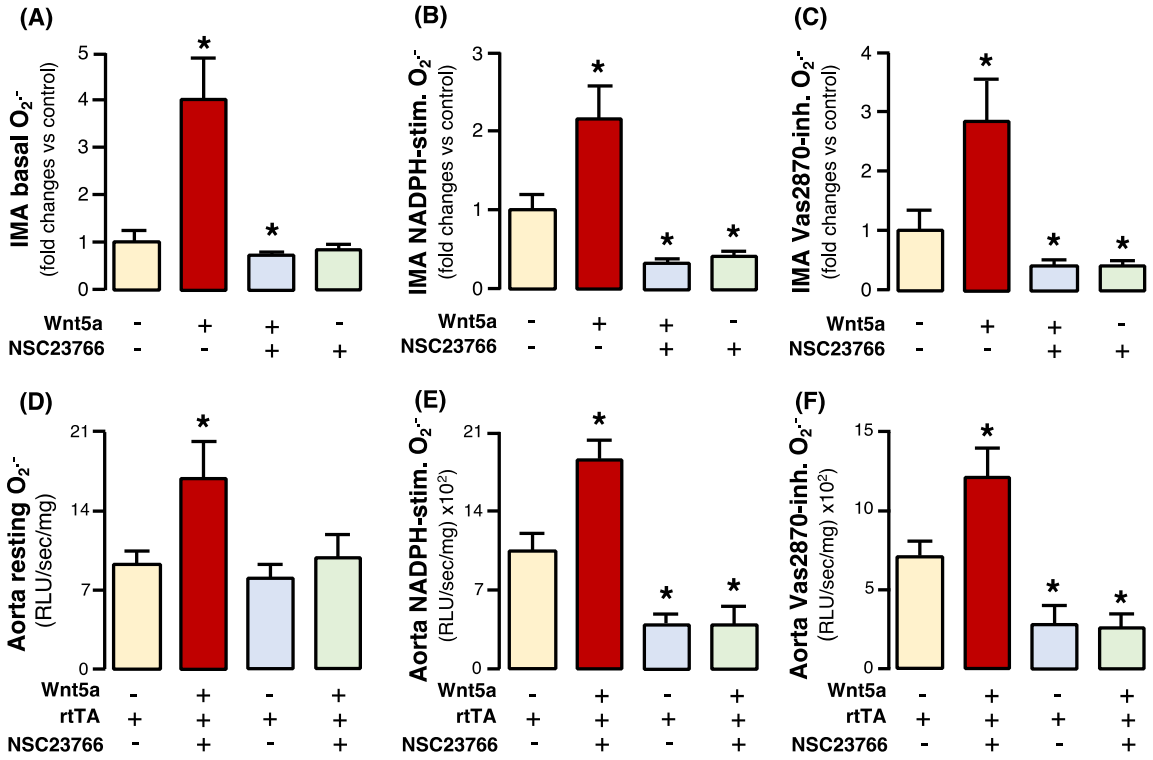

Figure 4.12: Rac1 activation mediates the effect of Wnt5a on arterial NADPH-oxidases activity. The specific Rac1 inhibitor NSC23766 abolished the ability of Wnt5a to increase basal, NADPH-stimulated or Vas2870-inhibitable superoxide (O_2^-) in human internal mammary arteries (IMA, panels A-C) or rtTA+/Wnt5a+ mouse aortae (panels D-F). *P<0.05 vs controls after post hoc analysis for multiple comparisons, n=19 for panels A-B, n=5 pairs for panels D-F. From I Akoumianakis *et al* (2), *Sci Transl Med* (Accepted).

As mentioned previously, Wnt5a has been regarded as a relatively specific non-canonical Wnt signalling ligand, especially in physiological concentrations such as the one used in this work. In line with these results, I demonstrated that Wnt5a induces JNK phosphorylation and Rac1 activation, which are hallmarks of non-canonical PCP Wnt signalling. To further confirm that canonical Wnt signalling does not account for the vascular effects of Wnt5a, primary human VSMC were incubated with Wnt5a at 100ng/ml or 400ng/ml, and β-catenin activation was tested. We observed that Wnt5a did not induce β-catenin

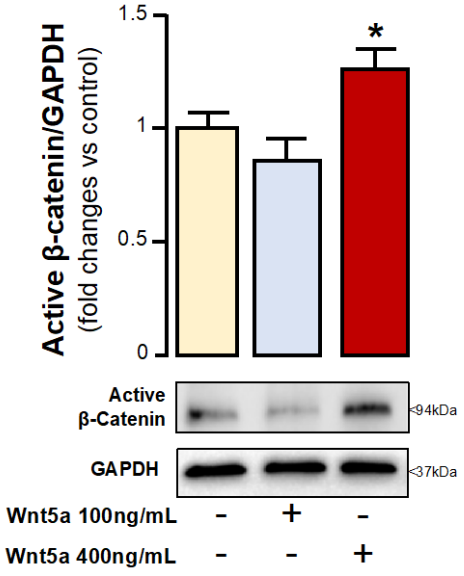

Figure 4.13: Physiological Wnt5a concentrations selectively activate non-canonical Wnt signalling. Wnt5a activated β-catenin only at the supra-physiological concentration of 400ng/ml. *P<0.05 vs control by Wilcoxon signed-rank test (n=5). From I Akoumianakis *et al* (2), *Sci Transl Med* (in Revision).

activation at the physiological concentration of 100ng/ml, in contrast with supra-physiological concentrations such as 400ng/ml (Fig. 4.13). This experiment was performed by Dr Fabio Sanna and is presented here as an additional proof-of-concept experiment to confirm the specificity of Wnt5a for non-canonical Wnt signalling.

4.3.7. Vascular smooth muscle cell-specific effects of Wnt5a

The results I have presented so far suggest an effect of Wnt5a on vascular NADPH-oxidases activity in humans with atherosclerosis. This was shown to be due to non-canonical Rac1 activation and was confirmed to be highly specific for non-canonical versus canonical Wnt signalling in human primary VSMCs. In this section, I describe a series of cell culture *in vitro* experiments that were mainly performed by Dr Fabio Sanna, while Dr Amy Chiu also contributed to some experimental work. These experiments provide further mechanistic insights and they are presented here for the sake of a more global understanding of the effects of Wnt5a, particularly originating from AT, on the muscular component of the vascular wall. These results were also presented in one of the journal papers supporting this thesis.

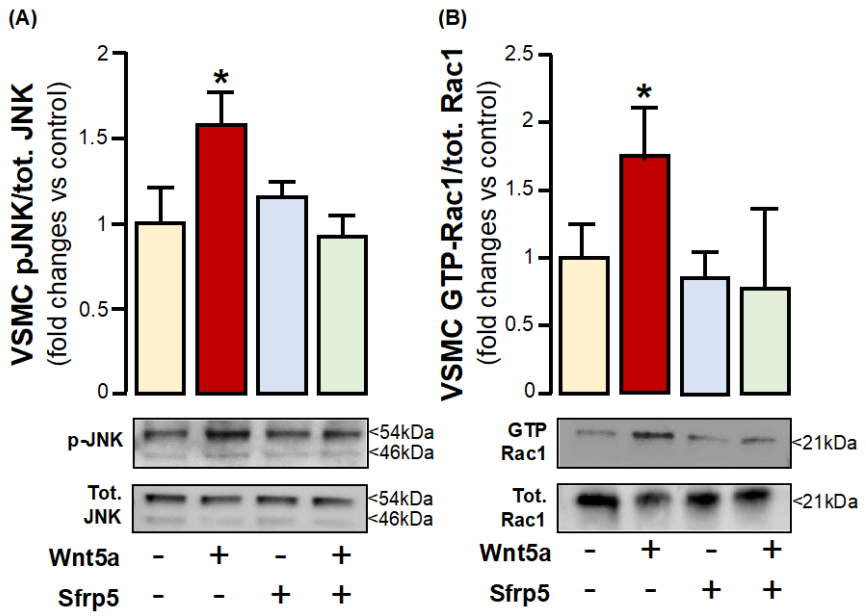

Figure 4.14: Wnt5a induces activation of the planar cell polarity (PCP) pathway in human primary vascular smooth muscle cells (VSMCs). Wnt5a (100ng/mL for 30min) induced c-Jun N-terminal kinase (JNK) phosphorylation (panel A) and GTP-activation of Rac1 in human VSMCs (panel B), both indicative of PCP activation. *P<0.05 vs control by Wilcoxon signed-rank test (n=5). From I Akoumianakis *et al* (2), *Sci Transl Med* (Accepted).

To explore whether adipocyte-derived Wnt5a can exert paracrine effects that control the redox state in the neighbouring VSMCs, the ability of Wnt5a to activate the PCP pathway (JNK-phosphorylation, Fig. 4.14A) and GTP-Rac1(Fig. 4.14B) was first confirmed in human primary VSMCs in culture, similarly to intact vessels. Furthermore, incubation with Wnt5a 100 ng/mL increased basal, NADPH-stimulated and Vas2870-inhibitable $O_2^{\cdot-}$ in VSMCs (Fig. 4.15A-C) similarly to intact vessels.

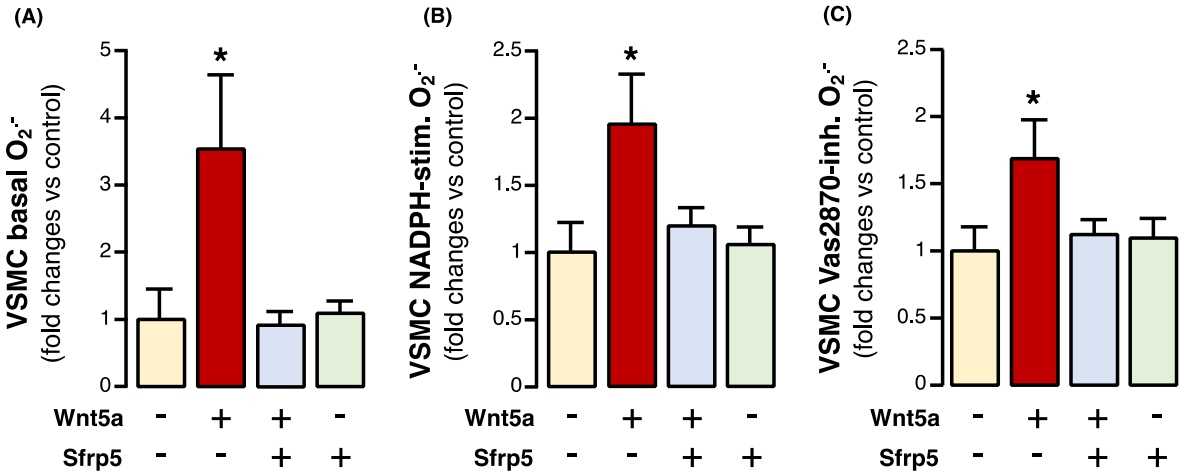

Figure 4.15: Wnt5a increases oxidative stress and NADPH-oxidases activity in human primary vascular smooth muscle cells (VSMCs). Wnt5a significantly increased basal (panel A), NADPH-stimulated (panel B) and Vas2870-inhibitable (panel C) superoxide ($O_2^{\cdot-}$) production in human primary VSMCs, which was reversed by its antagonist Sfrp5. *P<0.05 by Wilcoxon signed-rank tests, n=5 pairs. From I Akoumianakis *et al* (2), *Sci Transl Med* (Accepted).

Immortalised primary human preadipocytes endogenously expressing and secreting Wnt5a (Fig. 4.16A) were used, in which Wnt5a gene expression was knocked-down using shRNA (Fig. 4.16A). Co-culture of these adipocytes with human primary VSMCs revealed a significant reduction in basal $O_2^{\cdot-}$ in VSMCs co-cultured with Wnt5a-knockout (KO) adipocytes compared to sham control adipocytes (Fig. 4.16B). This reduction was due to a specific effect on the Nox2 isoform of NADPH-oxidase in VSMCs, as confirmed by the significant changes in gp91-dstat-inhibitable $O_2^{\cdot-}$ (gp91-dstat is a specific Nox2 inhibitor indicating the contribution of Nox2, Fig. 4.16C).

In the associations study (study 1), I demonstrated that the vascular gene expression of the Wnt receptors Fzd2 and Fzd5 was upregulated in obese study participants. As such, it is plausible that these receptors contribute significantly towards obesity-associated vascular oxidative stress via Wnt5a signalling. To test this hypothesis, Fzd2 and Fzs5 were knocked-down in VSMCs by using siRNA (Fig. 4.17A-C). Down-regulation of *FZD2* was ~96%, and prevented the Wnt5a-induced increase of basal, NADPH-stimulated and Vas2870-inhibitable $O_2^{\cdot-}$ in human VSMCs (Fig. 4.176D-F). Knocking down *FZD5* was less efficient in this model with ~65% reduction of its gene expression in human VSMCs and that was related with a borderline reduction of the Wnt5a-induced increase of basal (Fig. 4.17G) but not NADPH-stimulated (Fig. 4.17H) or Vas2870-inhibitable (Fig. 4.17I) $O_2^{\cdot-}$.

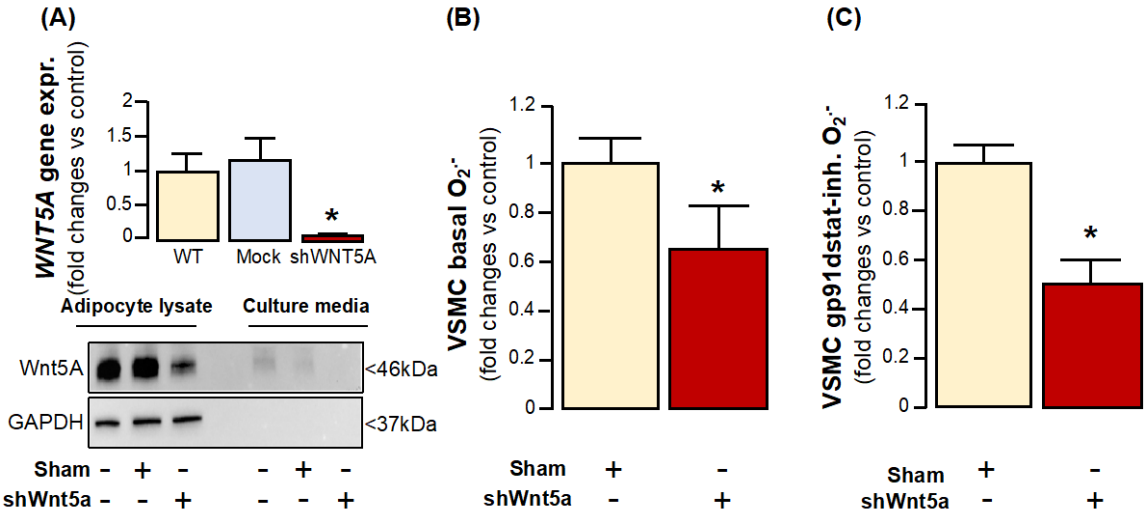

Figure 4.16: Paracrine effect of human primary adipocyte-derived Wnt5a on NADPH-oxidases activity in neighbouring human primary vascular smooth muscle cells (VSMCs). Wnt5a expression was knocked-down in human immortalised pre-adipocytes which are able to secrete wnt5a (panel G, n=3). VSMCs co-cultured with WNT5A-knockdown preadipocytes displayed lower basal and gp91 dstat-inhibitable $O_2^{\cdot-}$ production compared to VSMCs co-cultured with sham control preadipocytes, (panels H-I, n=5), confirming the concept that adipocyte-derived wnt5a can activate NOX2 isoform of NADPH oxidase in VSMCs in a paracrine way. *P<0.05 vs control after post hoc analysis for multiple comparisons. From I Akoumianakis *et al* (2), *Sci Transl Med* (Accepted).

To better understand the cellular effects of Wnt5a signalling on VSMC biology and the contribution of redox signalling in this context, human VSMCs were incubated with Wnt5a 100 ng/ml in the presence or absence of peg-SOD (100 IU/mL) for 8 hours, and microarray analysis was performed to evaluate the differential gene expression profile induced by Wnt5a

compared to non-treated controls. Wnt5a altered the expression of 1,890 differentially expressed genes (DEGs), of which 1,057 genes were upregulated and 833 were down regulated.

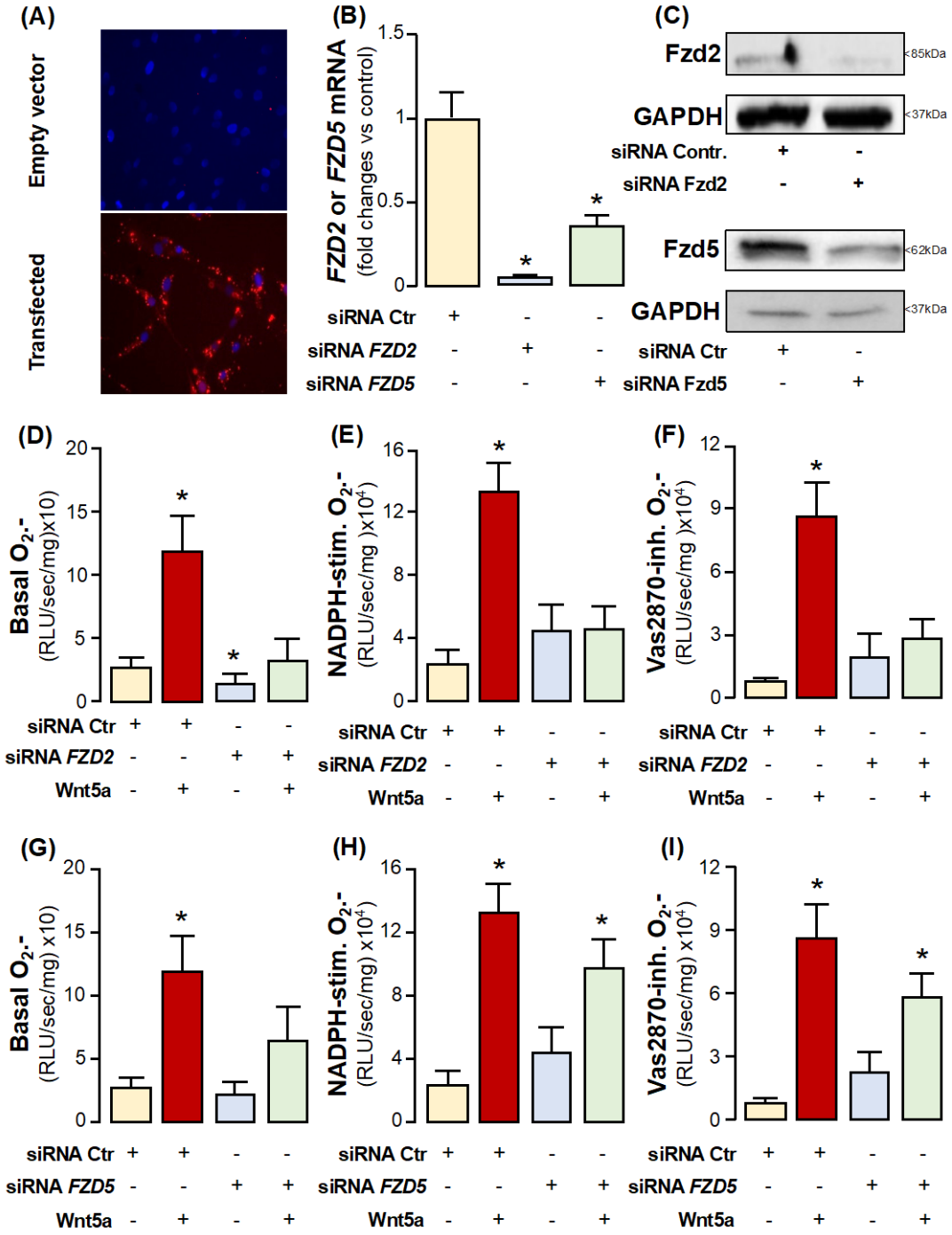

Figure 4.17: The pro-oxidant effects of Wnt5a in human vascular smooth muscle cells (VSMCs) are mediated by Frizzled 2 (Fzd2) and Frizzled 5 (Fzd5) receptors. Fzd2 and Fzd5 were knocked-down in human primary VSMCs, and transfection efficiency was confirmed by fluorescence lipofectamine RNAimax imaging (panel A), resulting in ~96% downregulation of FZD2 and ~65% downregulation of FZD5 (panel B, n=3). This was also confirmed at the protein level by Western blotting (panel C). Fzd2 knockdown reversed the ability of recombinant Wnt5a to induce basal, NADPH-stimulated and Vas2870-inhibitable $O_2^{\cdot-}$ production in VSMCs (panels D-F, n=5). On the other hand, knockdown of FZD5 reversed the ability of recombinant Wnt5a to induce basal but not NADPH-stimulated or Vas2870-inhibitable $O_2^{\cdot-}$ production (panels G-I, n=5). *P<0.05 vs control by Wilcoxon signed ranks tests (panels D-I) or paired t-test (panel B). From I Akoumianakis *et al* (2), *Sci Transl Med* (Accepted).

After performing a functional annotation using Gene Ontology (GO) database, these genes were found to be associated with biological processes such as cell growth, cell cycle, cell motility & migration. The effect of Wnt5a on several of those genes was reversed by peg-SOD, implying a redox-sensitive effect. Crucially, the top hit of the genes upregulated by Wnt5a was USP17, a member of a deubiquitinating enzyme multigene family within a tandemly repeated sequence (Burrows, McGrattan and Johnston, 2005). The ability of Wnt5a to increase the expression of USP17 was validated using quantitative real time polymerase chain reaction (q-RT-PCR) in primary VSMCs isolated from 10 patients that were treated with Wnt5a with or without peg-SOD (Fig. 4.18).

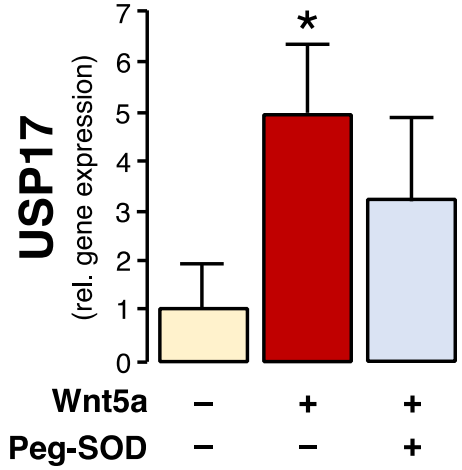

Figure 4.18: Wnt5a increases USP17 expression in a redox-sensitive manner in human vascular smooth muscle cells (VSMCs). Wnt5a markedly increased USP17 expression in human primary VSMCs after 8h, which was partially reversed by peg-SOD (n=10 pairs), suggesting a redox-sensitive mechanism. *P<0.05 vs control by Wilcoxon signed ranks test. From I Akoumianakis *et al* (2), *Sci Transl Med* (Accepted).

USP17 has been found to be involved in the activation of small GTPases such as Rac1 (De La Vega *et al.*, 2011). To address the mechanistic role of USP17 in Wnt5a-mediated Rac1 activation, USP17 was knocked down in HeLa cells using shRNA (Fig. 4.19) and these cells were treated with Wnt5a 100ng/mL for 8h (experiments performed by Dr Amy Chiu).

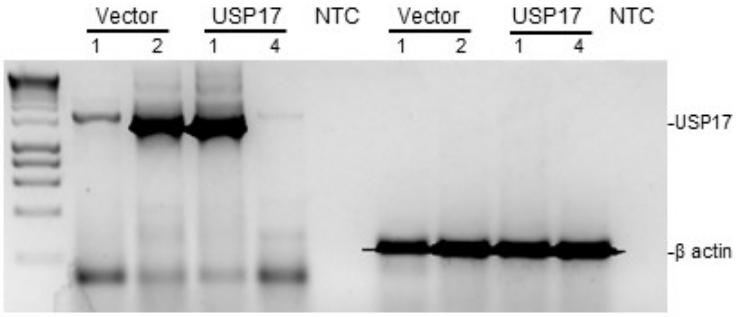

Figure 4.19: USP17 transfection in HeLa cells. HeLa cells were successfully transfected with shUSP17 (clones 1 & 4) or empty vector (clones 1 & 2), and cells demonstrating negligible expression of USP17 (clone 4) were passaged and used for downstream in vitro treatments with recombinant Wnt5a (100ng/mL). β actin was used as a housekeeping gene. NTC: negative control. From I Akoumianakis *et al* (2), *Sci Transl Med* (Accepted).

Wnt5a failed to induce persistent Rac1 activation in USP17-KO HeLa cells as opposed to empty vector control cells (Fig. 4.20). This proposes for the first time that USP17 is an important mediator of the Wnt5a-induced Rac1 activation, thus orchestrating the long-term effects of Wnt5a on Rac1-mediated redox signalling and comprising a potential therapeutic target.

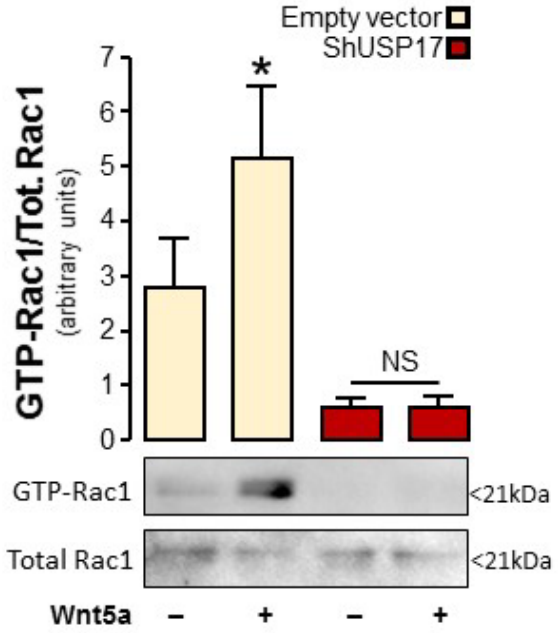

Figure 4.20: USP17 mediates the long-term effect of Wnt5a on Rac1 activation. Wnt5a failed to induce persistent Rac1 activation after 8h in USP17-knockdown HeLa cells. +P<0.05 vs untreated empty vector control by Wilcoxon signed rank test; NS by Wilcoxon signed rank test for Wnt5a-treated vs untreated shUSP17 cells. From I Akoumianakis e*t al* (2)*, Sci Transl Med* (Accepted).

4.3.7. Effects of Wnt5a on endothelial function and eNOS coupling

The results I have presented so far indicate that Wnt5a induces arterial NADPH-oxidases activity in humans with atherosclerosis via receptor-mediated, PCP-regulated Rac1 activation. I next explored the potential effects of Wnt5a on eNOS coupling, NO bioavailability and endothelial function (which are known to be significantly affected by oxidative stress) in human vessels.

Indeed, by using *ex vivo* models of human vessels, I found that incubation of IMA segments with recombinant Wnt5a 100ng/ml resulted in significant induction of eNOS uncoupling (Fig. 4.21A, evidenced by negative L-NAME delta $O_2^{\cdot-}$ values), which was reversed by Sfpr5. Investigating the underlying mechanism, I hypothesised that Wnt5a-induced oxidative stress

via NADPH-oxidases (as shown previously) could oxidise BH4, the key co-factor required to maintain eNOS coupling. Therefore, I incubated human IMA with Wnt5a 100ng/ml for 45min and subsequently measured vascular biopterins by HPLC. I observed that Wnt5a significantly reduced arterial BH4 (Fig. 4.21B) but not total biopterin content (Fig. 4.21C), thereby drastically reducing arterial BH4 bioavailability (Fig. 4.14D) and thus promoting eNOS uncoupling, which were reversed by Sfrp5.

To further determine the consequences of these observations on overall endothelial function, I used *ex vivo* models of human SV segments and I performed vasomotor studies at baseline and following Wnt5a 100ng/ml ± Sfrp5 300ng/ml incubations for 45min. Vasorelaxations in response to Ach, which are NO-mediated and endothelium-dependent, were evaluated. SNP

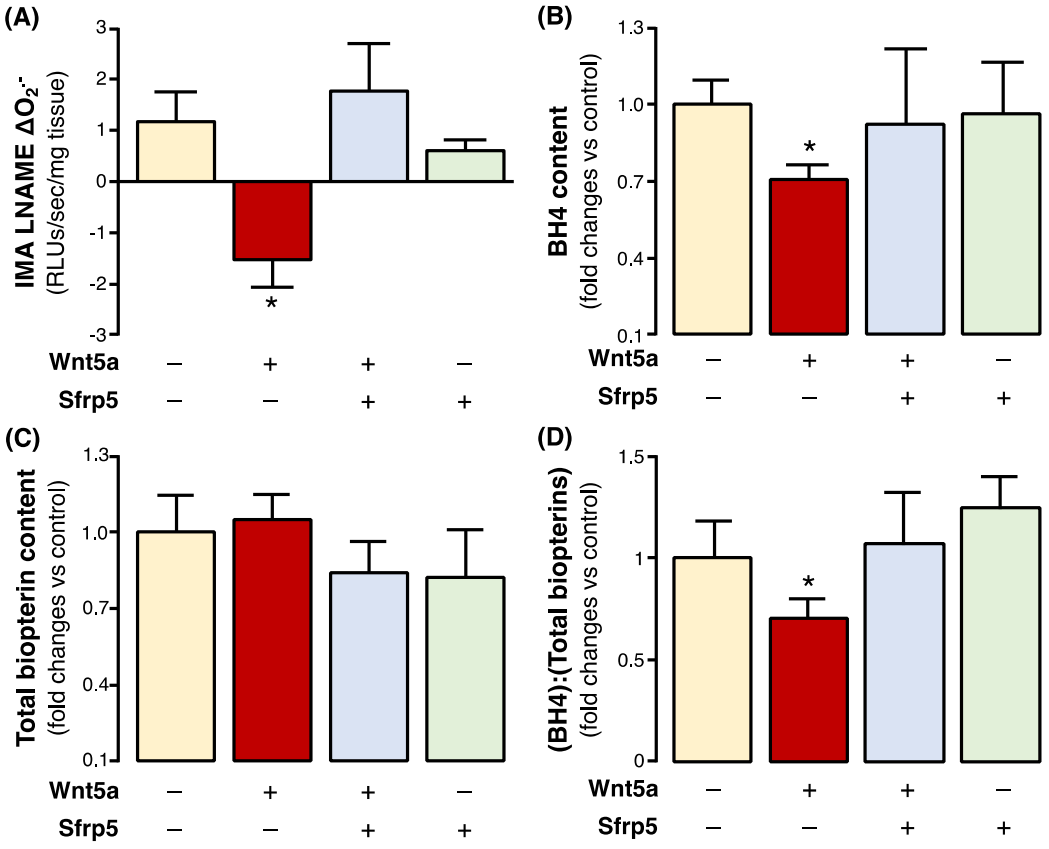

Figure 4.21: Wnt5a induces uncoupling of endothelial nitric oxide synthase (eNOS) via tetrahydrobiopterin (BH4) oxidation. Wnt5a directly induced eNOS uncoupling in internal mammary artery (IMA) segments, evidenced by negative L-NAME $\Delta O_2^{\cdot-}$ (panel A). This resulted from reduced BH4 (panel B) but not total biopterin (panel C), resulting in decreased BH4 bioavailability (panel D). *P<0.05 vs control by Wilcoxon signed-rank test (n=5).

vasorelaxations following eNOS inhibition by L-NAME were also performed to evaluate the VSMC component of vasorelaxation responses. I observed that Wnt5a impaired endothelial function as evidenced by blunted vasorelaxation response to Ach (Fig. 4.22A), without affecting SNP relaxations (Fig. 4.22B). These suggest a specific effect of Wnt5a on endothelial

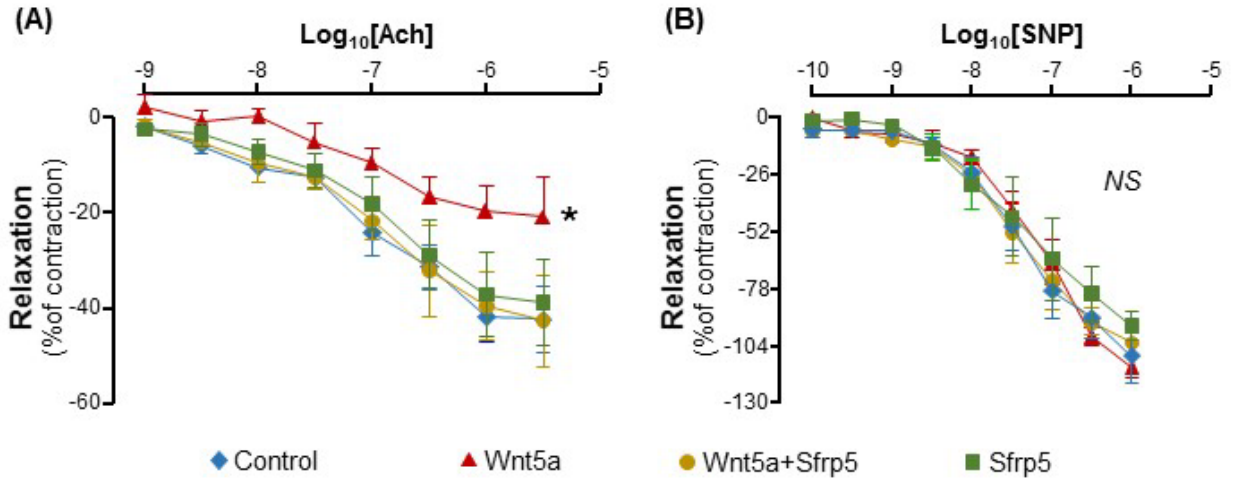

Figure 4.22: Wnt5a induces endothelial dysfunction in human vessels *ex vivo*. In *ex vivo* models of saphenous vein rings, Wnt5a 100ng/ml significantly impaired endothelium-dependent. Acetylcholine (Ach) mediated vasorelaxation following phenylephrine (PE) pre-constriction, an effect which was reversed by Sfrp5 (panel A). On the contrary, Wnt5a did not influence endothelium-independent vasorelaxation in response to sodium nitroprusside (SNP) following PE pre-constriction and endothelial nitric oxide synthase inhibition (panel B). These reflect a specific effect of Wnt5a on endothelial function. *P<0.05 vs control by two-way ANOVA for paired observations with group x treatment interaction.

function via reduced NO bioavailability resulting from arterial eNOS uncoupling.

4.4. Discussion

This work is the first to demonstrate that obesity leads to an imbalance between Wnt5a and Sfrp5 levels in both PVAT and other AT depots such as ThAT, affecting also their circulating levels in human atherosclerosis. In addition, my work indicates that obesity is associated with significant upregulation of Wnt5a receptors Fzd2 and Fzd5 in human arteries, which are involved in non-canonical Wnt signalling. By using *ex vivo* models of human vessels and an *in vivo* transgenic mouse model, I demonstrate that Wnt5a secreted by human AT leads to significant activation of arterial NADPH-oxidases, increasing $O_2^{\cdot-}$ generation. Furthermore, Wnt5a induces endothelial dysfunction and eNOS uncoupling resulting from oxidative

reduction of BH4 bioavailability in human arteries. These observations may explain the clinical association of Wnt5a with the CAD, captured in this work by the higher risk for calcified plaque progression and new-onset coronary calcification identified in patients with high plasma wnt5a levels. Therefore Wnt5a, its balance with Sfrp5, its receptors and downstream signalling network may be novel mechanistic links between obesity and vascular complications in humans and act as potential therapeutic targets for the prevention and treatment of such complications.

4.4.1. Links between Wnt5a signalling and metabolic disease in humans

AT tissue biology displays remarkable regional variability and is dysregulated in obesity (Akoumianakis and Antoniades, 2017b). Indeed, several studies have documented the biological discrepancy between visceral and superficial AT (Alexopoulos, Katritsis and Raggi, 2014) and identified inflamed visceral AT as a source of adipocytokines with detrimental paracrine and endocrine effects on the vasculature (Fuster *et al.*, 2016). Wnt ligands are expressed in human AT and they are believed to affect AT biology (Christodoulides *et al.*, 2009). Previous studies have shown that Wnt5a is expressed in the human AT (Catalán *et al.*, 2014), while the balance between Wnt5a and its decoy inhibitor Sfrp5 may be involved in the pathogenesis of obesity and diabetes (Catalán *et al.*, 2014). Indeed, Wnt5a signalling has been associated with a number of pathogenic AT phenotypes such as increased local inflammation (Fuster *et al.*, 2015) and IR (Buettner, Schlmerich and Bollheimer, 2007), while it may also affect adipogenesis in controversial ways (Christodoulides *et al.*, 2009). Although local Wnt5a secretion in AT is believed to regulate AT biology, little is known about the contribution of AT-derived Wnt5a in the endocrine/paracrine crosstalk between At and the human vasculature.

In this work, I firstly observed that Wnt5a is the most abundant Wnt ligand expressed in the human PVAT, and also one of the predominant Wnt ligands expressed in ThAT and ScAT.

This suggests that Wnt5a is likely a very important mediator of Wnt signalling pathways in AT, with potential paracrine and/or endocrine implications for the vascular wall. In addition, I observed that, in a cohort of 1,004 patients with CAD, Wnt5a bioavailability is increased in obese individuals, both in the systemic circulation and in ThAT (especially in the morbid obesity group, i.e., BMI>35kg/m^2), in consistence with previous studies linking Wnt5a with visceral adiposity (Lu *et al.*, 2013; Catalán *et al.*, 2014). Moreover, I observed that Wnt5a bioavailability is also increased in PVAT of obese individuals, a finding that has not been reported before and its significance is two-fold: a) it further supports the notion that Wnt5a signalling dysregulation in AT (especially deep AT depots as opposed to ScAT) accompanies obesity, especially advanced states of obesity (it may be of less importance in milder cases) b) it suggests (due to the close proximity of PVAT with the vascular wall) that AT-derived Wnt5a may quite possibly exert paracrine vascular effects that are enhanced in obesity. Wnt5a could thus be an advanced obesity-associated biomarker of vascular disease.

4.4.2. Association of Wnt5a signalling with vascular biology and disease in humans

As mentioned in Chapter 1, Wnt5a has recently been implicated in vascular disease pathogenesis (Foulquier *et al.*, 2018) via multiple biological processes which include regulation of vascular cell migration (Masckauchán *et al.*, 2006; Cheng *et al.*, 2008), local inflammation (Kim *et al.*, 2010), enhanced vascular calcification (Woldt *et al.*, 2012) and endothelial dysfunction (Bretón-Romero *et al.*, 2016). However, observational associations are lacking to strongly support a clinically relevant role for Wnt5a in vascular disease.

My work provides strong links between Wnt5a signalling and vascular disease at an observational level in humans, confirming the existing literature and taking it further in terms of clinical associations and mechanistic implications. Indeed, I first observed that obesity was

associated with significant upregulation of Wnt5a receptors Fzd2 and Fzd5 in the human arterial wall, increasing arterial sensitivity to non-canonical Wnt signalling. Considering that obesity is also associated with increased bioavailability of the Wnt5a ligand, it is plausible to hypothesise that these combined observations significantly enhance arterial Wnt5a signalling in humans with CAD. On the other hand, I showed (in a nested case-control study) a striking increase of plasma Wnt5a accompanied by reduced circulating Sfpr5 levels in patients with CAD compared to age-, sex- and BMI-matched non-CAD controls. This complements previous studies reporting increased Wnt5a expression in atherosclerotic vessels (Bhatt and Malgor, 2014), and it was found to be independent of other traditional risk factors for vascular disease. Importantly, plasma Wnt5a was positively and independently associated with both coronary calcification progression and new onset calcification in humans, suggesting that it has a clinically relevant role and a potential biomarker role in vascular disease progression, which has never been reported before. These results support the notion that Wnt5a is associated with vascular disease, and considering that it is also upregulated in obesity, it is plausible to hypothesise that Wnt5a comprises a novel mechanistic link between vascular and metabolic disease.

4.4.3. Novel interactions between Wnt5a signalling and arterial redox signalling in humans

Redox signalling is directly involved in multiple vascular diseases commonly presented as complications of obesity (Keaney *et al.*, 2003; Ceriello and Motz, 2004). NADPH-oxidases, in particular, comprise major sources of ROS in the human vascular wall and they have been consistently associated with vascular disease pathogenesis (Konior *et al.*, 2014). The activation of Nox1 and Nox2 isoforms of NADPH-oxidases is dependent on the activation and membrane translocation of Rac1 and $p47^{phox}$ cytoplasmic subunits in order to form the active enzymatic

complex (Guzik and Harrison, 2006). Given that non-canonical Wnt signalling has been linked with activation of small GTPases like Rac, I hypothesised that adipose tissue-derived Wnt5a may drive arterial oxidative stress via Rac1-mediated NADPH-oxidases activation in obesity, a hypothesis that has not been explored before.

My work reveals that both obesity and Wnt5a bioavailability (in the circulation and in PVAT) are associated with increased arterial NADPH-oxidases activity, further supporting the link between obesity and vascular oxidative stress and proposing a novel link between Wnt5a and vascular redox state. Crucially, the association of obesity with arterial NADPH-oxidases activity was dependent on PVAT Wnt5a bioavailability upon multivariate analysis, supporting the notion that Wnt5a may be the mechanistic link between obesity and vascular oxidative stress. I next confirmed the causal stimulatory effect of Wnt5a on NADPH-oxidases activity via non-canonical Rac1 activation, using *ex vivo* models of human arteries and an *in vivo* Wnt5a-overexpressing mouse model. Previous reports have suggested that Wnt5a may induce canonical Wnt signalling in VSMCs (Mill *et al.*, 2014); however, the experimental concentration of Wnt5a used *in vitro* was 300ng/mL in that study. Our work here suggests that Wnt5a is a rather specific non-canonical Wnt ligand at lower, physiological concentrations. The aforementioned findings comprise the first ever evidence linking Wnt5a with vascular NADPH-oxidases activity.

VMSC phenotype is crucial from the progression of atherosclerosis, since upon phenotypic switch, plaque VSMCs are believed to lose their contractile phenotype and assume migratory/proliferative and extracellular matrix remodelling properties which may propagate atherosclerotic plaque instability (Bennett, Sinha and Owens, 2016; Chappell *et al.*, 2016). Previous studies have linked Wnt5a signalling with reduced VSMCs apoptosis (Mill *et al.*, 2014), but this effect is attributed to canonical Wnt signalling achieved by using a supra-

physiological Wnt5a concentration *in vitro* (Mill *et al.*, 2014). We this in mind, the work presented in this thesis attempted to explore the VSMC-specific effect of Wnt5a and to provide further mechanistic insights to the molecular vascular effects of Wnt5a by using primary VSMCs *in vitro* models.

This work demonstrates now demonstrate that Wnt5a induces NADPH-activity in VSMCs, which results in a complex cascade of redox signalling events that influence the expression of multiple genes involved in processes such as cell migration, an effect that was reversed by peg-SOD, a scavenger of intracellular $O_2^{\cdot-}$. Interestingly, the top hit up-regulated by Wnt5a (and partly reversed by peg-SOD) in these cells is USP17, a deubiquitinating enzyme acting as a known activator of small GTPases like Rac (De La Vega *et al.*, 2011). The USP17/Rac1 link has previously been implicated in disease entities where cell motility plays a pivotal role (such as tumorigenesis) (McFarlane *et al.*, 2010). However, USP17 has never been implicated in vascular biology before, and neither has it ever been proposed as a downstream target of Wnt5a signalling. This work is the first to demonstrate that USP17 mediates the effects of Wnt5a on Rac1 activation, controlling vascular redox state, while the link between wnt5a and USP17 also appears to be partly redox-sensitive. The Wnt5a/USP17/Rac1/NADPH oxidases axis is thus identified as a highly novel potential therapeutic target to modify the vascular effects of obesity.

Previous reports have suggested that Wnt5a may be involved in endothelial dysfunction, particularly in the context of diabetes (Bretón-Romero *et al.*, 2016; Farb *et al.*, 2016). In these studies, Wnt5a was shown to induce vascular IR via JNK signalling and thus impair insulin-mediated eNOS Ser1177 phosphorylation and NO production in endothelial cells. However, the potential direct effects of Wnt5a signalling on eNOS function and endothelial function in human vascular tissue from real-life patients with atherosclerosis have not been investigated before. Considering the clear effect of Wnt5a on NADPH-oxidases activity in human vessels,

I hypothesised that this Wnt5a-induced increase in vascular oxidative stress could directly decrease NO bioavailability via inducing eNOS uncoupling resulting from oxidative BH4 depletion. Indeed, using *ex vivo* models of human vessels, I demonstrated that Wnt5a drastically reduced BH4 bioavailability and induced eNOS uncoupling, further stimulating $O_2^{\cdot-}$ production and promoting endothelial dysfunction in a mechanism that is redox-sensitive and independent of insulin-mediated eNOS activation as proposed in endothelial cells. As such, my work suggests that Wnt5a has a potent, direct effect on NADPH-oxidases activity which adversely influences eNOS coupling and endothelial function. These combined effects could partially explain the association of Wnt5a with CAD presence and progression, though other mechanisms are very likely to be involved besides redox regulation.

4.5. Conclusion

This work is the first to show that metabolic disease is associated with enhanced activation of non-canonical Wnt signalling in the human arterial wall, as a result of: a) a shift of the balance between Wnt5a and Sfrp5 towards in favour of the former, both in the circulation and in PVAT and b) up-regulation of the Wnt5a receptors Fzd2 and 5 on the arterial wall. This results into a Wnt5a-mediated activation of Rac1 and a downstream activation of vascular NADPH-oxidases, leading to arterial oxidative stress, BH4 oxidation, eNOS uncoupling and ultimately endothelial dysfunction (Fig. 4.16). Furthermore, Wnt5a signalling has a wide range of VSMC-specific consequences which are at least partly mediated via redox signalling, and may contribute to plaque progression. Finally, USP17 is, for the first time, identified as novel link between Wnt5a and Rac1 activation. At a clinical level, Wnt5a levels are independently associated with the presence of CAD and progression of calcified coronary atherosclerotic plaque burden, clearly identifying this molecule and its downstream signalling as novel

mechanistic links between metabolic disease and vascular complications, which may be of significant translational potential in cardiometabolic disease, something that warrants further

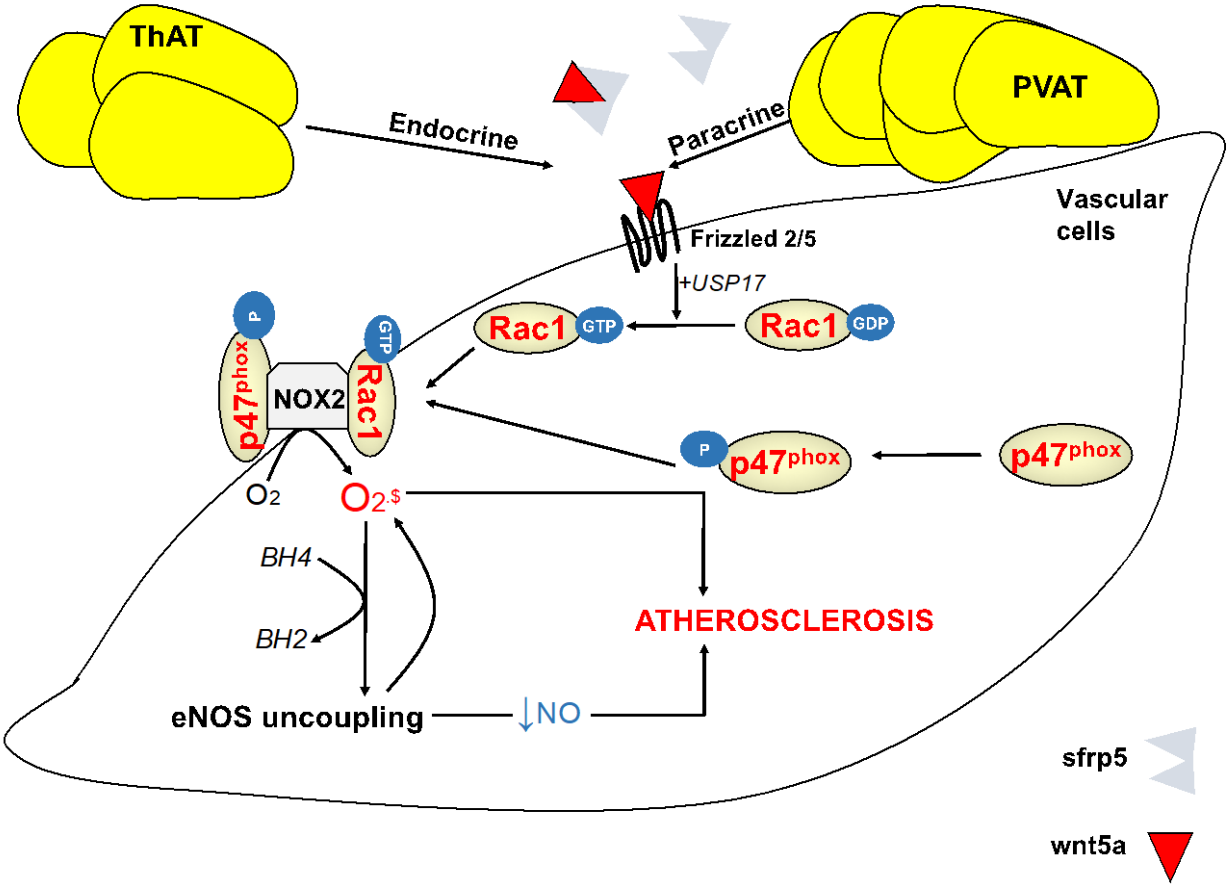

Figure 4.23: Summary of the effects of Wnt5a on arterial redox state. Wnt5a/Sfrp5 balance is dysregulated in the circulation and in adipose tissue (AT) depots such as thoracic AT (ThAT) and perivascular AT (PVAT), affecting the vasculature (vascular smooth muscle cells and endothelial cells) via endocrine and paracrine routes. In the vasculature, enhanced receptor-mediated Wnt signalling (presumably via receptors Fzd2 and Fzd5) induces non-canonical Rac1 GTP-activation followed by membrane translocation of active Rac1 and $p47^{phox}$ to stimulate the activity of NADPH-oxidases such as Nox2. Furthermore, USP17 is revealed as a novel enhancer of persistent Rac1 activation in response to Wnt5a. Wnt5a-mediated NADPH-oxidases activation results in increased superoxide ($O_2^{\cdot-}$) production followed by oxidation of tetrahydrobiopterin (BH4), leading to endothelial nitric oxide synthase (eNOS) uncoupling. This, in turn, results in further $O_2^{\cdot-}$ production and reduction of nitric oxide bioavailability. These combined effects are believed to contribute to atherogenesis.

investigation.

Chapter 5

Study limitations

This Chapter provides an outline of the study limitations which may pose certain caveats when attempting to generalise the conclusions to a broader context. These include: a) the lack of "healthy" control cohort for most clinical associations, b) the use of human non-atherosclerotic vessels as models of human atherosclerosis and c) the lack of vascular tissue from healthy, CVD-free humans for the *ex vivo* experiments.

5.1. Lack of healthy control cohort for clinical associations

When exploring the association of Wnt5a with vascular disease presence and progression, I utilised the unique availability of imaging data and plasma samples for healthy subjects as part of the ORFAN study, which allowed me to demonstrate that Wnt5a is independently associated with both the presence and progression of atherosclerosis (as explained in Chapter 4). Conversely, certain observational associations presented in this thesis could not be replicated in healthy subject groups without CVD. This may complicate the generalisation of certain conclusions of this thesis to a broader context of health and disease, although the mechanistic experiments I have performed provide strong evidence and make the thesis conclusions extremely plausible in real-life clinical settings. In the following paragraph, I explain the reasons for the lack of such healthy cohort controls, and I interrogate the relevance and implications of individual observational conclusions presented in this thesis.

The uniqueness of my work is largely based on the fact that I have used one of the most extensively phenotyped cohorts of vascular disease in the wold, and this allows for an invaluable link between clinical parameters and biological readouts in these patients. Therefore, many of the clinical associations presented in this thesis involve biological readout variables such as vascular and AT gene expression studies, vascular $O_2^{\cdot-}$ measurements and vascular vasomotor characteristics. Although these associations may help identify novel translational hypotheses, they are at the same time difficult to replicate in disease-free human cohorts due to lack of such biological material availability. Indeed, recruitment of CABG patients is virtually the only efficient and consistent way to gain access to human vascular tissue for the purposes of my project. Consequently, most of my findings are directly applicable to patients with atherosclerosis, but possibly not as readily generalisable in other study populations. However, this does not comprise a major limitation since the primary target subjects for this work were patients with atherosclerosis to start with. Nonetheless, I included healthy cohort controls whenever possible, such as in the case of linking plasma Wnt5a with CAD, where non-CAD formally recruited patients were available and less extensive bioresource was needed (limited to the availability of plasma samples).

In Chapter 3, I demonstrated that serum insulin is associated with impaired endothelial function and increased vascular oxidative stress in non-diabetic humans with CAD, while the combined effect of increased serum insulin and increased DPP4 activity was associated with adverse outcomes in CAD patients. These are highly novel findings which may have serious implications for diabetic patients with atherosclerosis, and they strongly suggest the presence of vascular IR in virtually all atherosclerosis patients and a potential benefit of DPP4 inhibition in that regard. However, it is not known if these conclusions can be generalised in all patients with DM. Indeed, the vasculature of diabetic patients without pre-existing evidence of inflammatory vascular disease (e.g., young T1DM patients) may respond differently to insulin,

and this would influence the efficiency of antidiabetic treatment accordingly. On the other hand, as mentioned previously, no vascular tissue from atherosclerosis-free patients was available, so replication (or not) of these findings in patients without vascular disease was not possible. In fact, it is quite likely that the insulin responses in such patients would be different, as per my hypothesis that human atherosclerosis is accompanied by vascular IR. In this work, this was supported by the *ex vivo* experiments done in healthy wild-type mice, which revealed differing effects of insulin as compared to human vessels from patients with atherosclerosis, further supporting the notion that there is a specific link between atherosclerosis and the presence of vascular IR.

In Chapter 4, I found that obesity is associated with increased Wnt5a bioavailability in both the circulation and AT (including PVAT) in CAD patients. This association has been shown before in non-CAD patients, and this served as good control for my work. On the other hand, such an association has never been published before for PVAT; unfortunately, access to PVAT from non-CAD patients would not be feasible. I further showed that both obesity and Wnt5a are associated with vascular oxidative stress, something which could not be tested in a non-CAD cohort as mentioned previously due to nature of the tissue models used. However, these associations are highly complemented by the relevant mechanistic experiments I have also performed, and they strongly support a role for AT-derived Wnt5a on obesity-related vascular disease via redox state regulation in CAD patients.

The OxHVF cohort also includes patients undergoing cardiac surgery for valve repair/replacement. Valve disease is the primary indication for such patients, and most of them do not suffer from CAD. As such, one would assume that they could be used as a healthy control cohort. However, these patients have severe myocardial disease which significantly interferes with cardiac biology and even systemic CVD compensatory mechanisms. As such,

assuming they could comprise a healthy, vascular disease-free study group is highly unreliable. Furthermore, since no access to vascular tissue (and thus vascular biology readouts) was available for such patients, their use in validating the associations described in this thesis would be very limited.

5.2. Use of non-atherosclerotic vessels as models of human atherosclerosis

For the purposes of this thesis, I used IMA and SV segments as models to study human vascular biology and vascular disease mechanisms, with a focus on atherosclerosis. However, these vessels are traditionally believed not to develop atherosclerosis (S.S., F.B. and A., 2018) and this is precisely why they are such popular vascular graft choices. This is certainly a study limitation for the study of human atherosclerosis, and one driven by logistic parameters since these are the most readily accessible types of human vessels for research. However, these vessels have been exposed to the main systemic atherosclerosis risk factors (i.e., smoking, diabetes, hyperlipidaemia, hypertension, high fat diet, systemic oxidative stress etc), and therefore can be assumed to reflect vascular biology in a real-life situation of systemic vascular disease. Besides, upon exposure to high pressure turbulent flow (i.e., after being grafted to the coronary circulation following CABG), IMA and SV may develop atherosclerosis (Grondin *et al.*, 1984), which suggests that these vessels do share certain pathophysiological responses to pro-atherogenic stimuli with other vessels that frequently develop atherosclerosis (such as the coronaries). On the other hand, I believe that studying human vessels, even those without atherosclerosis, is more important than the alternative which would be studying diseased arteries of animal atherosclerosis models. This is because of the often striking discrepancy amongst species regarding vascular biology; study of human vascular biology patterns in thus necessary if we hope to understand human vascular disease. Ideally, hypotheses should be tested in models of human vessels to assure relevance to human disease, then tested in animal models to confirm *in vivo* links with vascular disease. In the context of this thesis, certain

experiments were replicated in mouse aortae which served as controls or *in vivo* replications of the hypotheses tested, to further increase the relevance of the proposed mechanisms to vascular disease *in vivo*.

5.3. Lack of control vascular tissue from healthy humans

As mentioned previously, the IMA and SV segments studied in this thesis originate from patients with CAD, and they are thus related with a systemic inflammatory vascular disease environment which is further accompanied by a variety of demographic risk factors. Ideally, vascular tissue from healthy individuals would be required as an appropriate biological control for the various experiments presented previously. However, access to vascular segments from healthy individuals without vascular disease is not possible. Mouse samples were used instead to test individual hypotheses in different contexts i.e., in the absence of atherosclerosis (such as the wild type mouse experiments in Chapter 3) or as an *in vivo* replication of the vascular effects of Wnt5a (transgenic mouse experiments in Chapter 4).

Chapter 6

Discussion

This Chapter discusses the key findings of my thesis, summarising their significance, novelty and clinical relevance. Furthermore, these new findings are put into broader context, while translational and clinical implications as well as future research perspectives are reasoned.

6.1. The concept of vascular insulin resistance: novel perspectives

This work is the first to suggest that atherosclerosis is characterised by the presence of vascular IR irrespectively of systemic IR or diabetes. The consequences of vascular IR have been explored before, mainly in *in vitro* models of endothelial cells (e.g., insulin receptor knockout endothelial cells) as well as diabetic mouse models (King, Park and Li, 2016). Importantly, these studies have revealed that loss of normal insulin signalling in the vasculature may cause selective attenuation of Akt signalling, resulting in loss of the stimulatory effect of insulin on eNOS, NO production and vasorelaxation (Williams *et al.*, 1996; Rask-Madsen and King, 2007; King, Park and Li, 2016). On the other hand, this concept of vascular IR has never been put to a clinical context before. Furthermore, the underlying mechanisms are unknown, while vascular IR has silently been believed to be a bystander or marker of systemic IR and diabetes in humans (King, Park and Li, 2016). In this work, I demonstrate for the first time that

vascular IR is present at a cellular and molecular level in virtually all patients with atherosclerosis independently of the presence of systemic IR or diabetes, i.e., even in the absence of markers of systemic IR. This implies that atherosclerotic disease mechanisms directly promote vascular IR induction, via potential factors such as local inflammation, high fat diet or simply aging (Samuel and Shulman, 2012). This is in agreement with a previous report suggesting that he vasculature is amongst the first tissues to develop signs of molecular IR in a mouse model of diet-induced obesity (F. Kim *et al.*, 2008). More importantly, my work demonstrates that this presence of vascular IR not only blunts the protective vascular effects of insulin, but completely reverses the consequences of vascular insulin signalling. In other words, insulin is shown to have detrimental effects on vascular oxidative stress and endothelial function in patients with atherosclerosis due to the presence of vascular IR.

6.1.1. Clinical implications

The notion that inulin treatment directly induces vascular oxidative stress and impairs endothelial function in patients with atherosclerosis has serious implications for diabetes treatment. Insulin administration is the mainstay of treatment for T1DM patients, and often required in patients with severe T2DM (Kahn, Cooper and Del Prato, 2014; Shubrook *et al.*, 2017). On the other hand, aggressive glycaemic control with insulin treatment does not improve cardiovascular outcomes, despite hyperglycaemia being regarded as the major cause of diabetic vascular complications (Gerstein *et al.*, 2012; Marso *et al.*, 2017). This suggests that pleiotropic mechanisms govern vascular biology, and perhaps the vascular responses to insulin treatment, in the context of diabetes. Such mechanisms are likely to be multiple and complex, ranging from diabetic epigenetic modifications (Guzik and Cosentino, 2017) to, potentially, local adverse effects of molecular IR (Samuel and Shulman, 2012; King, Park and Li, 2016).

In this work, I demonstrated that insulin and synthetic insulin analogues often used in clinical practice directly induce vascular oxidative stress and impair endothelial function in patients with atherosclerosis, and this is due to the presence of vascular IR in these patients independently of the co-presence of systemic IR. My findings directly suggest that insulin treatment in an *in vivo* setting may have detrimental vascular effects, which may counterbalance the beneficial vascular effects of successful glycaemic control, and this could partially explain the neutral effect of insulin treatment of cardiovascular outcomes in diabetic patients. Consequently, vascular insulin sensitisation strategies are required and may help improve cardiovascular outcomes in insulin-treated diabetic patients (at least patients with both diabetes and atherosclerosis), which is a major clinical implication of this work.

DPP4 inhibitors are novel drugs which have been successfully used in diabetes treatment (Rehman *et al.*, 2017). Although they were initially believed to be relevant in diabetes management due to increasing incretin half-life, it has now become evident that they likely have pleiotropic effects on various tissues such as the vasculature (Fadini and Avogaro, 2011). Such effects may include amelioration of inflammation, reduction of oxidative stress, improvement of endothelial function and insulin-sensitizing properties (Fadini and Avogaro, 2011; Zeng *et al.*, 2014; Kornelius *et al.*, 2015). On the other hand, isolated DPP4 inhibition apparently has no significant effect on cardiovascular outcomes in diabetic patients based on recent randomised clinical trials (Scirica *et al.*, 2013; Green *et al.*, 2015), questioning its usefulness in preventing cardiovascular complications in diabetic patients.

In this thesis, I presented how DPP4 inhibition has a direct insulin-sensitising role in the human vasculature, which is able to reverse vascular responses to insulin. This raises thoughts as to whether combined insulin and DPP4 inhibition treatment could improve clinically relevant vascular phenotypes (or even cardiovascular clinical outcomes) in humans with diabetes *in*

vivo. The failure of isolated DPP4 inhibition to improve such outcomes in recent trials may be attributed to pharmacokinetics/pharmacodynamics parameters or complex endogenous interactions with actual DPP4 activity (in the systemic circulation or the vasculature), since a surprisingly complex balance has recently been suggested between DPP4 inhibition, systemic and local DPP4 activity (Ghorpade *et al.*, 2018). On the other hand, my *ex vivo* results suggest that DPP4 inhibition has minor vascular effects itself; it rather works as a facilitator of physiological signalling, and it is insulin that exerts strong antioxidant and vasoprotective effects under such conditions. Therefore, hypothesising that combination of insulin treatment with DPP4 inhibition could offer additive clinical cardiovascular benefit is quite plausible, and potentially calls for appropriate clinical trials in the future.

In this work, I also demonstrated that serum insulin and DPP4 activity levels may provide additive predictive potential with regards to vascular oxidative stress and, importantly, with mortality risk in patients with atherosclerosis. Indeed, patients in the high tertile for both serum insulin and serum DPP4 activity were found to have increased mortality risk in my study population compared to the rest of the study participants. Although such a finding should be replicated in larger validation cohorts in the future, it certainly raises the possibility that exploring the interaction of insulin with DPP4 activity at a systemic level may be a useful surrogate biomarker of peripheral IR with important predictive potential in patients with atherosclerosis.

6.2. Wnt5a and vascular redox signalling: implications in humans

The link of Wnt5a with vascular disease has been proposed in the past, but the mechanistic background of this association remains poorly explored. Indeed, Wnt5a appears to be upregulated in atherosclerotic plaques and it may have the ability to promote inflammation,

thrombosis and endothelial dysfunction (Bhatt and Malgor, 2014). On the other hand, Wnt5a signalling shares links with NADPH-oxidases activity via Rac1, although the interplay between the two has not been explored previously. NADPH-oxidases are able to orchestrate a wide spectrum of redox signalling pathways promoting inflammation, plaque instability and atherogenesis (Konior *et al.*, 2014). Hence, it would be plausible to assume that Wnt5a may promote atherogenesis at least partly via NADPH-oxidases activation. Furthermore, Wnt5a has been linked with dysregulation of VSMC phenotype (Mill *et al.*, 2014). However, this has been proposed to be mechanistically mediated via canonical Wnt signalling triggered with supra-physiological Wnt5a concentrations (Mill *et al.*, 2014). On the contrary, the effect of physiological Wnt5a signalling on VSMCs has not been explored.

This work is the first to demonstrate a direct link between non-canonical Wnt5a signalling and arterial oxidative stress in humans with atherosclerosis in the context of obesity. In particular, I demonstrated that Wnt5a bioavailability is increased in the systemic circulation as well as in visceral and perivascular AT depots of obese humans, which has been shown before but never in a CAD cohort (Lu *et al.*, 2013; Catalán *et al.*, 2014; Zuriaga *et al.*, 2017). I then went on to show that Wnt5a bioavailability in the circulation and in PVAT is associated with arterial NADPH-oxidases activity, which was shown to be the direct effect of non-canonical Rac1 activation in a series of *ex vivo* and mouse *in vivo* experiments. My results also reveal that Wnt5a induces oxidative depletion of vascular BH4, resulting in eNOS uncoupling, reduced NO bioavailability and endothelial dysfunction. Wnt5a hence has a strong oxidative pro-oxidant effect on the human vasculature with detrimental consequences on endothelial function in particular.

Focusing on the VMSC-specific effects of Wnt5a, my work in combination with Dr Fabio Sanna's contribution suggests that Wnt5a propagates redox-sensitive signalling in human

VSMCs, presumably as a direct consequence of NADPH-oxidase activation in these cells, which may be involved in a variety of biological processes such as VSMC migration (via differential gene regulation). Therefore, Wnt5a appears to have a profound, potentially detrimental effect on VSMC phenotype which may be associated with atherosclerosis progression. Crucially, this work is the first ever to suggest a link between Wnt5a, USP17 and Rac1 activation, which was suggested upon transcriptome screening and then validated and confirmed mechanistically *in vitro*. USP17 may be a novel means of targeting Wnt5a signalling, Rac1 activation and NADPH-oxidases activity in the vasculature and beyond.

Besides these *ex vivo* and *in vitro* effects, plasma Wnt5a bioavailability was independently associated with the presence and progression of CAD in humans at an observational level. This observation along with the aforementioned mechanistic experiments suggests that non-canonical Wnt5a and downstream signalling network (such as USP17) on the human vasculature could provide promising links with CAD, with translational potential.

6.2.1. Clinical implications

Identification of Wnt5a as a causal inducer of arterial oxidative stress and endothelial dysfunction in humans with atherosclerosis implies that downstream Wnt5a signalling could be a candidate target for therapeutic interventions. Considering that Wnt5a is revealed as a strong link between obesity and vascular disease, this may be of particular benefit in obese individuals. Indeed, although obesity is regarded as a risk factor for vascular disease, the molecular links of this relationship as poorly understood and largely attributed to a complex and interrelated spectrum of metabolic and inflammatory abnormalities which are not easily targeted. Identification of novel, obesity-specific, targets with vascular implications (such as Wnt5a) is thus needed.

The ambition to therapeutically target the Wnt pathway is not new. Wnt signalling (both canonical and non-canonical) has been implicated in various forms of carcinogenesis, and more recently in diseases such as osteoporosis autoimmune and inflammatory diseases (Marinou *et al.*, 2012; Schulte and Bryja, 2017; Wiese, Nusse and van Amerongen, 2018). On the other hand, Wnt pathways are universal signalling cascades that affect virtually all cell types and determine embryonic development (Zimmerman, Moon and Chien, 2012; Blagodatski, Poteryaev and Katanaev, 2014). As such, targeting Wnt signalling is inherently prone to non-specific, off-target side effects (tumorigenesis being the most important) and is challenging in cases where embryonic development is relevant (e.g., pregnant women). In addition, the interconnected Wnt ligand and receptor network makes targeting of a single ligand challenging. So far, attempts have mainly focused on targeting the canonical signalling pathway especially in the context of cancer (Zimmerman, Moon and Chien, 2012; Blagodatski, Poteryaev and Katanaev, 2014; Nusse and Clevers, 2017), but these efforts are still in their infancy. On the other hand, efficient targeting of non-canonical Wnt signalling has not been explored. Based on the findings of this thesis, Wnt5a signalling could be targeted either by targeting Wnt5a or its antagonist Sfrp5. On the other hand, both these approaches could have serious side effects. Experimental techniques achieving local administration of therapeutic agents (nanoparticle carriage) could be useful in this context (Petros and Desimone, 2010; Blanco, Shen and Ferrari, 2015), e.g., by targeting vascular or AT Wnt5a/Sfrp5. However such techniques are still immature. Finally, identification of USP17 as a link between Wnt5a and NADPH-oxidases suggests that this molecule could be targeted in the context of vascular disease, but given its wide range of effects (Burrows, McGrattan and Johnston, 2005; McFarlane *et al.*, 2010; De La Vega *et al.*, 2011; Lu *et al.*, 2018), this is something that requires further investigation.

In this work, plasma Wnt5a bioavailability was found to be independently associated with the presence and calcific progression of atherosclerotic plaques in humans. This finding was

observed retrospectively in a small cohort of patients and thus requires further exploration in larger validation cohorts, to determine whether Wnt5a can be of true predictive value with regards to the presence and progression of atherosclerosis or other cardiovascular clinical endpoints for that matter. However, it is possible that Wnt5a may have a clinically relevant biomarker role in vascular disease, especially in the context of obesity, which warrants further investigation.

6.3. Novel aspects of the interplay between metabolic & vascular disease

This thesis provides novel insights into the interplay between metabolic and vascular disease. It has been widely accepted that metabolic disease can contribute to vascular disease pathogenesis via multiple mechanisms involving systemic inflammation and metabolic abnormalities (e.g., hyperlipidaemia, hyperglycaemia). More recently, it became evident that AT is a dynamic regulator of this interaction by secreting products, or adipokines, the secretion of which is dysregulated in metabolic disease, having vascular consequences. Recent work has further suggested that vascular disease can be sensed by AT, either remote or close to the vascular wall (Margaritis *et al.*, 2013; Antonopoulos *et al.*, 2014, 2015). Such mutual interactions between the vascular wall and its surrounding PVAT result in paracrine signalling that may be harnessed therapeutically or diagnostically (Akoumianakis and Antoniades, 2017b; Antonopoulos *et al.*, 2017; Oikonomou *et al.*, 2018). This thesis expands on these concepts and reveals novel aspects of the crosstalk between metabolic and vascular disease.

6.3.1. Vascular disease modifies responses to insulin: implications for treatment of diabetes

In the first part of my thesis, I demonstrated that human atherosclerosis is associated with the presence of vascular IR irrespectively of systemic IR or diabetes. Importantly, this completely dysregulates vascular insulin signalling such that insulin treatment induces oxidative stress and endothelial dysfunction. Crucially, DPP4 inhibition appears to have novel insulin-sensitising roles in the human vasculature, completely reversing vascular IR.

These findings provide extremely significant implications for insulin treatment in diabetes. Insulin treatment is the mainstay of therapy for T1DM and a large fraction of T2DM cases, but my results suggest that it could have detrimental vascular effects, and vascular insulin sensitisation strategies may be required in such patients. In addition, my results provide a novel example of how the presence of vascular disease may itself be associated with locally dysregulated metabolic pathways even in the absence of systemic metabolic disease. This suggests that vascular responses to any metabolic intervention may be of clinical relevance and would warrant further investigation in the context of vascular and metabolic disease.

6.3.2. AT as a sensor of metabolic disease and vascular consequences: the example of Wnt5a

In the second part of my thesis, I revealed Wnt5a to be a novel inducer of arterial oxidative stress and redox-sensitive signalling which directly increases NADPH-oxidases activity, promotes eNOS uncoupling and causes endothelial dysfunction in humans, while also been linked with the presence of human CAD at an observational level. Importantly, I further revealed that obesity is associated with increased production of Wnt5a from PVAT and thoracic AT, increased Wnt5a bioavailability in the plasma and increased sensitivity of the human vasculature to Wnt5a signalling via increased Wnt receptor expression. Hence, Wnt5a may be a novel link between obesity and vascular complications.

This is another example supporting the broad notion that AT is a dynamic sensor of metabolic disease, altering its secretome and influencing vascular biology via vasoactive adipokines. Indeed, obesity is associated with increased AT secretion of Wnt5a, which is an molecule with direct deleterious effects for human vascular biology. Wnt5a is thus recognised as a novel link between obesity and vascular disease, and the AT secretome is once again identified as a promising target to modify vascular responses to metabolic disease.

6.3.3. Metabolic & vascular disease are involved in a dynamic, bidirectional crosstalk

Recent experimental and *in vivo* work has elegantly demonstrated that AT is in continuous, bidirectional crosstalk with the vascular wall, and this may be harnessed to provide diagnostic and therapeutic tools against CVD (Akoumianakis and Antoniades, 2017b; Antonopoulos *et al.*, 2017; Oikonomou *et al.*, 2018). My work further expands on that notion and demonstrates that vascular and metabolic disease may comprise an interrelated pathophysiological spectrum where changes in one of the two aspects influence the responses of the other. Indeed, metabolic disease may be able to directly drive vascular disease via the secretion of adipokines and molecules such as Wnt5a. On the other hand, metabolic disease can alter vascular responses to treatments such as insulin (via vascular IR); in other words, vascular disease (i.e., atherosclerosis) can cause a local metabolic signalling abnormality (i.e., vascular IR), which can determine clinical events of a certain treatment (i.e., insulin) in the context of systemic disease (i.e., DM). In summary, metabolic pathogenic parameters should always be considered when studying vascular disease while vascular phenotypes should be equally accounted for when targeting metabolic disease.

6.4. Future work

Throughout my DPhil, I have worked on acquiring material and data for the oxHVF cohort, which also formed the basis for the project-specific, hypothesis-driven mechanistic experiments of my thesis. This work has provided novel insights into the concept of vascular IR and the mechanistic vascular roles of AT-derived Wnt5a in humans, introducing new unanswered questions which warrant further investigation. At the same time, I have contributed to the expansion of the oxHVF cohort, one of the most extensive and well-phenotyped CVD cohorts worldwide, which comprises a powerful, ongoing target discovery project.

6.4.1. Understanding vascular insulin resistance in humans

My work links for the first time the presence of atherosclerosis with vascular IR in humans, irrespectively of systemic metabolic parameters, while revealing novel insulin-sensitizing roles for DPP4 inhibition. These exciting findings open new research directions with regards to: a) further exploration of the exact mechanisms establishing vascular IR and its consequences in humans, b) investigation of strategies to reverse vascular IR such as by deployment of DPP4 inhibition, and c) deciphering the spectrum of vascular roles of DPP4 inhibition.

As mentioned in Chapter 1, FFA and inflammatory pathways may contribute to molecular IR (Shulman, 2000; Matsuda and Shimomura, 2013; Khodabandehloo *et al.*, 2016). However, despite the fact that these factors may exist at a whole body level, my research suggests a dissociation of vascular IR from systemic IR development. One could assume that vascular inflammation could be associated with molecular IR at the vascular level (Natali *et al.*, 2006; Costa *et al.*, 2016), independently of systemic parameters. On the other hand, considering that my findings were observed in non-atherosclerotic IMA segments, it would seem plausible that

local inflammation is not necessary for the development of vascular IR. To this end, it is more likely that systemic parameters associated with the presence of atherosclerosis are also associated with increased risk of vascular IR susceptibility. Such factors could include age (in which case vascular IR could be a surrogate marker of senescence), high-fat diet or other traditional risk factors. Consistently, previous *in vivo* mouse work has suggested that the vascular wall is more susceptible to IR induction in response to high-fat diet compared to other tissues (F. Kim *et al.*, 2008). Better understanding of these potential causes of vascular IR could be of immense clinical benefit.

6.4.2. Exploring the spectrum of vascular Wnt5a signalling & consequences

As mentioned in Chapter 1, Wnt5a has been implicated to metabolic disease via non-canonical signalling that induces adipogenesis and inflammation, processes linked with pathophysiological entities such as obesity and systemic IR (Dandona, Aljada and Bandyopadhyay, 2004; Gu and Xu, 2013). Several studies have also associated Wnt5a with vascular disease, mainly via effects in macrophages and endothelial cells (Cheng *et al.*, 2008; Christman *et al.*, 2008; Kim *et al.*, 2010; Bhatt and Malgor, 2014; Bretón-Romero *et al.*, 2016). However, the role of Wnt5a in metabolic-vascular disease crosstalk and its downstream vascular signalling have not been adequately investigated in humans.

My thesis identifies Wnt5a as a direct link between metabolic and vascular disease, and unravels some novel molecular effects on Wnt5a on vascular NADPH-oxidases activity and eNOS coupling in humans, which have implications for disease mechanisms such as VSMC migration and endothelial dysfunction. These findings raise further questions as to the specific Wnt5a signalling pathways activated in individual vascular cell types. Further research is also warranted as to the *in vivo* and translational implications of targeting Wnt5a signalling.

In this work, Wnt5a was shown to stimulate non-canonical PCP signalling in intact arteries and primary VSMCs from humans with atherosclerosis. On the other hand, the fact that Wnt5a is able to induce eNOS uncoupling and endothelial dysfunction in intact vessels suggests an endothelium-specific effect which has not been adequately explored yet. Current work in our lab focuses on evaluating the relative activation of non-canonical Wnt signalling pathways (Ca^{2+}-dependent versus PCP) in endothelial cells, and how these could affect the main vascular redox enzymes, namely NADPH-oxidases and eNOS in these cells. This would provide a better characterisation of the vascular effects of Wnt5a in metabolic and vascular disease.

The vascular effects of Wnt5a should ideally be integrated in an *in vivo* animal model of atherosclerosis. This would prove a causal role for Wnt5a as a trigger of vascular disease and would justify further research to target Wnt5a signalling for therapeutic/diagnostic/predictive purposes. Future work in our lab will explore the effect of Wnt5a gain-of-function (globally and in AT) on atherosclerosis progression in ApoE-/- mice, which is expected to provide a definite answer as to whether Wnt5a can directly contribute to atherosclerosis development.

6.4.3. The Oxford cohort for heart, vessels and fat: an ongoing target discovery project

The projects presented on this thesis were designed and implemented on the basis of the OxHVF cohort, a large, unique cohort of patients undergoing cardiac surgery, which combines demographic, non-invasive imaging and biological *ex vivo* variables as well as follow-up clinical data for a variety of outcomes (e.g., hospitalisations, graft failure, mortality). This cohort provides an invaluable translational platform for the study of CVD mechanisms while directly linking them with clinical implications.

During my work as a DPhil student, I have worked towards expanding this cohort, being responsible for tissue collection, DNA and RNA extractions, *ex vivo* functional assay

implementation and archiving of all the biological material and data. This information is complemented by a huge amount of clinical data retrieved from clinical notes and national databases such as NHS Digital. In the era of big data bioinformatics analysis, this wealth of data can be used to generate hypotheses, identify new therapeutic targets and explore relevant clinical associations and outcomes. To this end, transcriptome profiling and metabolomics analysis in biological AT and IMA samples collected and processed by myself have recently been used to identify novel metabolic pathways dysregulated in obese AT and the vascular consequences of this, a project that is now moving towards the *ex vivo/in vitro* validation phase. In addition, genome-wide associations study for patients of the OxHVF cohort has been added to the pipeline, with the hope to identify novel mechanistic links with vascular redox state and disease progression.

References

Abhijit, S. *et al.* (2013) 'Hyperinsulinemia-induced vascular smooth muscle cell (VSMC) migration and proliferation is mediated by converging mechanisms of mitochondrial dysfunction and oxidative stress', *Molecular and Cellular Biochemistry*. doi: 10.1007/s11010-012-1478-5.

Afanas'ev, I. (2015) 'Mechanisms of Superoxide Signaling in Epigenetic Processes: Relation to Aging and Cancer', *Aging and Disease*. doi: 10.14336/AD.2014.0924.

Agatston, A. S. *et al.* (1990) 'Quantification of coronary artery calcium using ultrafast computed tomography', *Journal of the American College of Cardiology*. doi: 10.1016/0735-1097(90)90282-T.

Akoumianakis, I. and Antoniades, C. (2017a) 'Dipeptidyl peptidase IV inhibitors as novel regulators of vascular disease', *Vascular Pharmacology*. doi: 10.1016/j.vph.2017.07.001.

Akoumianakis, I. and Antoniades, C. (2017b) 'The interplay between adipose tissue and the cardiovascular system: Is fat always bad?', *Cardiovascular Research*. doi: 10.1093/cvr/cvx111.

Akoumianakis, I., Tarun, A. and Antoniades, C. (2016) 'Perivascular adipose tissue as a regulator of vascular disease pathogenesis: identifying novel therapeutic targets.', *British journal of pharmacology*. doi: 10.1111/bph.13666.

Alexopoulos, N., Katritsis, D. and Raggi, P. (2014) 'Visceral adipose tissue as a source of inflammation and promoter of atherosclerosis', *Atherosclerosis*. doi: 10.1016/j.atherosclerosis.2013.12.023.

Ameres, S. L. and Zamore, P. D. (2013) 'Diversifying microRNA sequence and function', *Nature Reviews Molecular Cell Biology*. doi: 10.1038/nrm3611.

American Diabetes Association (2009) 'Diagnosis and classification of diabetes mellitus', *Diabetes Care*. doi: 10.2337/dc09-S062.

Antonopoulos, A. S. *et al.* (2014) 'Reciprocal effects of systemic inflammation and brain natriuretic peptide on adiponectin biosynthesis in adipose tissue of patients with ischemic heart disease', *Arteriosclerosis, Thrombosis, and Vascular Biology*. doi: 10.1161/ATVBAHA.114.303828.

Antonopoulos, A. S. *et al.* (2015) 'Adiponectin as a link between type 2 diabetes and vascular NADPH oxidase activity in the human arterial wall: The regulatory role of perivascular adipose tissue', *Diabetes*. doi: 10.2337/db14-1011.

Antonopoulos, A. S. *et al.* (2016) 'From the BMI paradox to the obesity paradox: the obesity–mortality association in coronary heart disease', *Obesity Reviews*. doi: 10.1111/obr.12440.

Antonopoulos, A. S. *et al.* (2017) 'Detecting human coronary inflammation by imaging perivascular fat', *Science Translational Medicine*. doi: 10.1126/scitranslmed.aal2658.

Banerjee, M. and Vats, P. (2014) 'Reactive metabolites and antioxidant gene

polymorphisms in Type 2 diabetes mellitus', *Redox Biology*. doi: 10.1016/j.redox.2013.12.001.

Bartosz, G. (2009) 'Reactive oxygen species: Destroyers or messengers?', *Biochemical Pharmacology*. doi: 10.1016/j.bcp.2008.11.009.

Basuroy, S. *et al.* (2009) 'Nox4 NADPH oxidase mediates oxidative stress and apoptosis caused by TNF-alpha in cerebral vascular endothelial cells.', *American journal of physiology. Cell physiology*. doi: 10.1152/ajpcell.00381.2008.

Beckman, J. A. and Creager, M. A. (2016) 'Vascular complications of diabetes', *Circulation Research*. doi: 10.1161/CIRCRESAHA.115.306884.

Bedard, K. and Krause, K.-H. (2007) 'The NOX Family of ROS-Generating NADPH Oxidases: Physiology and Pathophysiology', *Physiological Reviews*. doi: 10.1152/physrev.00044.2005.

Bełtowski, J. *et al.* (2000) 'The effect of dietary-induced obesity on lipid peroxidation, antioxidant enzymes and total plasma antioxidant capacity.', *Journal of physiology and pharmacology : an official journal of the Polish Physiological Society*.

Bennett, M. R., Sinha, S. and Owens, G. K. (2016) 'Vascular Smooth Muscle Cells in Atherosclerosis', *Circulation Research*. doi: 10.1161/CIRCRESAHA.115.306361.

Benov, L. *et al.* (1998) 'Critical evaluation of the use of hydroethidine as a measure of superoxide anion radical.', *Free radical biology & medicine*. doi: 10.1016/S0891-5849(98)00163-4.

Bhatt, P. M. and Malgor, R. (2014) 'Wnt5a: A player in the pathogenesis of atherosclerosis and other inflammatory disorders', *Atherosclerosis*. doi: 10.1016/j.atherosclerosis.2014.08.027.

Bhupathiraju, S. N. and Hu, F. B. (2016) ‘Epidemiology of obesity and diabetes and their cardiovascular complications’, *Circulation Research*. doi: 10.1161/CIRCRESAHA.115.306825.

Blagodatski, A., Poteryaev, D. and Katanaev, V. L. (2014) ‘Targeting the Wnt pathways for therapies’, *Molecular and Cellular Therapies*. doi: 10.1186/2052-8426-2-28.

Blanco, E., Shen, H. and Ferrari, M. (2015) ‘Principles of nanoparticle design for overcoming biological barriers to drug delivery’, *Nature Biotechnology*. doi: 10.1038/nbt.3330.

Bretón-Romero, R. *et al.* (2016) ‘Endothelial dysfunction in human diabetes is mediated by Wnt5a-JNK signaling’, *Arteriosclerosis, Thrombosis, and Vascular Biology*. doi: 10.1161/ATVBAHA.115.306578.

Brouet, A. *et al.* (2001) ‘Hsp90 Ensures the Transition from the Early Ca2+-dependent to the Late Phosphorylation-dependent Activation of the Endothelial Nitric-oxide Synthase in Vascular Endothelial Growth Factor-exposed Endothelial Cells’, *Journal of Biological Chemistry*. doi: 10.1074/jbc.M101371200.

Brownlee, M. (2001) ‘Biochemistry and molecular cell biology of diabetic complications’, *Nature*. doi: 10.1038/414813a.

Brownlee, M. (2005) ‘The pathobiology of diabetic complications: A unifying mechanism’, in *Diabetes*. doi: 10.2337/diabetes.54.6.1615.

Buchanan, T. A., Watanabe, R. M. and Xiang, A. H. (2010) ‘Limitations in surrogate measures of insulin resistance’, *Journal of Clinical Endocrinology and Metabolism*. doi: 10.1210/jc.2010-2167.

Buettner, R., Sch??lmerich, J. and Bollheimer, L. C. (2007) ‘High-fat diets: Modeling the

metabolic disorders of human obesity in rodents', *Obesity*. doi: 10.1038/oby.2007.608.

Burrows, J. F., McGrattan, M. J. and Johnston, J. A. (2005) 'The DUB/USP17 deubiquitinating enzymes, a multigene family within a tandemly repeated sequence', *Genomics*. doi: 10.1016/j.ygeno.2004.11.013.

Buse, M. G. (2006) 'Hexosamines, insulin resistance, and the complications of diabetes: current status', *American Journal of Physiology-Endocrinology and Metabolism*. doi: 10.1152/ajpendo.00329.2005.

Catalán, V. *et al.* (2014) 'Activation of noncanonical wnt signaling through WNT5A in visceral adipose tissue of obese subjects is related to inflammation', *Journal of Clinical Endocrinology and Metabolism*. doi: 10.1210/jc.2014-1191.

Ceriello, A. and Motz, E. (2004) 'Is Oxidative Stress the Pathogenic Mechanism Underlying Insulin Resistance, Diabetes, and Cardiovascular Disease? The Common Soil Hypothesis Revisited', *Arteriosclerosis, Thrombosis, and Vascular Biology*. doi: 10.1161/01.ATV.0000122852.22604.78.

Chappell, J. *et al.* (2016) 'Extensive Proliferation of a Subset of Differentiated, yet Plastic, Medial Vascular Smooth Muscle Cells Contributes to Neointimal Formation in Mouse Injury and Atherosclerosis Models', *Circulation Research*. doi: 10.1161/CIRCRESAHA.116.309799.

Chen, J. *et al.* (2016) 'Advanced glycation endproducts induce apoptosis of endothelial progenitor cells by activating receptor RAGE and NADPH oxidase/JNK signaling axis', *American Journal of Translational Research*.

Cheng, C. *et al.* (2008) 'Wnt5a-mediated non-canonical Wnt signalling regulates human endothelial cell proliferation and migration', *Biochemical and Biophysical Research*

Communications. doi: 10.1016/j.bbrc.2007.10.166.

Chin, D. and Means, A. R. (2000) 'Calmodulin: A prototypical calcium sensor', *Trends in Cell Biology*. doi: 10.1016/S0962-8924(00)01800-6.

Christman, M. a *et al.* (2008) 'Wnt5a is expressed in murine and human atherosclerotic lesions.', *American journal of physiology. Heart and circulatory physiology*. doi: 10.1152/ajpheart.00982.2007.

Christodoulides, C. *et al.* (2009) 'Adipogenesis and WNT signalling', *Trends in Endocrinology and Metabolism*. doi: 10.1016/j.tem.2008.09.002.

Clevers, H. and Nusse, R. (2012) 'Wnt/β-catenin signaling and disease', *Cell*. doi: 10.1016/j.cell.2012.05.012.

Cosmi, F. *et al.* (2018) 'Treatment with insulin is associated with worse outcome in patients with chronic heart failure and diabetes', *European Journal of Heart Failure*. doi: 10.1002/ejhf.1146.

Costa, R. M. *et al.* (2016) 'TNF-α induces vascular insulin resistance via positive modulation of PTEN and decreased Akt/eNOS/NO signaling in high fat diet-fed mice', *Cardiovascular Diabetology*. doi: 10.1186/s12933-016-0443-0.

Crabtree, G. R. and Olson, E. N. (2002) 'NFAT signaling: Choreographing the social lives of cells', *Cell*. doi: 10.1016/S0092-8674(02)00699-2.

Dadu, R. T. and Ballantyne, C. M. (2014) 'Lipid lowering with PCSK9 inhibitors', *Nature Reviews Cardiology*. doi: 10.1038/nrcardio.2014.84.

Dandona, P., Aljada, A. and Bandyopadhyay, A. (2004) 'Inflammation: The link between insulin resistance, obesity and diabetes', *Trends in Immunology*. doi: 10.1016/j.it.2003.10.013.

Dassanayaka, S. and Jones, S. P. (2014) ‘O-GlcNAc and the cardiovascular system’, *Pharmacology and Therapeutics*. doi: 10.1016/j.pharmthera.2013.11.005.

Desco, M.-C. *et al.* (2002) ‘Xanthine oxidase is involved in free radical production in type 1 diabetes: protection by allopurinol.’, *Diabetes*. doi: 10.2337/diabetes.51.4.1118.

Després, J. P. (2006) ‘Is visceral obesity the cause of the metabolic syndrome?’, *Annals of Medicine*. doi: 10.1080/07853890500383895.

Dimitriadis, G. *et al.* (2011) ‘Insulin effects in muscle and adipose tissue’, *Diabetes Research and Clinical Practice*. doi: 10.1016/S0168-8227(11)70014-6.

Domingueti, C. P. *et al.* (2016) ‘Diabetes mellitus: The linkage between oxidative stress, inflammation, hypercoagulability and vascular complications’, *Journal of Diabetes and its Complications*. doi: 10.1016/j.jdiacomp.2015.12.018.

Doughan, A. K., Harrison, D. G. and Dikalov, S. I. (2008) ‘Molecular mechanisms of angiotensin II-mediated mitochondrial dysfunction: Linking mitochondrial oxidative damage and vascular endothelial dysfunction’, *Circulation Research*. doi: 10.1161/CIRCRESAHA.107.162800.

Duan, L. *et al.* (2017) ‘The regulatory role of DPP4 in atherosclerotic disease’, *Cardiovascular Diabetology*. doi: 10.1186/s12933-017-0558-y.

Duncan, E. R. *et al.* (2008) ‘Effect of endothelium-specific insulin resistance on endothelial function in vivo’, *Diabetes*. doi: 10.2337/db07-1111.

Eckel, N. *et al.* (2015) ‘Metabolically healthy obesity and cardiovascular events: A systematic review and meta-analysis’, *European Journal of Preventive Cardiology*. doi: 10.1177/2047487315623884.

Erdei, N. *et al.* (2006) ‘High-fat diet-induced reduction in nitric oxide-dependent

arteriolar dilation in rats: role of xanthine oxidase-derived superoxide anion', *American Journal of Physiology-Heart and Circulatory Physiology*. doi: 10.1152/ajpheart.00389.2006.

Esser, N. *et al.* (2014) 'Inflammation as a link between obesity, metabolic syndrome and type 2 diabetes', *Diabetes Research and Clinical Practice*. doi: 10.1016/j.diabres.2014.04.006.

Das Evcimen, N. and King, G. L. (2007) 'The role of protein kinase C activation and the vascular complications of diabetes', *Pharmacol Res*. doi: 10.1016/j.phrs.2007.04.016.

Fadini, G. P. and Avogaro, A. (2011) 'Cardiovascular effects of DPP-4 inhibition: Beyond GLP-1', *Vascular Pharmacology*. doi: 10.1016/j.vph.2011.05.001.

Farb, M. G. *et al.* (2016) 'WNT5A-JNK regulation of vascular insulin resistance in human obesity', *Vascular Medicine (United Kingdom)*. doi: 10.1177/1358863X16666693.

Farese, R. R. V. and Sajan, M. M. P. (2012) 'Atypical Protein Kinase C in Cardiometabolic Abnormalities', *Current opinion in lipidology*. doi: 10.1097/MOL.0b013e328352c4c7.Atypical.

Fisslthaler, B. *et al.* (2003) 'Insulin enhances the expression of the endothelial nitric oxide synthase in native endothelial cells: A dual role for Akt and AP-1', *Nitric Oxide - Biology and Chemistry*. doi: 10.1016/S1089-8603(03)00042-9.

for Disease Control, C., Prevention and others (2017) 'National Diabetes Statistics Report: Estimates of Diabetes and Its Burden in the United States. Atlanta, GA: Centers for Disease Control and Prevention; 2017', *US Department of Health and Human Services*. doi: 10.1177/1527154408322560.

Förstermann, U. (2008) 'Oxidative stress in vascular disease: Causes, defense mechanisms and potential therapies', *Nature Clinical Practice Cardiovascular Medicine*. doi:

10.1038/ncpcardio1211.

Förstermann, U. and Sessa, W. C. (2012) 'Nitric oxide synthases: Regulation and function', *European Heart Journal*. doi: 10.1093/eurheartj/ehr304.

Förstermann, U., Xia, N. and Li, H. (2017) 'Roles of vascular oxidative stress and nitric oxide in the pathogenesis of atherosclerosis', *Circulation Research*. doi: 10.1161/CIRCRESAHA.116.309326.

Foulquier, S. *et al.* (2018) 'WNT Signaling in Cardiac and Vascular Disease', *Pharmacological Reviews*. doi: 10.1124/pr.117.013896.

Frey, R. S. *et al.* (2002) 'PKCzeta regulates TNF-alpha-induced activation of NADPH oxidase in endothelial cells.', *Circulation research*. doi: 10.1161/01.RES.0000017631.28815.8E.

Fu, Z., R. Gilbert, E. and Liu, D. (2013) 'Regulation of Insulin Synthesis and Secretion and Pancreatic Beta-Cell Dysfunction in Diabetes', *Current Diabetes Reviews*. doi: 10.2174/157339913804143225.

Fukai, T. and Ushio-Fukai, M. (2011) 'Superoxide Dismutases: Role in Redox Signaling, Vascular Function, and Diseases', *Antioxidants & Redox Signaling*. doi: 10.1089/ars.2011.3999.

Furukawa, S. *et al.* (2004) 'Increased oxidative stress in obesity and its impact on metabolic syndrome', *The journal of clinical investigation*. doi: 10.1172/JCI200421625.1752.

Fuster, J. J. *et al.* (2015) 'Noncanonical Wnt Signaling Promotes Obesity-Induced Adipose Tissue Inflammation and Metabolic Dysfunction Independent of Adipose Tissue Expansion', *Diabetes*. doi: 10.2337/db14-1164.

Fuster, J. J. *et al.* (2016) 'Obesity-induced changes in adipose tissue microenvironment

and their impact on cardiovascular disease', *Circulation Research*. doi: 10.1161/CIRCRESAHA.115.306885.

Van Gaal, L. F. (2010) 'Mechanisms linking obesity with cardiovascular disease', *Diabetes, Obesity and Metabolism*. doi: 10.1038/nature05487.

Gamez-Mendez, A. M. *et al.* (2015) 'Oxidative stress-dependent coronary endothelial dysfunction in obese mice', *PLoS ONE*. doi: 10.1371/journal.pone.0138609.

Gao, L. and Mann, G. E. (2009) 'Vascular NAD(P)H oxidase activation in diabetes: A double-edged sword in redox signalling', *Cardiovascular Research*. doi: 10.1093/cvr/cvp031.

García-Cardeña, G. *et al.* (1998) 'Dynamic activation of endothelial nitric oxide synthase by Hsp90', *Nature*. doi: 10.1038/33934.

Gaya, and K. R. O. T. (2011) 'Diagnosis and management of maturity onset diabetes of the young (MODY)', *Bmj*. doi: 10.1136/bmj.d6044.

Gerstein, H. C. *et al.* (2012) 'Basal insulin and cardiovascular and other outcomes in dysglycemia 1', *N.Engl.J Med*. doi: 10.1056/NEJMoa1203858.

Ghorpade, D. S. *et al.* (2018) 'Hepatocyte-secreted DPP4 in obesity promotes adipose inflammation and insulin resistance', *Nature*. doi: 10.1038/nature26138.

Goldin, A. *et al.* (2006) 'Advanced glycation end products: Sparking the development of diabetic vascular injury', *Circulation*. doi: 10.1161/CIRCULATIONAHA.106.621854.

Gollasch, M. (2017) 'Adipose-Vascular Coupling and Potential Therapeutics', *Annual Review of Pharmacology and Toxicology*. doi: 10.1146/annurev-pharmtox-010716-104542.

Gorshkova, I. *et al.* (2008) 'Protein kinase C-epsilon regulates sphingosine 1-phosphate-mediated migration of human lung endothelial cells through activation of phospholipase D2,

protein kinase C-zeta, and Rac1', *J Biol Chem*. doi: 10.1074/jbc.M800250200.

Gratton, J. P. *et al.* (2000) 'Reconstitution of an endothelial nitric-oxide synthase (eNOS), hsp90, and caveolin-1 complex in vitro: Evidence that hsp90 facilitates calmodulin stimulated displacement of eNOS from caveolin-1', *Journal of Biological Chemistry*. doi: 10.1074/jbc.M001644200.

Green, J. B. *et al.* (2015) 'Effect of Sitagliptin on Cardiovascular Outcomes in Type 2 Diabetes', *New England Journal of Medicine*. doi: 10.1056/NEJMoa1501352.

Greif, M. *et al.* (2009) 'Pericardial Adipose Tissue Determined by Dual Source CT Is a Risk Factor for Coronary Atherosclerosis', *Arteriosclerosis, Thrombosis, and Vascular Biology*. doi: 10.1161/ATVBAHA.108.180653.

Griendling, K. K. *et al.* (2016) 'Measurement of Reactive Oxygen Species, Reactive Nitrogen Species, and Redox-Dependent Signaling in the Cardiovascular System: A Scientific Statement from the American Heart Association', *Circulation Research*. doi: 10.1161/RES.0000000000000110.

Grondin, C. M. *et al.* (1984) 'Comparison of late changes in internal mammary artery and saphenous vein grafts in two consecutive series of patients 10 years after operation', *Circulation*.

Gu, P. and Xu, A. (2013) 'Interplay between adipose tissue and blood vessels in obesity and vascular dysfunction.', *Reviews in endocrine & metabolic disorders*. doi: 10.1007/s11154-012-9230-8.

Gustafson, B. *et al.* (2013) 'Restricted adipogenesis in hypertrophic obesity: The role of WISP2, WNT, and BMP4', *Diabetes*. doi: 10.2337/db13-0473.

Guzik, T. J. *et al.* (2004) 'Systemic regulation of vascular NAD(P)H oxidase activity and

nox isoform expression in human arteries and veins', *Arteriosclerosis, Thrombosis, and Vascular Biology*. doi: 10.1161/01.ATV.0000139011.94634.9d.

Guzik, T. J. and Channon, K. M. (2005) 'Measurement of vascular reactive oxygen species production by chemiluminescence.', *Methods in molecular medicine*. doi: 10.1385/1-59259-850-1:073.

Guzik, T. J. and Cosentino, F. (2017) 'Epigenetics and Immunometabolism in Diabetes and Aging', *Antioxidants & Redox Signaling*. doi: 10.1089/ars.2017.7299.

Guzik, T. J. and Harrison, D. G. (2006) 'Vascular NADPH oxidases as drug targets for novel antioxidant strategies', *Drug Discovery Today*. doi: 10.1016/j.drudis.2006.04.003.

Hales, C. M. *et al.* (2018) 'Trends in Obesity and Severe Obesity Prevalence in US Youth and Adults by Sex and Age, 2007-2008 to 2015-2016', *JAMA*. doi: 10.1001/jama.2018.3060.

Han, M. S. *et al.* (2013) 'JNK expression by macrophages promotes obesity-induced insulin resistance and inflammation', *Science*. doi: 10.1126/science.1227568.

Hansson, G. K. (2005) 'Inflammation, atherosclerosis and coronary artery disease', *The New England Journal of Medicine*. doi: 10.1056/NEJM199408183310709.

Harcourt, B. E., Penfold, S. A. and Forbes, J. M. (2013) 'Coming full circle in diabetes mellitus: From complications to initiation', *Nature Reviews Endocrinology*. doi: 10.1038/nrendo.2012.236.

Hart, G. W. *et al.* (2011) 'Cross Talk Between O-GlcNAcylation and Phosphorylation: Roles in Signaling, Transcription, and Chronic Disease', *Annual Review of Biochemistry*. doi: 10.1146/annurev-biochem-060608-102511.

Henquin, J. C. (2000) 'Triggering and amplifying pathways of regulation of insulin secretion by glucose', *Diabetes*. doi: 10.2337/diabetes.49.11.1751.

Henquin, J. C. (2009) ‘Regulation of insulin secretion: A matter of phase control and amplitude modulation’, *Diabetologia*. doi: 10.1007/s00125-009-1314-y.

Herrington, W. *et al.* (2016) ‘Epidemiology of Atherosclerosis and the Potential to Reduce the Global Burden of Atherothrombotic Disease’, *Circulation Research*. doi: 10.1161/CIRCRESAHA.115.307611.

Hoffman, R. P., Vicini, P. and Cobelli, C. (2004) ‘Pubertal changes in HOMA and QUICKI: Relationship to hepatic and peripheral insulin sensitivity’, *Pediatric Diabetes*. doi: 10.1111/j.1399-543X.2004.00050.x.

Hotamisligil, G. S. *et al.* (1996) ‘IRS-1-mediated inhibition of insulin receptor tyrosine kinase activity in TNF-alpha- and obesity-induced insulin resistance.’, *Science*. doi: 10.1126/SCIENCE.271.5249.665.

Huang, P. L. (2009) ‘eNOS, metabolic syndrome and cardiovascular disease.’, *Trends in endocrinology and metabolism: TEM*. doi: 10.1016/j.tem.2009.03.005.

Hubert, H. B. *et al.* (1983) ‘Obesity as an independent risk factor for cardiovascular disease: A 26-year follow-up of participants in the Framingham Heart Study’, *Circulation*. doi: 10.1161/01.CIR.67.5.968.

Iacobellis, G. (2015) ‘Local and systemic effects of the multifaceted epicardial adipose tissue depot’, *Nature Reviews Endocrinology*. doi: 10.1038/nrendo.2015.58.

Ibrahim, M. M. (2010) ‘Subcutaneous and visceral adipose tissue: Structural and functional differences’, *Obesity Reviews*. doi: 10.1111/j.1467-789X.2009.00623.x.

Ishibashi, Y. *et al.* (2011) ‘Sitagliptin augments protective effects of GLP-1 against advanced glycation end product receptor axis in endothelial cells’, *Hormone and Metabolic Research*. doi: 10.1055/s-0031-1284383.

Issad, T., Masson, E. and Pagesy, P. (2010) 'O-GlcNAc modification, insulin signaling and diabetic complications', *Diabetes & Metabolism*. doi: 10.1016/j.diabet.2010.09.001.

James, R. G., Conrad, W. H. and Moon, R. T. (2008) 'β-Catenin-independent Wnt pathways: Signals, core proteins, and effectors', *Methods in Molecular Biology*. doi: 10.1007/978-1-59745-249-6_10.

Jiang, Z. Y. *et al.* (1999) 'Characterization of selective resistance to insulin signaling in the vasculature of obese Zucker (fa/fa) rats', *Journal of Clinical Investigation*. doi: 10.1172/JCI5971.

Jones, M. K. *et al.* (2004) 'Dual actions of nitric oxide on angiogenesis: Possible roles of PKC, ERK, and AP-1', *Biochemical and Biophysical Research Communications*. doi: 10.1016/j.bbrc.2004.04.055.

Kahn, B. and Flier, J. (2000) 'Obesity and insulin resistance', *The Journal of Clinical Investigation*. doi: 10.1172/JCI10842.

Kahn, S. E., Cooper, M. E. and Del Prato, S. (2014) 'Pathophysiology and treatment of type 2 diabetes: Perspectives on the past, present, and future', *The Lancet*. doi: 10.1016/S0140-6736(13)62154-6.

Kampmann, U. (2015) 'Gestational diabetes: A clinical update', *World Journal of Diabetes*. doi: 10.4239/wjd.v6.i8.1065.

Karbach, S. *et al.* (2014) 'eNOS uncoupling in cardiovascular diseases--the role of oxidative stress and inflammation.', *Current pharmaceutical design*. doi: 10.1155/2014/615312.

Katakam, P. V. G. *et al.* (2005) 'Impaired insulin-induced vasodilation in small coronary arteries of Zucker obese rats is mediated by reactive oxygen species.', *Am J Physiol Heart*

Circ Physiol. doi: 10.1152/ajpheart.00715.2004.

Katsarou, A. *et al.* (2017) 'Type 1 diabetes mellitus', *Nature Reviews Disease Primers*. doi: 10.1038/nrdp.2017.16.

Kaur, J. (2014) 'A comprehensive review on metabolic syndrome', *Cardiology Research and Practice*. doi: 10.1155/2014/943162.

Keaney, J. F. *et al.* (2003) 'Obesity and systemic oxidative stress: Clinical correlates of oxidative stress in the Framingham study', *Arteriosclerosis, Thrombosis, and Vascular Biology*. doi: 10.1161/01.ATV.0000058402.34138.11.

Kearney, M. T. (2013) 'Changing the way we think about endothelial cell insulin sensitivity, nitric oxide, and the pathophysiology of type 2 diabetes: The FoxO is loose', *Diabetes*. doi: 10.2337/db13-0183.

Keske, M. A. *et al.* (2016) 'Muscle microvascular blood flow responses in insulin resistance and ageing', *Journal of Physiology*. doi: 10.1113/jphysiol.2014.283549.

Khodabandehloo, H. *et al.* (2016) 'Molecular and cellular mechanisms linking inflammation to insulin resistance and β-cell dysfunction.', *Translational research : the journal of laboratory and clinical medicine*. doi: 10.1016/j.trsl.2015.08.011.

Kikuchi, A. *et al.* (2012) 'Wnt5a: Its signalling, functions and implication in diseases', *Acta Physiologica*. doi: 10.1111/j.1748-1716.2011.02294.x.

Kikuchi, A., Yamamoto, H. and Sato, A. (2009) 'Selective activation mechanisms of Wnt signaling pathways', *Trends in Cell Biology*. doi: 10.1016/j.tcb.2009.01.003.

Kim, F. *et al.* (2008) 'Vascular inflammation, insulin resistance, and reduced nitric oxide production precede the onset of peripheral insulin resistance', *Arteriosclerosis, Thrombosis, and Vascular Biology*. doi: 10.1161/ATVBAHA.108.169722.

Kim, J. *et al.* (2010) 'Wnt5a induces endothelial inflammation via beta-catenin-independent signaling.', *Journal of immunology (Baltimore, Md. : 1950)*. doi: 10.4049/jimmunol.1000181.

Kim, N. H., Yu, T. and Lee, D. H. (2014) 'The nonglycemic actions of dipeptidyl peptidase-4 inhibitors', *BioMed Research International*. doi: 10.1155/2014/368703.

Kim, S. H., Abbasi, F. and Reaven, G. M. (2004) 'Impact of degree of obesity on surrogate estimates of insulin resistance', *Diabetes Care*. doi: 10.2337/diacare.27.8.1998.

Kim, Y. *et al.* (2008) 'Hyaluronic acid targets CD44 and inhibits FcεRI signaling involving PKCδ, Rac1, ROS, and MAPK to exert anti-allergic effect', *Molecular Immunology*. doi: 10.1016/j.molimm.2008.01.008.

Kim, Y. S. *et al.* (2007) 'TNF-Induced Activation of the Nox1 NADPH Oxidase and Its Role in the Induction of Necrotic Cell Death', *Molecular Cell*. doi: 10.1016/j.molcel.2007.04.021.

King, G. L., Park, K. and Li, Q. (2016) 'Selective insulin resistance and the development of cardiovascular diseases in diabetes: The 2015 Edwin Bierman Award Lecture', *Diabetes*. doi: 10.2337/db16-0152.

Knatterud, G. L. *et al.* (1978) 'Effects of Hypoglycemic Agents on Vascular Complications in Patients With Adult-Onset Diabetes: VII. Mortality and Selected Nonfatal Events With Insulin Treatment', *JAMA: The Journal of the American Medical Association*. doi: 10.1001/jama.1978.03290010041020.

Konior, A. *et al.* (2014) 'NADPH Oxidases in Vascular Pathology', *Antioxidants & Redox Signaling*. doi: 10.1089/ars.2013.5607.

Konopatskaya, O. *et al.* (2003) 'Insulin and lysophosphatidylcholine synergistically

stimulate NO-dependent cGMP production in human endothelial cells', *Diabetic Medicine*. doi: 10.1046/j.1464-5491.2003.01039.x.

Korda, M. *et al.* (2008) 'Leptin-induced endothelial dysfunction in obesity', *AJP: Heart and Circulatory Physiology*. doi: 10.1152/ajpheart.00479.2008.

Kornelius, E. *et al.* (2015) 'DPP-4 Inhibitor Linagliptin Attenuates Aβ-induced Cytotoxicity through Activation of AMPK in Neuronal Cells', *CNS Neuroscience and Therapeutics*. doi: 10.1111/cns.12404.

De La Vega, M. *et al.* (2011) 'The deubiquitinating enzyme USP17 is essential for GTPase subcellular localization and cell motility', *Nature Communications*. doi: 10.1038/ncomms1243.

Lamers, D. *et al.* (2011) 'Dipeptidyl peptidase 4 is a novel adipokine potentially linking obesity to the metabolic syndrome', *Diabetes*. doi: 10.2337/db10-1707.

Lassègue, B. and Griendling, K. K. (2010) 'NADPH oxidases: Functions and pathologies in the vasculature', *Arteriosclerosis, Thrombosis, and Vascular Biology*. doi: 10.1161/ATVBAHA.108.181610.

Lassègue, B., San Martín, A. and Griendling, K. K. (2012) 'Biochemistry, physiology, and pathophysiology of NADPH oxidases in the cardiovascular system', *Circulation Research*. doi: 10.1161/CIRCRESAHA.111.243972.

Lastra, G. *et al.* (2017) 'Xanthine oxidase inhibition protects against Western diet-induced aortic stiffness and impaired vasorelaxation in female mice', *American Journal of Physiology - Regulatory, Integrative and Comparative Physiology*. doi: 10.1152/ajpregu.00483.2016.

Laudes, M. (2011) 'Role of WNT signalling in the determination of human mesenchymal

stem cells into preadipocytes', *Journal of Molecular Endocrinology*. doi: 10.1530/JME-10-0169.

Laugesen, E., Østergaard, J. A. and Leslie, R. D. G. (2015) 'Latent autoimmune diabetes of the adult: Current knowledge and uncertainty', *Diabetic Medicine*. doi: 10.1111/dme.12700.

Lee, B. W. *et al.* (2010) 'RAGE ligands induce apoptotic cell death of pancreatic beta-cells via oxidative stress', *International Journal of Molecular Medicine*. doi: 10.3892/ijmm.

Lee, H. Y., Després, J. P. and Koh, K. K. (2013) 'Perivascular adipose tissue in the pathogenesis of cardiovascular disease', *Atherosclerosis*. doi: 10.1016/j.atherosclerosis.2013.07.037.

Lee, Y. C. *et al.* (2011) 'Role of perivascular adipose tissue-derived methyl palmitate in vascular tone regulation and pathogenesis of hypertension', *Circulation*. doi: 10.1161/CIRCULATIONAHA.111.027375.

Li, H. and Förstermann, U. (2013) 'Uncoupling of endothelial NO synthase in atherosclerosis and vascular disease', *Current Opinion in Pharmacology*. doi: 10.1016/j.coph.2013.01.006.

Li, H., Horke, S. and Förstermann, U. (2013) 'Oxidative stress in vascular disease and its pharmacological prevention', *Trends in Pharmacological Sciences*. doi: 10.1016/j.tips.2013.03.007.

Li, H., Horke, S. and Förstermann, U. (2014) 'Vascular oxidative stress, nitric oxide and atherosclerosis', *Atherosclerosis*. doi: 10.1016/j.atherosclerosis.2014.09.001.

Li, J. M. and Shah, A. M. (2003) 'Mechanism of endothelial cell NADPH oxidase activation by angiotensin II: Role of the p47phox subunit', *Journal of Biological Chemistry*.

doi: 10.1074/jbc.M209793200.

Li, Y. *et al.* (2008) 'Sfrp5 coordinates foregut specification and morphogenesis by antagonizing both canonical and noncanonical Wnt11 signaling', *Genes and Development*. doi: 10.1101/gad.1687308.

Libby, P. (2012) 'Inflammation in atherosclerosis', *Arteriosclerosis, Thrombosis, and Vascular Biology*. doi: 10.1161/ATVBAHA.108.179705.

Lipska, K. J. and Krumholz, H. M. (2017) 'Is hemoglobin A1c the right outcome for studies of diabetes?', *JAMA - Journal of the American Medical Association*. doi: 10.1001/jama.2017.0029.

Liu, J. *et al.* (2010) 'Pericardial adipose tissue, atherosclerosis, and cardiovascular disease risk factors: the Jackson heart study', *Diabetes Care*. doi: 10.2337/dc10-0245.

Lizcano, J. M. and Alessi, D. R. (2002) 'The insulin signalling pathway', *Current Biology*. doi: 10.1016/S0960-9822(02)00777-7.

Logan, C. Y. and Nusse, R. (2004) 'THE WNT SIGNALING PATHWAY IN DEVELOPMENT AND DISEASE', *Annual Review of Cell and Developmental Biology*. doi: 10.1146/annurev.cellbio.20.010403.113126.

Loh, N. Y. *et al.* (2015) 'LRP5 regulates human body fat distribution by modulating adipose progenitor biology in a dose- and depot-specific fashion', *Cell Metabolism*. doi: 10.1016/j.cmet.2015.01.009.

Lorenzi, M. (2007) 'The polyol pathway as a mechanism for diabetic retinopathy: Attractive, elusive, and resilient', *Experimental Diabesity Research*. doi: 10.1155/2007/61038.

Lowell, B. B. and Shulman, G. I. (2005) 'Mitochondrial dysfunction and type 2

diabetes.', *Science (New York, N.Y.)*. doi: 10.1126/science.1104343.

Lu, C. H. *et al.* (2018) 'USP17 mediates macrophage-promoted inflammation and stemness in lung cancer cells by regulating TRAF2/TRAF3 complex formation', *Oncogene*. doi: 10.1038/s41388-018-0411-0.

Lu, Y. C. *et al.* (2013) 'Circulating secreted frizzled-related protein 5 (Sfrp5) and wingless-type MMTV integration site family member 5a (Wnt5a) levels in patients with type 2 diabetes mellitus', *Diabetes/Metabolism Research and Reviews*. doi: 10.1002/dmrr.2426.

Luo, X. *et al.* (2012) 'Increased plasma S-adenosyl-homocysteine levels induce the proliferation and migration of VSMCs through an oxidative stress-ERK1/2 pathway in apoE-/-mice', *Cardiovascular Research*. doi: 10.1093/cvr/cvs130.

Mahadev, K. *et al.* (2004) 'The NAD (P) H Oxidase Homolog Nox4 Modulates Insulin-Stimulated Generation of H 2 O 2 and Plays an Integral Role in Insulin Signal Transduction', *Molecular and cellular biology*. doi: 10.1128/MCB.24.5.1844.

Malgor, R. *et al.* (2014) 'Wnt5a, TLR2 and TLR4 are elevated in advanced human atherosclerotic lesions.', *Inflammation research : official journal of the European Histamine Research Society ... [et al.]*. doi: 10.1007/s00011-013-0697-x.

Marchesi, C. *et al.* (2009) 'Endothelial nitric oxide synthase uncoupling and perivascular adipose oxidative stress and inflammation contribute to vascular dysfunction in a rodent model of metabolic syndrome', *Hypertension*. doi: 10.1161/HYPERTENSIONAHA.109.138305.

Margaritis, M. *et al.* (2013) 'Interactions between vascular wall and perivascular adipose tissue reveal novel roles for adiponectin in the regulation of endothelial nitric oxide synthase function in human vessels', *Circulation*. doi: 10.1161/CIRCULATIONAHA.112.001133.

Margaritis, M. *et al.* (2017) 'Predictive value of telomere length on outcome following acute myocardial infarction: Evidence for contrasting effects of vascular vs. blood oxidative stress', *European Heart Journal*. doi: 10.1093/eurheartj/ehx177.

Margolis, D. J., Hoffstad, O. and Strom, B. L. (2008) 'Association between serious ischemic cardiac outcomes and medications used to treat diabetes', *Pharmacoepidemiology and Drug Safety*. doi: 10.1002/pds.1630.

Marinou, K. *et al.* (2012) 'Wnt signaling in cardiovascular physiology', *Trends in endocrinology and metabolism: TEM*. doi: 10.1016/j.tem.2012.06.001.

Marso, S. *et al.* (2016) 'Liraglutide and Cardiovascular Outcomes in Type 2 Diabetes', *New England Journal of Medicine*. doi: 10.1056/NEJMoa1603827.

Marso, S. P. *et al.* (2016) 'Liraglutide and Cardiovascular Outcomes in Type 2 Diabetes', *New England Journal of Medicine*. doi: 10.1056/NEJMoa1603827.

Marso, S. P. *et al.* (2017) 'Efficacy and Safety of Degludec versus Glargine in Type 2 Diabetes', *New England Journal of Medicine*. doi: 10.1056/NEJMoa1615692.

Masckauchán, T. N. H. *et al.* (2006) 'Wnt5a signaling induces proliferation and survival of endothelial cells in vitro and expression of MMP-1 and Tie-2.', *Molecular biology of the cell*. doi: 10.1091/mbc.E06-04-0320.

Matsuda, M. and Shimomura, I. (2013) 'Increased oxidative stress in obesity: Implications for metabolic syndrome, diabetes, hypertension, dyslipidemia, atherosclerosis, and cancer', *Obesity Research and Clinical Practice*. doi: 10.1016/j.orcp.2013.05.004.

Matsumoto, S. *et al.* (2003) 'Confirmation of superoxide generation via xanthine oxidase in streptozotocin-induced diabetic mice', *Free Radic Res*. doi: 10.1080/1071576031000107344.

McDonald, T. J. and Ellard, S. (2013) 'Maturity onset diabetes of the young: Identification and diagnosis', *Annals of Clinical Biochemistry*. doi: 10.1177/0004563213483458.

McEwen, L. N. *et al.* (2012) 'Predictors of mortality over 8 years in type 2 diabetic patients: Translating research into action for diabetes (TRIAD)', *Diabetes Care*. doi: 10.2337/dc11-2281.

McFarlane, C. *et al.* (2010) 'The deubiquitinating enzyme USP17 is highly expressed in tumor biopsies, is cell cycle regulated, and is required for G1-S progression', *Cancer Research*. doi: 10.1158/0008-5472.CAN-09-4152.

Mcneill, J. H. *et al.* (1998) 'Insulin-induced vasodilatation is dependent upon tetrahydro-biopterin synthesis', *Proceedings of the Western Pharmacology Society*.

de Mello, A. H. *et al.* (2018) 'Mitochondrial dysfunction in obesity', *Life Sciences*. doi: 10.1016/j.lfs.2017.11.019.

Mill, C. *et al.* (2014) 'Wnt5a-Induced Wnt1-Inducible secreted protein-1 suppresses vascular smooth muscle cell apoptosis induced by oxidative stress', *Arteriosclerosis, Thrombosis, and Vascular Biology*. doi: 10.1161/ATVBAHA.114.303922.

Minami, T. *et al.* (2003) 'Thrombin stimulation of vascular adhesion molecule-1 in endothelial cells is mediated by protein kinase C (PKC)-delta-NF-kappa B and PKC-zeta-GATA signaling pathways.', *The Journal of biological chemistry*. doi: 10.1074/jbc.M208974200.

Mittal, M. *et al.* (2014) 'Reactive Oxygen Species in Inflammation and Tissue Injury', *Antioxidants & Redox Signaling*. doi: 10.1089/ars.2012.5149.

Mochly-Rosen, D., Das, K. and Grimes, K. V (2012) 'Protein kinase C, an elusive

therapeutic target?', *Nature reviews.Drug discovery*. doi: 10.1038/nrd3871 [doi].

Montezano, A. C. *et al.* (2015) 'Oxidative stress and human hypertension: Vascular mechanisms, biomarkers, and novel therapies', *Canadian Journal of Cardiology*. doi: 10.1016/j.cjca.2015.02.008.

Mount, P. F., Kemp, B. E. and Power, D. A. (2007) 'Regulation of endothelial and myocardial NO synthesis by multi-site eNOS phosphorylation', *Journal of Molecular and Cellular Cardiology*. doi: 10.1016/j.yjmcc.2006.05.023.

Muniyappa, R. *et al.* (2007) 'Cardiovascular actions of insulin', *Endocrine Reviews*. doi: 10.1210/er.2007-0006.

Münzel, T. *et al.* (2002) 'Detection of superoxide in vascular tissue', *Arteriosclerosis, Thrombosis, and Vascular Biology*. doi: 10.1161/01.ATV.0000034022.11764.EC.

Napoli, C. *et al.* (2003) 'Deletion of the p66Shc longevity gene reduces systemic and tissue oxidative stress, vascular cell apoptosis, and early atherogenesis in mice fed a high-fat diet', *Proceedings of the National Academy of Sciences*. doi: 10.1073/pnas.0336359100.

Natali, A. *et al.* (2006) 'Clustering of insulin resistance with vascular dysfunction and low-grade inflammation in type 2 diabetes', *Diabetes*. doi: 10.2337/diabetes.55.04.06.db05-1076.

Naylor, R. N. *et al.* (2011) 'Genetics and pathophysiology of neonatal diabetes mellitus', *Journal of Diabetes Investigation*. doi: 10.1111/j.2040-1124.2011.00106.x.

Nolan, C. J. *et al.* (2015) 'Insulin resistance as a physiological defense against metabolic stress: Implications for the management of subsets of type 2 diabetes', *Diabetes*. doi: 10.2337/db14-0694.

Nomachi, A. *et al.* (2008) 'Receptor tyrosine kinase Ror2 mediates Wnt5a-induced

polarized cell migration by activating c-Jun N-terminal kinase via actin-binding protein filamin A', *Journal of Biological Chemistry*. doi: 10.1074/jbc.M802325200.

Nusse, R. and Clevers, H. (2017) 'Wnt/β-Catenin Signaling, Disease, and Emerging Therapeutic Modalities', *Cell*. doi: 10.1016/j.cell.2017.05.016.

Odegaard, J. I. and Chawla, A. (2013) 'Pleiotropic actions of insulin resistance and inflammation in metabolic homeostasis.', *Science (New York, N.Y.)*. doi: 10.1126/science.1230721.

Ohashi, M. *et al.* (2006) 'MnSOD deficiency increases endothelial dysfunction in ApoE-deficient mice', *Arteriosclerosis, Thrombosis, and Vascular Biology*. doi: 10.1161/01.ATV.0000238347.77590.c9.

Ohyama, K. *et al.* (2018) 'Coronary Adventitial and Perivascular Adipose Tissue Inflammation in Patients With Vasospastic Angina', *Journal of the American College of Cardiology*. doi: 10.1016/j.jacc.2017.11.046.

Oikonomou, E. K. *et al.* (2018) 'Non-invasive detection of coronary inflammation using computed tomography and prediction of residual cardiovascular risk (the CRISP CT study): a post-hoc analysis of prospective outcome data', *The Lancet*. doi: 10.1016/S0140-6736(18)31114-0.

Okerson, T. and Chilton, R. J. (2012) 'The Cardiovascular Effects of GLP-1 Receptor Agonists', *Cardiovascular Therapeutics*. doi: 10.1111/j.1755-5922.2010.00256.x.

Ott, C. *et al.* (2014) 'Role of advanced glycation end products in cellular signaling', *Redox Biology*. doi: 10.1016/j.redox.2013.12.016.

Ouchi, N. *et al.* (2010) 'Sfrp5 is an anti-inflammatory adipokine that modulates metabolic dysfunction in obesity', *Science*. doi: 10.1126/science.1188280.

Oyama, T. *et al.* (2006) 'The role of polyol pathway in high glucose-induced endothelial cell damages', *Diabetes Research and Clinical Practice*. doi: 10.1016/j.diabres.2006.02.010.

Pacher, P. (2006) 'Therapeutic Effects of Xanthine Oxidase Inhibitors: Renaissance Half a Century after the Discovery of Allopurinol', *Pharmacological Reviews*. doi: 10.1124/pr.58.1.6.

Pacher, P., Beckman, J. S. and Liaudet, L. (2007) 'Nitric oxide and peroxynitrite in health and disease.', *Physiological reviews*. doi: 10.1152/physrev.00029.2006.

Panday, A. *et al.* (2015) 'NADPH oxidases: An overview from structure to innate immunity-associated pathologies', *Cellular and Molecular Immunology*. doi: 10.1038/cmi.2014.89.

Paneni, F. *et al.* (2012) 'Gene silencing of the mitochondrial adaptor p66Shc suppresses vascular hyperglycemic memory in diabetes', *Circulation Research*. doi: 10.1161/CIRCRESAHA.112.266593.

Paneni, F. *et al.* (2013) 'Diabetes and vascular disease: Pathophysiology, clinical consequences, and medical therapy: Part i', *European Heart Journal*. doi: 10.1093/eurheartj/eht149.

Park, J.-S. *et al.* (2013) 'Epicardial adipose tissue thickness is a predictor for plaque vulnerability in patients with significant coronary artery disease.', *Atherosclerosis*. doi: 10.1016/j.atherosclerosis.2012.11.001.

Park, J. Y. *et al.* (2000) 'Induction of endothelin-1 expression by glucose: an effect of protein kinase C activation', *Diabetes*. doi: 10.2337/diabetes.49.7.1239.

Payne, G. A. *et al.* (2009) 'Periadventitial adipose tissue impairs coronary endothelial function via PKC-beta-dependent phosphorylation of nitric oxide synthase.', *American*

journal of physiology. Heart and circulatory physiology. doi: 10.1152/ajpheart.00116.2009.

Pereira, C. *et al.* (2008) 'Wnt5A/CaMKII signaling contributes to the inflammatory response of macrophages and is a target for the antiinflammatory action of activated protein C and interleukin-10', *Arteriosclerosis, Thrombosis, and Vascular Biology*. doi: 10.1161/ATVBAHA.107.157438.

Pessin, J. E. and Saltiel, A. R. (2000) 'Signaling pathways in insulin action: Molecular targets of insulin resistance', *Journal of Clinical Investigation*. doi: 10.1172/JCI10582.

Petros, R. A. and Desimone, J. M. (2010) 'Strategies in the design of nanoparticles for therapeutic applications', *Nature Reviews Drug Discovery*. doi: 10.1038/nrd2591.

Pfaffl, M. W. (2001) 'A new mathematical model for relative quantification in real-time RT-PCR', *Nucleic Acids Research*. doi: 10.1093/nar/29.9.e45.

Piché, M.-E. *et al.* (2018) 'Overview of Epidemiology and Contribution of Obesity and Body Fat Distribution to Cardiovascular Disease: An Update', *Progress in Cardiovascular Diseases*. doi: 10.1016/j.pcad.2018.06.004.

Polak, M. and Cavé, H. (2007) 'Neonatal diabetes mellitus: A disease linked to multiple mechanisms', *Orphanet Journal of Rare Diseases*. doi: 10.1186/1750-1172-2-12.

Potenza, M. A., Addabbo, F. and Montagnani, M. (2009) 'Vascular actions of insulin with implications for endothelial dysfunction.', *American journal of physiology. Endocrinology and metabolism*. doi: 10.1152/ajpendo.00297.2009.

Rajesh, M. *et al.* (2009) 'Xanthine oxidase inhibitor allopurinol attenuates the development of diabetic cardiomyopathy', *Journal of Cellular and Molecular Medicine*. doi: 10.1111/j.1582-4934.2008.00564.x.

Ramachandran, A. *et al.* (2002) 'Mitochondria, nitric oxide, and cardiovascular

dysfunction', *Free Radical Biology and Medicine*. doi: 10.1016/S0891-5849(02)01142-5.

RAMANA, K. V. *et al.* (2003) 'Nitric oxide regulates the polyol pathway of glucose metabolism in vascular smooth muscle cells', *The FASEB Journal*. doi: 10.1096/fj.02-0722com.

Rask-Madsen, C. and King, G. L. (2007) 'Mechanisms of Disease: endothelial dysfunction in insulin resistance and diabetes', *Nature Clinical Practice Endocrinology & Metabolism*. doi: 10.1038/ncpendmet0366.

Rask-Madsen, C. and King, G. L. (2013) 'Vascular complications of diabetes: Mechanisms of injury and protective factors', *Cell Metabolism*. doi: 10.1016/j.cmet.2012.11.012.

Rasouli, N. and Kern, P. A. (2008) 'Adipocytokines and the metabolic complications of obesity', *Journal of Clinical Endocrinology and Metabolism*. doi: 10.1210/jc.2008-1613.

Rauner, M. *et al.* (2012) 'WNT5A is induced by inflammatory mediators in bone marrow stromal cells and regulates cytokine and chemokine production', *Journal of Bone and Mineral Research*. doi: 10.1002/jbmr.1488.

Ray, R. M., Vaidya, R. J. and Johnson, L. R. (2007) 'MEK/ERK regulates adherens junctions and migration through Rac1', *Cell Motility and the Cytoskeleton*. doi: 10.1002/cm.20172.

Rehman, M. B. *et al.* (2017) 'Efficacy and safety of DPP-4 inhibitors in patients with type 2 diabetes: Meta-analysis of placebo-controlled randomized clinical trials', *Diabetes and Metabolism*. doi: 10.1016/j.diabet.2016.09.005.

Renner, S. *et al.* (2016) 'Incretin actions and consequences of incretin-based therapies: Lessons from complementary animal models', *Journal of Pathology*. doi: 10.1002/path.4655.

Reya, T. and Clevers, H. (2005) 'Wnt signalling in stem cells and cancer', *Nature*. doi: 10.1038/nature03319.

Roberts, C. K. *et al.* (2006) 'Oxidative stress and dysregulation of NAD(P)H oxidase and antioxidant enzymes in diet-induced metabolic syndrome', *Metabolism: Clinical and Experimental*. doi: 10.1016/j.metabol.2006.02.022.

Rorsman, P. and Braun, M. (2013) 'Regulation of Insulin Secretion in Human Pancreatic Islets', *Annual Review of Physiology*. doi: 10.1146/annurev-physiol-030212-183754.

Roumie, C. L. *et al.* (2014) 'Association between intensification of metformin treatment with insulin vs sulfonylureas and cardiovascular events and all-cause mortality among patients with diabetes', *JAMA - Journal of the American Medical Association*. doi: 10.1001/jama.2014.4312.

Rydén, L. *et al.* (2013) 'ESC guidelines on diabetes, pre-diabetes, and cardiovascular diseases developed in collaboration with the EASD', *European Heart Journal*. doi: 10.1093/eurheartj/eht108.

S.S., M., F.B., S. and A., C. (2018) 'Atherosclerosis of the Internal Mammary Artery: Intravascular Ultrasound and Virtual Histology Imaging', *Journal of Invasive Cardiology*.

Saely, C. H., Geiger, K. and Drexel, H. (2011) 'Brown versus white adipose tissue: A mini-review', *Gerontology*. doi: 10.1159/000321319.

Samuel, V. T. and Shulman, G. I. (2012) 'Mechanisms for insulin resistance: Common threads and missing links', *Cell*. doi: 10.1016/j.cell.2012.02.017.

San José, G., Bidegain, J., Robador, P. A., *et al.* (2009) 'Insulin-induced NADPH oxidase activation promotes proliferation and matrix metalloproteinase activation in monocytes/macrophages.', *Free radical biology & medicine*. doi:

10.1016/j.freeradbiomed.2009.01.009.

San José, G., Bidegain, J., Robador, P. A., *et al.* (2009) 'Insulin-induced NADPH oxidase activation promotes proliferation and matrix metalloproteinase activation in monocytes/macrophages', *Free Radical Biology and Medicine*. doi: 10.1016/j.freeradbiomed.2009.01.009.

San Martin, A. *et al.* (2007) 'Nox1-based NADPH oxidase-derived superoxide is required for VSMC activation by advanced glycation end-products', *Free Radical Biology and Medicine*. doi: 10.1016/j.freeradbiomed.2007.02.002.

Sarzani, R. *et al.* (2011) 'Carotid artery atherosclerosis in hypertensive patients with a functional LDL receptor-related protein 6 gene variant', *Nutrition, Metabolism and Cardiovascular Diseases*. doi: 10.1016/j.numecd.2009.08.004.

Savini, I. *et al.* (2013) 'Obesity-associated oxidative stress: Strategies finalized to improve redox state', *International Journal of Molecular Sciences*. doi: 10.3390/ijms140510497.

Schalkwijk, C. G. and Stehouwer, C. D. (2005) 'Vascular complications in diabetes mellitus: the role of endothelial dysfunction', *Clin Sci (Lond)*. doi: CS20050025 [pii]\r10.1042/CS20050025.

Scherrer, U. *et al.* (1994) 'Nitric oxide release accounts for insulin's vascular effects in humans', *Journal of Clinical Investigation*. doi: 10.1172/JCI117621.

Schulman, I. H. and Zhou, M.-S. (2009) 'Vascular insulin resistance: a potential link between cardiovascular and metabolic diseases.', *Current hypertension reports*. doi: 10.1007/s11906-009-0010-0.

Schulte, G. and Bryja, V. (2017) 'WNT signalling: mechanisms and therapeutic

opportunities', *British Journal of Pharmacology*. doi: 10.1111/bph.14065.

Scirica, B. M. *et al.* (2013) 'Saxagliptin and cardiovascular outcomes in patients with type 2 diabetes mellitus.', *The New England journal of medicine*. doi: 10.1056/NEJMoa1307684.

Semba, R. D. *et al.* (2014) 'The role of O-GlcNAc signaling in the pathogenesis of diabetic retinopathy', *Proteomics - Clinical Applications*. doi: 10.1002/prca.201300076.

Shah, B. R., Retnakaran, R. and Booth, G. L. (2008) 'Increased risk of cardiovascular disease in young women following gestational diabetes mellitus', *Diabetes Care*. doi: 10.2337/dc08-0706.

Shubrook, J. *et al.* (2017) 'Standards of medical care in diabetes—2017 abridged for primary care providers', *Clinical Diabetes*. doi: 10.2337/cd16-0067.

Shulman, G. I. (2000) 'Cellular mechanisms of insulin resistance', *The Journal of Clinical Investigation*. doi: 10.1172/JCI10583.On.

Siegel-Axel, D. I. and Häring, H. U. (2016) 'Perivascular adipose tissue: An unique fat compartment relevant for the cardiometabolic syndrome', *Reviews in Endocrine and Metabolic Disorders*. doi: 10.1007/s11154-016-9346-3.

Sinha, S. K. *et al.* (2016) 'Epicardial Adipose Tissue Thickness and Its Association With the Presence and Severity of Coronary Artery Disease in Clinical Setting: A Cross-Sectional Observational Study', *Journal of Clinical Medicine Research*. doi: 10.14740/jocmr2468w.

Slusarski, D. C., Corces, V. G. and Moon, R. T. (1997) 'Interaction of Wnt and a Frizzled homologue triggers G-protein-linked phosphatidylinositol signalling', *Nature*. doi: 10.1038/37138.

Sobrevia, L. and González, M. (2009) 'A role for insulin on L-arginine transport in fetal

endothelial dysfunction in hyperglycaemia.', *Current vascular pharmacology*. doi: 10.2174/157016109789043919.

Spaight, C. *et al.* (2016) 'Gestational diabetes mellitus', *Endocrine Development*. doi: 10.1159/000439413.

Steinberg, S. F. (2015) 'Mechanisms for redox-regulation of protein kinase C', *Frontiers in Pharmacology*. doi: 10.3389/fphar.2015.00128.

Stenstrom, G. *et al.* (2005) 'Latent Autoimmune Diabetes in Adults: Definition, Prevalence, -Cell Function, and Treatment', *Diabetes*. doi: 10.2337/diabetes.54.suppl_2.S68.

Takada, I. *et al.* (2007) 'A histone lysine methyltransferase activated by non-canonical Wnt signalling suppresses PPAR-gamma transactivation.', *Nature cell biology*. doi: 10.1038/ncb1647.

Tan, S. X. *et al.* (2015) 'Selective insulin resistance in adipocytes', *Journal of Biological Chemistry*. doi: 10.1074/jbc.M114.623686.

Thannickal, V. J. and Fanburg, B. L. (2000) 'Reactive oxygen species in cell signaling.', *American journal of physiology. Lung cellular and molecular physiology*. doi: 10.1164/rccm.2206007.

Thomou, T. *et al.* (2017) 'Adipose-derived circulating miRNAs regulate gene expression in other tissues', *Nature*. doi: 10.1038/nature21365.

Thompson, D. S. *et al.* (2014) 'Limitations of fasting indices in the measurement of insulin sensitivity in Afro-Caribbean adults', *BMC Research Notes*. doi: 10.1186/1756-0500-7-98.

Thorens, B. (2011) 'Brain glucose sensing and neural regulation of insulin and glucagon secretion', *Diabetes, Obesity and Metabolism*. doi: 10.1111/j.1463-1326.2011.01453.x.

Tilg, H. and Moschen, A. R. (2006) 'Adipocytokines: Mediators linking adipose tissue, inflammation and immunity', *Nature Reviews Immunology*. doi: 10.1038/nri1937.

Todorčević, M. *et al.* (2017) 'A cellular model for the investigation of depot specific human adipocyte biology', *Adipocyte*. doi: 10.1080/21623945.2016.1277052.

Tsuneki, H. *et al.* (2008) 'Age-related insulin resistance in hypothalamus and peripheral tissues of orexin knockout mice', *Diabetologia*. doi: 10.1007/s00125-008-0929-8.

Tune, J. D. *et al.* (2017) 'Cardiovascular consequences of metabolic syndrome', *Translational Research*. doi: 10.1016/j.trsl.2017.01.001.

Turner, R. (1998) 'Intensive blood-glucose control with sulphonylureas or insulin compared with conventional treatment and risk of complications in patients with type 2 diabetes (UKPDS 33)', *Lancet*. doi: 10.1016/S0140-6736(98)07019-6.

Ueland, T. *et al.* (2009) 'Dickkopf-1 enhances inflammatory interaction between platelets and endothelial cells and shows increased expression in atherosclerosis', *Arteriosclerosis, Thrombosis, and Vascular Biology*. doi: 10.1161/ATVBAHA.109.189761.

Valko, M. *et al.* (2007) 'Free radicals and antioxidants in normal physiological functions and human disease', *The International Journal of Biochemistry & Cell Biology*. doi: 10.1016/j.biocel.2006.07.001.

Vásquez-Vivar, J. *et al.* (1997) 'Superoxide anion formation from lucigenin: An electron spin resonance spin-trapping study', *FEBS Letters*. doi: 10.1016/S0014-5793(97)00036-7.

Veal, E. A., Day, A. M. and Morgan, B. A. (2007) 'Hydrogen Peroxide Sensing and Signaling', *Molecular Cell*. doi: 10.1016/j.molcel.2007.03.016.

Very, N. *et al.* (2018) 'Cross-dysregulation of O-GlcNAcylation and PI3K/AKT/mTOR axis in human chronic diseases', *Frontiers in Endocrinology*. doi: 10.3389/fendo.2018.00602.

Vlassara, H. and Uribarri, J. (2014) 'Advanced glycation end products (AGE) and diabetes: Cause, effect, or both?', *Current Diabetes Reports*. doi: 10.1007/s11892-013-0453-1.

Wajchenberg, B. L. (2000) 'Subcutaneous and visceral adipose tissue: Their relation to the metabolic syndrome', *Endocrine Reviews*. doi: 10.1210/edrv.21.6.0415.

Wang, G. X., Zhao, X. Y. and Lin, J. D. (2015) 'The brown fat secretome: Metabolic functions beyond thermogenesis', *Trends in Endocrinology and Metabolism*. doi: 10.1016/j.tem.2015.03.002.

Wanstall, J. C. *et al.* (2001) 'Vascular smooth muscle relaxation mediated by nitric oxide donors: A comparison with acetylcholine, nitric oxide and nitroxyl ion', *British Journal of Pharmacology*. doi: 10.1038/sj.bjp.0704269.

Warboys, C. M., Toh, H. B. and Fraser, P. A. (2009) 'Role of NADPH oxidase in retinal microvascular permeability increase by RAGE activation', *Investigative Ophthalmology and Visual Science*. doi: 10.1167/iovs.08-2730.

Weber, C. and Noels, H. (2011) 'Atherosclerosis: Current pathogenesis and therapeutic options', *Nature Medicine*. doi: 10.1038/nm.2538.

Wellen, K. E. and Hotamisligil, G. S. (2003) 'Obesity-induced inflammatory changes in adipose tissue', *Journal of Clinical Investigation*. doi: 10.1172/JCI20514.

WHO (2011) *Waist Circumference and Waist–Hip Ratio*, *WHO Expert*.

Wiese, K. E., Nusse, R. and van Amerongen, R. (2018) 'Wnt signalling: conquering complexity', *Development*. doi: 10.1242/dev.165902.

Williams, S. B. *et al.* (1996) 'Impaired nitric oxide-mediated vasodilation in patients with non-insulin-dependent diabetes mellitus', *J Am Coll Cardiol*. doi: 0735-1097(95)00522-6

[pii].

Woldt, E. *et al.* (2012) 'The nuclear hormone receptor PPARγ counteracts vascular calcification by inhibiting Wnt5a signalling in vascular smooth muscle cells', *Nature Communications*. doi: 10.1038/ncomms2087.

Xia, N. *et al.* (2016) 'Uncoupling of Endothelial Nitric Oxide Synthase in Perivascular Adipose Tissue of Diet-Induced Obese Mice', *Arteriosclerosis, Thrombosis, and Vascular Biology*. doi: 10.1161/ATVBAHA.115.306263.

Yan, L.-J. *et al.* (2016) 'Sources and implications of NADH/NAD+ redox imbalance in diabetes and its complications', *Diabetes, Metabolic Syndrome and Obesity: Targets and Therapy*. doi: 10.2147/DMSO.S106087.

Yudkin, J. S., Eringa, E. and Stehouwer, C. D. A. (2005) '"Vasocrine" signalling from perivascular fat: A mechanism linking insulin resistance to vascular disease', *Lancet*. doi: 10.1016/S0140-6736(05)66585-3.

Zeng, G. *et al.* (2000) 'Roles for insulin receptor, PI3-kinase, and Akt in insulin-signaling pathways related to production of nitric oxide in human vascular endothelial cells', *Circulation*. doi: 10.1161/01.CIR.101.13.1539.

Zeng, Y. *et al.* (2014) 'The DPP-4 inhibitor sitagliptin attenuates the progress of atherosclerosis in apolipoprotein-E-knockout mice via AMPK- and MAPK-dependent mechanisms', *Cardiovascular Diabetology*. doi: 10.1186/1475-2840-13-32.

Zhao, H. *et al.* (2005) 'Detection and characterization of the product of hydroethidine and intracellular superoxide by HPLC and limitations of fluorescence.', *Proceedings of the National Academy of Sciences of the United States of America*. doi: 10.1073/pnas.0501719102.

Zhao, Y. *et al.* (2014) 'Wnt5a Promotes Inflammatory Responses via Nuclear Factor κB (NF-κB) and Mitogen-activated Protein Kinase (MAPK) Pathways in Human Dental Pulp Cells.', *The Journal of biological chemistry*. doi: 10.1074/jbc.M113.546523.

Zimmerman, Z. F., Moon, R. T. and Chien, A. J. (2012) 'Targeting Wnt pathways in disease', *Cold Spring Harbor Perspectives in Biology*. doi: 10.1101/cshperspect.a008086.

Zuriaga, M. A. *et al.* (2017) 'Activation of non-canonical WNT signaling in human visceral adipose tissue contributes to local and systemic inflammation', *Scientific Reports*. doi: 10.1038/s41598-017-17509-5.